ISSN 1007-9327 (print)
ISSN 2219-2840 (online)

World Journal of *Gastroenterology*

World J Gastroenterol 2019 November 21; 25(43): 6373-6482

Published by Baishideng Publishing Group Inc

World Journal of Gastroenterology

Contents

Weekly Volume 25 Number 43 November 21, 2019

MINIREVIEWS

ORIGINAL ARTICLE

Basic Study

Case Control Study

Retrospective Cohort Study

Retrospective Study

Observational Study

Contents

World Journal of Gastroenterology

Volume 25 Number 43 November 21, 2019

ABOUT COVER

Editorial board member of *World Journal of Gastroenterology*, Haruhiko Sugimura, MD, PhD, Professor, Department of Tumor Pathology, Hamamatsu University School of Medicine, Hamamatsu 431-3192, Japan.

AIMS AND SCOPE

The primary aim of *World Journal of Gastroenterology* (*WJG*, *World J Gastroenterol*) is to provide scholars and readers from various fields of gastroenterology and hepatology with a platform to publish high-quality basic and clinical research articles and communicate their research findings online.

WJG mainly publishes articles reporting research results and findings obtained in the field of gastroenterology and hepatology and covering a wide range of topics including gastroenterology, hepatology, gastrointestinal endoscopy, gastrointestinal surgery, gastrointestinal oncology, and pediatric gastroenterology.

INDEXING/ABSTRACTING

The *WJG* is now indexed in Current Contents®/Clinical Medicine, Science Citation Index Expanded (also known as SciSearch®), Journal Citation Reports®, Index Medicus, MEDLINE, PubMed, PubMed Central, and Scopus. The 2019 edition of Journal Citation Report® cites the 2018 impact factor for *WJG* as 3.411 (5-year impact factor: 3.579), ranking *WJG* as 35th among 84 journals in gastroenterology and hepatology (quartile in category Q2). CiteScore (2018): 3.43.

RESPONSIBLE EDITORS FOR THIS ISSUE

NAME OF JOURNAL
World Journal of Gastroenterology

ISSN
ISSN 1007-9327 (print) ISSN 2219-2840 (online)

LAUNCH DATE
October 1, 1995

FREQUENCY
Weekly

EDITORS-IN-CHIEF
Subrata Ghosh, Andrzej S Tarnawski

EDITORIAL BOARD MEMBERS
http://www.wjgnet.com/1007-9327/editorialboard.htm

EDITORIAL OFFICE
Ze-Mao Gong, Director

PUBLICATION DATE
November 21, 2019

INSTRUCTIONS TO AUTHORS
https://www.wjgnet.com/bpg/gerinfo/204

GUIDELINES FOR ETHICS DOCUMENTS
https://www.wjgnet.com/bpg/GerInfo/287

GUIDELINES FOR NON-NATIVE SPEAKERS OF ENGLISH
https://www.wjgnet.com/bpg/gerinfo/240

PUBLICATION MISCONDUCT
https://www.wjgnet.com/bpg/gerinfo/208

ARTICLE PROCESSING CHARGE
https://www.wjgnet.com/bpg/gerinfo/242

STEPS FOR SUBMITTING MANUSCRIPTS
https://www.wjgnet.com/bpg/GerInfo/239

ONLINE SUBMISSION
https://www.f6publishing.com

World Journal of Gastroenterology

Submit a Manuscript: https://www.f6publishing.com

World J Gastroenterol 2019 November 21; 25(43): 6373-6385

DOI: 10.3748/wjg.v25.i43.6373

ISSN 1007-9327 (print) ISSN 2219-2840 (online)

MINIREVIEWS

Current status of associating liver partition with portal vein ligation for staged hepatectomy: Comparison with two-stage hepatectomy and strategies for better outcomes

Kin Pan Au, Albert Chi Yan Chan

ORCID number: Kin Pan Au (0000-0002-7138-9805); Albert Chi Yan Chan (0000-0002-1383-2952).

Author contributions: Au KP did the literature review and wrote the manuscript; Chan ACY supervised the study and made revision to the manuscript; Both authors approved the submitted version of the manuscript.

Conflict-of-interest statement: The authors have no conflict of interest.

Manuscript source: Unsolicited manuscript

Received: May 27, 2019
Peer-review started: May 27, 2019
First decision: July 21, 2019
Revised: July 31, 2019
Accepted: August 7, 2019
Article in press: August 7, 2019
Published online: November 21, 2019

Kin Pan Au, Department of Surgery, Queen Mary Hospital, Hong Kong, China

Albert Chi Yan Chan, Department of Surgery and State Key Laboratory for Liver Research, The University of Hong Kong, Hong Kong, China

Corresponding author: Albert Chi Yan Chan, FRCS (Ed), Associate Professor, Department of Surgery, The University of Hong Kong, 102 Pok Fu Lam Road, Hong Kong, China.
acchan@hku.hk
Telephone: +86-852-22553025

Abstract

Since its introduction in 2012, associating liver partition with portal vein ligation for staged hepatectomy (ALPPS) has significantly expanded the pool of candidates for liver resection. It offers patients with insufficient liver function a chance of a cure. ALPPS is most controversial when its high morbidity and mortality is concerned. Operative mortality is usually a result of post-hepatectomy liver failure and can be minimized with careful patient selection. Elderly patients have limited reserve for tolerating the demanding operation. Patients with colorectal liver metastasis have normal liver and are ideal candidates. ALPPS for cholangiocarcinoma is technically challenging and associated with fair outcomes. Patients with hepatocellular carcinoma have chronic liver disease and limited parenchymal hypertrophy. However, in selected patients with limited hepatic fibrosis satisfactory outcomes have been produced. During the inter-stage period, serum bilirubin and creatinine level and presence of surgical complication predict mortality after stage II. Kinetic growth rate and hepatobiliary scintigraphy also guide the decision whether to postpone or omit stage II surgery. The outcomes of ALPPS have been improved by a combination of technical modifications. In patients with challenging anatomy, partial ALPPS potentially reduces morbidity, but remnant hypertrophy may compare unfavorably to a complete split. When compared to conventional two-stage hepatectomy with portal vein embolization or portal vein ligation, ALPPS offers a higher resection rate for colorectal liver metastasis without increased morbidity or mortality. While ALPPS has obvious theoretical oncological advantages over two-stage hepatectomy, the long-term outcomes are yet to be determined.

Key words: Associating liver partition with portal vein ligation for staged hepatectomy; Two-stage hepatectomy; Patient selection; Surgical outcomes

P-Reviewer: Aoki T, Donati M
S-Editor: Ma RY
L-Editor: Filipodia
E-Editor: Ma YJ

Core tip: Associating liver partition with portal vein ligation for staged hepatectomy (ALPPS) is associated with high morbidity and mortality. Operative mortality is usually a result of post-hepatectomy liver failure. Young patients with colorectal liver metastasis are ideal candidates. ALPPS for cholangiocarcinoma is associated with fair outcomes. In patients with challenging anatomy, partial ALPPS reduces morbidity, but remnant hypertrophy may compare unfavorably to a complete split. When compared to conventional two-stage hepatectomy with portal vein embolization or portal vein ligation, ALPPS has a higher resection rate. However, the long-term outcomes are yet to be determined.

Citation: Au KP, Chan ACY. Current status of associating liver partition with portal vein ligation for staged hepatectomy: Comparison with two-stage hepatectomy and strategies for better outcomes. *World J Gastroenterol* 2019; 25(43): 6373-6385
URL: https://www.wjgnet.com/1007-9327/full/v25/i43/6373.htm
DOI: https://dx.doi.org/10.3748/wjg.v25.i43.6373

INTRODUCTION

Functional reserve of future liver remnant (FLR) is the most important factor limiting surgical resection of liver tumors. In the last decade, extensive liver resection with a marginal FLR has been tackled with two-stage hepatectomy (TSH)[1]. Portal vein occlusion with surgical ligation or radiological embolization is performed in the first stage to induce hypertrophy of FLR. Redistribution of portal flow constitutes a stimulus to hypertrophy. Introduced in 2012, associating liver partition with portal vein ligation for staged hepatectomy (ALPPS) encompasses parenchymal splitting and portal vein ligation in the first stage[2]. Complete redistribution of portal blood flow accelerates and enhances magnitude of FLR hypertrophy. Accelerated hepatic regeneration also minimizes disease progression during the inter-stage period and exclusion from surgery. ALPPS significantly expanded the pool of candidates for liver resection but was associated with significant operative morbidity and mortality[3]. Early results of this novel procedure have been more readily reported and may provide insights on how to improve the outcomes. The objective of this review is to summarize current available literature to compare the efficacy of ALPPS *vs* conventional TSH and to determine the strategies to make ALPPS a better surgery.

ALPPS: BETTER THAN TWO-STAGE HEPATECTOMY?

The principle of oncological liver resection is complete tumor clearance while preserving adequate functional liver remnant. Inadequate FLR and extensive bilobar disease are common contraindications to curative resection. Before the era of ALPPS, TSH with portal vein embolization (PVE) or portal vein ligation (PVL) was validated to enlarge FLR prior to major hepatectomy. PVE boosted the FLR by 12%-62% over 3-8 wk[4-9]. In patients with diffuse bilobar disease, resection was achieved through a staged approach. In the first operation, tumors in the intended FLR were resected, *i.e.* clean-up resection and PVL is performed. The remnant was allowed to undergo hypertrophy while disease progression was controlled with systemic therapy before tumor clearance was completed in the second stage operation. ALPPS has been compared to TSH with PVE or PVL in terms of operative and oncological outcomes in recent publications.

Operative outcomes

ALPPS consistently offered a more pronounced hypertrophy rate (50%-80% *vs* 10%-40%) over a shorter interval (7-11 d *vs* 20-103 d), enabled higher resection rate (80%-100% *vs* 60%-90%)[4-10] (Table 1). However, the inception of ALPPS was also met by criticism for the associated morbidity and mortality. In the initial series reported by Schnizbauer *et al*[2], operative mortality was 12%. The international registry reported a major morbidity (Clavien-Dindo IIIa or above) rate of 40% and an operative mortality rate of 9%[3]. From the captioned series a 20%-40% major complication rate (Clavien-

Dindo grade IIIa or above) was generally reported for both approaches[4-10]. Bile leak, intra-abdominal collection and pleural effusions were common complications encountered[9]. Pooled data from a meta-analysis did not reveal a statistically significant difference in overall morbidity. However, a comparison in terms of major morbidity had not been made[12]. Occurrence of post-hepatectomy liver failure (PHLF) (10% *vs* 14%, OR = 0.86) and 90-d mortality (9% *vs* 5%, OR = 1.44) were similar among patients operated with both approaches[12].

Sandstrom *et al*[13] conducted a prospective randomized LIGRO trial to compare ALPPS and TSH in 100 patients with colorectal liver metastasis (CRLM) and FLR/estimated standard liver volume (ESLV) < 30%. The mean FLR/ESLV ratios were 22% and 21% in the ALPPS and TSH groups, respectively. Of the 48 patients in the ALPPS group, 44 (92%) attained satisfactory FLR/ESLV, *i.e*. 30% and completed stage II hepatectomy within 14 d. In contrast, thirteen (27%) patients in the TSH group (n = 49) never acquired sufficient remnant volume, and eight (16%) suffered disease progression preventing them from proceeding with second stage hepatectomy. It was noteworthy to highlight that twelve (24% of TSH arm) of them were successfully treated with rescue ALPPS. The prospective trial confirmed a higher resection rate (92% *vs* 57%, P < 0.001) for ALPPS with similar major morbidity (43% *vs* 43%, P = 0.99) and 90-d mortality (8% *vs* 6%, P = 0.68) with TSH.

Oncological outcomes

CRLM is the most common indication for ALPPS. Theoretically accelerated remnant growth in ALPPS shortens the interval to definitive resection and minimizes dropout due to disease progression. Skepticism remains while a manipulated hemiliver with high tumor load is left *in vivo* within an immunosuppressed and stressed environment, and that rapid hypertrophy could trigger residual tumor progression[14,15]. In the setting of TSH for CRLM, tumor progression has been documented radiologically by accelerated tumor growth, and pathologically by increased mitotic rate and Ki67 index[16-19]. However, similar findings were not observed in ALPPS patients. Tanaka *et al*[8] compared Ki67 expression in both approaches showing significantly induced of Ki67 index in PVE but not ALPPS patients. Joechle *et al*[20] concluded that markers of tumor proliferation and angiogenesis were similar among patients undergoing ALPPS and standard liver resection.

Oldhafer *et al*[21] reported frequent early recurrence after ALPPS for CRLM. Over a median follow up of 7 mo, six out of seven patients (86%) developed recurrence. The median disease-free survival (DFS) was 7 mo (3-13 mo). However, the outcomes could have been accounted for by the relatively advanced disease status. The mean number of tumors was 7.6 (3-14), and the mean tumor diameter was 4.9 cm (1.7-11.3 cm). From the registry, the 1- and 2-year overall survival (OS) for CRLM were 76% and 62%, respectively[3], comparable with a 67% 3-year OS reported for a large series of TSH[22]. While most case-control studies reported heterogeneous indications, comparison of CRLM outcomes was limited to two small retrospective series (Table 1). Ratti *et al*[6] compared 12 patients who underwent ALPPS with 36 TSH controls matched in terms of loco-regional staging and liver tumor status. With minimal dropout in the TSH arm (6%), 1-year overall (92% *vs* 94%) and DFS (67% *vs* 80%) were comparable. R0 resection rate was 100% among patients with completed resection procedures in both arms.

Adam *et al*[9] reported median OS was lower for the ALPPS arm at 2-year (42% *vs* 77%, P = 0.006) despite a higher completion rate (100% *vs* 63%, P < 0.001). This result compared unfavorably with registry data (2-year OS = 62%) and had to be interpreted with caution. R0 resection rates were low (17.6% *vs* 19.5%, P = 0.67) in both arms. Indeed, most patient in this series, irrespective of treatment arm, recurred early (1-year DFS 0% *vs* 10%, P = 0.21). An advanced preoperative disease status could be the culprit. Six (35%) and twelve (29%) patients had extrahepatic disease upon surgery in the ALPPS and TSH arms, respectively, and the median number of liver metastases were ten (compared to five reported in Ratti *et al*[6]). The inferior oncological outcomes could be the results of aggressive tumor biology rather than the choice of surgical approach.

In the more recent LIGRO trial, R0 resection rates were not different between ALPPS and TSH (77% *vs* 57%, P = 0.11), but survival data has yet to be available[13]. Long term oncological outcome of ALPPS is sparse due to its recent introduction. Whether ALPPS's conceptual advantages would translate to actual benefits over TSH remains unanswered.

Table 1 Associating liver partition with portal vein ligation for staged hepatectomy *vs* two-stage hepatectomy, *n* (%)

	n	Tumor	Preoperative FLR/ESLV in %	FLR increase in %	Interval in d	Complete planned resection	Major morbidity, ≥ IIIa		PHLF, ≥ B	HM	OS	DFS
							Stage I	Stage II				
Case control												
Schadde *et al*[3], 2014	48/83	CRLM/HCC/CC	0.47/0.53[b]	-		48 (100)/54 (64)					-	-
Shindoh *et al*[4], 2013	25/144	CRLM/HCC/CC	-	74 (21-192)/62 (0-379)	9 (5-28)/31 (12-385)	-	10 (40)/34 (33)		-	3 (12)/6 (6)	-	-
Croome *et al*[5], 2015	15/53	CRLM/HCC/CC	20 ± 4/31 ± 14	84 ± 8/36 ± 27	-	15 (100)/42 (79)	-	-	2 (13)/12 (23)[c]	0/2 (4)	-	-
Ratti *et al*[6], 2015	12/36	CRLM	22/23	47/41	11/31	12 (100)/34 (94.4)	0/1 (2.8)	5 (42)/6 (18)[d]	0/2 (5.9)	1 (8.3)/1 (2.9)	1 yr: 92%/94%	1 yr: 67%/80%
Tanaka *et al*[8], 2015	11/54	CRLM/NET	34 ± 10/31 ± 10	52 (33-94)/22 (34-68)[e]	-	11 (100)/48 (89)	1 (9)/4 (8)	3 (27)/8 (17)	5 (45)/5 (9)	1 (9)/1 (2)	-	-
Adam *et al*[9], 2016	17/41	CRLM	24/30	50/33	12/103	17 (100)/26 (63.4)	4 (24)/7 (17)	4 (24)/10 (38)	0/1 (3.8)	0/2 (4.9)	2 yr: 42%/77%	1 yr: 0%/10%
Matsuo *et al*[11], 2016	8/14	CRLM/CC	-	-	11 ± 2/52 ± 33	-	1(13)/4 (29)		2 (25)/8 (57)	0/0	-	-
Chia *et al*[7], 2018	10/29	HCC/CRLM	22 (12-29)/22 (15-32)	48 (39-97)/12 (4-42)	7 (7-9)/20 (18-29)	8 (80)/12 (59)	3 (30)[f]	2 (25)[g]/3 (17.6)[h]	2 (25)/0[c]	1 (3.4)/0	-	-
Meta-analysis												
Zhou *et al*[12], 2017	201/518	-	-	WMD +40%	WMD -27%	97%/73%	OR 2.4[i]	OR 4.0[i]	10%/14%			
Randomized controlled trial												
Sandstrom *et al*[13], 2018[j]	48/49	CRLM	22.4 ± 4.3/21.2 ± 5.1	68 ± 38/36 ± 18	11 ± 11/43 ± 15	44 (92)/28 (57)	19 (43)/12 (43)[k]		4 (8.3)/3 (6.1)	4 (8.3)/3 (6.1)	-	-

[a]Among completed procedures.
[b] Future liver remnant/body weight.
[c]50-50 criteria.
[d]Bile leak (*n* = 1), intra-abdominal abscess (*n* = 3).
[e]Week 1.
[f]Pleural effusion (*n* = 2), wound dehiscence (*n* = 1).
[g]Pleural effusion (*n* = 1), post-hepatectomy liver failure (*n* = 1).
[h]Bowel ischemia (*n* = 1), acute renal failure (*n* = 1), pleural effusion (*n* = 1).
[i]All morbidity.
[j]Combined results of portal vein embolization (*n* = 27) and staged hepatectomy (*n* = 22) compared with associating liver partition with portal vein ligation for staged hepatectomy (*n* = 48).
[k]Clavien-Dindo IIIa or above. CC: Cholangiocarcinoma; CRLM: Colorectal liver metastasis; Cx: Complications; DFS: Disease-free survival; ESLV: Estimated standard liver volume; FLR: Future liver remnant; HCC: Hepatocellular carcinoma; HM: Hospital mortality; NET: Neuroendocrine tumor; OS: Overall survival; PHLF: Post-hepatectomy liver failure; WMD: Weighed mean difference.

RISK FACTORS FOR MORBIDITY AND MORTALITY

The major morbidity associated with ALPPS were PHLF and bile leak. Understanding the risk factors allow better patient selection for better outcomes.

PHLF

PHLF accounted for 75% of ALPPS related mortality[3,22]. Using the 50-50 criteria[23], the international registry reported a 9% PHLF rate. Despite a rapid median volume gain of 80% before stage II, 80% of the patients with PHLF had an FLR of more than 30% of the total liver volume prior to stage II. Critics suggested that rapid remnant expansion in ALPPS was partly a result of tissue edema rather than pure hypertrophy[24]. There was also concern if the increase in volume had been paralleled by a corresponding increase in function[25,26]. The query was supported by the discrepancies between

volume gain and functional assessment using hepatobiliary scintigraphy. Inter-stage functional increment assessed by (99m)Tc-Mebrofenin scan only attained half the value of volume expansion[27]. This may in part explain the remarkable PHLF rate after ALPPS stage II despite satisfactory volume.

In an analysis of 320 patients in the registry to identify risk factors for 90-d mortality[22], the single most important risk factor was patient age > 60 years (OR = 14.3, P = 0.001). Inter-stage biochemical parameters were also predictive of mortality. Model of end-stage liver disease score > 10 prior to stage II (OR = 4.9, P = 0.006) and liver failure defined by International Study Group of Liver Surgery (prolonged international normalized ratio and raised serum bilirubin) at day 5 after stage I (OR = 3.9, P = 0.011)[28] were independent risk factors for PHLF after ALPPS. These were simple, objective and reproducible laboratory parameters that allowed clinicians to assess the risk of proceeding to stage II operation.

Another study based on data collected from the registry generated a risk model for prediction of operative mortality after ALPPS (Table 2)[29]. Stage I poor risk indicators included advanced age (> 67, OR = 5.7) and biliary malignancy (OR = 3.8). Stage II predictors included cumulative stage I risk score (OR = 1.9), severe stage I complication (> IIIb, OR = 3.4) and serum level of bilirubin (OR 4.4) and creatinine (OR 5.4). Perhaps patient selection is most important before stage I. Advanced age was given a risk score of 3, while biliary tumor and non-CRLM/non-biliary tumor were given scores of 2 and 1, respectively. A total score of 0, 1, 2, 3, 4 and 5 were associated with operative mortality of 3%, 5%, 9%, 15%, 24% and 37%, respectively. The risk model provided an objective prediction of mortality. The message behind was straightforward: By avoiding elderly patients the total risk score was capped as 2, *i.e*. a mortality of 9%. Furthermore, this score provided guidance for a decision to postpone or omit stage II operation. The inclusion of serum bilirubin and creatinine level suggested postponing stage II until liver and renal function improved and was in concordance with the observation of higher mortality when stage II was proceeded with a high model for end-stage liver disease score (> 10, OR = 4.9, P = 0.006)[22]. Nonetheless, it was worthy to highlight that the addition of stage I cumulative score, *i.e*., age, indication and stage I complications implied that presence of these poor risk factors despite normal liver and renal function still incurred stage II operative risk.

From experience in PVE, we learned that FLR growth rate was related to hepatic regenerative potential[30,31]. A kinetic growth rate of > 2%/wk was associated with fewer PHLF after hepatectomy. Its significance in ALPPS was investigated by Kambakamba *et al*[32] in a retrospective series of 38 procedures. It appeared to be a more reliable predictor of PHLF than FLR volume alone. Kinetic growth rate ≥ 6%/d and FLR > 30% at 1 wk after ALPPS stage I were associated with no PHLF. It compared closely to the median kinetic growth rate in the registry of 7%/d[3]. On the other hand, Serenari *et al*[33] deployed hepatobiliary scintigraphy with (99m) Tc-Mebrofenin scan for inter-stage remnant function assessment and developed a model termed 'The HIBA index' to predict PHLF. In their cohort of 20 patients, a cut off value of less than 15% predicted PHLF by a sensitivity of 100% and a specificity of 94%. These results indicated that hepatobiliary scintigraphy could be a useful adjunct to biochemical test and liver volumetry to assess remnant function. Patients with suboptimal remnant function could be allowed more time for further hypertrophy and safe resection.

Bile leak

One of the most commonly reported surgical complications associated with ALPPS in the early days was bile leakage. According to the registry, bile leak occurred in 17% of ALPPS procedures[3]. The most common site of leakage occurred at the transection surface from the deportalized liver due to ischemia of segment IV when the portal vein was ligated, and the parenchymal split was between the left medial and lateral section parenchymal partition. The risk is particularly high for ALPPS performed for right trisectionectomy[34]. This was in particular an important issue in right trisectionectomy when the segment IV was instantly deprived of both portal and arterial perfusion that in turn resulted in necrosis followed by bile leakage and sepsis.

Cholangiocarcinoma is another risk factor for bile leak[35]. Hilar dissection is technically difficult due to tumor infiltration. Portal lymphadenectomy further deprived the transection plane of blood supply[36]. ALPPS associated morbidities were closely related to procedural complexity. Indeed from the registry independent risk factors for severe complications (Clavien-Dindo IIIb or above) were prolonged stage I operating time (more than 300 min) (OR = 4.42, P = 0.004), blood transfusion (OR = 5.26, P = 0.001) and non-CRLM (OR = 2.73, P = 0.049)[3]. ALPPS for hilar cholangiocarcinoma was not only associated with more bile leak but also more PHLF and operative mortality[35,37].

Table 2 Risk modelling proposed by Linecker *et al*[29]

Risk modelling	Risk points	OR (95%CI)
Pre-stage I variables		
CRLM	0	1
Non-CRLM/non-biliary	1	1.925 (0.808-4.585)
Biliary	2	3.767 (1.800-7.822)
Age ≥ 67	3	5.668 (2.843-11.300)
Pre-stage II variables		
Pre-stage I score	0.66	1.925 (1.527-2.426)
Inter-stage complications ≥3b	1.2	3.350 (1.280-8.769)
Bilirubin	1.5	4.439 (1.699-11.600)
Creatinine	1.7	5.454 (1.606-18.520)

CI: Confidence interval; CRLM: Colorectal liver metastasis; OR: Odds ratio.

STRATEGIES TO IMPROVE OUTCOMES

Many innovative surgeries faced unfavorable outcomes when they were first introduced. With accumulation of experience, improved outcomes were achieved with more cautious patient selection and more sophisticated technical refinements. A well-established international registry allowed information regarding ALPPS to be systematically collected[3]. With better understanding and insights into the procedure hepatobiliary surgeons could better select the suitable candidates and further refine their techniques to achieve more desirable outcomes.

Patient selection

Patient factor: Elderly patients are poor candidates for ALPPS. From the international registry, patients older than 60 years of age had more severe complications (Clavien-Dindo IIIb or above) (OR = 3.76, P = 0.007)[3] and higher mortality (OR = 14.3, P = 0.001)[22]. Moreover, inferior OS were consistently observed for elderly patients with CRLM[3] and hepatocellular carcinoma (HCC)[38]. ALPPS is a physiologically challenging operation. Although a chronological cut-off may be impractical, it is rational to avoid ALPPS in patients with advanced physiological age. They have limited reserve to survive major complications, which are not uncommonly encountered. In these patients, TSH can be considered alternatively.

FLR volume: For major hepatectomy, an FLR to ESLV ratio of 25% is mandatory to ensure adequate postoperative liver function in patients with normal liver[39-41]. The requirement is 30% in patients with underlying liver disease *e.g.*, cirrhosis, cholestasis, *etc*[40]. When FLR deems insufficient, TSH with PVE or PVL is an established strategy, which induces 10%-30% FLR hypertrophy over 4-6 wk[42]. However, inadequate hypertrophy and disease progression prevent 10%-40% patients from proceeding stage II hepatectomy[4-6,11,43,44].

ALPPS offers accelerated and pronounced hypertrophy. A 40%-80% hypertrophy is consistently observed over 7-10 d[4-6,11,43,44]. Conceptually, ALPPS would be most beneficial when FLR is extremely marginal or risk of inter-stage disease progression is high, *i.e.* aggressive and extensive tumor, for PVE/PVL would unlikely be effective. When ALPPS was compared head-to-head against PVE/PVL in the prospective LIGRO trial, the inclusion FLR/ESLV was defined as less than 30%[13]. A lower FLR/ESLV was generally accepted for ALPPS. Ratti *et al*[45] suggested performing ALPPS for patients with FLR less than 20% who were not expected to achieve sufficient remnant volume with conventional TSH. Consensus has not been reached on the ideal indicating FLR for ALPPS. Perhaps it would be rational to accept higher procedural risks when sufficient remnant growth is unlikely with conventional TSH. Reviewing current experience through the international registry, the median pre-stage I FLR was 21% (interquartile range: 17%-27%) of ESLV[3]. FLR hypertrophied by 80% over a 7-d interval producing an FLR to ESLV ratio of 40% (interquartile range: 31%-47%)[3]. ALPPS for extremely marginal ALPPS should be reserved for good risk patients in experienced centers, while increased operative morbidity and mortality should be expected. Patients with less marginal remnant volume can be considered for TSH.

Disease factor - CRLM: CRLM is the leading indication for ALPPS. To date, more

than 400 ALPPS have been performed for CRLM worldwide, including 220 right trisectionectomies and over 180 right hepatectomies[46]. Normal liver function and favorable tumor biology confers advantageous operative and oncological outcomes. Data from the registry concluded CRLM as an independent predictor of fewer severe complications (OR = 0.37, P = 0.049)[3]. Major morbidity (Clavien-Dindo 3a or above) occurred in 36% of CRLM patients, and the figure was further reduced to 29% when only patients younger than 60 years of age were selected[3].

ALPPS was initially performed for unresectable CRLM primarily due to inadequate FLR[23]. Patients with tumors in the FLR were not included. Subsequently patients with tumors in the FLR were also operated on with a cleaning procedure of the FLR performed in stage I adopting from conventional TSH[14]. Apart from portal vein ligation and parenchymal partition, any tumor involvement of the FLR was resected. Provided tumor clearance of the FLR is feasible, bilobar CRLM was not considered a contraindication[47-49]. ALPPS has been reported for patients with extrahepatic diseases in small numbers[50,51]. The long term oncological outcomes require further validation. There is better acceptance for extrahepatic metastasis amendable to future surgical treatment[45]. After all, it complied with the principle of surgical oncology, *i.e*. to achieve R0 resection.

From registry data ALPPS achieved a 1- and 2-year OS of 76% and 62%, respectively for patients with CRLM. The corresponding 1- and 2-year DFS were 59% and 41%, respectively[3]. The tumor status and the proportion of patients receiving preoperative chemotherapy were not specified. Given the systemic disease nature, the importance of chemotherapy response could not be overemphasized. Chemotherapy response could be objectively defined with radiological and biochemical assessment[3]. Patients with favorable response to chemotherapy are more likely to secure disease control after local treatment. We learned from conventional TSH and standard liver resection that selection by chemotherapy response resulted in improved oncological outcomes[22,52]. Indeed, the pioneering surgeon of ALPPS suggested that ALPPS was not indicated for CRLM patients without prior chemotherapy[46].

The major concerns for chemotherapy as well as targeted therapy were the potential drawbacks of reduced remnant growth and increased operative complications. Kremer *et al*[53] retrospectively compared eleven ALPPS patients who received preoperative chemotherapy with eight controls. It was observed that chemotherapy impaired remnant hypertrophy (FLR hypertrophy 59+/-22% *vs* 98+/-35%, P = 0.027). There seemed to be no impact on operative morbidity and mortality. A safe time interval between chemotherapy and surgery has not been proposed. Experience from conventional hepatectomy showed that an interval shorter than 4 wk was associated with more surgical complications (11% *vs* 5.5/2.6% for 5-8/9-12 wk, P = 0.009)[54]. It is reasonable to wait for more than 4 wk for a more demanding ALPPS. While neoadjuvant chemotherapy selects patients with favorable tumor biology, the surgeon must be aware of its potential effects on ALPPS.

Disease factor - hilar cholangiocarcinoma: Hilar cholangiocarcinoma necessitates extensive parenchymal and biliary resection for tumor clearance. Not uncommonly, resection is hindered by inadequate FLR. Limited numbers of ALPPS has been performed for Klatskin tumor with much debate elicited for its safety. Patients with Klatskin tumor suffered from cholestasis and recurrent biliary sepsis both contributing to impaired hepatic regeneration[55] and increased septic complications[35]. Furthermore, tumor infiltration renders hilar dissection challenging. In fact, technical complexity in ALPPS has been closely associated with morbidity and mortality[56]. From registry data we learned that prolonged stage I operating time (more than 300 min) (OR = 4.42, P = 0.004) and blood transfusion (OR = 5.26, P = 0.001) were independent risk factors for severe complications[3]. When ALPPS was performed for Klatskin tumor, 90-d mortality was reported as an exceedingly high 48%[37]. In the study by Li *et al*[35], bile leak and PHLF occurred more frequently in patients operated for hilar cholangiocarcinoma.

Oncological outcomes were also far from satisfactory. In a case-control study conducted by Olthof *et al*[37], the median OS of cholangiocarcinoma patients undergoing ALPPS was 6 mo comparing unfavorably to matched controls with similar remnant volume and tumor status undergoing conventional hepatectomy (6 mo *vs* 27 mo, P = 0.06). After all, the operative techniques of ALPPS conflicts with the oncological principles of bile duct cancer surgery. In the early periods hilar dissection was performed with complete lymphadenectomy of the hepatoduodenal ligament to allow clear identification of portal structures[2,57,58]. However, extensive portal dissection has been criticized for inducing segment IV ischemia and subsequent bile leaks[36]. Shifting away from extensive hepatoduodenal ligament dissection, lymphatic clearance could have been jeopardized. Nonetheless, there is no data in the literature to evaluate the adequacy of lymphatic clearance in ALPPS for bile duct cancers, and

further studies are warranted.

Disease factor - HCC: Vennarecci *et al*[59] reported the feasibility of ALPPS in chronic liver disease with their early experience in three HCC patients. Considering cirrhotic livers have diminished regenerative capacity, the safety profile may be different in this context. Two studies looked into the degree of hypertrophy, kinetic growth and operative outcomes among HCC patients in the international registry and from a Singaporean tertiary center, respectively[7,38] (Table 3). When compared to patients with normal liver, HCC patients consistently underwent less rapid (5%-19% FLR per day *vs* 9%-35% FLR per day) and less extensive hypertrophy (40%-47% *vs* 76%-138% increase in FLR). From 13 patients whose pathological details were available, both degree of hypertrophy (105%, 48%, 26% and 15% for grade 1, 2, 3 fibrosis and cirrhosis, $P = 0.013$) and kinetic growth (12, 4.7, 3.0 and 1.5 mL/d for grade 1, 2, 3 fibrosis and cirrhosis, $P = 0.033$) correlated directly with the degree of fibrosis[38]. Albeit comparing inferiorly to normal liver, ALPPS still induce substantial hypertrophy in fibrotic liver, especially when the degree of fibrosis is limited. In a recent series of 35 ALPPS performed in our center, the hypertrophy rate compared favorably to patients treated with PVE (5.1 mL/d *vs* 0.9 mL/d, $P < 0.001$)[60]. A median volume gain of 45.1% was achieved over a median interval of 6 d.

Pooled data from 35 patients in the international registry revealed a discouraging 31% mortality for patients with chronic liver disease[38]. However, more promising results have been produced in our center[60]. Thirty-five HCC patients started with a median FLR/ESLV ratio of 27%. All patients proceeded to stage II. Operative mortality was kept to 9% comparable to CRLM patients in the international registry[3]. These results indicated that chronic liver disease is not an absolute contraindication for ALPPS. Patients with low grade fibrosis are better candidates for the procedure, and a longer inter-stage interval is desirable to allow sufficient liver hypertrophy[61,62]. Vivarelli *et al*[63] suggested preoperative liver biopsy to determine the degree of liver fibrosis after observing a PHLF in a patient with fibrotic liver undergoing ALPPS. From our experience ALPPS candidates could be effectively selected by reviewing the surrogate markers reflecting the degree of liver fibrosis and portal hypertension, *i.e.* platelet count and indocyanine green clearance. Indocyanine green retention test correlated with the degree of portal hypertension[64,65] and mortality in major hepatectomy[66]. The role of indocyanine green clearance warrants further investigation to better understand its relationship with growth parameters and operative outcomes.

Not uncommonly, HCC is associated with portal venous invasion. When a tumor has invaded the right portal vein, PVE is neither technically feasible nor effective. Even PVL has little chance of further increasing the FLR volume as no further portal blood flow is redistributed. Alternatively, ALPPS could be a strategy to induce hypertrophy in HCC with portal tumor thrombus. Successful cases have been reported indicating technical feasibility[67,68]. An additional benefit conferred by ALPPS is the shortened inter-stage period. With a tumor thrombus in situ, disease is likely to progress while awaiting conventional second stage hepatectomy.

Technical refinements

Preservation of middle hepatic vein: In the initial description of ALPPS, parenchymal partition was performed with division of the middle hepatic vein[2]. However, with significant morbidity observed following ischemic necrosis and bile leak, it was proposed that the middle hepatic vein could be preserved as the venous outflow of segment IV without jeopardizing parenchymal hypertrophy[69]. With a patent outflow, venous congestion and ischemia could be reduced. It has now become the preferred technique by most hepatobiliary surgeons. A questionnaire survey indicated that 70% surgeons routinely preserved the middle hepatic vein during ALPPS stage I[70].

Surgical management of hepatoduodenal ligament: A complete hilar dissection and ske-letonization of the hepatoduodenal ligament was performed in the classical approach to ALPPS. This allowed hilar vascular pedicles to be clearly identified but potentially contributed to complete devascularization of segment IV[36]. In the aforementioned questionnaire survey, 39% of the surgeons believed that skeletonization of the hepatoduodenal ligament was indicated[70]. Currently there is no consensus on the surgical approach to hepatoduodenal ligament. In ALPPS where lymphatic clearance is not indicated for oncological grounds, consideration can be given to limit hilar dissection to avoid potential detrimental effects on segment IV ischemia.

Anterior approach: The anterior approach to hepatectomy was initially proposed for bulky liver tumor with invasion of surrounding structures[71]. It entails portal pedicle division and complete parenchymal transection before right liver mobilization,

Table 3 Associating liver partition with portal vein ligation for staged hepatectomy for hepatocellular carcinoma, *n* (%)

	n	Tumor	FLR in mL		Hypertrophy		Kinetic growth in %/d	Severe Cx, ≥ IIIB	PHLF, 50-50	90-d mortality
			Stage I	Stage II	Absolute in mL	Relative in %				
Case control										
D'Haese *et al*[38], 2016	35/225	HCC/CRLM	420 (346-540)/340 (260-433)	639 (541-855)/617 (487-724)	206 (172-277)/252 (186-348)	47 (26-69)/76 (50-108)	4.7 (2.8-8.9)/9.1 (5.8-14.3)	14 (27)/54 (17)	14 (40)/42 (19)	11 (31)/15 (7)
Chia *et al*[43], 2018	9/4	HCC/non-HCC	381 (280-422)/313 (177-550)	-	154 (86-166)/251 (248-344)	40 (22-65)/138 (92-139)	19 (6-24)/35 (31-39)	1 (14)/0	2 (29)/1 (25)	1 (11)/0

CRLM: Colorectal liver metastasis; Cx: Complication; FLR: Future liver remnant; HCC: Hepatocellular carcinoma; PHLF: Post-hepatectomy liver failure.

minimizing bleeding and tumor spillage during the process. The concept of anterior approach has been adopted to ALPPS[72,73]. During stage I, hepatic parenchyma is split without prior right liver mobilization. In stage II, right liver is mobilized after division of right hepatic artery, bile duct and hepatic veins. In the setting of ALPPS, anterior approach could be more challenging given that the arterial and biliary pedicles had to be preserved during transection. Chan *et al*[73] prospective series of 13 patients indicated that complete parenchymal split was feasible and safe with anterior approach. Occurrence of perihepatic adhesions was minimized during stage II. Thirty-seven percent of the ALPPS procedures in the registry were performed using the anterior approach[74]. With reduced tissue manipulation tumor spillage was minimal. This was particularly important in the setting of ALPPS, where the tumor is left in torso during the inter-stage period. Further evaluation is required before any oncological benefit of anterior approach ALPPS could be ascertained. With the potential benefits the anterior approach appears to be the preferred procedure, especially when a bulky tumor is handled. Nevertheless, it would be rather challenging to combine a complex procedure with an advanced technical approach. Without reduced vascular control more difficult bleeding would be encountered during parenchymal transection. Anterior approach ALPPS is best reserved for hepatobiliary surgeons who excel in both ALPPS and anterior approach for conventional hepatectomy.

Partial ALPPS: Schlegel *et al*[75] concluded from canine model that accelerated regeneration in ALPPS was not solely related to redistribution of blood flow but also the presence of circulating factors secondary to tissue injury. Plasma levels of IL-6 were elevated after ALPPS, and injection of post-ALPPS plasma into mice treated with PVL produced comparable remnant hypertrophy. On this basis Petrowsky *et al*[76] proposed a technical modification of ALPPS with partial parenchymal partition, *i.e.* 50%-80% in an attempt to preserve collateral blood supply and reduce operative morbidity. The middle hepatic vein was preserved in stage I. Termed as partial ALPPS, the modified procedure was associated with zero mortality and a more favorable complication profile in the initial series of six patients[76]. Partial ALPPS effectively induced the same degree of FLR hypertrophy as a complete split (median hypertrophy 60% *vs* 61% in 7 d). The operative boundary for partial partition was subsequently defined as dissection to the level of middle hepatic vein as opposed to the inferior vena cava in complete ALPPS[77].

However, the effectiveness of partial split appeared to be limited in chronic hepatitis. Chan *et al*[78] compared partial and complete ALPPS in 25 patients with HCC. Partial split failed to induce a similar degree of hypertrophy as in complete split (17.5 mL/d *vs* 31.2 mL/d, $P = 0.022$). Perioperative morbidity and mortality were not decreased. After all, current evidence is based on limited experience and partial ALPPS could be further validated in larger cohorts. Perhaps partial ALPPS is most effective when liver function is normal, and a complete split is technically difficult. When a sizable tumor is situated close to the middle hepatic vein or inferior vena cava, parenchymal transection to the vena cava could be impeded by troublesome bleeding from engorged hepatic veins[78]. Partial ALPPS potentially reduced bleeding and subsequent complications. The difficult transection is probably better tolerated in stage II when the remnant has undergone hypertrophy and the procedure is expedited after full mobilization of the right liver and division of the arterial and biliary pedicles. Slower hypertrophy and delayed stage II operation are the potential drawbacks.

CONCLUSION

ALPPS challenged the concept of unresectability and stretched the limit of liver surgery. When performed for CRLM, ALPPS was associated with similar mortalities and morbidities as with TSH. Mortality is usually a result of PHLF, and it can be minimized with careful patient selection. The benefit of ALPPS is maximized when performed for young patients with very borderline remnant volume. Various technical modifications have been proposed to improve the surgical outcomes of ALPPS. Preservation of the middle hepatic vein during stage I minimized morbidities and did not affect remnant growth. In patients with challenging anatomy, partial ALPPS potentially reduces morbidity but remnant hypertrophy may compare unfavorably to a complete split. Whether the theoretical advantages of ALPPS translate to actuarial survival benefits warrants further studies.

REFERENCES

1 **Clavien PA**, Petrowsky H, DeOliveira ML, Graf R. Strategies for safer liver surgery and partial liver transplantation. *N Engl J Med* 2007; **356**: 1545-1559 [PMID: 17429086 DOI: 10.1056/NEJMra065156]

2 **Narita M**, Oussoultzoglou E, Ikai I, Bachellier P, Jaeck D. Right portal vein ligation combined with in situ splitting induces rapid left lateral liver lobe hypertrophy enabling 2-staged extended right hepatic resection in small-for-size settings. *Ann Surg* 2012; **256**: e7-8; author reply e16-17 [PMID: 22868374 DOI: 10.1097/SLA.0b013e318265fd51]

3 **Schadde E**, Ardiles V, Robles-Campos R, Malago M, Machado M, Hernandez-Alejandro R, Soubrane O, Schnitzbauer AA, Raptis D, Tschuor C, Petrowsky H, De Santibanes E, Clavien PA; ALPPS Registry Group. Early survival and safety of ALPPS: first report of the International ALPPS Registry. *Ann Surg* 2014; **260**: 829-36; discussion 836-8 [PMID: 25379854 DOI: 10.1097/SLA.0000000000000947]

4 **Shindoh J**, Vauthey JN, Zimmitti G, Curley SA, Huang SY, Mahvash A, Gupta S, Wallace MJ, Aloia TA. Analysis of the efficacy of portal vein embolization for patients with extensive liver malignancy and very low future liver remnant volume, including a comparison with the associating liver partition with portal vein ligation for staged hepatectomy approach. *J Am Coll Surg* 2013; **217**: 126-133; discussion 133-134 [PMID: 23632095 DOI: 10.1016/j.jamcollsurg.2013.03.004]

5 **Croome KP**, Hernandez-Alejandro R, Parker M, Heimbach J, Rosen C, Nagorney DM. Is the liver kinetic growth rate in ALPPS unprecedented when compared with PVE and living donor liver transplant? A multicentre analysis. *HPB (Oxford)* 2015; **17**: 477-484 [PMID: 25728543 DOI: 10.1111/hpb.12386]

6 **Ratti F**, Schadde E, Masetti M, Massani M, Zanello M, Serenari M, Cipriani F, Bonariol L, Bassi N, Aldrighetti L, Jovine E. Strategies to Increase the Resectability of Patients with Colorectal Liver Metastases: A Multi-center Case-Match Analysis of ALPPS and Conventional Two-Stage Hepatectomy. *Ann Surg Oncol* 2015; **22**: 1933-1942 [PMID: 25564160 DOI: 10.1245/s10434-014-4291-4]

7 **Chia DKA**, Yeo Z, Loh SEK, Iyer SG, Madhavan K, Kow AWC. ALPPS for Hepatocellular Carcinoma Is Associated with Decreased Liver Remnant Growth. *J Gastrointest Surg* 2018; **22**: 973-980 [PMID: 29380118 DOI: 10.1007/s11605-018-3697-x]

8 **Tanaka K**, Matsuo K, Murakami T, Kawaguchi D, Hiroshima Y, Koda K, Endo I, Ichikawa Y, Taguri M, Tanabe M. Associating liver partition and portal vein ligation for staged hepatectomy (ALPPS): short-term outcome, functional changes in the future liver remnant, and tumor growth activity. *Eur J Surg Oncol* 2015; **41**: 506-512 [PMID: 25704556 DOI: 10.1016/j.ejso.2015.01.031]

9 **Adam R**, Imai K, Castro Benitez C, Allard MA, Vibert E, Sa Cunha A, Cherqui D, Baba H, Castaing D. Outcome after associating liver partition and portal vein ligation for staged hepatectomy and conventional two-stage hepatectomy for colorectal liver metastases. *Br J Surg* 2016; **103**: 1521-1529 [PMID: 27517369 DOI: 10.1002/bjs.10256]

10 **Schadde E**, Ardiles V, Slankamenac K, Tschuor C, Sergeant G, Amacker N, Baumgart J, Croome K, Hernandez-Alejandro R, Lang H, de Santibañes E, Clavien PA. ALPPS offers a better chance of complete resection in patients with primarily unresectable liver tumors compared with conventional-staged hepatectomies: results of a multicenter analysis. *World J Surg* 2014; **38**: 1510-1519 [PMID: 24748319 DOI: 10.1007/s00268-014-2513-3]

11 **Matsuo K**, Murakami T, Kawaguchi D, Hiroshima Y, Koda K, Yamazaki K, Ishida Y, Tanaka K. Histologic features after surgery associating liver partition and portal vein ligation for staged hepatectomy versus those after hepatectomy with portal vein embolization. *Surgery* 2016; **159**: 1289-1298 [PMID: 26775576 DOI: 10.1016/j.surg.2015.12.004]

12 **Zhou Z**, Xu M, Lin N, Pan C, Zhou B, Zhong Y, Xu R. Associating liver partition and portal vein ligation for staged hepatectomy versus conventional two-stage hepatectomy: a systematic review and meta-analysis. *World J Surg Oncol* 2017; **15**: 227 [PMID: 29258518 DOI: 10.1186/s12957-017-1295-0]

13 **Sandström P**, Røsok BI, Sparrelid E, Larsen PN, Larsson AL, Lindell G, Schultz NA, Bjørnbeth BA, Isaksson B, Rizell M, Björnsson B. ALPPS Improves Resectability Compared With Conventional Two-stage Hepatectomy in Patients With Advanced Colorectal Liver Metastasis: Results From a Scandinavian Multicenter Randomized Controlled Trial (LIGRO Trial). *Ann Surg* 2018; **267**: 833-840 [PMID: 28902669 DOI: 10.1097/SLA.0000000000002511]

14 **Fernando A**, Alvarez VA, Eduardo de Santibañes. The ALPPS Approach for the Management of Colorectal Carcinoma Liver Metastases. Current Colorectal Cancer Reports. 2013; 168-77

15 **Aloia TA**, Vauthey JN. Associating liver partition and portal vein ligation for staged hepatectomy (ALPPS): what is gained and what is lost? *Ann Surg* 2012; **256**: e9; author reply e16-e19; author reply e19 [PMID: 22868369 DOI: 10.1097/SLA.0b013e318265fd3e]

16 **de Graaf W**, van den Esschert JW, van Lienden KP, van Gulik TM. Induction of tumor growth after preoperative portal vein embolization: is it a real problem? *Ann Surg Oncol* 2009; **16**: 423-430 [PMID: 19050974 DOI: 10.1245/s10434-008-0222-6]

17 **Kokudo N**, Tada K, Seki M, Ohta H, Azekura K, Ueno M, Ohta K, Yamaguchi T, Matsubara T, Takahashi T, Nakajima T, Muto T, Ikari T, Yanagisawa A, Kato Y. Proliferative activity of intrahepatic

colorectal metastases after preoperative hemihepatic portal vein embolization. *Hepatology* 2001; **34**: 267-272 [PMID: 11481611 DOI: 10.1053/jhep.2001.26513]
18 **Hoekstra LT**, van Lienden KP, Doets A, Busch OR, Gouma DJ, van Gulik TM. Tumor progression after preoperative portal vein embolization. *Ann Surg* 2012; **256**: 812-817; discussion 817-818 [PMID: 23095626 DOI: 10.1097/SLA.0b013e3182733f09]
19 **Pamecha V**, Levene A, Grillo F, Woodward N, Dhillon A, Davidson BR. Effect of portal vein embolisation on the growth rate of colorectal liver metastases. *Br J Cancer* 2009; **100**: 617-622 [PMID: 19209170 DOI: 10.1038/sj.bjc.6604872]
20 **Joechle K**, Moser C, Ruemmele P, Schmidt KM, Werner JM, Geissler EK, Schlitt HJ, Lang SA. ALPPS (associating liver partition and portal vein ligation for staged hepatectomy) does not affect proliferation, apoptosis, or angiogenesis as compared to standard liver resection for colorectal liver metastases. *World J Surg Oncol* 2017; **15**: 57 [PMID: 28270160 DOI: 10.1186/s12957-017-1121-8]
21 **Oldhafer KJ**, Donati M, Jenner RM, Stang A, Stavrou GA. ALPPS for patients with colorectal liver metastases: effective liver hypertrophy, but early tumor recurrence. *World J Surg* 2014; **38**: 1504-1509 [PMID: 24326456 DOI: 10.1007/s00268-013-2401-2]
22 **Brouquet A**, Abdalla EK, Kopetz S, Garrett CR, Overman MJ, Eng C, Andreou A, Loyer EM, Madoff DC, Curley SA, Vauthey JN. High survival rate after two-stage resection of advanced colorectal liver metastases: response-based selection and complete resection define outcome. *J Clin Oncol* 2011; **29**: 1083-1090 [PMID: 21263087 DOI: 10.1200/JCO.2010.32.6132]
23 **Balzan S**, Belghiti J, Farges O, Ogata S, Sauvanet A, Delefosse D, Durand F. The "50-50 criteria" on postoperative day 5: an accurate predictor of liver failure and death after hepatectomy. *Ann Surg* 2005; **242**: 824-828, discussion 828-discussion 829 [PMID: 16327492 DOI: 10.1097/01.sla.0000189131.90876.9e]
24 **Aloia TA**. Insights into ALPPS. *Eur J Surg Oncol* 2015; **41**: 610-611 [PMID: 25716333 DOI: 10.1016/j.ejso.2015.02.001]
25 **Cieslak KP**, Olthof PB, van Lienden KP, Besselink MG, Busch OR, van Gulik TM, Bennink RJ. Assessment of Liver Function Using (99m)Tc-Mebrofenin Hepatobiliary Scintigraphy in ALPPS (Associating Liver Partition and Portal Vein Ligation for Staged Hepatectomy). *Case Rep Gastroenterol* 2015; **9**: 353-360 [PMID: 26675783 DOI: 10.1159/000441385]
26 **Truant S**, Baillet C, Deshorgue AC, Leteurtre E, Hebbar M, Ernst O, Huglo D, Pruvot FR. Drop of Total Liver Function in the Interstages of the New Associating Liver Partition and Portal Vein Ligation for Staged Hepatectomy Technique: Analysis of the "Auxiliary Liver" by HIDA Scintigraphy. *Ann Surg* 2016; **263**: e33-e34 [PMID: 26756764 DOI: 10.1097/SLA.0000000000001603]
27 **Sparrelid E**, Jonas E, Tzortzakakis A, Dahlén U, Murquist G, Brismar T, Axelsson R, Isaksson B. Dynamic Evaluation of Liver Volume and Function in Associating Liver Partition and Portal Vein Ligation for Staged Hepatectomy. *J Gastrointest Surg* 2017; **21**: 967-974 [PMID: 28283924 DOI: 10.1007/s11605-017-3389-y]
28 **Rahbari NN**, Garden OJ, Padbury R, Brooke-Smith M, Crawford M, Adam R, Koch M, Makuuchi M, Dematteo RP, Christophi C, Banting S, Usatoff V, Nagino M, Maddern G, Hugh TJ, Vauthey JN, Greig P, Rees M, Yokoyama Y, Fan ST, Nimura Y, Figueras J, Capussotti L, Büchler MW, Weitz J. Posthepatectomy liver failure: a definition and grading by the International Study Group of Liver Surgery (ISGLS). *Surgery* 2011; **149**: 713-724 [PMID: 21236455 DOI: 10.1016/j.surg.2010.10.001]
29 **Linecker M**, Stavrou GA, Oldhafer KJ, Jenner RM, Seifert B, Lurje G, Bednarsch J, Neumann U, Capobianco I, Nadalin S, Robles-Campos R, de Santibañes E, Malagó M, Lesurtel M, Clavien PA, Petrowsky H. The ALPPS Risk Score: Avoiding Futile Use of ALPPS. *Ann Surg* 2016; **264**: 763-771 [PMID: 27455156 DOI: 10.1097/SLA.0000000000001914]
30 **Shindoh J**, Truty MJ, Aloia TA, Curley SA, Zimmitti G, Huang SY, Mahvash A, Gupta S, Wallace MJ, Vauthey JN. Kinetic growth rate after portal vein embolization predicts posthepatectomy outcomes: toward zero liver-related mortality in patients with colorectal liver metastases and small future liver remnant. *J Am Coll Surg* 2013; **216**: 201-209 [PMID: 23219349 DOI: 10.1016/j.jamcollsurg.2012.10.018]
31 **Leung U**, Simpson AL, Araujo RL, Gönen M, McAuliffe C, Miga MI, Parada EP, Allen PJ, D'Angelica MI, Kingham TP, DeMatteo RP, Fong Y, Jarnagin WR. Remnant growth rate after portal vein embolization is a good early predictor of post-hepatectomy liver failure. *J Am Coll Surg* 2014; **219**: 620-630 [PMID: 25158914 DOI: 10.1016/j.jamcollsurg.2014.04.022]
32 **Kambakamba P**, Stocker D, Reiner CS, Nguyen-Kim TD, Linecker M, Eshmuminov D, Petrowsky H, Clavien PA, Lesurtel M. Liver kinetic growth rate predicts postoperative liver failure after ALPPS. *HPB (Oxford)* 2016; **18**: 800-805 [PMID: 27524732 DOI: 10.1016/j.hpb.2016.07.005]
33 **Serenari M**, Collaud C, Alvarez FA, de Santibañes M, Giunta D, Pekolj J, Ardiles V, de Santibañes E. Interstage Assessment of Remnant Liver Function in ALPPS Using Hepatobiliary Scintigraphy: Prediction of Posthepatectomy Liver Failure and Introduction of the HIBA Index. *Ann Surg* 2018; **267**: 1141-1147 [PMID: 28121683 DOI: 10.1097/SLA.0000000000002150]
34 **Alghamdi T**, Viebahn C, Justinger C, Lorf T. Arterial Blood Supply of Liver Segment IV and Its Possible Surgical Consequences. *Am J Transplant* 2017; **17**: 1064-1070 [PMID: 27775870 DOI: 10.1111/ajt.14089]
35 **Li J**, Girotti P, Königsrainer I, Ladurner R, Königsrainer A, Nadalin S. ALPPS in right trisectionectomy: a safe procedure to avoid postoperative liver failure? *J Gastrointest Surg* 2013; **17**: 956-961 [PMID: 23288719 DOI: 10.1007/s11605-012-2132-y]
36 **Hernandez-Alejandro R**, Bertens KA, Pineda-Solis K, Croome KP. Can we improve the morbidity and mortality associated with the associating liver partition with portal vein ligation for staged hepatectomy (ALPPS) procedure in the management of colorectal liver metastases? *Surgery* 2015; **157**: 194-201 [PMID: 25282528 DOI: 10.1016/j.surg.2014.08.041]
37 **Olthof PB**, Coelen RJS, Wiggers JK, Groot Koerkamp B, Malago M, Hernandez-Alejandro R, Topp SA, Vivarelli M, Aldrighetti LA, Robles Campos R, Oldhafer KJ, Jarnagin WR, van Gulik TM. High mortality after ALPPS for perihilar cholangiocarcinoma: case-control analysis including the first series from the international ALPPS registry. *HPB (Oxford)* 2017; **19**: 381-387 [PMID: 28279621 DOI: 10.1016/j.hpb.2016.10.008]
38 **D'Haese JG**, Neumann J, Weniger M, Pratschke S, Björnsson B, Ardiles V, Chapman W, Hernandez-Alejandro R, Soubrane O, Robles-Campos R, Stojanovic M, Dalla Valle R, Chan AC, Coenen M, Guba M, Werner J, Schadde E, Angele MK. Should ALPPS be Used for Liver Resection in Intermediate-Stage HCC? *Ann Surg Oncol* 2016; **23**: 1335-1343 [PMID: 26646946 DOI: 10.1245/s10434-015-5007-0]
39 **Shoup M**, Gonen M, D'Angelica M, Jarnagin WR, DeMatteo RP, Schwartz LH, Tuorto S, Blumgart LH, Fong Y. Volumetric analysis predicts hepatic dysfunction in patients undergoing major liver resection. *J*

Gastrointest Surg 2003; **7**: 325-330 [PMID: 12654556]
40 **Ferrero A**, Viganò L, Polastri R, Muratore A, Eminefendic H, Regge D, Capussotti L. Postoperative liver dysfunction and future remnant liver: where is the limit? Results of a prospective study. *World J Surg* 2007; **31**: 1643-1651 [PMID: 17551779 DOI: 10.1007/s00268-007-9123-2]
41 **Guglielmi A**, Ruzzenente A, Conci S, Valdegamberi A, Iacono C. How much remnant is enough in liver resection? *Dig Surg* 2012; **29**: 6-17 [PMID: 22441614 DOI: 10.1159/000335713]
42 **Abulkhir A**, Limongelli P, Healey AJ, Damrah O, Tait P, Jackson J, Habib N, Jiao LR. Preoperative portal vein embolization for major liver resection: a meta-analysis. *Ann Surg* 2008; **247**: 49-57 [PMID: 18156923 DOI: 10.1097/SLA.0b013e31815f6e5b]
43 **Chia DKA**, Yeo Z, Loh SEK, Iyer SG, Bonney GK, Madhavan K, Kow AWC. Greater hypertrophy can be achieved with associating liver partition with portal vein ligation for staged hepatectomy compared to conventional staged hepatectomy, but with a higher price to pay? *Am J Surg* 2018; **215**: 131-137 [PMID: 28859921 DOI: 10.1016/j.amjsurg.2017.08.013]
44 **Røsok BI**, Björnsson B, Sparrelid E, Hasselgren K, Pomianowska E, Gasslander T, Bjørnbeth BA, Isaksson B, Sandström P. Scandinavian multicenter study on the safety and feasibility of the associating liver partition and portal vein ligation for staged hepatectomy procedure. *Surgery* 2016; **159**: 1279-1286 [PMID: 26606881 DOI: 10.1016/j.surg.2015.10.004]
45 **Ratti F**, Cipriani F, Gagliano A, Catena M, Paganelli M, Aldrighetti L. Defining indications to ALPPS procedure: technical aspects and open issues. *Updates Surg* 2014; **66**: 41-49 [PMID: 24343420 DOI: 10.1007/s13304-013-0243-y]
46 **Schnitzbauer AA**, Schadde E, Linecker M, Machado MA, Adam R, Malago M, Clavien PA, de Santibanes E, Bechstein WO. Indicating ALPPS for Colorectal Liver Metastases: A Critical Analysis of Patients in the International ALPPS Registry. *Surgery* 2018; **164**: 387-394 [PMID: 29803563 DOI: 10.1016/j.surg.2018.02.026]
47 **Alvarez FA**, Ardiles V, de Santibañes M, Pekolj J, de Santibañes E. Associating liver partition and portal vein ligation for staged hepatectomy offers high oncological feasibility with adequate patient safety: a prospective study at a single center. *Ann Surg* 2015; **261**: 723-732 [PMID: 25493362 DOI: 10.1097/SLA.0000000000001046]
48 **Torzilli G**, Adam R, Viganò L, Imai K, Goransky J, Fontana A, Toso C, Majno P, de Santibañes E. Surgery of Colorectal Liver Metastases: Pushing the Limits. *Liver Cancer* 2016; **6**: 80-89 [PMID: 27995092 DOI: 10.1159/000449495]
49 **Vondran FWR**, Oldhafer F, Ringe KI, Wirth TC, Kleine M, Jäger MD, Klempnauer J, Bektas H. Associating Liver Partition and Portal vein ligation for Staged hepatectomy after pre-operative chemotherapy. *ANZ J Surg* 2018; **88**: E324-E328 [PMID: 28419692 DOI: 10.1111/ans.13944]
50 **Watanabe H**, Okada M, Kaji Y, Satouchi M, Sato Y, Yamabe Y, Onaya H, Endo M, Sone M, Arai Y. [New response evaluation criteria in solid tumours-revised RECIST guideline (version 1.1)]. *Gan To Kagaku Ryoho* 2009; **36**: 2495-2501 [PMID: 20009446]
51 **Björnsson B**, Sparrelid E, Røsok B, Pomianowska E, Hasselgren K, Gasslander T, Bjørnbeth BA, Isaksson B, Sandström P. Associating liver partition and portal vein ligation for staged hepatectomy in patients with colorectal liver metastases--Intermediate oncological results. *Eur J Surg Oncol* 2016; **42**: 531-537 [PMID: 26830731 DOI: 10.1016/j.ejso.2015.12.013]
52 **Araujo RL**, Riechelmann RP, Fong Y. Patient selection for the surgical treatment of resectable colorectal liver metastases. *J Surg Oncol* 2017; **115**: 213-220 [PMID: 27778357 DOI: 10.1002/jso.24482]
53 **Kremer M**, Manzini G, Hristov B, Polychronidis G, Mokry T, Sommer CM, Mehrabi A, Weitz J, Büchler MW, Schemmer P. Impact of Neoadjuvant Chemotherapy on Hypertrophy of the Future Liver Remnant after Associating Liver Partition and Portal Vein Ligation for Staged Hepatectomy. *J Am Coll Surg* 2015; **221**: 717-728.e1 [PMID: 26232303 DOI: 10.1016/j.jamcollsurg.2015.05.017]
54 **Welsh FK**, Tilney HS, Tekkis PP, John TG, Rees M. Safe liver resection following chemotherapy for colorectal metastases is a matter of timing. *Br J Cancer* 2007; **96**: 1037-1042 [PMID: 17353923 DOI: 10.1038/sj.bjc.6603670]
55 **Yokoyama Y**, Nagino M, Nimura Y. Mechanism of impaired hepatic regeneration in cholestatic liver. *J Hepatobiliary Pancreat Surg* 2007; **14**: 159-166 [PMID: 17384907 DOI: 10.1007/s00534-006-1125-1]
56 **Truant S**, Scatton O, Dokmak S, Regimbeau JM, Lucidi V, Laurent A, Gauzolino R, Castro Benitez C, Pequignot A, Donckier V, Lim C, Blanleuil ML, Brustia R, Le Treut YP, Soubrane O, Azoulay D, Farges O, Adam R, Pruvot FR; e-HPBchir Study Group from the Association de Chirurgie Hépato-Biliaire et de Transplantation (ACHBT). Associating liver partition and portal vein ligation for staged hepatectomy (ALPPS): impact of the inter-stages course on morbi-mortality and implications for management. *Eur J Surg Oncol* 2015; **41**: 674-682 [PMID: 25630689 DOI: 10.1016/j.ejso.2015.01.004]
57 **Fernando A**, Alvarez JI, Lastiri J, Ulla M, Bonadeo Lassalle F. Nuevo Metodo de Regeneracion hepatica. *CIRUGI´A ESPAN˜ OLA* 2011; **89**: 645-649
58 **Sala S**, Ardiles V, Ulla M, Alvarez F, Pekolj J, de Santibañes E. Our initial experience with ALPPS technique: encouraging results. *Updates Surg* 2012; **64**: 167-172 [PMID: 22903531 DOI: 10.1007/s13304-012-0175-y]
59 **Vennarecci G**, Laurenzi A, Levi Sandri GB, Busi Rizzi E, Cristofaro M, Montalbano M, Piselli P, Andreoli A, D'Offizi G, Ettorre GM. The ALPPS procedure for hepatocellular carcinoma. *Eur J Surg Oncol* 2014; **40**: 982-988 [PMID: 24767805 DOI: 10.1016/j.ejso.2014.04.002]
60 **Chan A**, Chok KSH, Lo CM. Outcome of Associating Liver Partition and Portal Vein Ligation for Staged Hepatectomy (ALPPS) vs Portal Vein Embolisation (PVE) for Hepatocellular Carcinoma. *J Am Coll Surg* 2017; **25**: e32 [DOI: 10.1016/j.jamcollsurg.2017.07.604]
61 **Yamanaka N**, Okamoto E, Kawamura E, Kato T, Oriyama T, Fujimoto J, Furukawa K, Tanaka T, Tomoda F, Tanaka W. Dynamics of normal and injured human liver regeneration after hepatectomy as assessed on the basis of computed tomography and liver function. *Hepatology* 1993; **18**: 79-85 [PMID: 8392029]
62 **Nagasue N**, Yukaya H, Ogawa Y, Kohno H, Nakamura T. Human liver regeneration after major hepatic resection. A study of normal liver and livers with chronic hepatitis and cirrhosis. *Ann Surg* 1987; **206**: 30-39 [PMID: 3038039 DOI: 10.1097/00000658-198707000-00005]
63 **Vivarelli M**, Vincenzi P, Montalti R, Fava G, Tavio M, Coletta M, Vecchi A, Nicolini D, Agostini A, Ahmed EA, Giovagnoni A, Mocchegiani F. ALPPS Procedure for Extended Liver Resections: A Single Centre Experience and a Systematic Review. *PLoS One* 2015; **10**: e0144019 [PMID: 26700646 DOI: 10.1371/journal.pone.0144019]
64 **Lisotti A**, Azzaroli F, Buonfiglioli F, Montagnani M, Cecinato P, Turco L, Calvanese C, Simoni P,

Guardigli M, Arena R, Cucchetti A, Colecchia A, Festi D, Golfieri R, Mazzella G. Indocyanine green retention test as a noninvasive marker of portal hypertension and esophageal varices in compensated liver cirrhosis. *Hepatology* 2014; **59**: 643-650 [PMID: 24038116 DOI: 10.1002/hep.26700]

65 **Lisotti A**, Azzaroli F, Cucchetti A, Buonfiglioli F, Cecinato P, Calvanese C, Simoni P, Arena R, Montagnani M, Golfieri R, Colecchia A, Festi D, Mazzella G. Relationship between indocyanine green retention test, decompensation and survival in patients with Child-Pugh A cirrhosis and portal hypertension. *Liver Int* 2016; **36**: 1313-1321 [PMID: 26786880 DOI: 10.1111/liv.13070]

66 **Fan ST**, Lai EC, Lo CM, Ng IO, Wong J. Hospital mortality of major hepatectomy for hepatocellular carcinoma associated with cirrhosis. *Arch Surg* 1995; **130**: 198-203 [PMID: 7848092 DOI: 10.1001/archsurg.1995.01430020088017]

67 **Vennarecci G**, Laurenzi A, Santoro R, Colasanti M, Lepiane P, Ettorre GM. The ALPPS procedure: a surgical option for hepatocellular carcinoma with major vascular invasion. *World J Surg* 2014; **38**: 1498-1503 [PMID: 24146197 DOI: 10.1007/s00268-013-2296-y]

68 **Cavaness KM**, Doyle MB, Lin Y, Maynard E, Chapman WC. Using ALPPS to induce rapid liver hypertrophy in a patient with hepatic fibrosis and portal vein thrombosis. *J Gastrointest Surg* 2013; **17**: 207-212 [PMID: 22996934 DOI: 10.1007/s11605-012-2029-9]

69 **Donati M**, Basile F, Oldhafer KJ. Present status and future perspectives of ALPPS (associating liver partition and portal vein ligation for staged hepatectomy). *Future Oncol* 2015; **11**: 2255-2258 [PMID: 26260803 DOI: 10.2217/fon.15.145]

70 **Buac S**, Schadde E, Schnitzbauer AA, Vogt K, Hernandez-Alejandro R. The many faces of ALPPS: surgical indications and techniques among surgeons collaborating in the international registry. *HPB (Oxford)* 2016; **18**: 442-448 [PMID: 27154808 DOI: 10.1016/j.hpb.2016.01.547]

71 **Lai EC**, Fan ST, Lo CM, Chu KM, Liu CL. Anterior approach for difficult major right hepatectomy. *World J Surg* 1996; **20**: 314-7; discussion 318 [PMID: 8661837]

72 **Chan AC**, Pang R, Poon RT. Simplifying the ALPPS procedure by the anterior approach. *Ann Surg* 2014; **260**: e3 [PMID: 24866543 DOI: 10.1097/SLA.0000000000000736]

73 **Chan AC**, Poon RT, Lo CM. Modified Anterior Approach for the ALPPS Procedure: How We Do It. *World J Surg* 2015; **39**: 2831-2835 [PMID: 26239774 DOI: 10.1007/s00268-015-3174-6]

74 **Ardiles V**, Schadde E, Santibanes E, Clavien PA. Commentary on "Happy marriage or "dangerous liaison": ALPPS and the anterior approach". *Ann Surg* 2014; **260**: e4 [PMID: 25350653 DOI: 10.1097/SLA.0000000000000735]

75 **Schlegel A**, Lesurtel M, Melloul E, Limani P, Tschuor C, Graf R, Humar B, Clavien PA. ALPPS: from human to mice highlighting accelerated and novel mechanisms of liver regeneration. *Ann Surg* 2014; **260**: 839-46; discussion 846-7 [PMID: 25379855 DOI: 10.1097/SLA.0000000000000949]

76 **Petrowsky H**, Györi G, de Oliveira M, Lesurtel M, Clavien PA. Is partial-ALPPS safer than ALPPS? A single-center experience. *Ann Surg* 2015; **261**: e90-e92 [PMID: 25706390 DOI: 10.1097/SLA.0000000000001087]

77 **Cai YL**, Song PP, Tang W, Cheng NS. An updated systematic review of the evolution of ALPPS and evaluation of its advantages and disadvantages in accordance with current evidence. *Medicine (Baltimore)* 2016; **95**: e3941 [PMID: 27311006 DOI: 10.1097/MD.0000000000003941]

78 **Chan ACY**, Chok K, Dai JWC, Lo CM. Impact of split completeness on future liver remnant hypertrophy in associating liver partition and portal vein ligation for staged hepatectomy (ALPPS) in hepatocellular carcinoma: Complete-ALPPS versus partial-ALPPS. *Surgery* 2017; **161**: 357-364 [PMID: 27596751 DOI: 10.1016/j.surg.2016.07.029]

World Journal of Gastroenterology

Submit a Manuscript: https://www.f6publishing.com

World J Gastroenterol 2019 November 21; 25(43): 6386-6403

DOI: 10.3748/wjg.v25.i43.6386

ISSN 1007-9327 (print) ISSN 2219-2840 (online)

ORIGINAL ARTICLE

Basic Study

Ubiquitin-conjugating enzyme E2T knockdown suppresses hepatocellular tumorigenesis *via* inducing cell cycle arrest and apoptosis

Jian Guo, Mu Wang, Jun-Ping Wang, Chang-Xin Wu

ORCID number: Jian Guo (0000-0002-9028-9308); Mu Wang (0000-0002-5526-8149); Jun-Ping Wang (0000-0002-7517-9936); Chang-Xin Wu (0000-0002-7416-1662).

Author contributions: Wu CX designed the research; Guo J performed the majority of experiments and wrote the paper; Wang JP and Wang M coordinated the research.

Institutional review board statement: This study was approved by the ethics committee of The Affiliated People's Hospital of Shanxi Medical University.

Institutional animal care and use committee statement: All procedures involving animals were reviewed and approved by the Institutional Animal Care and Use Committee of The Affiliated People's Hospital of Shanxi Medical University (IACUC protocol number: 20171236).

Conflict-of-interest statement: No potential conflicts of interest are disclosed.

Data sharing statement: Data are available from the first author at guo10121012@163.com

ARRIVE guidelines statement: The authors have read the ARRIVE guidelines, and the manuscript was prepared and revised according to the ARRIVE guidelines.

Jian Guo, Institute of Biotechnology, Key Laboratory of Chemical Biology and Molecular Engineering of Ministry of Education, Institute of Biotechnology, Shanxi University, Taiyuan 030006, Shanxi Province, China

Jian Guo, Department of General Surgery, Shanxi Provincial People's Hospital, the Affiliated People's Hospital of Shanxi Medical University, Taiyuan 030012, Shanxi Province, China

Mu Wang, Department of Neurology, Shanxi Provincial People's Hospital, the Affiliated People's Hospital of Shanxi Medical University, Taiyuan 030012, Shanxi Province, China

Jun-Ping Wang, Department of Gastroenterology, Shanxi Provincial People's Hospital, the Affiliated People's Hospital of Shanxi Medical University, Taiyuan 030001, Shanxi Province, China

Chang-Xin Wu, The Institutes of Biomedical Sciences, Shanxi University, Taiyuan 03006, Shanxi Province, China

Chang-Xin Wu, Key Laboratory of Molecular Biology and Biochemistry of Ministry of Education, Shanxi University, Taiyuan 030006, Shanxi Province, China

Corresponding author: Chang-Xin Wu, PhD, Professor, The Institutes of Biomedical Sciences, Shanxi University, Taiyuan 030006, Shanxi Province, China. cxw20@sxu.edu.cn
Telephone: +86-351-4960141
Fax: +86-351-4960123

Abstract

BACKGROUND

Hepatocellular carcinoma (HCC) is now the most common primary liver malignancy worldwide, and multiple risk factors attribute to the occurrence and development of HCC. Recently, increasing studies suggest that ubiquitin-conjugating enzyme E2T (UBE2T) serves as a promising prognostic factor in human cancers, although the molecular mechanism of UBE2T in HCC remains unclear.

AIM

To investigate the clinical relevance and role of UBE2T in HCC development.

METHODS

UBE2T expression in HCC tissues from the TCGA database and its association with patient survival were analyzed. A lentivirus-mediated strategy was used to

Manuscript source: Unsolicited manuscript

Received: January 16, 2019
Peer-review started: January 16, 2019
First decision: February 13, 2019
Revised: September 10, 2019
Accepted: September 13, 2019
Article in press: September 13, 2019
Published online: November 21, 2019

P-Reviewer: Gougelet A, Lim SJ
S-Editor: Yan JP
L-Editor: Wang TQ
E-Editor: Ma YJ

knock down UBE2T in HCC cells. qRT-PCR and Western blot assays were performed to check the effect of UBE2T silencing in HCC cells. Cell growth *in vitro* and *in vivo* was analyzed by multiparametric high-content screening and the xenograft tumorigenicity assay, respectively. Cell cycle distribution and apoptosis were determined by flow cytometry. The genes regulated by UBE2T were profiled by microarray assay.

RESULTS
UBE2T was overexpressed in HCC tissues compared with paired and non-paired normal tissues. High expression of UBE2T predicted a poor overall survival in HCC patients. *In vitro*, lentivirus-mediated UBE2T knockdown significantly reduced the viability of both SMMC-7721 and BEL-7404 cells. *In vivo*, the xenograft tumorigenesis of SMMC-7721 cells was largely attenuated by UBE2T silencing. The cell cycle was arrested at G1/S phase in SMMC-7721 and BEL-7404 cells with UBE2T knockdown. Furthermore, apoptosis was increased by UBE2T knockdown. At the molecular level, numerous genes were dysregulated after UBE2T silencing, including IL-1B, FOSL1, PTGS2, and BMP6.

CONCLUSION
UBE2T plays an important role in cell cycle progression, apoptosis, and HCC development.

Key words: Hepatocellular carcinoma; Ubiquitin-conjugating enzyme E2T; Cell cycle; Apoptosis; Tumorigenesis

Core tip: Ubiquitin-conjugating enzyme E2T (UBE2T) is a member of the ubiquitin-proteasome family. Although it has been reported that UBE2T promotes the growth of hepatocellular carcinoma (HCC) cells, the role of UBE2T in the HCC cell cycle, apoptosis, and tumorigenesis is unclear. UBE2T was highly expressed in HCC tissues, and its expression was correlated with the survival of HCC patients. Silencing of UBE2T reduced the viability and xenograft tumor growth of HCC cells. Additionally, cell cycle arrest and apoptosis were induced by UBE2T knockdown. Numerous genes were regulated by UBE2T silencing in HCC cells. Therefore, UBE2T is a novel diagnostic and therapeutic target for HCC.

Citation: Guo J, Wang M, Wang JP, Wu CX. Ubiquitin-conjugating enzyme E2T knockdown suppresses hepatocellular tumorigenesis *via* inducing cell cycle arrest and apoptosis. *World J Gastroenterol* 2019; 25(43): 6386-6403
URL: https://www.wjgnet.com/1007-9327/full/v25/i43/6386.htm
DOI: https://dx.doi.org/10.3748/wjg.v25.i43.6386

INTRODUCTION

Hepatocellular carcinoma (HCC), which accounts for more than 90% of primary liver cancers, is the fifth most common malignancy and the third leading cause of cancer-related deaths worldwide[1]. Virus infections [including hepatitis B virus and hepatitis C virus (HCV)], obesity, inflammation, fibrosis, and cirrhosis are the major risk factors for HCC[2]. Genetic studies have identified that TP53, β-catenin, and TERT are the most frequently mutated genes in HCC[3-5]. However, effective drugs are lacking for this disease. Therefore, novel factors triggering HCC remain to be identified that may benefit the diagnosis and treatment of HCC patients.

Ubiquitin-conjugating enzyme E2T (UBE2T), also known as HSPC150, belongs to the E2 family of the ubiquitin-proteasome pathway. UBE2T activates FANCD2 mono-ubiquitination, and it was first identified in a patient with Fanconi anemia[6,7]. Recently, increasing evidence has reported that UBE2T is involved in cancer development. UBE2T is highly expressed in prostate cancer tissues and correlates with the metastatic stage and survival of patients. UBE2T promotes the proliferation, migration, and tumor development of prostate cancer cells[8]. Moreover, the upregulation of UBE2T is also found in other cancer types, such as breast and lung

cancers[9]. *In vitro*, UBE2T accelerates the growth of HCC cells *via* destabilizing P53 protein abundance[10]. However, the role of UBE2T in HCC carcinogenesis requires more in-depth investigation.

In this study, we found that UBE2T was overexpressed in HCC specimens. We hypothesized that UBE2T functions as an oncogene in HCC. To this aim, we used a lentivirus to knock down UBE2T in two HCC cell lines and analyzed the cell proliferation and xenograft tumorigenesis. Furthermore, cell cycle distribution, apoptosis, and gene expression were analyzed to investigate the potential mechanisms. We found that UBE2T knockdown inhibited the viability and tumor development of HCC cells. Cell cycle arrest and apoptosis were induced by UBE2T silencing. Various genes were downregulated or upregulated by UBE2T knockdown. We suggest that UBE2T is a promising oncogene in HCC.

MATERIALS AND METHODS

UBE2T expression analysis based on The Cancer Genome Atlas database

The transcript analysis of UBE2T in HCC patients was performed based on The Cancer Genome Atlas (TCGA, http://cancergenome.nih.gov). Fifty pairs of HCC and adjacent normal tissues and a total of 543 samples (373 tumor tissues and 169 normal tissues) were available for this study. The expression of UBE2T was analyzed in cancer and normal tissues. The patients were divided into UBE2T high expression and UBE2T low expression groups and subjected to overall survival analysis. The pathological characteristics of grade, T stage, and tumor stage were analyzed between these two groups.

Cell culture

The HCC cell lines BEL-7404 and SMMC-7721 were obtained from the American Type Culture Collection (United States) and the Cell Bank of the Chinese Academy of Sciences (China). The cells were cultured in Dulbecco modified Eagle's medium (Invitrogen) containing 10% fetal bovine serum (Gibco) as well as 1% penicillin and streptomycin (Corning). The cells were cultured in a 37 °C incubator with 5% CO_2.

Lentivirus-mediated UBE2T knockdown assay

UBE2T was knocked down using the lentivirus vector pGCSIL-GFP in BEL-7404 and SMMC-7721 cells. The targeted sequences (ShUBE2T, 5′-ACCTCCTCAGAT CCGATTT-3′ and ShCtrl, 5′-TTCTCCGAACGTGTCACGT-3′) were synthesized and inserted into the pGCSIL-GFP vector. pHelper1.0 and Helper2.0 served as the packaging vectors. Briefly, ShCtrl or ShUBE2T pGCSIL-GFP vectors were co-transfected with pHelper1.0 and Helper2.0 vectors into 293T cells using Lipofectamine 2000 (Invitrogen). After 48 or 72 h, the viral supernatants were harvested and filtered through 0.45 μm filters. The viral supernatants were used to infect the BEL-7404 and SMMC-7721 cells, and the infection efficiency was determined by qRT-PCR and Western blot assays.

Total RNA isolation and quantitative real-time PCR

RNA was harvested from indicated cells using TRIzol reagent (Invitrogen) and an RNA isolation kit (CWBIO, China) following the manufacturer's instructions. Equal amounts of RNA were subjected to reverse transcription with M-MLV reverse transcriptase (Promega). The qRT-PCR experiment was performed using the SYBR master mixture (Takara) on a real-time PCR machine TP800 (Takara). The primer sequences are listed in Table 1. The expression of the targeted genes was normalized to GAPDH.

Western blot analysis

The proteins were collected from the indicated cells with lysis buffer (Beyotime), and the concentration was analyzed with a BCA protein assay kit (Beyotime). The proteins were separated on a 10% or 12% SDS-PAGE gel and subsequently transferred to PVDF membranes (Millipore, United States). The membranes were then blocked with 5% nonfat milk for at least 60 min at room temperature. After incubating with primary antibodies overnight at 4 °C, the membranes were incubated with secondary antibodies and washed three times with PBS-T. The proteins on the membranes were detected using chemiluminescence (Thermo Fisher Scientific). The antibody against UBE2T (SAB1104968) was from Sigma. The antibodies against GAPDH (ab9485), ITGA2 (ab133557), FOSL1 (ab124722), PTGS2 (ab15191), IL1B (ab9722), and BMP6 (ab155963) were from Abcam. All the secondary antibodies were from Santa Cruz.

Multiparametric high-content screening (HCS) of viable cells

Table 1 The primers of target genes

Gene	Primer sequence	
UBE2T	Forward	TTGATTCTGCTGGAAGGATTTG
	Reverse	CAGTTGCGATGTTGAGGGAT
PTGS2	Forward	CTCCTGTGCCTGATGATTGC
	Reverse	CAGCCCGTTGGTGAAAGC
IL1B	Forward	TCCTGTTGTCTACACCAATGCCCA
	Reverse	GAACCAAATGTGGCCGTGGTTTCT
RAC2	Forward	GAAGCATCTACCCGTTCACTC
	Reverse	AGTTGTGGCAGCAACCATCT
ITGA2	Forward	CCTACAATGTTGGTCTCCCAGA
	Reverse	AGTAACCAGTTGCCTTTTGGATT
IL1A	Forward	AGATGCCTGAGATACCCAAAACC
	Reverse	CCAAGCACACCCAGTAGTCT
FOSL1	Forward	ACCCTCCCTAACTCCTTTCA
	Reverse	CTGGAGTTGGATGTGGGATA
SOD2	Forward	TGGACAAACCTCAGCCCT
	Reverse	TGAAACCAAGCCAACCC
BMP6	Forward	TCAACTTATCCCAGATTCCTGA
	Reverse	CCATACTACACGGGTGTCCAA
BCL2L1	Forward	CTGAATCGGAGATGGAGACC
	Reverse	GAGCTGGGATGTCAGGTCA
GSTO1	Forward	GCATACCCAGGGAAGAAGCT
	Reverse	AGAATTGCCACCAAAGAAGG
ITGA5	Forward	GGCTTCAACTTAGACGCGGAG
	Reverse	TGGCTGGTATTAGCCTTGGGT
ENC1	Forward	ACATGGTAGTGCAACTCTTGTC
	Reverse	TTCAGGTCATAGCTGATCCAGT
IL1RAP	Forward	CAAAGTGATGCCTCAGAACG
	Reverse	CTGCCTAGTCCAATACCAGATC
MET	Forward	AGTCATAGGAAGAGGGCATT
	Reverse	CTTCACTTCGCAGGCAGA
SOCS3	Forward	GCCTCAAGACCTTCAGCTCCAA
	Reverse	CTCCAGTAGAAGCCGCTCTCCT
PRKAR1A	Forward	GTTTTCGGTCTCCTTTATCGC
	Reverse	ACTGGTTGCCCATTCATTGTT
RPL31	Forward	CTCGGGCACTCAAAGAGATTC
	Reverse	CGGATTCGGTATGGCACATTC
PPARGC1A	Forward	TCTGAGTCTGTATGGAGTGACAT
	Reverse	CCAAGTCGTTCACATCTAGTTCA
RPL13A	Forward	GCCATCGTGGCTAAACAGGTA
	Reverse	GTTGGTGTTCATCCGCTTGC
NQO1	Forward	AGGCAGTGCTTTCCATCA
	Reverse	CAGGCGTTTCTTCCATCC
ABCC1	Forward	GTCGGGGCATATTCCTGGC
	Reverse	CTGAAGACTGAACTCCCTTCCT
RPL32	Forward	ACCCAGAGGCATTGACAACA
	Reverse	GAGCGATCTCGGCACAGTAA
GCLM	Forward	ATCAGTGGGCACAGGTAAA
	Reverse	CAGAAAGCAGTTCTTTTGGA
FYN	Forward	GGATGCCAAGGCTTACCGAT
	Reverse	GGGCTCCTCAGACACCACTG
HMOX1	Forward	AAGACTGCGTTCCTGCTCAAC
	Reverse	AAAGCCCTACAGCAACTGTCG

SCNN1A	Forward	AGTTCCACCGCTCCTACCGA
	Reverse	GTCCGAGTTGAGGTTGATGTTG
GSTA4	Forward	ACTATCCCAACGGAAGAGGC
	Reverse	CAGGTGGTTACCATCCTGCA
MAP2K6	Forward	GAAGCATTTGAACAACCTCAGAC
	Reverse	CCTGGCTATTTACTGTGGCTC
PIK3C2B	Forward	TTCCTCCACTGTAGACTTGCTT
	Reverse	AGCCGAATGTCAATGTCAAACT
GAPDH	Forward	TGACTTCAACAGCGACACCCA
	Reverse	CACCCTGTTGCTGTAGCCAAA

The HCS assay was performed to detect cell viability. ShCtrl and ShUBE2T SMMC-7721 or BEL-7404 cells were seeded in 96-well plates and cultured for 5 d. The viable cells were scanned by the detection of intensity and distribution of fluorescence. The images were collected using a 20 × objective fluorescence-imaging microscope and analyzed with ArrayScan HCS software (Cellomics Inc.).

Xenografted tumor growth assay

A total of 5 × 10^6 ShCtrl and ShUBE2T SMMC-7721 cells were subcutaneously implanted into the immune-deficient nude mice (BALB/c, 4 wk old, n = 8 per group). The tumor volume was analyzed using the following formula: V = 0.5 × ab^2 (a = long diameter of the tumor, b = short diameter of the tumor). The tumor weight was measured by day 42 after the implantation. This study was approved by the ethics committee of The Affiliated People's Hospital of Shanxi Medical University.

Cell cycle analysis

Propidium iodide (PI) staining was used to detect the cell cycle distribution of ShCtrl and ShUBE2T SMMC-7721 or BEL-7404 cells. In brief, the SMMC-7721 or BEL-7404 cells expressing shRNA lentivirus against Ctrl or UBE2T were seeded in six-well plates. When reaching 80% density, the cell nuclei were stained with PI. PI absorbance was then measured by flow cytometry (FACSCalibur, Becton Dickinson).

Apoptosis analysis

The apoptosis of ShCtrl and ShUBE2T SMMC-7721 or BEL-7404 cells was determined with an Annexin-V-APC kit (Ebioscience, United States) according to the manufacturer's instructions. Briefly, the indicated cells were washed with PBS and resuspended with staining buffer. A total of 5 μL of annexin V-APC regent was added into a total of 100 μL cell suspension, and the mixture was maintained at room temperature for 15 min. Then, flow cytometry was used to detect cell apoptosis (FACSCalibur, Becton-Dickinson, United States).

Gene expression profiling by microarray assay

Gene expression profiling was measured by the Affymetrix human GeneChip prime view. RNA was extracted from ShCtrl and ShUBE2T SMMC-7721 cells using TRIzol reagent. The difference in the gene expression was considered significant when the fold change > 2 and when $P < 0.05$. The pathway enrichment and gene networks were analyzed using the Ingenuity Pathway Analysis.

Statistical analysis

SPSS version 16.0 software was used to analyze the data as shown by the mean ± standard error of the mean (SEM) of three independent experiments. The difference between the two groups was analyzed by the unpaired Student's t-test. One-way ANOVA was applied when more than two groups were analyzed. For survival analysis, the Kaplan-Meier method was applied to analyze the correction between UBE2T expression and the overall survival rate, which was determined using the log-rank test. The median value was used as the cutoff for classification of patients into high and low expression groups. The difference was considered significant at $P < 0.05$.

RESULTS

UBE2T expression is increased in HCC tissues

UBE2T is overexpressed in various cancer patients. We initially analyzed the abundance of UBE2T in HCC patients based on the TCGA database. UBE2T was

highly expressed in 50 HCC specimens compared their adjacent normal tissues (Figure 1A and B). The expression of UBE2T was then analyzed in HCC and nonpaired normal tissues. The results showed that UBE2T was significantly overexpressed in 373 HCC tissues compared to 169 normal liver tissues (Figure 1C). In addition, high expression of UBE2T was positively correlated with grade, T stage, and the pathological stage of HCC patients (Table 2). The patients in the UBE2T high expression group exhibited a poorer overall survival than those in the low expression group (Figure 1D). Taken together, the results demonstrate that UBE2T is abundant in HCC tissues and correlates with HCC progression and survival.

UBE2T knockdown inhibits the proliferation and xenograft tumorigenesis of HCC cells

We next determined the effect of UBE2T on HCC cell viability using the multi-parametric HCS assay. UBE2T was knocked down using the lentivirus-mediated strategy. The qRT-PCR and Western blot assays showed that UBE2T was efficiently silenced in SMMC-7721 and BEL-7404 cells (Figure 2A-D). The HCS results indicated that UBE2T knockdown clearly decreased the viability of SMMC-7721 and BEL-7404 cells (Figure 2E-H).

To explore the role of UBE2T in HCC tumorigenesis, we implanted SMMC-7721 cells carrying the ShCtrl or ShUBE2T lentivirus. The tumors were harvested and photographed 42 d after implantation. The images showed that the tumor size of the ShUBE2T group was clearly smaller than that of the ShCtrl group (Figure 3A). The tumor growth curve suggested that UBE2T knockdown suppressed the tumor initiation and progression of SMMC-7721 cells (Figure 3B). Likewise, the tumor weight was decreased in UBE2T-silenced tumors compared with ShCtrl tumors (Figure 3C). Therefore, UBE2T is essential for the proliferation and carcinogenesis of both SMMC-7721 and BEL7404 cells.

Knockdown of UBE2T induces G1/S cell cycle arrest and apoptosis

Aberrant cell cycle progression and suppressed apoptosis are hallmarks of cancer. We then analyzed whether UBE2T regulated the cell cycle and apoptosis of HCC cells. Using PI staining and analysis by flow cytometry, we found that UBE2T knockdown in SMMC-7721 cells resulted in increased G1 phase and decreased S phase distribution. The G2/M phase remained unchanged (Figure 4A). Consistent results were observed in ShCtrl and ShUBE2T BEL-7404 cells (Figure 4B).

Next, Annexin-V-APC staining was used to determine the apoptosis of ShCtrl and ShUBE2T HCC cells. The results showed that UBE2T knockdown led to increased apoptosis of both SMMC-7721 and BEL-7404 cells (Figure 5). Taken together, the results show that UBE2T silencing induces G1/S cell cycle arrest and enhances apoptosis in HCC cells.

Expression profiling of UBE2T regulated genes

To explore the downstream factors regulated by UBE2T in HCC, ShCtrl and ShUBE2T SMMC-7721 cells were subjected to gene chip analysis. A total of 354 genes were upregulated while 276 downregulated in the UBE2T knockdown cells compared with ShCtrl cells (Figure 6A). The pathway enrichment analysis showed that acute phase response signaling, osteoarthritis pathway, interleukin (IL)-6 signaling, type I diabetes mellitus signaling, and HMGB1 signaling were significantly activated by UBE2T knockdown, while IGF-1 signaling was suppressed (Figure 6B). Based on the previous studies and our data, a possible regulation network for UBE2T is presented in Figure 6C. We then performed Western blot and qRT-PCR assays to verify the GeneChip results. We found that PTGS2, IL-1B, RAC2, ITGA2, IL-1A, FOSL1, SOD2, bone morphogenetic protein (BMP) 6, BCL2L1, GSTO1, IGTA5, ENC1, IL-1RAP, MET, SOCS3, and PRKAR1A were upregulated, while RPL31, PPARGC1A, RPL13A, NQO1, ABCC1, RPL32, GCLM, FYN, HMOX1, SCNN1A, GSTA4, MAP2K6, and PIK3c2b were downregulated by UBE2T knockdown (Figure 6D and E).

DISCUSSION

HCC is one of the most malignant tumors, with a poor 5-year survival rate. It has been shown that HCC is a chronic disease, where non-alcoholic fatty liver disease and non-alcoholic steatohepatitis are risk factors for HCC[11,12]. Even though a large number of studies have identified that some critical genes, such as TP53 and β-catenin, and several important signaling pathways, including Wnt/β-catenin and PI3K/AKT/mTOR, play essential roles in HCC[5,13,14], effective drugs targeting these genes or signaling pathways are still scarce. Therefore, identifying novel genes contributing to this disease may help us develop effective targeted treatments.

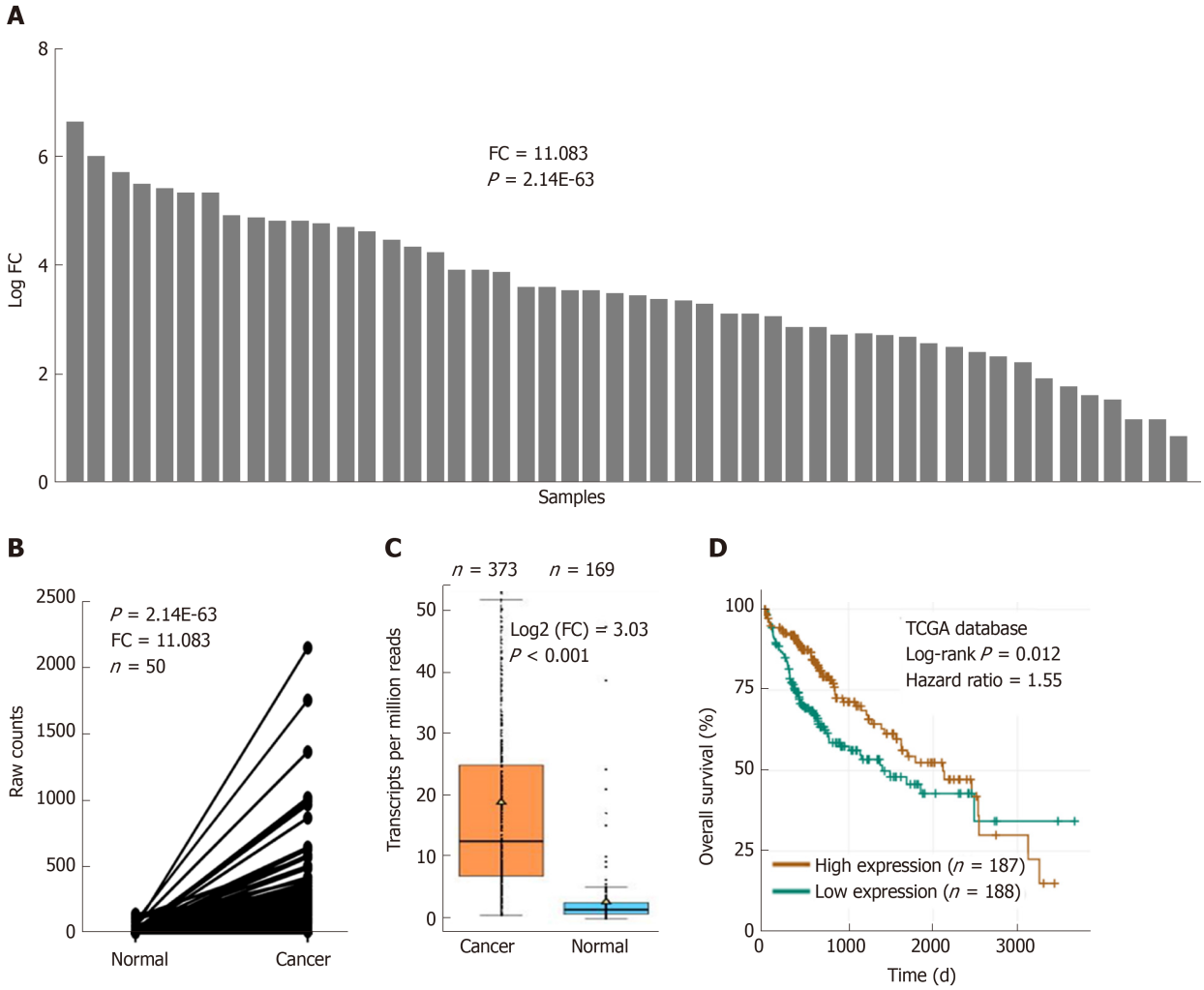

Figure 1 Ubiquitin-conjugating enzyme E2T is overexpressed in hepatocellular carcinoma. A and B: The relative expression of ubiquitin-conjugating enzyme E2T (UBE2T) in hepatocellular carcinoma (HCC) and adjacent normal tissues based on The Cancer Genome Atlas (TCGA) database (fold change =11.083, n = 50, P = 2.14E-63); C: UBE2T mRNA expression in HCC (n = 373) and normal (n = 169) tissues based on the TCGA database. P < 0.001; D: The overall survival of HCC patients who were divided into the UBE2T high expression group (n = 186) and the UBE2T low expression group (n = 187). P = 0.012. FC: Fold change; TCGA: The Cancer Genome Atlas.

A recent profiling study based on the database of TCGA showed that most of the cancer types harbor at least one driver signaling pathway. In HCC, the cell cycle and Wnt signaling pathways are the most frequently altered signaling[15]. Based on the TCGA database, we initially found that UBE2T was clearly overexpressed in HCC patients. And a previous study suggested that UBE2T expression was elevated in HCC tissues with higher pathological grade and vascular invasion according to TCGA cohort[10]. UBE2T acts as a member of ubiquitin-conjugating enzymes[16]. Notably, UBE2T locates at 1q32.1 and the gain of 1q in most human cancers may contribute to the aberrant upregulation of UBE2T[8]. Previously, several studies have illustrated the function of UBE2T in cancer development. For example, UBE2T expression is linked with the poor outcome of breast and lung cancers[9]. UBE2T is also overexpressed in prostate cancer and contributes to the growth of prostate cancer[8]. Furthermore, the knockdown of upregulated UBE2T suppresses cell and/or tumor growth in bladder cancer and gastric cancer[17,18]. The involvement of UBE2T was also reported in HCC cell growth *in vitro*. UBE2T potentiated HCC cell growth by increasing the ubiquitination level of p53[10]. However, the *in vivo* function of UBE2T in HCC is still unknown. Based on the TCGA database, UBE2T was highly expressed in HCC tissues; hence, we knocked down UBE2T in HCC SMMC-7721 and BEL-7404 cells. We showed that UBE2T silencing suppressed the growth of both cells *in vitro* and the xenograft tumor development of SMMC-7721 cells *in vivo*. These results indicate that UBE2T may be a functional oncogene in HCC. Moreover, UBE2T is critical for HCC cell growth and proliferation.

Cancer cells have accelerated cell cycle progression and reduced apoptosis[19]. Targeting cell cycle proteins has been used in cancer patients[20]. In bladder cancer,

Table 2 Relationship between ubiquitin-conjugating enzyme E2T expression and clinicopathological parameters by The Cancer Genome Atlas

		Expression of UBE2T		Total	*P* value
		Low	High		
Grade					0.000
	G1/2	137	95	232	
	G3/4	47	87	134	
Total		184	182	366	
T stage					0.001
	T1	108	73	181	
	T2	38	56	94	
	T3/4	38	55	93	
Total		184	184	368	
Pathological stage					0.002
	I	101	70	171	
	II	36	50	86	
	III/IV	37	53	90	
Total		174	173	347	

UBE2T: Ubiquitin-conjugating enzyme E2T.

UBE2T has been found to negatively regulate the cell cycle process of G2/M transition and apoptosis[17]. Therefore, we investigated the role of UBE2T in the HCC cell cycle. We found that, although changes in the G2/M phase of the cell cycle in HCC cells remained minimal after UBE2T knockdown, the percentage of cells in the G1 phase was increased and that in the S phase was decreased in both ShUBE2T SMMC-7721 and BEL-7404 cells. These results suggest that UBE2T knockdown suppresses the cell cycle progression in both bladder cancer and HCC cells, while it exhibits a distinct function in regulating cell cycle phases in different cancers. Consistent with the results in bladder cancer, UBE2T silencing enhanced apoptosis in HCC cells.

Some studies have illustrated the downstream substrates of UBE2T in various cancers. UBE2T activates the AKT/GSK3β/β-catenin pathway and triggers nasopharyngeal carcinoma progression[21]. UBE2T knockdown suppresses the phosphorylation of both PI3K and AKT in osteosarcoma[22]. In addition, UBE2T interacts with the BRCA1/BARD1 complex and promotes the development and progression of breast cancer[16]. To explore the downstream targets regulated by UBE2T, we performed GeneChip analysis in ShCtrl and ShUBE2T SMMC-7721 cells. We identified hundreds of genes that are regulated by UBE2T. The pathway enrichment and regulation network analyses showed the potential signaling pathways and the central genes downstream of UBE2T. As the GeneChip results indicated, multiple genes were dys-regulated upon UBE2T silencing, including ITGA2, FOSL1, PTGS2, IL-1β, and BMP6. ITGA2 subunit forms a heterodimer with the beta 1 subunit to mediate the adhesion of extracellular matrix, involved in tumor cell proliferation, apoptosis, and migration. Blockade of ITGA2 induces apoptosis and inhibits cell migration in gastric cancer, which might partially explain the ability of UBE2T silencing to inhibit HCC growth[23]. FOSL1 is a member of the FOS family, involved in cancer cell progression and maintenance of the transformed state in several cell types. Further studies suggest that FOSL1 is mainly involved in late tumor stages, including epithelial-to-mesenchymal transition and tumor invasion[24]. Prostaglandin endoperoxide synthases (also known as COX) are the rate-limiting enzymes in the conversion of arachidonic acid into prostaglandins. As one of the isoforms, PTGS2 could activate PEG2, which functions as a regulator in cell proliferation, apoptosis, and invasion[25]. The IL-1 family are proinflammatory cytokines involved in tumor growth, invasion, and distant metastasis in various cancers. A study revealed that the genotypes of IL-1 beta is associated with the prognosis of HCV-related HCC[26]. BMPs belong to the superfamily of the transforming growth factor-β. BMP6 is required to mediate the self-renewal and differentiation of several types of stem cells, and the deficiency of BMP6 may lead to cancer[27]. Taken together, all of these factors may contribute to the UBE2T silencing-induced deceleration of progression in HCC. These results provide clues for further mechanistic studies of UBE2T in HCC and other cancers.

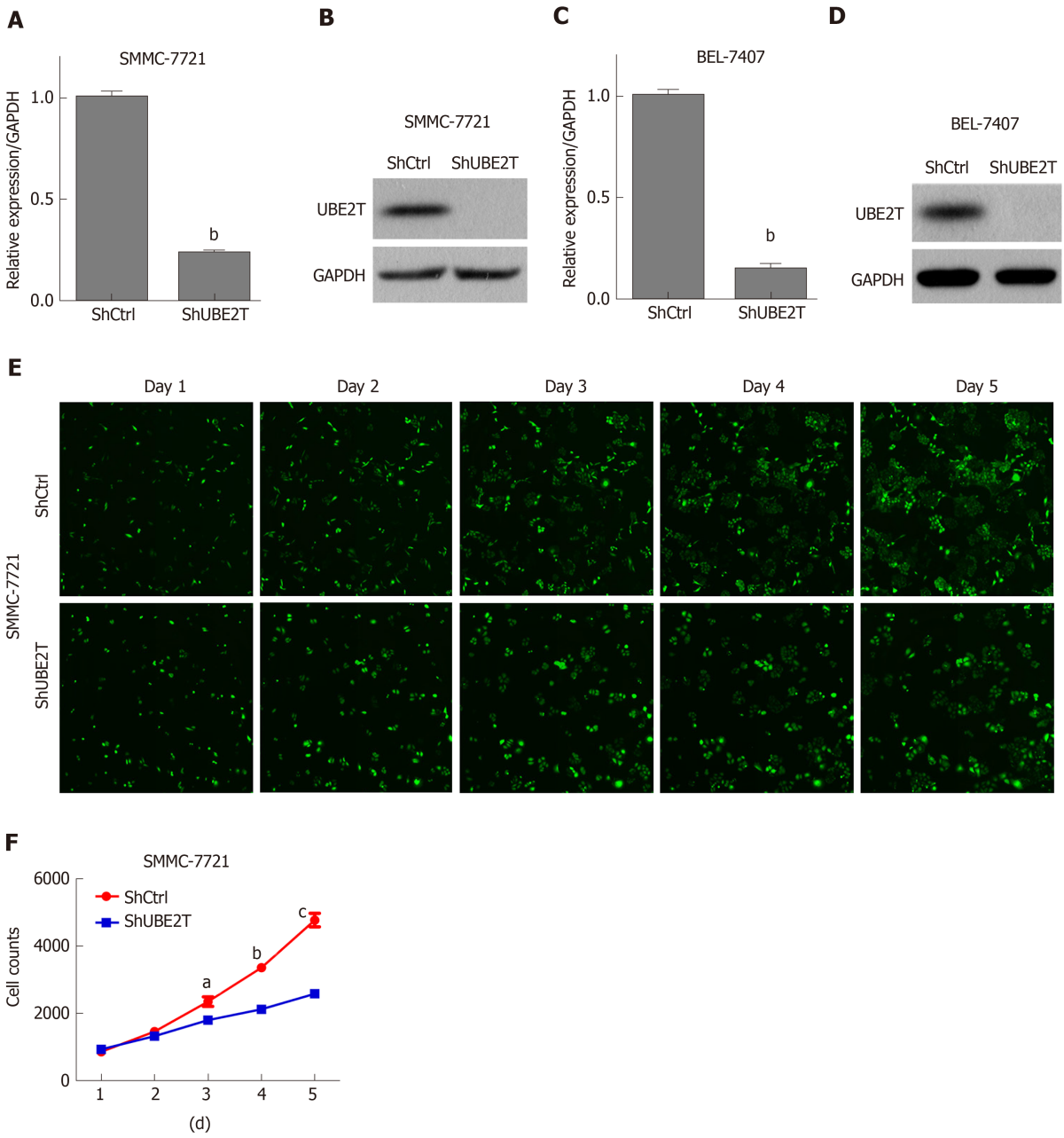
A
SMMC-7721
Relative expression/GAPDH
1.0
0.5
0.0
b
ShCtrl
ShUBE2T
B
SMMC-7721
ShCtrl
ShUBE2T
UBE2T
GAPDH
C
BEL-7407
Relative expression/GAPDH
1.0
0.5
0.0
b
ShCtrl
ShUBE2T
D
BEL-7407
ShCtrl
ShUBE2T
UBE2T
GAPDH
E
Day 1
Day 2
Day 3
Day 4
Day 5
SMMC-7721
ShCtrl
ShUBE2T
F
SMMC-7721
ShCtrl
ShUBE2T
Cell counts
6000
4000
2000
0
a
b
c
1
2
3
4
5
(d)

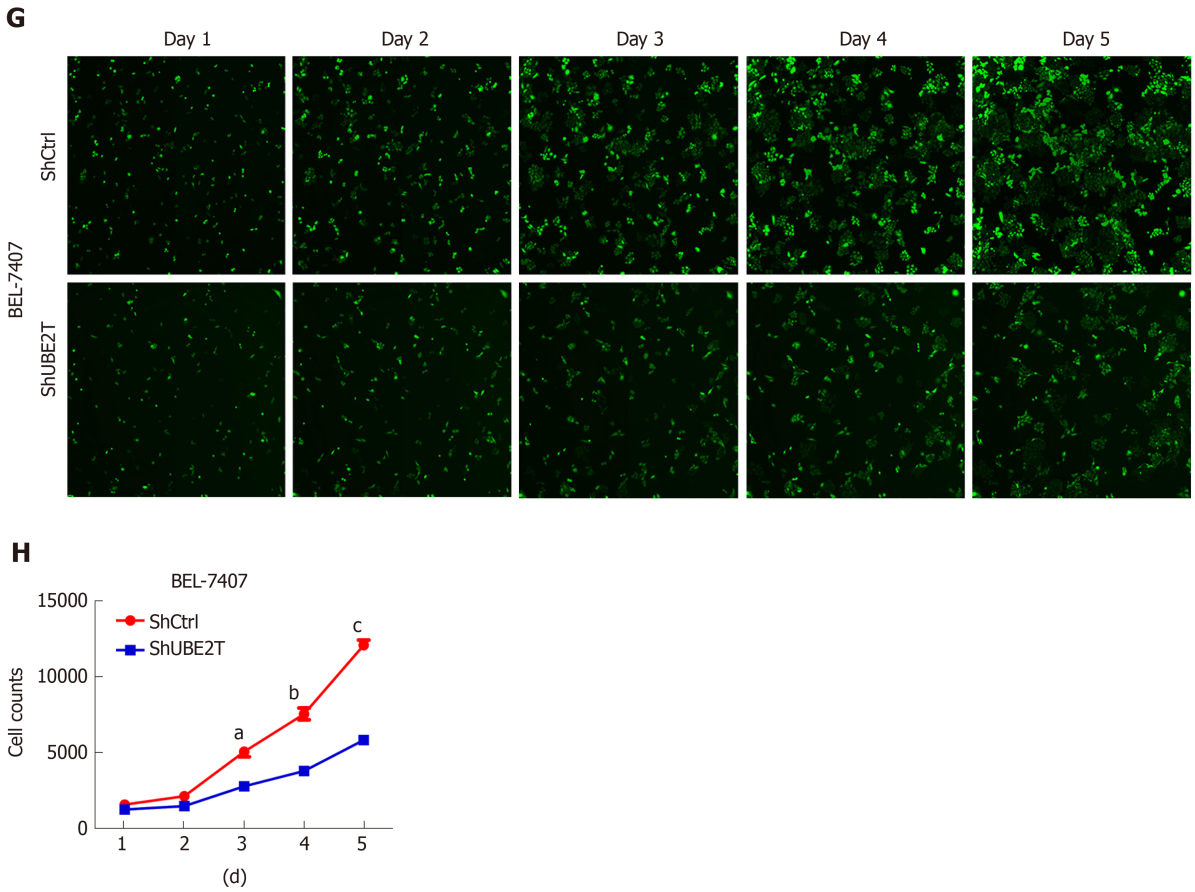

Figure 2 Ubiquitin-conjugating enzyme E2T knockdown reduces the viability of hepatocellular carcinoma cells. A and B: ShCtrl or ShUBE2T SMMC-7721 cells were subjected to qRT-PCR and Western blot analyses of UBE2T. GAPDH served as an internal control. $^{b}P < 0.01$; C and D: ShCtrl or ShUBE2T BEL-7404 cells were subjected to qRT-PCR and Western blot analyses of UBE2T. GAPDH served as an internal control. $^{b}P < 0.01$; E and F: ShCtrl or ShUBE2T SMMC-7721 cells were subjected to multiparametric high-content screening (HCS) analysis of cell viability from day 1 to day 5. Representative images of HCS and quantification of HCS. $^{a}P < 0.05$, $^{b}P < 0.01$, $^{c}P < 0.001$; G and H: ShCtrl or ShUBE2T BEL-7404 cells were subjected to multiparametric HCS analysis of cell viability from day 1 to day 5; G: Representative images of HCS; H: Quantification of HCS. $^{a}P < 0.05$, $^{b}P < 0.01$, $^{c}P < 0.001$. UBE2T: Ubiquitin-conjugating enzyme E2T.

In summary, UBE2T is overexpressed in HCC specimens. Downregulation of UBE2T suppresses HCC cell and tumor growth, at least partly through arrested cell cycle progression and enhanced apoptosis. Numerous genes are regulated by UBE2T. Therefore, UBE2T acts as a potential oncogene and is significantly involved in HCC.

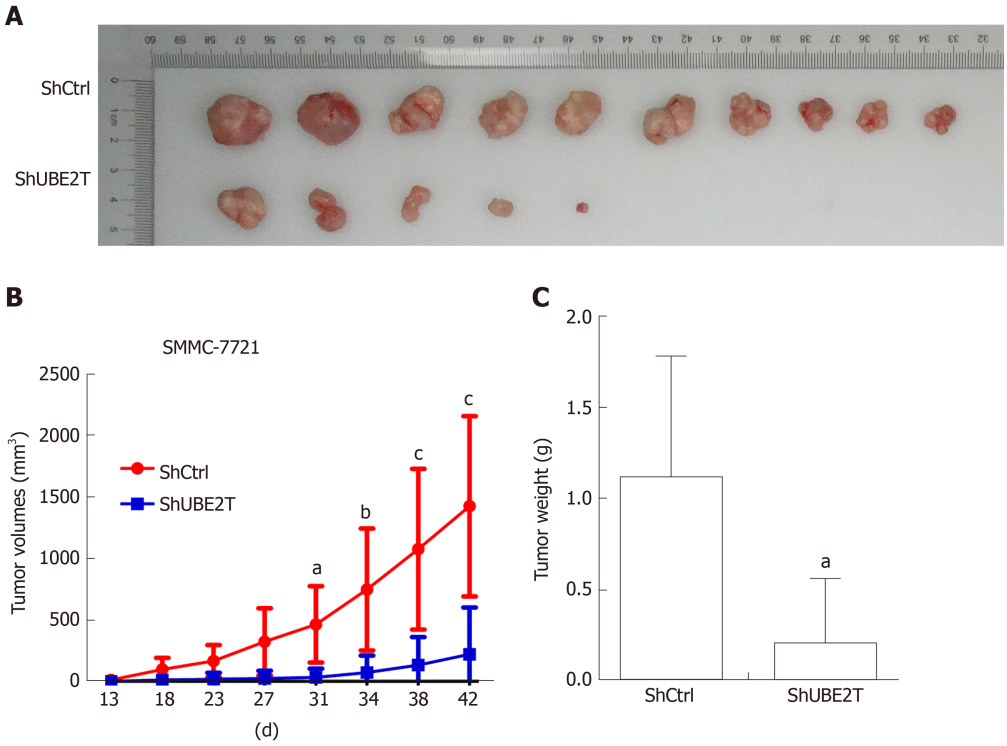

Figure 3 Ubiquitin-conjugating enzyme E2T reduction inhibits the xenograft tumor growth of SMMC-7721 cells. A: Representative images of xenograft tumors derived from nude mice implanted with ShCtrl and ShUBE2T SMMC-7721 cells. *n* = 8 per group; B: Xenograft tumor growth in nude mice implanted with ShCtrl and ShUBE2T SMMC-7721 cells from day 13 to 42. *n* = 8 per group. $^{a}P < 0.05$, $^{b}P < 0.01$, $^{c}P < 0.001$; C: ShCtrl and ShUBE2T xenograft tumor weight 42 d after implantation. $^{b}P < 0.01$.

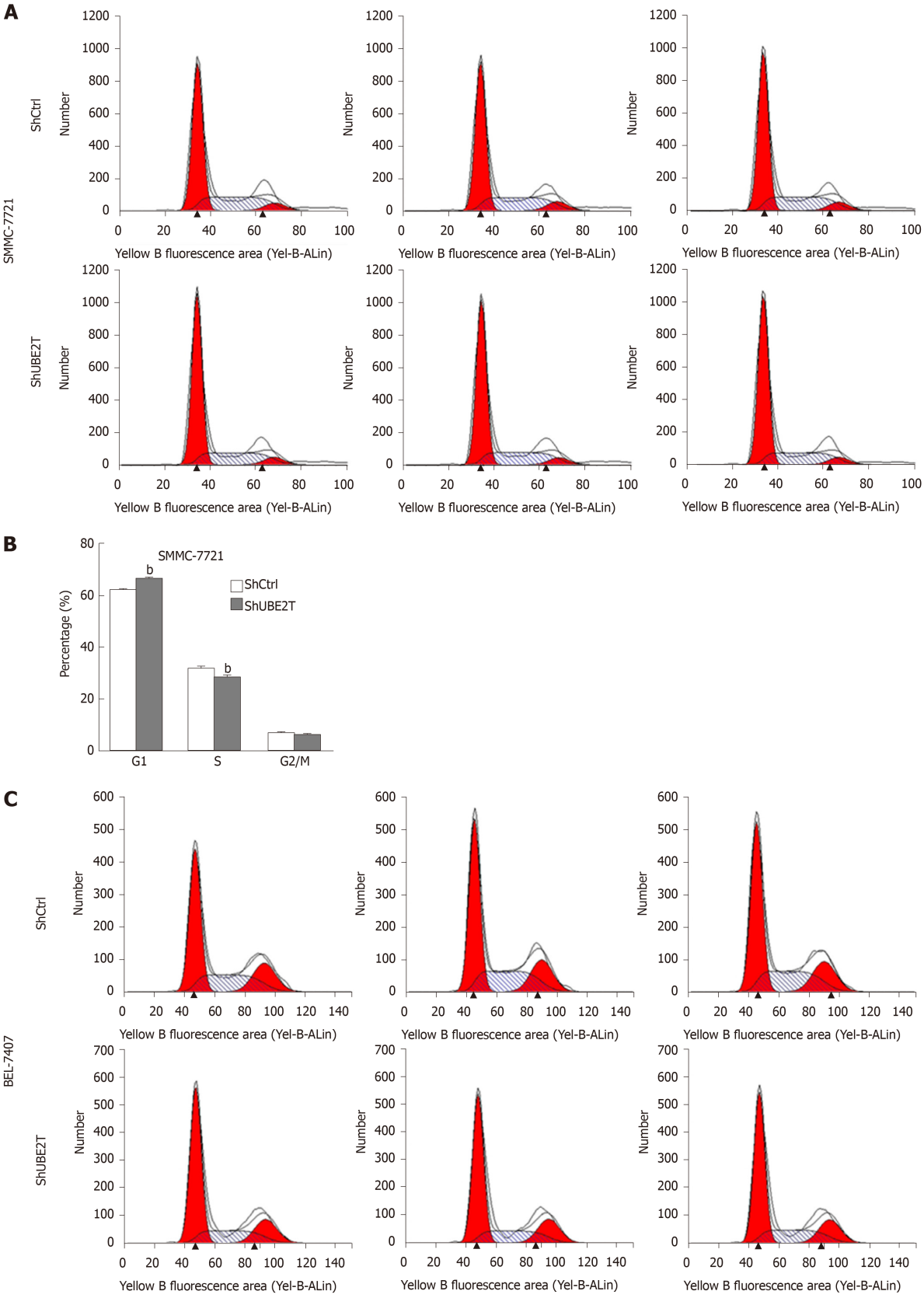
A
SMMC-7721
ShCtrl
ShUBE2T
Number
Yellow B fluorescence area (Yel-B-ALin)
B
SMMC-7721
ShCtrl
ShUBE2T
Percentage (%)
G1
S
G2/M
C
BEL-7407
ShCtrl
ShUBE2T
Number
Yellow B fluorescence area (Yel-B-ALin)

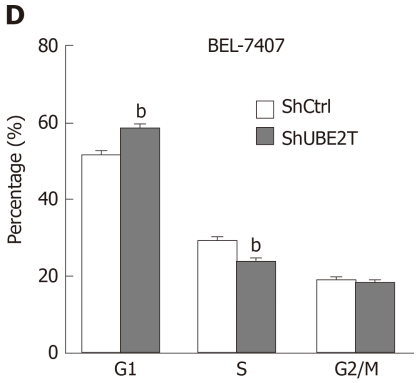

Figure 4 Ubiquitin-conjugating enzyme E2T silencing results in suppressed cell cycle progression in hepatocellular carcinoma cells. A and B: Cell cycle distribution analysis by flow cytometry indicating that ubiquitin-conjugating enzyme E2T (UBE2T) knockdown caused increased G1 phase and decreased S phase in SMMC-7721 cells. $^{b}P < 0.01$; C and D: Cell cycle distribution analysis by flow cytometry indicating that UBE2T knockdown caused increased G1 phase and decreased S phase in BEL-7404 cells. $^{b}P < 0.01$.

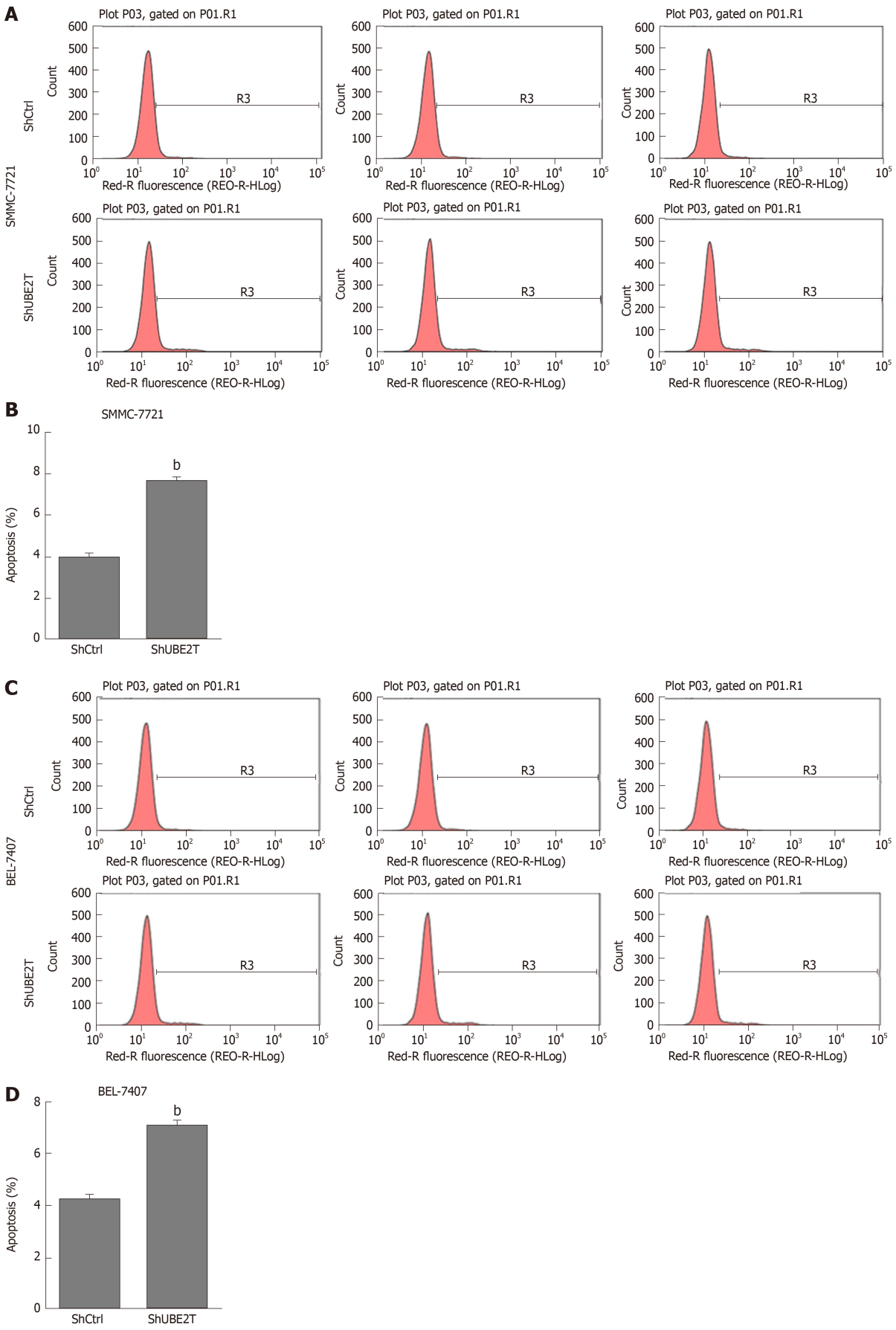

Figure 5 Ubiquitin-conjugating enzyme E2T knockdown enhances apoptosis in hepatocellular carcinoma cells. A and B: Apoptosis in ShCtrl and ShUBE2T SMMC-7721 cells was detected by flow cytometry. Representative flow cytometry plots and apoptosis quantification are shown. $^{b}P < 0.01$; C and D: The apoptosis of ShCtrl and ShUBE2T BEL-7404 cells was detected by flow cytometry. Representative flow cytometry plots and apoptosis quantification are shown. $^{b}P < 0.01$.

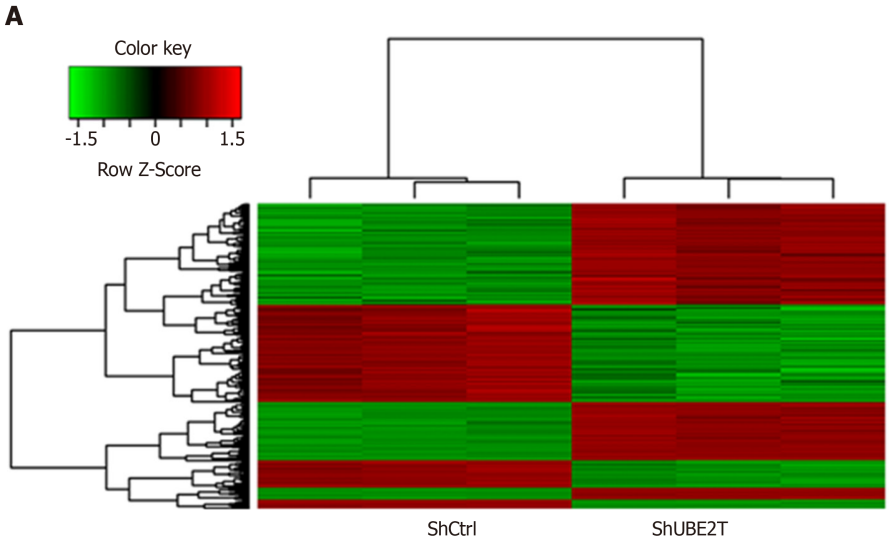
A
Color key
-1.5
0
1.5
Row Z-Score
ShCtrl
ShUBE2T

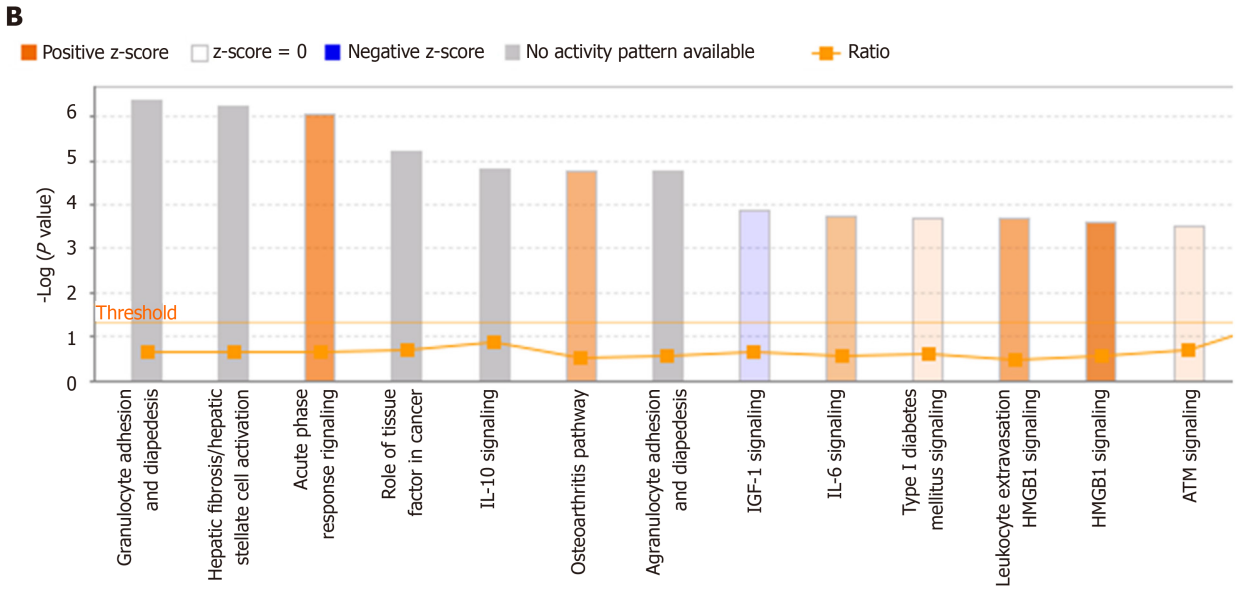
B
Positive z-score
z-score = 0
Negative z-score
No activity pattern available
Ratio
-Log (P value)
Threshold
Granulocyte adhesion and diapedesis
Hepatic fibrosis/hepatic stellate cell activation
Acute phase response rignaling
Role of tissue factor in cancer
IL-10 signaling
Osteoarthritis pathway
Agranulocyte adhesion and diapedesis
IGF-1 signaling
IL-6 signaling
Type I diabetes mellitus signaling
Leukocyte extravasation HMGB1 signaling
HMGB1 signaling
ATM signaling

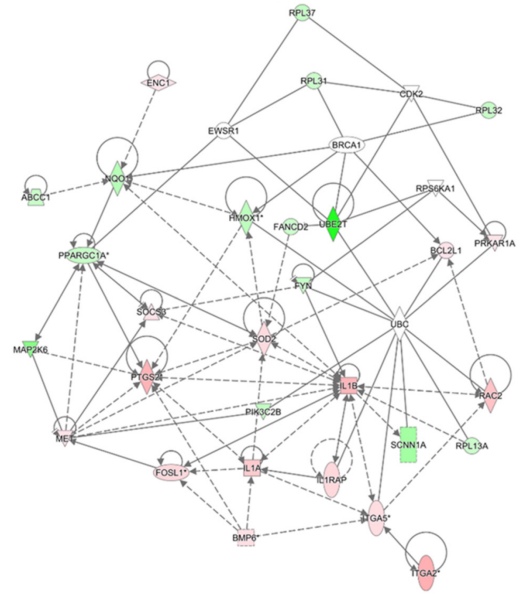
C
RPL37
ENC1
RPL31
CDK2
RPL32
EWSR1
BRCA1
NQO1
ABCC1
RPS6KA1
HMOX1
FANCD2
UBE2T
PPARGC1A
BCL2L1
PRKAR1A
FYN
SOCS2
UBC
SOD2
MAP2K6
PTGS2
IL1B
RAC2
PIK3C2B
MET
SCNN1A
RPL13A
FOSL1
IL1A
IL1RAP
PTGA5
BMP6
ITGA2

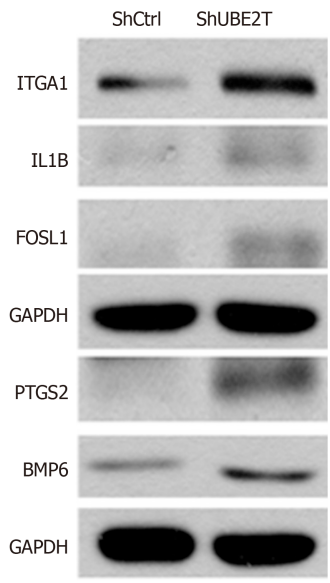
D
ShCtrl
ShUBE2T
ITGA1
IL1B
FOSL1
GAPDH
PTGS2
BMP6
GAPDH

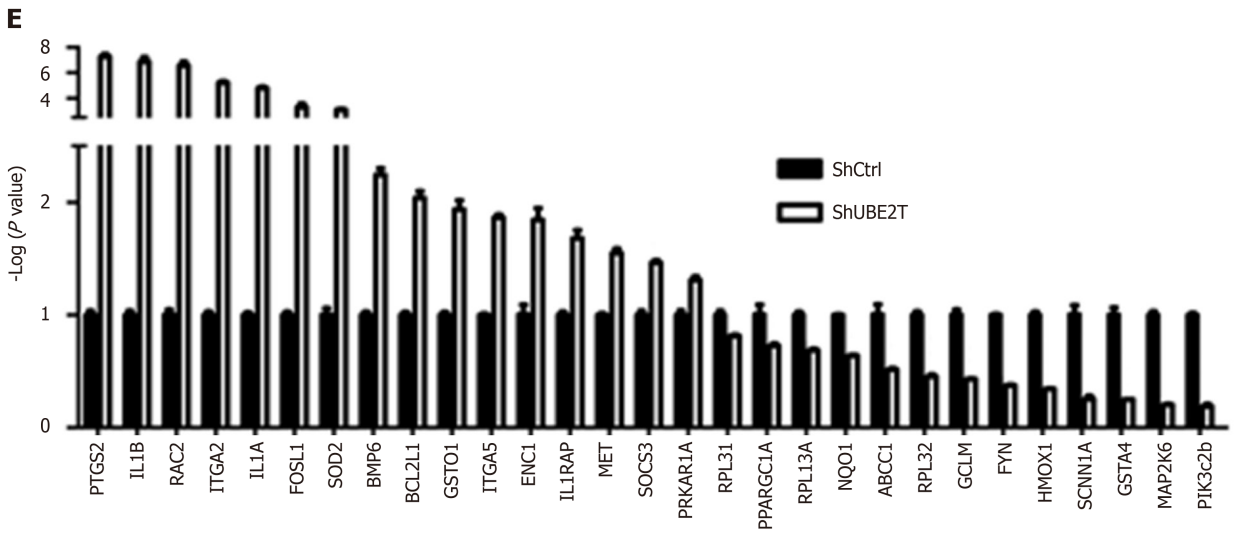

Figure 6 Dys-regulated genes in SMMC-7721 cells with ubiquitin-conjugating enzyme E2T knockdown. A: GeneChip assay showed that a total of 630 genes were regulated by ubiquitin-conjugating enzyme E2T (UBE2T) knockdown in SMMC-7721 cells (354 genes were upregulated and 276 genes downregulated) ($P < 0.05$, fold change > 2); B: The pathway enrichment analysis was performed using IPA software. Orange indicates activated pathways, and blue indicates suppressed pathways; C: Possible regulation network for UBE2T. The map shows upregulated SOD2 and its potential downstream targets. Pink box indicates upregulated genes, and green box indicates downregulated genes; D: qRT-PCR analysis of the indicated genes in ShCtrl and ShUBE2T SMMC-7721 cells. $^{a}P < 0.05$, $^{b}P < 0.01$, $^{c}P < 0.001$; E: ShCtrl and ShUBE2T SMMC-7721 cells were subjected to Western blot analysis.

ARTICLE HIGHLIGHTS

Research background

Hepatocellular carcinoma (HCC) is one of most common malignant tumors with a poor prognosis. Increasing studies indicated that dysregulation of ubiquitin-conjugating enzyme E2T (UBE2T) contributes to the development of human cancers. However, whether UBE2T is involved in the progression of HCC is unclear.

Research motivation

Previous studies have illustrated the critical role of UBE2T in the progression of various tumors, and our study will suggest the role of UBE2T in regulating the occurrence and development of HCC.

Research objectives

To investigate the biological function of UBE2T in HCC cell proliferation and progression *in vitro* by gain-of-function and loss-of-function strategies, and provides significant insights into the underlying molecular mechanisms of UBE2T involved in the development of HCC, which may contribute to the future research of more effective diagnosis and treatment.

Research methods

The expression of UBE2T in HCC tissues was obtained from The Cancer Genome Atlas database. *In vitro* experiments using lentivirus-medicated approach were performed to examine cell growth, cell cycle distribution, and apoptosis by CCK8 assay and flow cytometry, respectively. The xenograft tumorigenicity assay was performed to determine the capacity of cell proliferation *in vivo*. The whole genome expression profile was analyzed by microarray assay.

Research results

In this study, we identified remarkable overexpression of UBE2T in HCC tissues, which closely corrected with a poor overall survival in HCC patients. The results of *in vitro* experiments suggested a critical role of UBE2T in cell viability, cell cycle, and apoptosis of HCC. In both SMMC-7721 and BEL-7404 cells, the HCC cell proliferation was obviously inhibited, cell cycle was arrested at G1/S phase, and apoptosis was significantly promoted by lentivirus-medicated UBE2T knockdown. Moreover, the growth of SMMC-7721 cells with UBE2T knockdown in xenografts was significantly inhibited *in vivo*. The microarray assay confirmed that UBE2T silencing contributed to the dysregulation of numerous genes, including IL-1B, FOSL1, PTGS2, and BMP6.

Research conclusions

In conclusion, UBE2T is significantly involved in HCC cell proliferation, cell cycle, and apoptosis.

Research perspectives

Our study may provide a novel potential diagnostic and therapeutic target for HCC

intervention.

REFERENCES

1 **Sia D**, Villanueva A, Friedman SL, Llovet JM. Liver Cancer Cell of Origin, Molecular Class, and Effects on Patient Prognosis. *Gastroenterology* 2017; **152**: 745-761 [PMID: 28043904 DOI: 10.1053/j.gastro.2016.11.048]

2 **Arzumanyan A**, Reis HM, Feitelson MA. Pathogenic mechanisms in HBV- and HCV-associated hepatocellular carcinoma. *Nat Rev Cancer* 2013; **13**: 123-135 [PMID: 23344543 DOI: 10.1038/nrc3449]

3 **Schulze K**, Imbeaud S, Letouzé E, Alexandrov LB, Calderaro J, Rebouissou S, Couchy G, Meiller C, Shinde J, Soysouvanh F, Calatayud AL, Pinyol R, Pelletier L, Balabaud C, Laurent A, Blanc JF, Mazzaferro V, Calvo F, Villanueva A, Nault JC, Bioulac-Sage P, Stratton MR, Llovet JM, Zucman-Rossi J. Exome sequencing of hepatocellular carcinomas identifies new mutational signatures and potential therapeutic targets. *Nat Genet* 2015; **47**: 505-511 [PMID: 25822088 DOI: 10.1038/ng.3252]

4 **Tornesello ML**, Buonaguro L, Tatangelo F, Botti G, Izzo F, Buonaguro FM. Mutations in TP53, CTNNB1 and PIK3CA genes in hepatocellular carcinoma associated with hepatitis B and hepatitis C virus infections. *Genomics* 2013; **102**: 74-83 [PMID: 23583669 DOI: 10.1016/j.ygeno.2013.04.001]

5 **Farazi PA**, DePinho RA. Hepatocellular carcinoma pathogenesis: from genes to environment. *Nat Rev Cancer* 2006; **6**: 674-687 [PMID: 16929323 DOI: 10.1038/nrc1934]

6 **Machida YJ**, Machida Y, Chen Y, Gurtan AM, Kupfer GM, D'Andrea AD, Dutta A. UBE2T is the E2 in the Fanconi anemia pathway and undergoes negative autoregulation. *Mol Cell* 2006; **23**: 589-596 [PMID: 16916645 DOI: 10.1016/j.molcel.2006.06.024]

7 **Alpi A**, Langevin F, Mosedale G, Machida YJ, Dutta A, Patel KJ. UBE2T, the Fanconi anemia core complex, and FANCD2 are recruited independently to chromatin: a basis for the regulation of FANCD2 monoubiquitination. *Mol Cell Biol* 2007; **27**: 8421-8430 [PMID: 17938197 DOI: 10.1128/mcb.00504-07]

8 **Wen M**, Kwon Y, Wang Y, Mao JH, Wei G. Elevated expression of UBE2T exhibits oncogenic properties in human prostate cancer. *Oncotarget* 2015; **6**: 25226-25239 [PMID: 26308072 DOI: 10.18632/oncotarget.4712]

9 **Perez-Peña J**, Corrales-Sánchez V, Amir E, Pandiella A, Ocana A. Ubiquitin-conjugating enzyme E2T (UBE2T) and denticleless protein homolog (DTL) are linked to poor outcome in breast and lung cancers. *Sci Rep* 2017; **7**: 17530 [PMID: 29235520 DOI: 10.1038/s41598-017-17836-7]

10 **Liu LP**, Yang M, Peng QZ, Li MY, Zhang YS, Guo YH, Chen Y, Bao SY. UBE2T promotes hepatocellular carcinoma cell growth via ubiquitination of p53. *Biochem Biophys Res Commun* 2017; **493**: 20-27 [PMID: 28935368 DOI: 10.1016/j.bbrc.2017.09.091]

11 **Font-Burgada J**, Sun B, Karin M. Obesity and Cancer: The Oil that Feeds the Flame. *Cell Metab* 2016; **23**: 48-62 [PMID: 26771116 DOI: 10.1016/j.cmet.2015.12.015]

12 **Alexander J**, Torbenson M, Wu TT, Yeh MM. Non-alcoholic fatty liver disease contributes to hepatocarcinogenesis in non-cirrhotic liver: a clinical and pathological study. *J Gastroenterol Hepatol* 2013; **28**: 848-854 [PMID: 23302015 DOI: 10.1111/jgh.12116]

13 **Villanueva A**, Chiang DY, Newell P, Peix J, Thung S, Alsinet C, Tovar V, Roayaie S, Minguez B, Sole M, Battiston C, Van Laarhoven S, Fiel MI, Di Feo A, Hoshida Y, Yea S, Toffanin S, Ramos A, Martignetti JA, Mazzaferro V, Bruix J, Waxman S, Schwartz M, Meyerson M, Friedman SL, Llovet JM. Pivotal role of mTOR signaling in hepatocellular carcinoma. *Gastroenterology* 2008; **135**: 1972-1983, 1983.e1-1983.11 [PMID: 18929564 DOI: 10.1053/j.gastro.2008.08.008]

14 **Kenerson HL**, Yeh MM, Kazami M, Jiang X, Riehle KJ, McIntyre RL, Park JO, Kwon S, Campbell JS, Yeung RS. Akt and mTORC1 have different roles during liver tumorigenesis in mice. *Gastroenterology* 2013; **144**: 1055-1065 [PMID: 23376645 DOI: 10.1053/j.gastro.2013.01.053]

15 **Sanchez-Vega F**, Mina M, Armenia J, Chatila WK, Luna A, La KC, Dimitriadoy S, Liu DL, Kantheti HS, Saghafinia S, Chakravarty D, Daian F, Gao Q, Bailey MH, Liang WW, Foltz SM, Shmulevich I, Ding L, Heins Z, Ochoa A, Gross B, Gao J, Zhang H, Kundra R, Kandoth C, Bahceci I, Dervishi L, Dogrusoz U, Zhou W, Shen H, Laird PW, Way GP, Greene CS, Liang H, Xiao Y, Wang C, Iavarone A, Berger AH, Bivona TG, Lazar AJ, Hammer GD, Giordano T, Kwong LN, McArthur G, Huang C, Tward AD, Frederick MJ, McCormick F, Meyerson M; Cancer Genome Atlas Research Network, Van Allen EM, Cherniack AD, Ciriello G, Sander C, Schultz N. Oncogenic Signaling Pathways in The Cancer Genome Atlas. *Cell* 2018; **173**: 321-337.e10 [PMID: 29625050 DOI: 10.1016/j.cell.2018.03.035]

16 **Ueki T**, Park JH, Nishidate T, Kijima K, Hirata K, Nakamura Y, Katagiri T. Ubiquitination and downregulation of BRCA1 by ubiquitin-conjugating enzyme E2T overexpression in human breast cancer cells. *Cancer Res* 2009; **69**: 8752-8760 [PMID: 19887602 DOI: 10.1158/0008-5472.CAN-09-1809]

17 **Gong YQ**, Peng D, Ning XH, Yang XY, Li XS, Zhou LQ, Guo YL. UBE2T silencing suppresses proliferation and induces cell cycle arrest and apoptosis in bladder cancer cells. *Oncol Lett* 2016; **12**: 4485-4492 [PMID: 28101210 DOI: 10.3892/ol.2016.5237]

18 **Luo C**, Yao Y, Yu Z, Zhou H, Guo L, Zhang J, Cao H, Zhang G, Li Y, Jiao Z. UBE2T knockdown inhibits gastric cancer progression. *Oncotarget* 2017; **8**: 32639-32654 [PMID: 28427240 DOI: 10.18632/oncotarget.15947]

19 **Hanahan D**, Weinberg RA. Hallmarks of cancer: the next generation. *Cell* 2011; **144**: 646-674 [PMID: 21376230 DOI: 10.1016/j.cell.2011.02.013]

20 **Otto T**, Sicinski P. Cell cycle proteins as promising targets in cancer therapy. *Nat Rev Cancer* 2017; **17**: 93-115 [PMID: 28127048 DOI: 10.1038/nrc.2016.138]

21 **Hu W**, Xiao L, Cao C, Hua S, Wu D. UBE2T promotes nasopharyngeal carcinoma cell proliferation, invasion, and metastasis by activating the AKT/GSK3β/β-catenin pathway. *Oncotarget* 2016; **7**: 15161-15172 [PMID: 26943030 DOI: 10.18632/oncotarget.7805]

22 **Wang Y**, Leng H, Chen H, Wang L, Jiang N, Huo X, Yu B. Knockdown of UBE2T Inhibits Osteosarcoma Cell Proliferation, Migration, and Invasion by Suppressing the PI3K/Akt Signaling Pathway. *Oncol Res* 2016; **24**: 361-369 [PMID: 27712593 DOI: 10.3727/096504016x14685034103310]

23 **Chuang YC**, Wu HY, Lin YL, Tzou SC, Chuang CH, Jian TY, Chen PR, Chang YC, Lin CH, Huang TH, Wang CC, Chan YL, Liao KW. Blockade of ITGA2 Induces Apoptosis and Inhibits Cell Migration in Gastric Cancer. *Biol Proced Online* 2018; **20**: 10 [PMID: 29743821 DOI: 10.1186/s12575-018-0073-x]

24 **Maurus K**, Hufnagel A, Geiger F, Graf S, Berking C, Heinemann A, Paschen A, Kneitz S, Stigloher C, Geissinger E, Otto C, Bosserhoff A, Schartl M, Meierjohann S. The AP-1 transcription factor FOSL1

causes melanocyte reprogramming and transformation. *Oncogene* 2017; **36**: 5110-5121 [PMID: 28481878 DOI: 10.1038/onc.2017.135]

25 **Kunzmann AT**, Murray LJ, Cardwell CR, McShane CM, McMenamin UC, Cantwell MM. PTGS2 (Cyclooxygenase-2) expression and survival among colorectal cancer patients: a systematic review. *Cancer Epidemiol Biomarkers Prev* 2013; **22**: 1490-1497 [PMID: 23810915 DOI: 10.1158/1055-9965.EPI-13-0263]

26 **Okamoto K**, Ishida C, Ikebuchi Y, Mandai M, Mimura K, Murawaki Y, Yuasa I. The genotypes of IL-1 beta and MMP-3 are associated with the prognosis of HCV-related hepatocellular carcinoma. *Intern Med* 2010; **49**: 887-895 [PMID: 20467172 DOI: 10.2169/internalmedicine.49.3268]

27 **Wang H**, Yuan Q, Sun M, Niu M, Wen L, Fu H, Zhou F, Chen Z, Yao C, Hou J, Shen R, Lin Q, Liu W, Jia R, Li Z, He Z. BMP6 Regulates Proliferation and Apoptosis of Human Sertoli Cells Via Smad2/3 and Cyclin D1 Pathway and DACH1 and TFAP2A Activation. *Sci Rep* 2017; **7**: 45298 [PMID: 28387750 DOI: 10.1038/srep45298]

World Journal of Gastroenterology

Submit a Manuscript: https://www.f6publishing.com

World J Gastroenterol 2019 November 21; 25(43): 6404-6415

DOI: 10.3748/wjg.v25.i43.6404

ISSN 1007-9327 (print) ISSN 2219-2840 (online)

ORIGINAL ARTICLE

Basic Study

Mitochondrial metabolomic profiling for elucidating the alleviating potential of *Polygonatum kingianum* against high-fat diet-induced nonalcoholic fatty liver disease

Xing-Xin Yang, Jia-Di Wei, Jian-Kang Mu, Xin Liu, Feng-Jiao Li, Yan-Qin Li, Wen Gu, Jing-Ping Li, Jie Yu

ORCID number: Xing-Xin Yang (0000-0001-6594-772X); Jia-Di Wei (0000-0002-8108-0457); Jian-Kang Mu (0000-0001-9189-2515); Xin Liu (0000-0003-4788-5275); Feng-Jiao Li (0000-0001-9897-8258); Yan-Qin Li (0000-0001-7609-3790); Wen Gu (0000-0003-3766-5180); Jing-Ping Li (0000-0002-7452-6342); Jie Yu (0000-0001-8100-8896).

Author contributions: Yang XX and Mu JK wrote the manuscript; Wei JD, Yang XX, and Li FJ performed the experiments; Liu X provided technical support and suggestions; Mu JK, Li YQ, Gu W, and Li JP participated in writing and modifying the manuscript; Yang XX and Yu J designed the study; The final manuscript has been approved by all the co-authors; Yang XX, Wei JD and Mu JK contributed equally to this work.

Supported by the National Natural Science Foundation of China, No. 81660596; the National Natural Science Foundation of China, No. 81760733; the Science and Technology Project of Yunnan China, No. 2017FF117-013; the Application and Basis Research Project of Yunnan China, No. 201801CH00227; and the Science and Technology Project of Yunnan China, No. 2016FD050.

Institutional review board statement: This study was reviewed and approved by the Institutional Ethical Committee on Animal Care and Experimentations of Yunnan University of Chinese Medicine.

Xing-Xin Yang, Jia-Di Wei, Jian-Kang Mu, Feng-Jiao Li, Yan-Qin Li, Wen Gu, Jing-Ping Li, Jie Yu, College of Pharmaceutical Science, Yunnan University of Chinese Medicine, Kunming 650500, Yunnan Province, China

Xin Liu, Beijing Entry-Exit Inspection and Quarantine Bureau, Beijing 100026, China

Corresponding author: Jie Yu, PhD, Professor, College of Pharmaceutical Science, Yunnan University of Chinese Medicine, 1076 Yuhua Road, Kunming 650500, Yunnan Province, China. cz.yujie@gmail.com
Telephone: +86-871-65933303
Fax: +86-871-65933303

Abstract

BACKGROUND

Developing mitochondrial regulators/nutrients from natural products to remedy mitochondrial dysfunction represent attractive strategies for therapy of non-alcoholic fatty liver disease (NAFLD). *Polygonatum kingianum* (PK) has been traditionally used in China as a medicinal and nutritional ingredient for centuries and can alleviate high-fat diet (HFD)-induced NAFLD by promoting mitochondrial functions. To date, the underlying molecular mechanism of PK for treating mitochondrial dysfunctions and thus alleviating NAFLD remains unclear.

AIM

To identify the molecular mechanism behind the mitochondrial regulatory action of PK against HFD-induced NAFLD in rats.

METHODS

NAFLD model was induced in rats with HFD. The rats were intragastrically administered PK (4 g/kg per day) for 14 wk. Metabolites in hepatic mitochondrial samples were profiled through ultra-high performance liquid chromatography/mass spectrometry followed by multivariate statistical analysis to find the potential biomarkers and metabolic pathways.

RESULTS

PK significantly restored the metabolites' levels in the mitochondrial samples. Ten potential biomarkers were identified in the analyzed samples. These biomarkers are involved in riboflavin metabolism.

Institutional animal care and use committee statement: Approval from the Institutional Ethical Committee on Animal Care and Experimentations of Yunnan University of Chinese Medicine was obtained for this study.

Conflict-of-interest statement: The authors declare no conflict of interest associated with this manuscript.

Data sharing statement: No additional data are available.

ARRIVE guidelines statement: The authors have read the ARRIVE guidelines, and the manuscript was prepared and revised according to the ARRIVE guidelines.

Manuscript source: Unsolicited manuscript

Received: September 2, 2019
Peer-review started: September 2, 2019
First decision: September 19, 2019
Revised: October 15, 2019
Accepted: October 30, 2019
Article in press: October 30, 2019
Published online: November 21, 2019

P-Reviewer: Adams JD, Shimizu Y
S-Editor: Tang JZ
L-Editor: Filipodia
E-Editor: Ma YJ

CONCLUSION
PK can alleviate HFD-induced NAFLD by regulating the riboflavin metabolism and further improving the mitochondrial functions. Thus, PK is a promising mitochondrial regulator/nutrient for alleviating NAFLD-associated diseases.

Key words: Metabolomics; Mitochondria; Multivariate statistical analysis; Non-alcoholic fatty liver; *Polygonatum kingianum*; Ultra-high performance liquid chromatography/mass spectrometry

Core tip: We identified the molecular mechanism behind the mitochondrial regulatory action of *Polygonatum kingianum* against high-fat diet (HFD)-induced non-alcoholic fatty liver disease (NAFLD) in rats using an integrated mitochondrial metabolomic method. The results indicated that *Polygonatum kingianum* can alleviate HFD-induced NAFLD by regulating riboflavin metabolism, increasing flavin mononucleotide content and further improving mitochondrial functions. *Polygonatum kingianum* as a promising mitochondrial regulator/nutrient can alleviate NAFLD-associated diseases.

Citation: Yang XX, Wei JD, Mu JK, Liu X, Li FJ, Li YQ, Gu W, Li JP, Yu J. Mitochondrial metabolomic profiling for elucidating the alleviating potential of *Polygonatum kingianum* against high-fat diet-induced nonalcoholic fatty liver disease. *World J Gastroenterol* 2019; 25(43): 6404-6415
URL: https://www.wjgnet.com/1007-9327/full/v25/i43/6404.htm
DOI: https://dx.doi.org/10.3748/wjg.v25.i43.6404

INTRODUCTION

Non-alcoholic fatty liver disease (NAFLD), the most prevalent chronic liver disease, is characterized by the accumulation of lipids in the liver, and it can progress to inflammatory non-alcoholic steatohepatitis, fibrosis, cirrhosis, and hepatocellular carcinoma and eventually culminate in liver failure[1,2]. Apart from dieting and regular exercising, no other treatment is recommended for NAFLD[3].

Although the underlying mechanism of NAFLD has not yet been clarified, mitochondrial dysfunction might be involved in the pathogenesis and development of NAFLD[1,4]. Mitochondria play a crucial role in energy production, apoptotic cell death, oxidative stress, calcium homeostasis, and lipid metabolism[5]. Recent scientific reports suggest that natural products, such as Shexiang Baoxin Pill, *Cyclocarya paliurus*, and epigallocatechin gallate can treat NAFLD by regulating the mitochondrial function[6]. Thus, mitochondrial regulators/nutrients can be developed from natural products that which can be utilized for regulating NAFLD-associated mitochondrial dysfunction.

Polygonatum kingianum (PK) has been traditionally used in China as a medicinal and nutritional ingredient for centuries. Many varieties of compounds have been isolated from PK, such as polysaccharides, steroidal saponins, triterpenoid saponins, homoisoflavanones, flavonoids, alkaloids, lignins, and lectins. Among these compounds, the main active compounds are polysaccharides, steroidal saponins, triterpenoid saponins, and homoisoflavanones[7]. PK possesses various pharmacological activities, such as immuno-stimulatory, anti-aging, blood glucose, and lipid regulatory properties[8,9]. Our previous studies have reported that PK can alleviate high-fat diet (HFD)-induced NAFLD by significantly promoting mitochondrial functions. Therefore, the herb can be utilized for treating mitochondrial dysfunction and alleviate NAFLD as a mitochondrial regulator/nutrient[6]. Additionally, PK can alleviate HFD-induced dyslipidemia through remedying a large number of endogenous metabolites in serum, urine, and liver samples[10]. However, the underlying molecular mechanism of PK for treating mitochondrial dysfunctions and thus alleviating NAFLD remains unclear.

Metabolomics can comprehensively profile and characterize the intermediates and end products of cellular metabolism in body fluids, tissues, cells, *etc*. It is a novel approach for evaluating the efficacies and the mechanism of action of natural drugs[11]. However, metabolic profiling of whole cell (body fluid or tissue) is probably

unsuitable for monitoring mitochondrial alterations after drug treatment (though mitochondria contribute a small fraction to cellular contents). Thus, mitochondrial metabolomics can be applied for studying mitochondria-related diseases, as this technique can identify potential functional alterations in multiple metabolic pathways and signaling networks at the subcellular level[12].

The present study was aimed at elucidating the underlying molecular mechanism of PK for regulating mitochondrial dysfunction and thus alleviating HFD-induced NAFLD in rats. An integrated mitochondrial metabolomic method, based on ultra-high performance liquid chromatography/mass spectrometry (UHPLC/MS), was applied for analyzing mitochondrial samples from rat liver (Figure 1). The results indicate that PK can alleviate HFD-induced NAFLD by regulating many endogenous mitochondrial metabolites in hepatic mitochondrial samples. Thus, PK may be applied as a promising mitochondrial regulator/nutrient for alleviating NAFLD-associated diseases.

MATERIALS AND METHODS

Chemicals, reagents, and materials

HPLC-grade acetonitrile and formic acid were purchased from Merck (Darmstadt, Germany). Basic rodent diet was purchased from Suzhou Shuangshi Experimental Animal Feed Technology Co., Ltd. (Suzhou, China). Simvastatin was provided by Hangzhou Merck East Pharmaceutical Co., Ltd. (Hangzhou, China). High-purity deionized-water was prepared with a Milli-Q System (Millipore, Bedford, MA, United States). Cholesterol, refined lard, and eggs were supplied by Beijing Boao Extension Co., Ltd. (Beijing, China), Sichuan Green Island Co., Ltd. (Chengdu, China), and Wal-Mart Supermarket (Kunming, China), respectively. All other reagents were of analytical grade. The rhizome of PK was obtained from Wenshan Shengnong Trueborn Medicinal Materials Cultivation Cooperation Society (Wenshan, China) on 7 April 2017. Samples were authenticated by Professor Jie Yu, and a voucher specimen of PK (No. 8426) was deposited in College of Pharmaceutical Science, Yunnan University of Chinese Medicine (Kunming, China).

Preparation of PK extract

PK was extracted following a previously described method[6]. Briefly, the dried rhizome of PK was permeated in a five-fold volume of Shaoxing Rice Wine (Beijing Ershang Wangzhihe Food Co., Ltd., Beijing, China) and then steamed in a steam sterilizer (LDZX-50 KBS, Shanghai Shenan Medical Instrument Factory, Shanghai, China) for 2.5 h at 120 °C. The steamed samples were dried at 60 °C. Then, the obtained materials were pulverized, immersed in seven-fold volumes of water for 30 min and decocted for 60 min. The extracted liquids were filtered and collected. The filter residues were decocted with seven-fold volumes of water for another 60 min, and the extracted solution was leached. The filtrates were mixed and concentrated by an rotatory evaporator (R-210; Büchi Labortechnik AG, Flawil, Switzerland) under reduced pressure at 50 °C. The concentrates were then lyophilized by an freeze dryer (FD5-3; SIM International Group Co. Ltd., Newark, DE, United States). The powder was preserved in a desiccator until use.

Animal experiments

The animal experiments were performed following the Guide for the Care and Use of Laboratory Animals as published by the US National Institutes of Health and approved by the Institutional Ethical Committee on Animal Care and Experimentations of Yunnan University of Chinese Medicine (R-0620160026) (Kunming, China). Special care was taken to minimize the animals' suffering.

Male Sprague-Dawley rats (200 ± 50 g) were supplied by Dashuo Biotech Co., Ltd. (Chengdu, China). The animals were bred under a controlled environment (60 ± 10% humidity; 22 ± 1 °C temperature; and a 12 h/12 h light/dark cycle) with *ad libitum* access to commercial laboratory food and tap water. Rats were randomized into four groups (n = 5 rats per group), including normal control (normal saline), model (normal saline), simvastatin (1.8 mg/kg per day), and PK groups (4 g/kg). They were intragastrically administered with the tested samples (or normal saline) once a day for 14 wk. Simvastatin and PK were separately dissolved in normal saline. NAFLD was triggered by feeding with HFD (comprised of 1% cholesterol, 10% refined lard, 10% eggs, and 79% basic feed) for 14 wk in all groups except the normal group. After the last administration, rats were fasted for 12 h and anesthetized by chloral hydrate. The liver was collected and stored at 80 °C until use.

Sample pretreatment for UHPLC/MS analysis

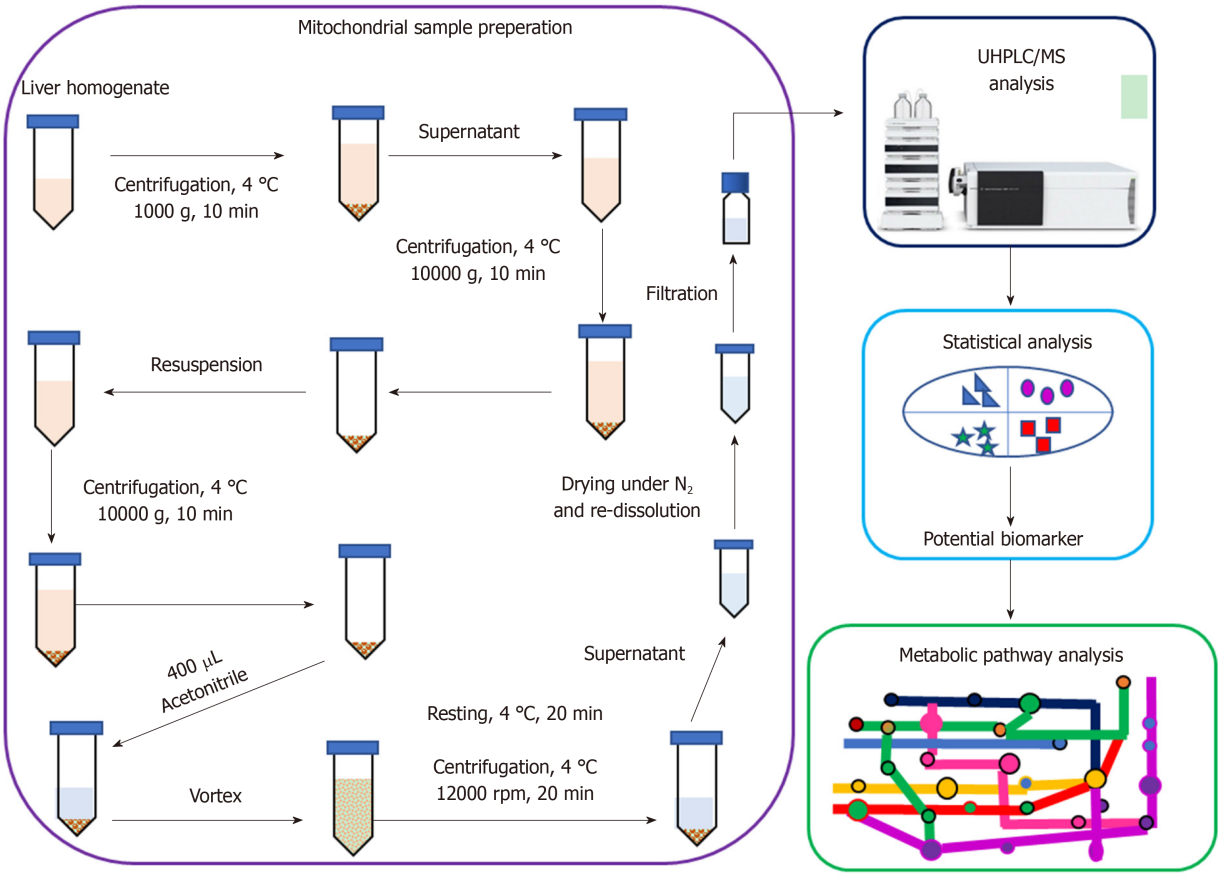

Figure 1 The workflow of the integrated mitochondrial metabolomic method based on ultra-high performance liquid chromatography/mass spectrometry analysis of liver mitochondria. UHPLC/MS: Ultra-high performance liquid chromatography/mass spectrometry.

Firstly, liver mitochondria were isolated following a previously described method[5]. Briefly, rat liver (0.1 g) was quickly placed into ice-cold isolation buffer (210 nmol/L mannitol, 70 nmol/L sucrose, 10 nmol/L Tris base, 1 nmol/L EDTA, and 0.5 nmol/L EGTA, pH 7.4) to remove blood, minced into 1 mm^3, and then homogenized with isolation buffer with a Dounce glass homogenizer (Kimble/Kontes, Vineland, NJ, United States). After centrifuging at 1000 × *g* for 10 min, the supernatant was collected and centrifuged at 10000 × *g* for 10 min. The pellet was resuspended in isolation buffer and centrifuged at 10000 × *g* for 10 min to isolate mitochondria. Next, the isolated mitochondria were resuspended in 400 μL of acetonitrile. After vortex-mixing and allowing to stand for 20 min at 4 °C, the samples were centrifuged at 12000 rpm for 15 min at 4 °C. The collected supernatants were dried under a nitrogen stream. The residues were re-dissolved in acetonitrile (100 μL) for mitochondrial metabolomics analysis.

Condition of UHPLC/MS

UHPLC/MS analyses were performed using a UHPLC (Dionex Ultimate 3000 system) coupled with a hybrid quadrupole-orbitrap mass spectrometer (Thermo Scientific Q-Exactive TM) with a heated-electrospray ionization probe (Thermo Fisher Scientific, San Jose, CA, United States). The UHPLC system comprised of a quaternary pump, a temperature controlled autosampler, a column box, and a photodiode array detector.

The UHPLC conditions were as follows: (1) Chromatographic column: Thermo C18 column (100 mm × 2.1 mm I.D., 1.9 μm); (2) Column temperature: 30 °C; (3) Mobile phase: Acetonitrile (A) and 0.1% formic acid (B) with a gradient program (0-3 min, 5% A; 3-5 min, 5% A-23% A; 5-10 min, 23% A-43% A; 10-13 min, 43% A-64% A; 13-16 min, 64% A-85% A; 16-18 min, 85% A-100% A; 18-20 min, 100% A-100% A); (4) flow rate: 0.2 mL/min; and (5) Sample injection volume: 4 μL.

Mass spectrometry conditions were as follows: (1) Mode: Positive and negative ion; (2) Heat block and curved desolvation line temperature: 250 °C; nebulizing nitrogen gas flow: 1.5 L/min; interface voltage: (+) 3.5 kV, (-) 2.8 kV; (3) Dynamic exclusion time: 10 s; (4) Mass range: MS, m/z 100-1000; MS^2 and MS^3, m/z 50-1000; and (5) Workstation: Xcalibur 3.0.63 for liquid chromatography coupled with data processing,

molecular prediction, and precise molecular weight calculations.

Data processing

All the UHPLC/MS files were exported in Xcalibur Raw File (.raw) format and transformed to *.cdf format by Xcalibur 2.0 software (Thermo Fisher Scientific, Waltham, MA, United States). Then, the transformed file was transferred to XCMS online to extract all data (grouping and comparison). Afterward, multivariate data analysis, including principal components analysis (PCA) and orthogonal partial least squares discriminant analysis (OPLS-DA), was undertaken through SIMCA-P 14.1 software (Umetrics, Umeå, Sweden). Next, potential biomarkers were chosen in conformity with the parameters of variable importance in the projection (VIP > 1.0) from OPLS-DA. The metabolites were identified using the METLIN database and compared with previously reported data. Additionally, biochemical reactions involving the confirmed metabolites were searched by the Kyoto Encyclopedia of Genes and Genomes in MetaboAnalyst 4.0 online.

RESULTS

Metabolomic profiling of liver mitochondria

Isolation conditions of the mitochondrial samples on the UHPLC column were optimized regarding peak number and peak shape. Figure 2 displays the representative total ion current profiles of the mitochondrial samples in the four groups at positive and negative ion modes. Many metabolites of the mitochondrial samples were profiled by UHPLC/MS. Furthermore, remarkable differences were noticed in peak number and intensity between the four groups, indicating different metabolomic states in different groups. Thus, the endogenous metabolites in the liver mitochondria were significantly changed after the 14 wk of HFD-feeding and administration of PK and simvastatin. In addition, the significant differences between PK and simvastatin groups indicated the different regulatory mechanisms of the two drugs to the metabolites in the mitochondrial samples.

Multivariate statistical analysis of the metabolomic data

PCA and OPLS-DA are commonly applied for multivariate data analysis due to their ability to analyze highly multivariate, collinear, and possibly incomplete data. Figure 3 shows the PCA score plots of mitochondrial samples in positive and negative ion modes. In the negative ion mode, the normal and model groups were significantly separated, indicating significant differences in the metabolic state between them. The sample sets of PK group showed a tendency to close the normal group and were nearer to the control group than the simvastatin group. In the positive ion mode, the four groups were almost separated, although significant differences were noticed among the sample sets within the same group. Moreover, the normal and model groups were significantly separated, while the PK group approached to the normal group and were nearer to the normal group than the simvastatin group. This phenomenon suggested that PK treatment significantly prevented HFD-induced pathological changes in a better manner than simvastatin.

OPLS-DA was performed to validate further the sample isolation process in the four groups, maximize separation between the groups, and find biomarkers in them (Figure 4). The four groups were also remarkably isolated in positive and negative ion modes. The PK and simvastatin groups were both near to the control group, which further demonstrated that PK strongly impeded HFD-induced pathological changes.

We evaluated the constituent changes after treatment; an S-Plot loading diagram was developed on the basis of OPLS-DA. Each point in Figure 5 represents a variable, *i.e*. the biomarker responsible for the dissimilarity between the model and PK groups. The importance of each variable to the classification was assessed with the VIP value, and the ingredients with VIP > 1.0 were chosen as potential biomarkers.

Potential biomarker identification

Ten molecules were identified from the mitochondrial samples, including eight in the negative ion mode and two in the positive ion mode. Chemically, these compounds were organic acids, amino acids, nucleosides, and organic salts (Table 1).

Metabolic pathway analysis

Pathways (influence values greater than 0.1) were chosen as the metabolic pathways[13]. Pathway impact plots were established to visualize the impact of the altered metabolic pathways (Figure 6). Based on the results, the main intervened pathways in mitochondrial samples involved riboflavin metabolism (Table 2).

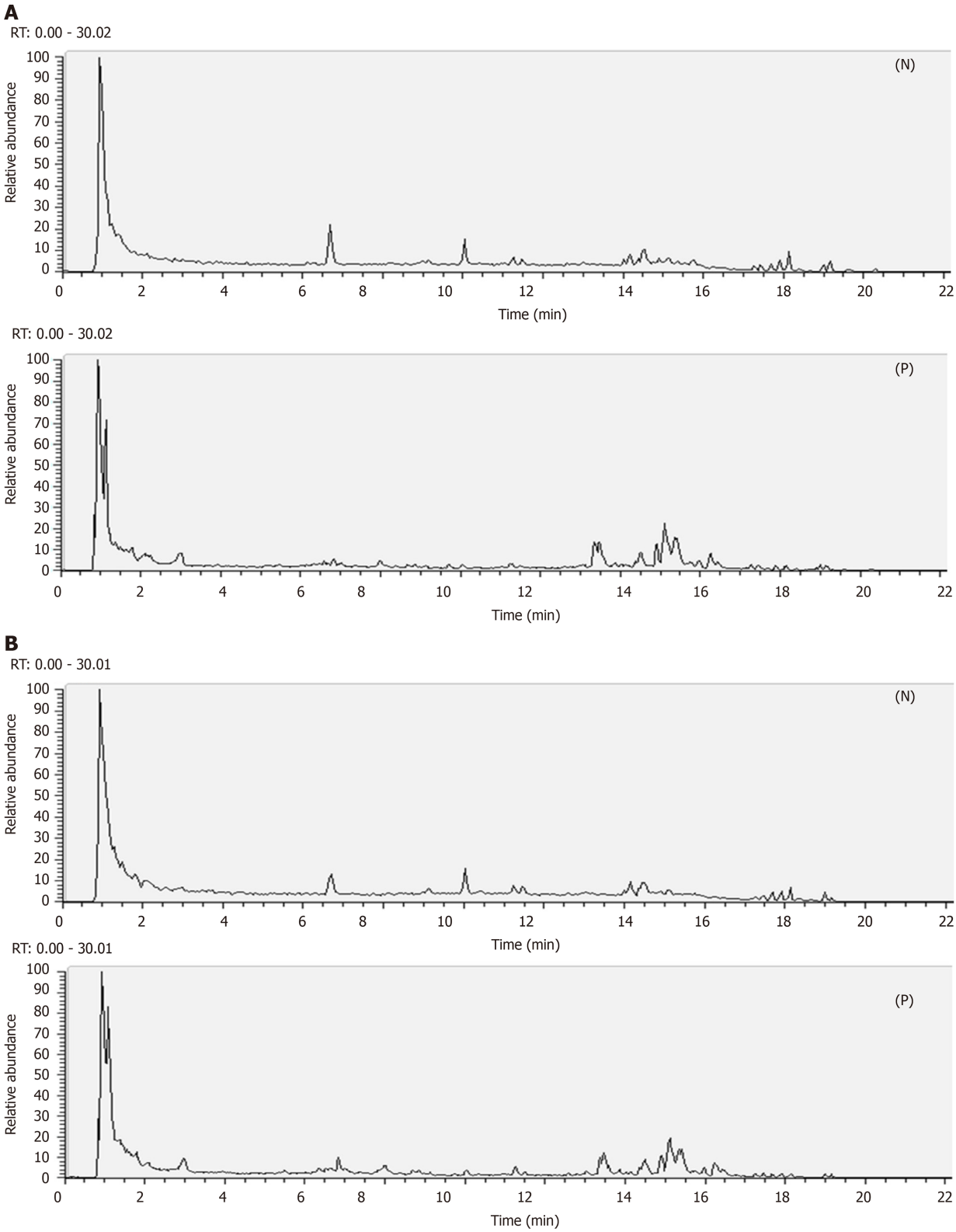
A
RT: 0.00 - 30.02
(N)
Relative abundance
Time (min)
RT: 0.00 - 30.02
(P)
Relative abundance
Time (min)
B
RT: 0.00 - 30.01
(N)
Relative abundance
Time (min)
RT: 0.00 - 30.01
(P)
Relative abundance
Time (min)

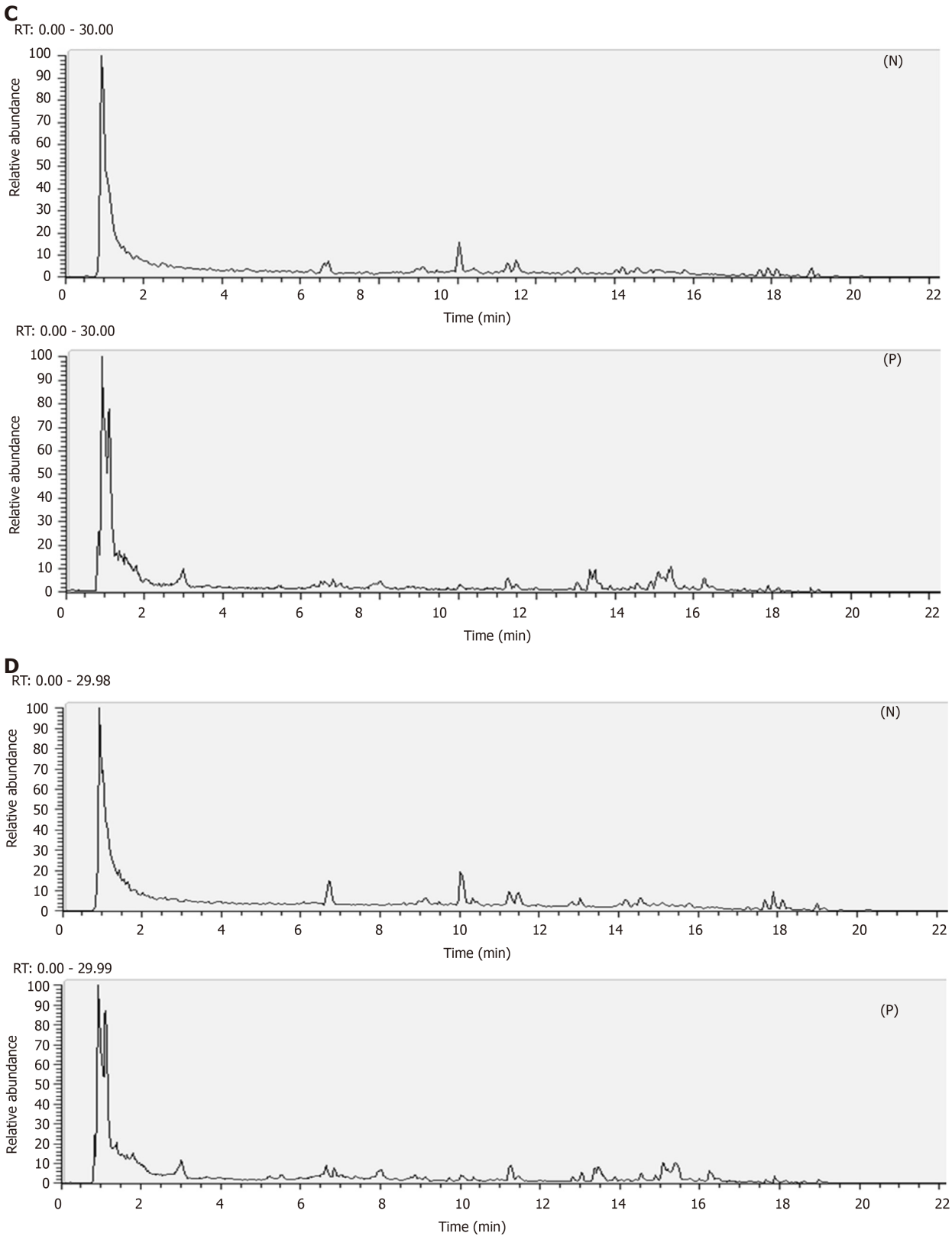

Figure 2 Representative total ion current profiles of the mitochondrial samples in the negative and positive ion mode. Significant differences were observed in peak number and intensity between the four groups, indicating different metabolomic states in the different groups. A: Control group; B: Model group; C: *Polygonatum kingianum* group; D: Simvastatin group; N: Negative; P: Positive.

DISCUSSION

NAFLD, a chronic liver disease, is associated with excessive lipid accumulation in the liver[14]. Mitochondrial dysfunction is the underlying mechanism of NAFLD. In our previous investigation, PK was established as a potential mitochondrial regulator. PK

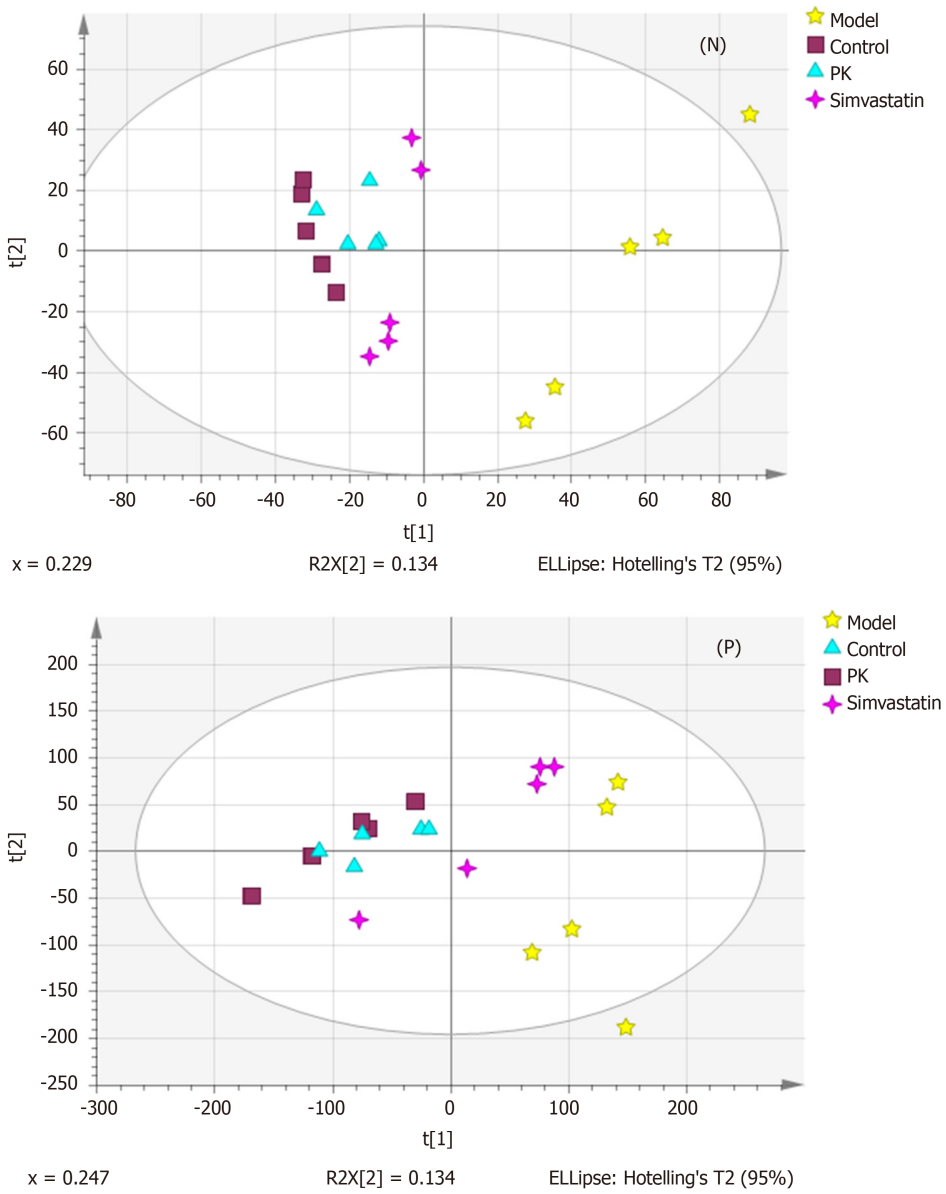

Figure 3 Principal components analysis score plots of the mitochondrial samples in the negative and positive ion mode. Although the significant differences were noticed among the sample sets within the same group, the four groups were almost separated, indicating significant differences in the metabolic state between them. PK: *Polygonatum kingianum*; N: Negative; P: Positive.

can treat mitochondrial dysfunctions and alleviate HFD-induced NAFLD. In the present study, a mitochondrial metabolomic method, based on UHPLC/MS analysis of hepatic mitochondrial samples, was applied for investigating the underlying mechanism of PK for regulating mitochondrial function and treating HFD-induced NAFLD in rats. PK and simvastatin showed the different regulatory mechanisms to the metabolites in the mitochondrial samples. Moreover, PK significantly prevented HFD-induced pathological changes in a better manner than simvastatin, which may be attributed to the multifarious constituents and pharmacological mechanism of PK.

In the present study, 10 potential biomarkers involved in riboflavin metabolism were identified from the mitochondrial samples. Flavin mononucleotide (FMN), also known as riboflavin-5-phosphate, is involved in riboflavin metabolism. FMN, an auxiliary group of flavoproteins, is involved in the electron transport mechanism of the biological oxidation processes (*e.g.*, respiration). This biomolecule is synthesized by riboflavin kinase from riboflavin (vitamin B2). Intracellular free radicals are produced at mitochondria, which can oxidize the mitochondrial enzyme complexes and induce mitochondrial respiratory dysfunction. FMN is the active auxiliary group of the flavoproteins in mitochondrial complex I. Studies have shown that FMN can increase the activity of mitochondrial complex I and promote oxygen consumption rate during mitochondrial respiration[15]. Additionally, FMN can be hydrolyzed to riboflavin and phosphoric acid by phosphatase enzyme. Riboflavin, an auxiliary

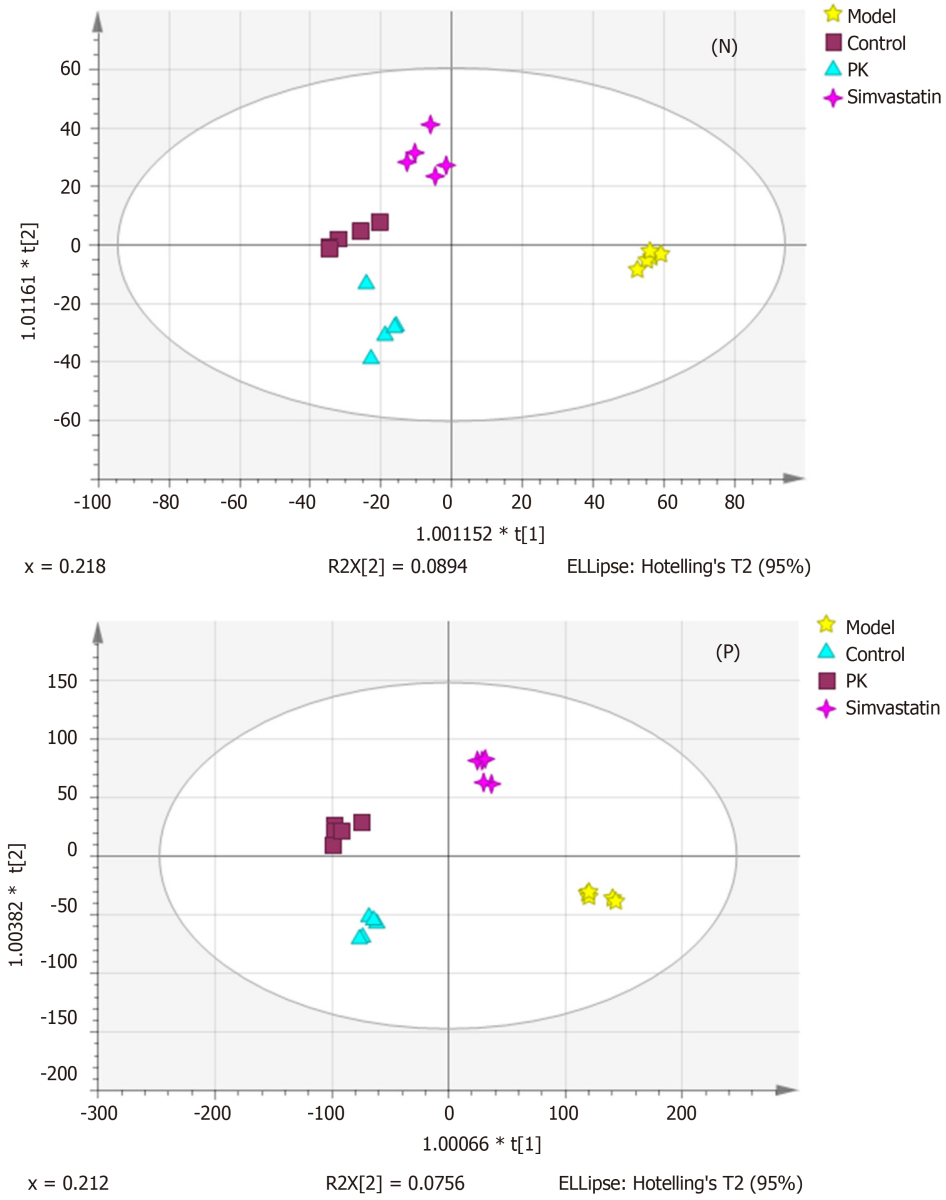

Figure 4 Orthogonal partial least squares discriminant analysis score plots of the mitochondrial samples in the negative and positive ion mode. The four groups were significantly separated, suggesting remarkable differences in the metabolic state between them. PK: *Polygonatum kingianum*; N: Negative; P: Positive.

group of flavin dehydrogenases, serves as a hydrogen donor in bio-oxidation. Lack of riboflavin would impair electron transport in the respiratory chain and result in insufficient ATP production. Thus, bio-oxidation and metabolic statuses are affected in the body. Hepatic proteomic analysis identified that riboflavin deficiency might cause a significant decrease in the expression of key proteins that are involved in the beta-oxidation of fatty acid, electron transport of respiratory chain and tricarboxylic acid cycle, and fat accumulation[16]. In this study, FMN content was significantly reduced after HFD-feeding, which caused mitochondrial respiratory dysfunction. However, the FMN content was remarkably increased after the treatment of PK extract, suggesting an increase in the activity of mitochondrial complex I and oxygen consumption during mitochondrial respiration and ATP production. Higher FMN content resisted fat accumulation in the NAFLD rats. The results indicated that PK extract improved mitochondrial function by accelerating riboflavin metabolism and enhancing FMN content in hepatic mitochondria and thus alleviated NAFLD.

In conclusion, PK extract significantly restored different endogenous metabolites (including riboflavin) in the hepatic mitochondrial samples from HFD-induced NAFLD rats. The results suggest that PK can alleviate HFD-induced NAFLD by regulating riboflavin metabolism, increasing FMN content, and further improving mitochondrial functions. Thus, PK as a promising mitochondrial regulator/nutrient can alleviate NAFLD-associated diseases.

Table 1 Potential biomarkers identified from mitochondrial samples

Retention time, min	Molecular weight, Da	VIP	Potential biomarker	Formula	Change trend Model-PKRP
ESI-					
15.0667	338.208	1.57637	PGJ2	$C_{20}H_{30}O_4$	Up
5.52016	203.082	1.39807	Ascorbate-2-sulfate	$C_6H_8O_9S$	Down
2.09975	267.074	1.36283	Allopurinol-1-ribonucleoside	$C_{10}H_{12}N_4O_5$	Down
1.78773	298.069	1.33035	D-4'-Phosphopantothenate	$C_9H_{18}NO_8P$	Up
15.384	293.18	1.24297	Sodium tetradecyl sulfate	$C_{14}H_{30}O_4S$	Up
20.3338	383.189	1.19012	Bortezomib	$C_{19}H_{25}BN_4O_4$	Up
3.96113	254.08	1.14379	Pantothenic acid	$C_9H_{17}NO_5$	Up
6.51405	455.097	1.11557	Flavin mononucleotide	$C_{17}H_{21}N_4O_9P$	Up
ESI+					
7.0308	301.208	1.53312	Pinolenic acid	$C_{18}H_{30}O_2$	Up
1.09652	266.124	1.44566	N6-Methyl-2'-deoxyadenosine	$C_{11}H_{15}N_5O_3$	Up

VIP: Variable importance in the projection; ESI: Electrospray ionization.

Table 2 Results of metabolic pathway analysis in mitochondrial samples

No	Pathway	Match status	*P*-value	Impact	Details
1	Riboflavin metabolism	1/11	0.031049	0.33333	KEGG
1	1	1	1	1	1

KEGG: Kyoto Encyclopedia of Genes and Genomes.

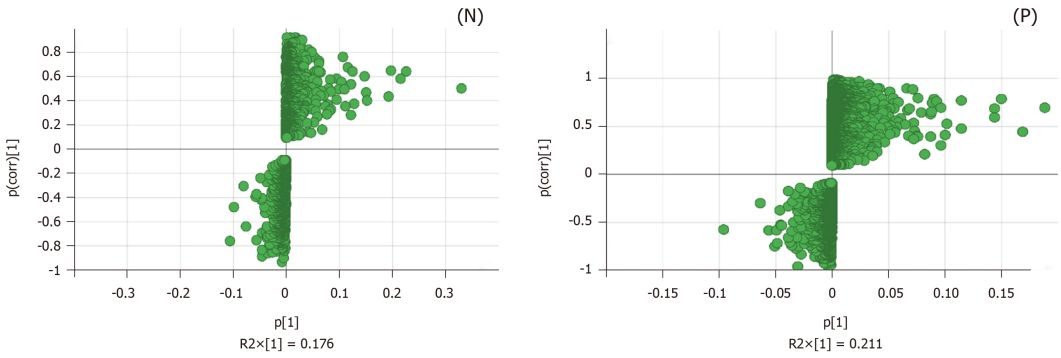

Figure 5 S-plot loading diagram of the model and *Polygonatum kingianum* groups' mitochondrial samples in the negative and positive ion mode. Each point represents a variable that shows the biomarker that caused the difference between the model and *Polygonatum kingianum* groups. N: Negative; P: Positive.

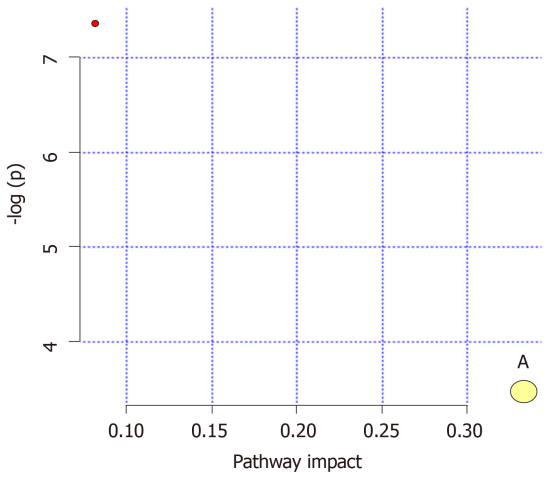

Figure 6 Analysis of metabolic pathways of the mitochondrial samples. A: Riboflavin metabolism.

ARTICLE HIGHLIGHTS

Research background

Non-alcoholic fatty liver disease (NAFLD) is the most prevalent chronic liver disease. Mitochondrial dysfunction is the mechanism of NAFLD. Developing mitochondrial regulators/nutrients from natural products to remedy mitochondrial dysfunction represents an attractive strategy for NAFLD therapy. *Polygonatum kingianum* (PK) has been traditionally used in China as a medicinal and nutritional ingredient for centuries and can alleviate high-fat diet (HFD)-induced NAFLD by significantly promoting mitochondrial functions.

Research motivation

To date, the underlying molecular mechanism of PK for treating mitochondrial dysfunctions and thus alleviating NAFLD remains unclear.

Research objectives

We aimed to identify the molecular mechanism behind the mitochondrial regulatory action of PK against HFD-induced NAFLD in rats.

Research methods

NAFLD model was induced in rats with HFD. The rats were intragastrically administered PK (4 g/kg per day) for 14 wk. Metabolites in hepatic mitochondrial samples were profiled through ultra-high performance liquid chromatography/mass spectrometry followed by multivariate statistical analysis to find the potential biomarkers and metabolic pathways.

Research results

PK significantly restored the metabolites' levels in the mitochondrial samples. Ten potential biomarkers were identified in the analyzed samples. These biomarkers are involved in riboflavin metabolism.

Research conclusions

PK can alleviate HFD-induced NAFLD by regulating riboflavin metabolism and further improving the mitochondrial functions.

Research perspectives

PK is a promising mitochondrial regulator/nutrient for alleviating NAFLD-associated diseases.

REFERENCES

1 **Le J**, Jia W, Sun Y. Sennoside A protects mitochondrial structure and function to improve high-fat diet-induced hepatic steatosis by targeting VDAC1. *Biochem Biophys Res Commun* 2018; **500**: 484-489 [PMID: 29673597 DOI: 10.1016/j.bbrc.2018.04.108]

2 **Im AR**, Kim YH, Kim YH, Yang WK, Kim SH, Song KH. Dolichos lablab Protects Against Nonalcoholic Fatty Liver Disease in Mice Fed High-Fat Diets. *J Med Food* 2017; **20**: 1222-1232 [PMID: 29090980 DOI: 10.1089/jmf.2017.4036]

3 **Lindquist C**, Bjørndal B, Rossmann CR, Svardal A, Hallström S, Berge RK. A fatty acid analogue targeting mitochondria exerts a plasma triacylglycerol lowering effect in rats with impaired carnitine biosynthesis. *PLos One* 2018; **13**: e0194978 [PMID: 29590220 DOI: 10.1371/journal.pone.0194978]

4 **Simões ICM**, Fontes A, Pinton P, Zischka H, Wieckowski MR. Mitochondria in non-alcoholic fatty liver disease. *Int J Biochem Cell Biol* 2018; **95**: 93-99 [PMID: 29288054 DOI: 10.1016/j.biocel.2017.12.019]

5 **Pathania D**, Millard M, Neamati N. Opportunities in discovery and delivery of anticancer drugs targeting mitochondria and cancer cell metabolism. *Adv Drug Deliv Rev* 2009; **61**: 1250-1275 [PMID: 19716393 DOI: 10.1016/j.addr.2009.05.010]

6 **Yang XX**, Wang X, Shi TT, Dong JC, Li FJ, Zeng LX, Yang M, Gu W, Li JP, Yu J. Mitochondrial dysfunction in high-fat diet-induced nonalcoholic fatty liver disease: The alleviating effect and its mechanism of Polygonatum kingianum. *Biomed Pharmacother* 2019; **117**: 109083 [PMID: 31387169 DOI: 10.1016/j.biopha.2019.109083]

7 **Zhao P**, Zhao C, Li X, Gao Q, Huang L, Xiao P, Gao W. The genus Polygonatum: A review of ethnopharmacology, phytochemistry and pharmacology. *J Ethnopharmacol* 2018; **214**: 274-291 [PMID: 29246502 DOI: 10.1016/j.jep.2017.12.006]

8 **Yan H**, Lu J, Wang Y, Gu W, Yang X, Yu J. Intake of total saponins and polysaccharides from Polygonatum kingianum affects the gut microbiota in diabetic rats. *Phytomedicine* 2017; **26**: 45-54 [PMID: 28257664 DOI: 10.1016/j.phymed.2017.01.007]

9 **Lu JM**, Wang YF, Yan HL, Lin P, Gu W, Yu J. Antidiabetic effect of total saponins from Polygonatum kingianum in streptozotocin-induced daibetic rats. *J Ethnopharmacol* 2016; **179**: 291-300 [PMID: 26743227 DOI: 10.1016/j.jep.2015.12.057]

10 **Yang XX**, Wei JD, Mu JK, Liu X, Dong JC, Zeng LX, Gu W, Li JP, Yu J. Integrated metabolomic profiling for analysis of antilipidemic effects of *Polygonatum kingianum* extract on dyslipidemia in rats. *World J Gastroenterol* 2018; **24**: 5505-5524 [PMID: 30622379 DOI: 10.3748/wjg.v24.i48.5505]

11 **Tao Y**, Chen X, Li W, Cai B, Di L, Shi L, Hu L. Global and untargeted metabolomics evidence of the protective effect of different extracts of Dipsacus asper Wall. ex C.B. Clarke on estrogen deficiency after ovariectomia in rats. *J Ethnopharmacol* 2017; **199**: 20-29 [PMID: 28132861 DOI: 10.1016/j.jep.2017.01.050]

12 **Liu X**, Xu G. Recent advances in using mass spectrometry for mitochondrial metabolomics and lipidomics - A review. *Anal Chim Acta* 2018; **1037**: 3-12 [PMID: 30292306 DOI: 10.1016/j.aca.2017.11.080]

13 **Xie HH**, Xie T, Xu JY, Shen CS, Lai ZJ, Xu NS, Wang SC, Shan JJ. Metabolomics study of aconitine and benzoylaconine induced reproductive toxicity in BeWo cell. *Fenxi Huaxue* 2015; **43**: 1808–1813 [DOI: 10.1016/S1872-2040(15)60881-7]

14 **Priore P**, Cavallo A, Gnoni A, Damiano F, Gnoni GV, Siculella L. Modulation of hepatic lipid metabolism by olive oil and its phenols in nonalcoholic fatty liver disease. *IUBMB Life* 2015; **67**: 9-17 [PMID: 25631376 DOI: 10.1002/iub.1340]

15 **Holt PJ**, Efremov RG, Nakamaru-Ogiso E, Sazanov LA. Reversible FMN dissociation from Escherichia coli respiratory complex I. *Biochim Biophys Acta* 2016; **1857**: 1777-1785 [PMID: 27555334 DOI: 10.1016/j.bbabio.2016.08.008]

16 **Tang J**, Hegeman MA, Hu J, Xie M, Shi W, Jiang Y, de Boer V, Guo Y, Hou S, Keijer J. Severe riboflavin deficiency induces alterations in the hepatic proteome of starter Pekin ducks. *Br J Nutr* 2017; **118**: 641-650 [PMID: 29185933 DOI: 10.1017/S0007114517002641]

World Journal of Gastroenterology

Submit a Manuscript: https://www.f6publishing.com

World J Gastroenterol 2019 November 21; 25(43): 6416-6429

DOI: 10.3748/wjg.v25.i43.6416

ISSN 1007-9327 (print) ISSN 2219-2840 (online)

ORIGINAL ARTICLE

Case Control Study

Altered profiles of fecal metabolites correlate with visceral hypersensitivity and may contribute to symptom severity of diarrhea-predominant irritable bowel syndrome

Wen-Xue Zhang, Yu Zhang, Geng Qin, Kai-Min Li, Wei Wei, Su-Yun Li, Shu-Kun Yao

ORCID number: Wen-Xue Zhang (0000-0002-5720-3314); Yu Zhang (0000-0003-0764-0599); Geng Qin (0000-0002-1197-2011); Kai-Min Li (0000-0002-5498-5875); Wei Wei (0000-0002-8388-0423); Su-Yun Li (0000-0002-2473-1348); Shu-Kun Yao (0000-0002-8512-2589).

Author contributions: Zhang WX designed and performed the study, analyzed the data and drafted the manuscript; Zhang Y, Qin G and Wei W collected material and clinical data from patients; Li KM gave guidance and support on experimental procedure and data interpretation; Li SY contributed to design of the study and analysis of data; Yao SK designed the study, supervised the study performance, revised the manuscript, and obtained the funding.

Supported by the National Key Technology Support Program for the "12th Five-Year Plan" of China, No. 2014BAI08B00; and the Research Projects on Biomedical Transformation of China-Japan Friendship Hospital, No. PYBZ1815.

Institutional review board statement: This study was approved by the Ethics Committee of China-Japan Friendship Hospital, Beijing, China.

Informed consent statement: All study participants provided written informed consent prior to study enrollment.

Conflict-of-interest statement: All

Wen-Xue Zhang, Yu Zhang, Geng Qin, Wei Wei, Graduate School, Peking Union Medical College and Chinese Academy of Medical Sciences, Beijing 100730, China

Wen-Xue Zhang, Yu Zhang, Geng Qin, Wei Wei, Shu-Kun Yao, Department of Gastroenterology, China-Japan Friendship Hospital, Beijing 100029, China

Kai-Min Li, School of Biological Science and Medical Engineering, Beihang University, Beijing 100191, China

Su-Yun Li, Department of Epidemiology and Health Statistics, School of Public Health, Qingdao University, Qingdao 266071, Shandong Province, China

Corresponding author: Shu-Kun Yao, MD, PhD, Professor, Department of Gastroenterology, China-Japan Friendship Hospital, 2nd Yinghua East Road, Chaoyang District, Beijing 100029, China. shukunyao@126.com
Telephone: +86-10-84205108
Fax: +86-10-84205108

Abstract

BACKGROUND

Fecal metabolites are associated with gut visceral sensitivity, mucosal immune function and intestinal barrier function, all of which have critical roles in the pathogenesis of irritable bowel syndrome (IBS). However, the metabolic profile and pathophysiology of IBS are still unclear. We hypothesized that altered profiles of fecal metabolites might be involved in the pathogenesis of IBS with predominant diarrhea (IBS-D).

AIM

To investigate the fecal metabolite composition and the role of metabolites in IBS-D pathophysiology.

METHODS

Thirty IBS-D patients and 15 age- and sex-matched healthy controls (HCs) underwent clinical and psychological assessments, including the IBS Symptom Severity System (IBS-SSS), an Italian modified version of the Bowel Disease Questionnaire, the Bristol Stool Form Scale (BSFS), the Hospital Anxiety and Depression Scale, and the Visceral Sensitivity Index. Visceral sensitivity to rectal distension was tested using high-resolution manometry system by the same investigator. Fecal metabolites, including amino acids and organic acids, were

authors report no conflicts of interest.

Data sharing statement: Technical appendix, statistical code, and dataset available from the first author at zhangwenxue048@163.com.

STROBE statement: The authors have read the STROBE Statement, and the manuscript was prepared and revised according to the STROBE Statement.

Manuscript source: Unsolicited manuscript

Received: September 19, 2019
Peer-review started: September 19, 2019
First decision: October 14, 2019
Revised: October 19, 2019
Accepted: November 1, 2019
Article in press: November 1, 2019
Published online: November 21, 2019

P-Reviewer: Carroccio A, Kamiya T, O'Malley D
S-Editor: Tang JZ
L-Editor: Ma JY
E-Editor: Ma YJ

measured by targeted metabolomics approaches. Correlation analyses between these parameters were performed.

RESULTS

The patients presented with increased stool water content, more psychological symptoms and increased visceral hypersensitivity compared with the controls. In fecal metabolites, His [IBS-D: 0.0642 (0.0388, 0.1484), HC: 0.2636 (0.0780, 0.3966), P = 0.012], Ala [IBS-D: 0.5095 (0.2826, 0.9183), HC: 1.0118 (0.6135, 1.4335), P = 0.041], Tyr [IBS-D: 0.1024 (0.0173, 0.4527), HC: 0.5665 (0.2436, 1.3447), P = 0.018], Phe [IBS-D: 0.1511 (0.0775, 0.3248), HC: 0.3967 (0.1388, 0.7550), P = 0.028], and Trp [IBS-D: 0.0323 (0.0001, 0.0826), HC: 0.0834 (0.0170, 0.1759), P = 0.046] were decreased in IBS-D patients, but isohexanoate [IBS-D: 0.0127 (0.0060, 0.0246), HC: 0.0070 (0.0023, 0.0106), P = 0.028] was significantly increased. Only Tyr was mildly correlated with BSFS scores in all subjects (r = -0.347, P = 0.019). A possible potential biomarker panel was identified to correlate with IBS-SSS score ($R^2_{Adjusted}$ = 0.693, P < 0.001). In this regression model, the levels of Tyr, Val, hexanoate, fumarate, and pyruvate were significantly associated with the symptom severity of IBS-D. Furthermore, visceral sensation, including abdominal pain and visceral hypersensitivity, was correlated with isovalerate, valerate and isohexanoate.

CONCLUSION

Altered profiles of fecal metabolites may be one of the origins or exacerbating factors of symptoms in IBS-D *via* increasing visceral sensitivity.

Key words: Fecal metabolite; Irritable bowel syndrome; Amino acids; Organic acids; Short chain fatty acids; Visceral hypersensitivity

Core tip: We comprehensively assessed the clinical and psychological characteristics of irritable bowel syndrome with predominant diarrhea (IBS-D) , visceral sensitivity, and fecal metabolites. As expected, the data confirmed that metabolite compositions were different in subjects with or without IBS-D and the levels of some metabolites were significantly correlated with IBS Symptom Severity System score, visceral sensitivity, and the severity or frequency of abdominal pain. Furthermore, a potential biomarker panel was identified to correlate with the symptom severity of IBS-D. These preliminary findings provide some clues for IBS-D pathogenesis and for the search for biomarkers in symptom severity.

Citation: Zhang WX, Zhang Y, Qin G, Li KM, Wei W, Li SY, Yao SK. Altered profiles of fecal metabolites correlate with visceral hypersensitivity and may contribute to symptom severity of diarrhea-predominant irritable bowel syndrome. *World J Gastroenterol* 2019; 25(43): 6416-6429
URL: https://www.wjgnet.com/1007-9327/full/v25/i43/6416.htm
DOI: https://dx.doi.org/10.3748/wjg.v25.i43.6416

INTRODUCTION

Irritable bowel syndrome (IBS) is a highly prevalent functional bowel disorder, and is characterized by chronic abdominal pain related to disordered bowel habits without evidence of organic diseases[1,2]. Patients with IBS often have psychological disturbances and gastrointestinal symptoms, all of which decline health-related quality of life (QOL)[3,4]. As defined by the Rome IV criteria, IBS is classified into four subtypes: IBS with predominant diarrhea (IBS-D), IBS with predominant constipation, IBS with mixed bowel habits, and IBS unclassified. Among these subtypes, IBS-D accounts for 39.0%-61.9% of IBS cases[5,6] and especially impairs QOL[7]. Although the pathogenesis is complicated, dysregulation of the brain-gut axis, increased gut mucosal immune activation, increased intestinal permeability, and visceral hypersensitivity may be involved[8,9].

The gastrointestinal tract represents the largest surface to the outside world and is a

sensory organ[10]. Metabolites in the intestine, as sensory information, are communicated with the gastrointestinal innervation, enteroendocrine hormonal signaling system, immune system, and the local tissue defense system[11,12]. Previous studies have demonstrated that dietary amino acids, which regulate the expression of anti-inflammatory cytokines and pro-inflammatory cytokines, are associated with intestinal inflammation[13-19]. Moreover, amino acids played significant roles in regulating the expression of tight junction proteins, oxidative stress and the apoptosis of enterocytes[19-24], all of which were critical factors for the functions of the intestinal barrier[25,26]. However, the role of amino acids in IBS-D pathogenesis is still unclear.

An increasing number of studies have indicated that organic acids, especially short chain fatty acids (SCFA), are one of the origins of symptoms in IBS with immunological and regulatory functions[27-31]. A recent study suggested that fecal microbial metabolites induced the release of serotonin (5-HT) from enterochromaffin (EC) cells and were involved in visceral hypersensitivity through modulating sensory neurons[32]. Bellono *et al*[32] also reported that EC cells were polymodal chemosensors and were activated by multiple metabolites. In addition, targeted metabolomics, the measurement of defined groups of metabolites, provided a particularly powerful tool for synchronously quantifying multiple metabolites.

Other studies reported that metabolite compositions were different in patients with IBS from those in healthy controls (HCs)[33-35]. Only a few articles reported that some fecal metabolites were correlated with symptoms in IBS[30,36]. Nevertheless, these studies only measured several kinds of SCFA in fecal samples and did not extensively investigate the relationships between metabolites and IBS symptoms as well as visceral sensitivity.

The aims of this study were to compare fecal metabolites in subjects with or without IBS-D and to explore the associations of metabolites with clinical and experimental parameters.

MATERIALS AND METHODS

Subjects

Based on the sample size of other studies[30,35], 30 patients were recruited from outpatient clinics at a teaching hospital in Beijing, China, together with 15 age- and sex-matched HCs. Patients were eligible for the study if they were 18 years or older and met the Rome IV criteria for IBS-D. HCs were recruited from asymptomatic individuals who had undergone colorectal cancer screening or polyposis follow-up and had negative results. Subjects were excluded if they had a history of major abdominal surgery, organic diseases such as celiac disease, other painful disorders such as dysmenorrhea or psychiatric disorders or were pregnant, lactating or unable to come off any of the following medications: probiotics, antibiotics, analgesics, stool bulking agents, lactulose, prokinetics, histamine antagonists, mast cell stabilizers or antidepressants within 2 wk.

All subjects gave written informed consent before participation. The study protocol was approved by the Ethics Committee of the China-Japan Friendship Hospital (No. 2015-33).

Procedure

Sixty-one patients with IBS-D-like symptoms were referred to the gastroenterological department. Nineteen patients (31.1%) refused to participate, and 12 patients were excluded for severe mental disorder (two patients), colon mucosal inflammation (five patients), a history of abdominal surgery (two patients), lactose intolerance (two patients) and poor compliance (one patient). Finally, 30 IBS-D patients and 15 HCs were included in this study.

After enrollment, the clinical and psychological states were assessed. Then, visceral sensitivity was measured after obtaining stool samples. Each fecal sample was collected with sterile plastic tube after defecation. Samples were frozen in liquid nitrogen immediately and stored at -80 °C.

Clinical and psychological assessments

The degree of symptoms was assessed using the previously validated IBS Symptom Severity System (IBS-SSS)[37]. The total score ranged from 0 to 500 and was summed from five individual scores: Abdominal pain (severity and days of pain), abdominal distension, dissatisfaction with bowel habits and life interference. IBS-D severity was then classified as mild (75-174), moderate (175-299) or severe (300-500).

Each IBS-D patient was invited to complete an Italian modified version of the bowel disease questionnaire (BDQ) to evaluate the severity of abdominal pain during

the prior 2 wk[38]. Symptom scores ranged from 0 to 4 according to the influence of symptoms on patients' daily activities: 0, absent; 1, mild (not influencing daily activities); 2, relevant (diverting from daily activities but not urging modification); 3, severe (influencing daily activities markedly enough to urge modifications); and 4, extremely severe (precluding daily activities). Symptom frequency was also graded 0-4 (0, absent; 1, up to 1 d/wk; 2, 2 or 3 d/wk; 3, 4-6 d/wk; and 4, daily).

The Bristol Stool Form Scale (BSFS), a 7-point scale, was used to measure stool form. The Hospital Anxiety and Depression Scale, which consists of 14 items (7 anxiety items and 7 depression items), was used to evaluate the severity of anxiety and depression symptoms[39,40].

The validated Visceral Sensitivity Index (VSI) scale is a measure of anxiety specifically related to gastrointestinal sensations and symptoms[41]. It consists of 15 items with scores ranging from 0 (no gastrointestinal-specific anxiety or visceral hypersensitivity) to 5 (severe gastrointestinal-specific anxiety and visceral hypersensitivity)[42].

Visceral sensitivity test

After glycerin enema and digital rectal examination, a ManoScan™ high-resolution anorectal catheter (ANN1522) (Given Imaging, Los Angeles, CA, United States) with a latex balloon at the tip was inserted into the rectum. After three min for adapting to the catheter, the balloon was manually inflated with air at a speed of 2 mL/s, and thresholds for initial perception, urgency, and discomfort/pain were recorded[43]. A ManoScan 360™ high-resolution manometry system (Model A100) and ManoView™ AR Analysis Software 2.1 were used in the test.

Selection of fecal metabolites

Thirty-one metabolites were selected based on extensive literature search, using the following criteria: (1) Metabolites are different in subjects with or without IBS or potentially discriminate between subjects with healthy gut function and IBS patients; (2) Metabolites are related to one or more gut health parameters[44]; and (3) Metabolites can be measured in fecal samples by a targeted metabolomics method. Amino acids are associated with intestinal inflammation and barrier[45]. Organic acids, which are produced by gut microbiota, are able to modulate multiple pathological and physiological processes[30]. Based on this, lactate, pyruvate, fumarate, SCFA (i.e., acetate, propionate, butyrate, valerate, hexanoate, isobutyrate, isovalerate, and isohexanoate), and 20 amino acids making up the proteins were selected for this study.

Measurement of biomarkers

Organic acid analysis: A total of 750 μL methanol was added to fecal samples (50-150 mg), and the sample was ground for 1 min, homogenized for 30 min and centrifuged at 10000 rpm for 10 min. The fecal supernatant was transferred into a tube, and 50 mg Na_2SO_4 was added. After one night at 4 °C, the aliquot was centrifuged at 14000 rpm for 20 min, and the supernatant was retained for subsequent analyses. Similar to previous reports[46], fecal SCFA was measured by gas chromatography-mass spectrometry after derivatization reaction. Liquid chromatography-mass spectrometry was employed to quantify the levels of other organic acids, *i.e.*, lactate, pyruvate, and fumarate, as described previously[47].

Amino acid analysis: After freeze-drying, 5 mg fecal sample was added to 1 ml purified water and incubated on a shaking table for 60 min at 37 °C. The supernatant was prepared by centrifugation at 12000 rpm for 5 min. Ultra-performance liquid chromatographic analysis was performed to quantify the levels of amino acids as described by Boogers *et al*[48].

Statistical analysis

SPSS (IBM-SPSS Statistics, Chicago, IL, United States) version 21.0 was used for statistical analysis. The Gibbs sampler based left - censored missing value imputation approach (GSimp) was used to measure the metabolite levels that were below the detection limit[49]. Normally distributed data are presented as the mean ± SD, and abnormally distributed data are expressed as the median (Q1, Q3). Levels of individual metabolites were compared between groups using the Mann-Whitney *U* test. Linear correlations between multiple metabolites and IBS-SSS score, maximum tolerable threshold or BDQ scores were analyzed using multiple linear regression (stepwise). Spearman's correlation analysis was used for correlations between individual metabolites and BDQ scores. A P value ≤ 0.05 was considered to be significant.

RESULTS

Characteristics of study subjects

Thirty IBS-D patients (22 males and 8 females) and 15 HCs (11 males and 4 females) were enrolled in this study (Table 1). There were no significant differences between the groups in age (P = 0.299), sex (P = 1.00), or body mass index (P = 0.219).

In IBS-D patients, the duration of disease ranged from 0.5 to 20.5 years (median 7.5 years). According to the IBS-SSS scores (261.7 ± 40.4), 23 patients (76.7%) had moderate and 7 (23.3%) had severe IBS-D. The scores of the BSFS [IBS-D: 6.0 (6.0, 6.0), HC: 4.0 (4.0, 4.0)], anxiety [IBS-D: 6.0 (3.0, 9.0), HC: 2.0 (1.0, 4.0)] and VSI [IBS-D: 34.0 (17.0, 45.3), HC: 5.0 (2.0, 15.0)] were significantly higher in IBS-D patients than in HCs. The score of depression showed a tendency to increase in IBS-D patients but failed to reach a significant level.

Visceral sensitivity test

Three parameters for assessing visceral sensitivity, including the first sensation threshold, defecating sensation threshold, and maximum tolerable threshold to rectal distension stimulation, were measured. Scores of the defecating sensation threshold [IBS-D: 50.0 (40.0, 90.0), HC: 80.0 (60.0, 110.0); P = 0.032] and maximum tolerable threshold [IBS-D: 100.0 (80.0, 142.5), HC: 200.0 (150.0, 210.0); P < 0.001] were significantly lower in the patients than those in the HCs (Figure 1). There was no difference between the two groups in the first sensation threshold [IBS-D: 40.0 (30.0, 60.0), HC: 40.0 (30.0, 50.0); P = 0.315].

Amino acids

In the control group, Gln was detected in only one subject. Cys was detected in six IBS-D patients and in two controls. The prevalence of Gly, Glu, Thr, Ala, Val, and Leu detection was 100%, and the prevalence of detection of other amino acids ranged from 66.7% to 96.7%. There was no difference in the amount of amino acids in subjects with or without IBS-D. Differences were observed for individual amino acids including His [IBS-D: 0.0642 (0.0388, 0.1484), HC: 0.2636 (0.0780, 0.3966), P = 0.012], Ala [IBS-D: 0.5095 (0.2826, 0.9183), HC: 1.0118 (0.6135, 1.4335), P = 0.041], Tyr [IBS-D: 0.1024 (0.0173, 0.4527), HC: 0.5665 (0.2436, 1.3447), P = 0.018], Phe [IBS-D: 0.1511 (0.0775, 0.3248), HC: 0.3967 (0.1388, 0.7550), P = 0.028], and Trp [IBS-D: 0.0323 (0.0001, 0.0826), HC: 0.0834 (0.0170, 0.1759), P = 0.046] (Table 2). Only Tyr was mildly correlated with BSFS scores in all subjects (r = -0.347, P = 0.019) (Table 3). There were no statistically significant associations between BSFS scores and the levels of His, Ala, Tyr, Phe, or Trp in IBS-D group or HC group.

Organic acids

Propionate was detected in only four IBS-D patients and four controls. Acetate was not detected in five controls, and the prevalence of detection of other organic acids was 100%. Only isohexanoate [IBS-D: 0.0127 (0.0060, 0.0246), HC: 0.0070 (0.0023, 0.0106), P = 0.028] was elevated in the IBS-D patients (Table 2). The level of isobutyrate was higher in the IBS-D group than in the controls, but the difference did not reach statistical significance. There were no differences in the amounts of SCFA or organic acids in subjects with or without IBS-D (Table 2).

Correlation of fecal microbial metabolites with IBS-SSS score

A statistically significant regression equation was found (R^2_{Adjusted} = 0.693, F = 11.893, P < 0.001). The levels of fumarate and Val had a significant negative association with IBS-SSS score but hexanoate, pyruvate and Tyr had a positive association (Table 4, Figure 2A). In collinearity diagnostics, the eigenvalues and condition indices ranged from 0.071 to 3.897 and from 1.000 to 7.394, respectively (Table 5). The residual obeyed a normal distribution.

Correlation of metabolites with maximum tolerable threshold to rectal distension stimulation

After taking a root of the maximum tolerable threshold, a multiple linear regression model using the stepwise method was applied. In the control group, no metabolites were included in the regression model. In IBS-D patients, associations with isovalerate and valerate for the maximum tolerable threshold (R^2_{Adjusted} = 0.255, F = 5.957, P = 0.007) are shown in Table 6 and Figure 2B. The eigenvalues and condition indices ranged from 0.040 to 2.286 and from 1.000 to 7.580, respectively (Table 5). A lower maximum tolerable threshold was associated with increased isohexanoate in all subjects (R^2_{Adjusted} = 0.079, F = 4.789, P =0.034) (Table 6, Figure 2C). The residual also obeyed a normal distribution.

Table 1 Demographics, clinical characteristics and psychological states of study subjects

Features	IBS-D patients	Controls	*P* value
n	30	15	NA
Age (yr)	30.0 (28.0, 41.3)	28.0 (25.0, 37.0)	0.299
Gender (male:female)	22:8	11:4	1.000
Body mass index (kg/m^2)	23.8 ± 3.9	22.4 ± 2.8	0.219
Duration of disease (yr)	7.5 (1.5, 10.1)	NA	NA
IBS-SSS	261.7 ± 40.4	NA	NA
Severity of abdominal pain	1.0 (1.0, 2.0)[b]	0.0 (0.0, 0.0)	< 0.001
Frequency of abdominal pain	2.0 (1.0, 4.0)[b]	0.0 (0.0, 0.0)	< 0.001
BSFS score	6.0 (6.0,6.0)[b]	4.0 (4.0, 4.0)	< 0.001
HADS anxiety score	6.0 (3.0, 9.0)[b]	2.0 (1.0, 4.0)	0.002
HADS depression score	4.0 (1.0, 7.3)	2.0 (2.0, 5.0)	0.350
VSI score	34.0 (17.0, 45.3)[b]	5.0 (2.0, 15.0)	< 0.001

[b]$P < 0.01$ *vs* controls. The data are presented as the mean ± SD or the median (Q1, Q3). IBS-D: Irritable bowel syndrome with predominant diarrhea; IBS-SSS: IBS symptom severity scale; BSFS: Bristol stool form scale; HADS: Hospital anxiety and depression scale; VSI: Visceral sensitivity index; NA: Not applicable.

Correlation of BDQ scores with isovalerate, valerate or isohexanoate

In HCs, there was no statistically significant association between BDQ scores and isovalerate, valerate or isohexanoate levels. In the IBS-D group, Spearman's rank correlation showed that the level of isovalerate was positively correlated with the severity or frequency of abdominal pain. In addition, isohexanoate was significantly correlated with the frequency of abdominal pain in IBS-D patients (Table 7). In all subjects, only isohexanoate was significantly associated with the severity or frequency of abdominal pain (Table 7).

DISCUSSION

Overwhelming evidence has shown that luminal contents play important roles in gastrointestinal function[10,32]. Although the effects of fecal metabolites in the pathogenesis of IBS are being discovered, there has been evidence that some metabolites in feces are correlated with symptoms in IBS patients[30,36]. We comprehensively assessed the clinical and psychological characteristics of IBS-D patients, visceral sensitivity and fecal metabolites. As expected, these data confirmed the difference in fecal metabolite compositions between IBS-D patients and HCs, and the levels of some metabolites were significantly correlated with IBS-SSS score, visceral sensitivity and the severity or frequency of abdominal pain.

More male patients were recruited in our study, although the morbidity rate of IBS is significantly higher in females. The reasons were as follows: on the one hand, more female patients refused to participate due to reluctance to visceral sensitivity test or distrust. On the other hand, women with a history of dysmenorrheal or cesarean section were excluded.

His, Ala, Tyr, Phe, and Trp were decreased in IBS-D patients compared to controls and were almost unassociated with stool form. Furthermore, the amount of amino acids was not different in subjects with or without IBS. These findings revealed that differences in individual amino acids would be mainly due to differences in the amino acid composition rather than stool water content.

Amino acids in the intestine have critical roles in the expression of tight junction proteins and are closely connected with the apoptosis or proliferation of gastrointestinal epithelial cells[19-22,24,50], all of which are important factors for the functions of the intestinal barrier. Trp enhanced the expression of tight junction proteins (occluden-1, occluden-2, occludin, claudin-3, and claudin-4) in the intestine and was beneficial for mucosal growth or maintenance[51,52]. Increased intestinal permeability is one of the pathophysiological changes in IBS.

Furthermore, increased gut mucosal immune activation was also involved in IBS. Aromatic amino acids, including Trp, Phe, and Tyr, attenuated gastrointestinal inflammation[53]. Inflammatory mediators are also one of the main etiological factors in ulcerative colitis. A previous study demonstrated that Trp and His were significantly lower in ulcerative colitis patients than in controls[54]. However, the functions of amino

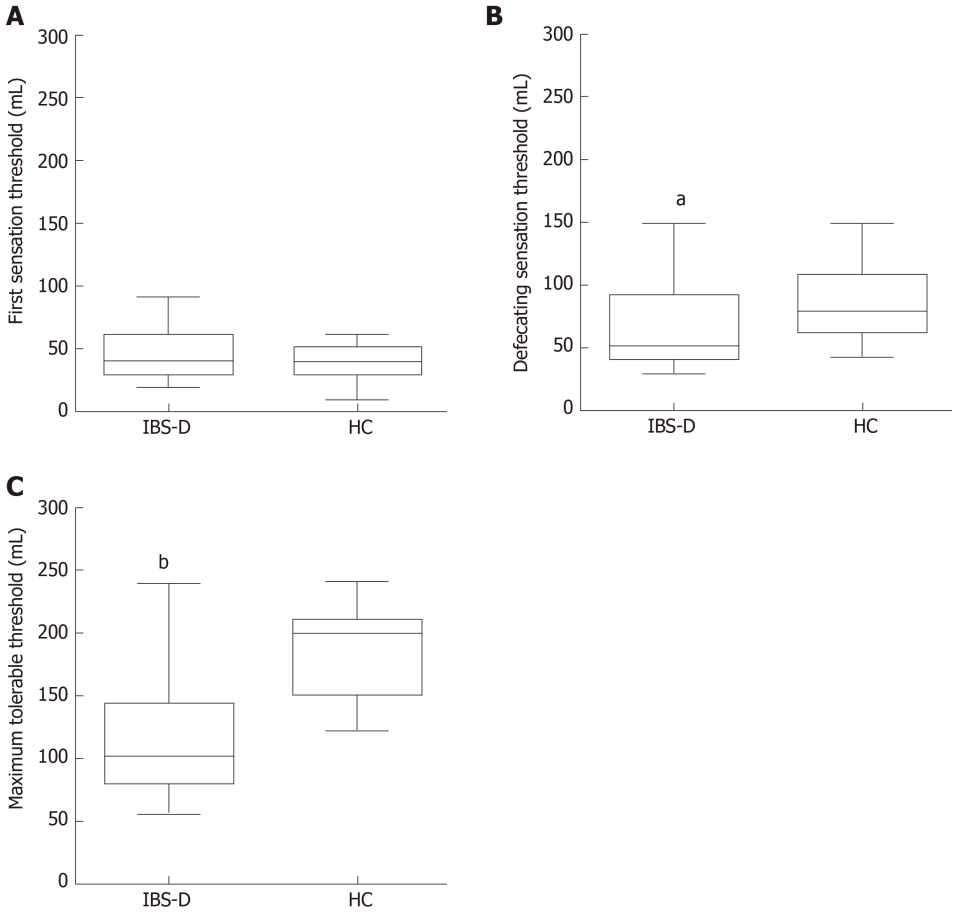

Figure 1 Visceral sensation thresholds to rectal distension stimulation. A: The first sensation threshold showed no significant difference between the two groups ($P = 0.315$). B: The score of the defecating sensation threshold was significantly decreased in the patients ($P = 0.032$). C: The maximum tolerable threshold was also lower in patients with irritable bowel syndrome with predominant diarrhea than in controls ($P < 0.001$). Box means the interquartile range; line inside the boxes indicates the median; the two whiskers indicate the 5th percentile and 95th percentile of the data. $^{a}P < 0.05$ *vs* healthy control (HC); $^{b}P < 0.01$ *vs* HC. IBS-D: Irritable bowel syndrome with predominant diarrhea; HC: Healthy control.

acids in IBS patients are still unclear. Further study is required to analyze the correlation between decreased individual amino acids and increased intestinal permeability or gut mucosal immune activation in IBS.

The association between the gut microbiota and IBS has been studied extensively. One study transplanting fecal microbiota from IBS-D patients into mice demonstrated that the microbiota played significant roles in gut function, and supported the point that bacteria would contribute to IBS[55]. The findings indicate differences in microbiota between IBS and healthy volunteers, but the results have been inconsistent[56,57]. After dietary treatment, the symptoms of IBS were controlled, but the phylotype of the intestinal microbiota remained unchanged[58]. As important as the phylotype, the function of the microbiota might add mechanistic insight[27,28,30]. The function could be measured as metabolites in the feces. SCFA, as a large group of fecal microbial metabolites, have been described as the link between the host and the microbes[29,31,59].

In this study, the association between SCFA (isohexanoate, isovalerate or valerate) and visceral sensation (abdominal pain or visceral hypersensitivity) indicates that increased chemical stimuli could be one of the origins or exacerbating factors in IBS-D. However, in IBS patients, the chemical stimuli and chemosensitivity are largely unknown. The gastrointestinal tract receives sensory innervation[10]. Some sensory neurons terminate close to the mucosal epithelium and sense chemical stimuli by connecting to enteroendocrine cells or immune cells[8,11,32,60,61]. Previous studies have shown that butyrate is increased in IBS-D patients and induces colonic hypersensitivity in rats[62,63]. However, other studies observed the conflicting results that the level of butyrate was decreased in patients or was not significantly different between patients and controls[36,59]. At the same time, there was no statistically significant association between butyrate and visceral sensation in this and other studies[36]. A recent study suggested that SCFA, especially isovalerate and isobutyrate, was involved in visceral hypersensitivity[32], which contributed to abdominal pain.

Table 2 Levels of partial fecal metabolites in irritable bowel syndrome with predominant diarrhea patients and controls

Metabolites	Prevalence of detection	IBS-D patients (μmol/g)	Controls (μmol/g)	*P* value
His	93.3%	0.0642 (0.0388, 0.1484)[a]	0.2636 (0.0780, 0.3966)	0.012
Ala	100.0%	0.5095 (0.2826, 0.9183)[a]	1.0118 (0.6135, 1.4335)	0.041
Tyr	88.9%	0.1024 (0.0173, 0.4527)[a]	0.5665 (0.2436, 1.3447)	0.018
Phe	97.8%	0.1511 (0.0775, 0.3248)[a]	0.3967 (0.1388, 0.7550)	0.028
Trp	77.8%	0.0323 (0.0001, 0.0826)[a]	0.0834 (0.0170, 0.1759)	0.046
Val	100.0%	0.2710 (0.1208, 0.5729)	0.3661 (0.2960, 1.0122)	0.079
Asp	97.8%	0.3086 (0.1797, 0.6904)	0.4875 (0.1939, 0.6591)	0.647
Fumarate	100.0%	0.0042 (0.0026, 0.0108)	0.0019 (0.0014, 0.0078)	0.051
Pyruvate	100.0%	0.0067 (0.0023, 0.0719)	0.0071 (0.0022, 0.0882)	0.718
Butyrate	100.0%	4.3819 (2.4060, 9.0920)	5.8539 (1.5193, 12.8616)	0.613
Isobutyrate	100.0%	6.8609 (0.5068, 8.9326)	2.1277 (0.5470, 10.4635)	0.962
Valerate	100.0%	0.2024 (0.0331, 0.8245)	0.2059 (0.0497, 1.2489)	0.485
Isovalerate	100.0%	0.1218 (0.0495, 0.3227)	0.1661 (0.0416, 0.2581)	0.866
Hexanoate	100.0%	0.0254 (0.0189, 0.0513)	0.0383 (0.0153, 0.0539)	0.613
Isohexanoate	100.0%	0.0127 (0.0060, 0.0246)[a]	0.0070 (0.0023, 0.0106)	0.028
Amino acids	NA	7.2873 (3.4177, 10.7709)	8.0603 (6.1393, 12.3225)	0.336
SCFA	NA	25.8082 (18.5826, 38.5067)	26.8452 (5.7182, 70.6763)	0.904
Organic acids	NA	26.6708 (20.0617, 38.5860)	26.9449 (5.8047, 71.4057)	0.866

[a]$P < 0.05$ *vs* controls. The data are presented as the median (Q1, Q3). IBS-D: Irritable bowel syndrome with predominant diarrhea; SCFA: Short chain fatty acids; NA: Not applicable.

Therefore, our current results are basically in accordance with the recent concept of visceral sensation.

The current methods of symptom-based diagnosis and the assessment of IBS severity are inherently limiting[64]. There is a pressing need for biomarkers of symptom severity and treatment response in IBS[65]. In the present study, a biomarker panel was identified to correlate with the symptom severity of IBS ($R^2_{Adjusted} = 0.693$, $P < 0.001$). This indicates a potential biomarker to objectively quantify symptom severity and assess responsiveness to treatments. However, this hypothesis needs to be verified further.

This preliminary study has some limitations. First, because only IBS-D patients were included in this study, the conclusions may not be generalized to other IBS subtypes. Second, the sample size is relatively small, which may undermine the reliability of the conclusions. Further research with a larger number of subjects should be conducted to verify our conclusions. Third, our conclusions were based on an observational study, which cannot make cause and effect inferences. Therefore, conclusions need to be further verified by high-grade evidence. Fourth, isovalerate was simultaneously positively correlated with the maximum tolerable threshold and the severity or frequency of abdominal pain. The reason for this conflict is still unclear. Finally, diet was not standardized during the study period. Habitual diet determines the repertoire of microbial metabolites[66], but food components also plays a significant role in the pathophysiology of IBS[67-69]. Although diet was not standardized in this and other studies[30,34,35], it should be noted that some food components may only relate to fecal metabolite composition but not IBS pathophysiology. It is necessary to standardize diet in the future study.

In summary, this study provides new evidence that metabolite compositions are different in subjects with or without IBS-D and altered profiles of fecal metabolites may be one of the origins or exacerbating factors in IBS-D. Furthermore, a significant correlation was observed between metabolites and symptom severity in the IBS-D group. This preliminary study lays a basis to further explore the role of fecal metabolites in IBS-D pathogenesis and to search for fecal biomarkers in symptom severity.

Table 3 Correlation of bristol stool form scale scores with the levels of His, Ala, Tyr, Phe, or Trp

Metabolites	IBS-D		Controls		All subjects	
	r	*P* value	*r*	*P* value	*r*	*P* value
His	0.057	0.764	0.423	0.117	-0.279	0.064
Ala	-0.026	0.892	0.338	0.218	-0.252	0.095
Tyr	-0.208	0.271	0.423	0.117	-0.347[1]	0.019
Phe	0.002	0.994	0.465	0.081	-0.250	0.098
Trp	-0.114	0.548	0.423	0.117	-0.268	0.075

[1]There was association between parameters ($P < 0.05$). IBS-D: Irritable bowel syndrome with predominant diarrhea.

Table 4 Multiple linear regression model for irritable bowel syndrome symptom severity scale score

Metabolites	Unstandardized coefficients		Standardized coefficients β	*t*	*P* value	Collinearity statistics	
	b	SE				Tolerance	VIF
Hexanoate[1]	116.194	29.961	0.420	3.878	0.001	0.903	1.107
Fumarate[1]	-1733.224	490.683	-0.383	-3.532	0.002	0.902	1.108
Pyruvate[1]	140.381	28.619	0.528	4.905	< 0.001	0.915	1.092
Asp	-15.303	7.943	-0.221	-1.927	0.066	0.807	1.240
Tyr[1]	60.960	15.019	0.763	4.059	< 0.001	0.300	3.333
Val[1]	-82.922	26.139	-0.626	-3.172	0.004	0.272	3.671

[1]Metabolite which was correlated with irritable bowel syndrome symptom severity scale score ($P< 0.01$); SE: Standard error; VIF: Variance inflation factor.

Table 5 Collinearity diagnostics of models

Models	Dimensions	Collinearity diagnostics	
		Eigenvalues	Condition indices
Multiple linear regression model for IBS-SSS score in IBS-D group	1	3.897	1.000
	2	1.008	1.966
	3	0.751	2.278
	4	0.643	2.462
	5	0.407	3.093
	6	0.222	4.186
	7	0.071	7.394
Multiple linear regression model for maximum tolerable threshold in IBS-D group	1	2.286	1.000
	2	0.675	1.841
	3	0.040	7.580

IBS-D: Irritable bowel syndrome with predominant diarrhea; IBS-SSS: Irritable bowel syndrome symptom severity scale score.

Table 6 Multiple linear regression model for maximum tolerable threshold

Groups	Metabolites	Unstandardized coefficients		Standar-dized coefficients β	*t*	*P* value	Collinearity statistics	
		b	SE				Tolerance	VIF
IBS-D	Isovalerate[2]	5.451	1.824	1.525	2.989	0.006	0.099	10.132
	Valerate[1]	-2.171	0.946	-1.171	-2.295	0.030	0.099	10.132
All subjects	Isohexanoate[1]	-40.910	18.695	-0.317	-2.188	0.034	NA	NA

[1]Metabolite which was correlated with maximum tolerable threshold ($P < 0.05$).
[2]Metabolite which was correlated with maximum tolerable threshold ($P < 0.01$); SE: Standard error; VIF: Variance inflation factor; IBS-D: Irritable bowel syndrome with predominant diarrhea; NA: Not applicable.

Table 7 Correlation of bowel disease questionnaire scores with isovalerate or isohexanoate

Groups	Metabolites	Frequency of abdominal pain		Severity of abdominal pain	
		r	*P* value	*r*	*P* value
IBS-D	Isovalerate	0.475[2]	0.008	0.377[1]	0.040
	Isohexanoate	0.414[1]	0.023	0.097	0.612
All subjects	Isovalerate	0.200	0.188	0.143	0.350
	Isohexanoate	0.473[2]	0.001	0.371[1]	0.012

[1]There was association between parameters ($P < 0.05$).
[2]There was association between parameters ($P < 0.01$). IBS-D: Irritable bowel syndrome with predominant diarrhea.

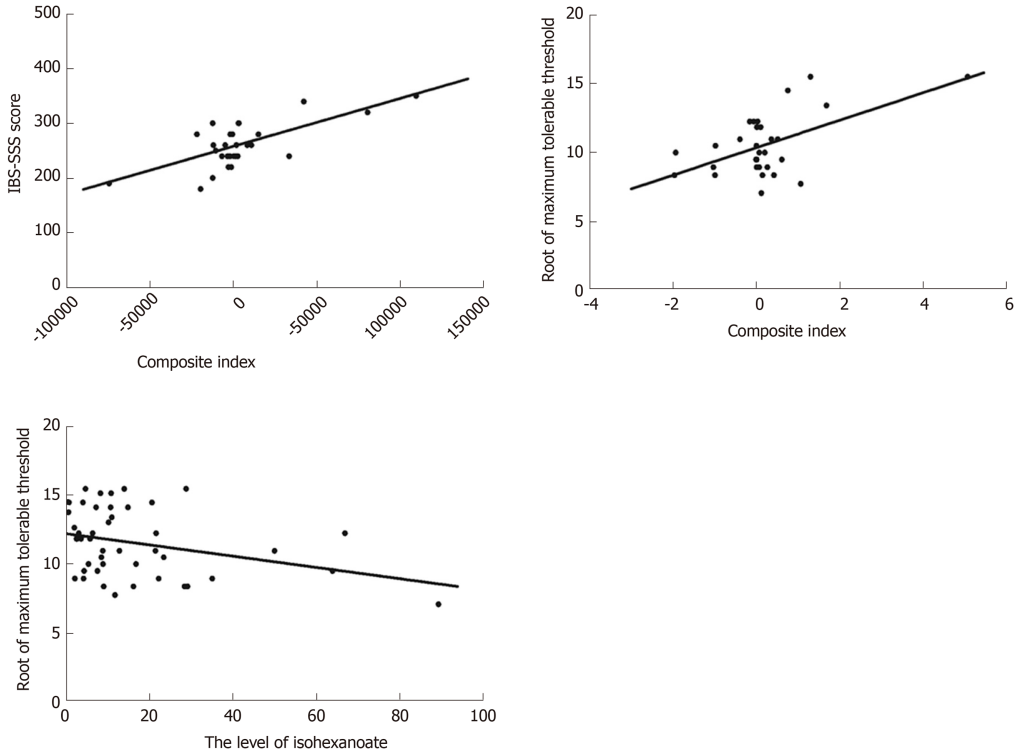

Figure 2 Correlation of fecal microbial metabolites with irritable bowel syndrome symptom severity scale score or maximum tolerable threshold. A: Correlation of fecal microbial metabolites with irritable bowel syndrome symptom severity scale score in irritable bowel syndrome with predominant diarrhea (IBS-D) patients ($R^2_{Adjusted} = 0.693$, $P < 0.001$). The composite index was the sum of score based on linear combination of metabolites using the coefficients listed in Table 4. B: Correlation of metabolites with maximum tolerable threshold in IBS-D patients ($R^2_{Adjusted} = 0.255$, $P = 0.007$); The composite index was the sum of scores based on linear combination of isovalerate and valerate using the coefficients listed in Table 6. C: Correlation of metabolites with maximum tolerable threshold in all subjects ($R^2_{Adjusted} = 0.079$, $P = 0.034$).

ARTICLE HIGHLIGHTS

Research background

Irritable bowel syndrome (IBS) is a highly prevalent functional bowel disorder and the pathogenesis is complicated. Fecal metabolites are associated with gut visceral sensitivity, mucosal immune function and intestinal barrier function, all of which have critical roles in the pathogenesis of IBS.

Research motivation

A few articles reported that patients diagnosed with IBS had metabolite compositions that were different from those of healthy controls. However, the role of metabolites in IBS pathophysiology is unclear. The study of fecal metabolites might add insight to investigate IBS.

Research objectives

IBS with predominant diarrhea (IBS-D) is the major subtype of IBS. The aims of this study were to compare fecal metabolites in subjects with or without IBS-D and to explore the associations of metabolites with clinical and experimental parameters.

Research methods

Participants underwent clinical and psychological assessments, including the IBS Symptom Severity System, an Italian modified version of the Bowel Disease Questionnaire, the Bristol Stool Form Scale, the Hospital Anxiety and Depression Scale, and the VSI, along with visceral sensitivity testing. Fecal metabolites were measured by targeted metabolomics approaches. Correlation analyses between these parameters were performed. SPSS (IBM-SPSS Statistics, Chicago, IL, United States) version 21.0 was used for statistical analysis.

Research results

The patients presented with more psychological symptoms and increased visceral hypersensitivity compared with the controls. In fecal metabolites, His, Ala, Tyr, Phe, and Trp were decreased in IBS-D patients, but isohexanoate was increased. Abdominal pain or visceral hypersensitivity was correlated with isovalerate, valerate and isohexanoate. Furthermore, a significant correlation was observed between metabolites and symptom severity.

Research conclusions

This study presented evidence that metabolite compositions were different in subjects with or without IBS-D and some metabolites might be one of the origins or exacerbating factors of symptoms *via* increasing visceral sensitivity. This study also demonstrated a possible potential biomarker panel of symptom severity. The authors believe that this study provides some clues for IBS-D pathogenesis and for the search for biomarkers in symptom severity.

Research perspectives

This preliminary study investigated the possible role of fecal metabolites in IBS pathophysiology. In the future, we will focus on the following aspects. First, as the present study did not standardize diet and could not make cause and effect inferences, conclusions need to be further verified by additional well-designed clinical and basic studies. Second, the present study focused on IBS-D patients, and the conclusions may not be generalized to other IBS subtypes. We will investigate the role of fecal metabolites in pathophysiology of other IBS subtypes in future studies.

ACKNOWLEDGEMENTS

We thank Dr. Du SY for enrollment of participants.

REFERENCES

1 **Chang L**, Toner BB, Fukudo S, Guthrie E, Locke GR, Norton NJ, Sperber AD. Gender, age, society, culture, and the patient's perspective in the functional gastrointestinal disorders. *Gastroenterology* 2006; **130**: 1435-1446 [PMID: 16678557 DOI: 10.1053/j.gastro.2005.09.071]

2 **Mearin F**, Lacy BE, Chang L, Chey WD, Lembo AJ, Simren M, Spiller R. Bowel Disorders. *Gastroenterology* 2016; **150**: 1393-1407.e5 [DOI: 10.1053/j.gastro.2016.02.031]

3 **Amouretti M**, Le Pen C, Gaudin AF, Bommelaer G, Frexinos J, Ruszniewski P, Poynard T, Maurel F, Priol G, El Hasnaoui A. Impact of irritable bowel syndrome (IBS) on health-related quality of life (HRQOL). *Gastroenterol Clin Biol* 2006; **30**: 241-246 [PMID: 16565657 DOI: 10.1016/s0399-8320(06)73160-8]

4 **Longstreth GF**, Thompson WG, Chey WD, Houghton LA, Mearin F, Spiller RC. Functional bowel disorders. *Gastroenterology* 2006; **130**: 1480-1491 [PMID: 16678561 DOI: 10.1053/j.gastro.2005.11.061]

5 **Bai T**, Xia J, Jiang Y, Cao H, Zhao Y, Zhang L, Wang H, Song J, Hou X. Comparison of the Rome IV and Rome III criteria for IBS diagnosis: A cross-sectional survey. *J Gastroenterol Hepatol* 2017; **32**: 1018-1025 [PMID: 27862281 DOI: 10.1111/jgh.13642]

6 **Ersryd A**, Posserud I, Abrahamsson H, Simrén M. Subtyping the irritable bowel syndrome by predominant bowel habit: Rome II versus Rome III. *Aliment Pharmacol Ther* 2007; **26**: 953-961 [PMID: 17767480 DOI: 10.1111/j.1365-2036.2007.03422.x]

7 **Hungin AP**, Whorwell PJ, Tack J, Mearin F. The prevalence, patterns and impact of irritable bowel syndrome: an international survey of 40,000 subjects. *Aliment Pharmacol Ther* 2003; **17**: 643-650 [PMID: 12641512 DOI: 10.1046/j.1365-2036.2003.01456.x]

8 **Fukudo S**, Nomura T, Muranaka M, Taguchi F. Brain-gut response to stress and cholinergic stimulation in irritable bowel syndrome. A preliminary study. *J Clin Gastroenterol* 1993; **17**: 133-141 [PMID: 8031340 DOI: 10.1097/00004836-199309000-00009]

9 **Kassam Z**, Collins SM, Moayyedi P. Peripheral mechanisms in irritable bowel syndrome. *N Engl J Med* 2013; **368**: 577-578 [PMID: 23388018 DOI: 10.1056/NEJMc1214185]

10 **Furness JB RL**, Cho HJ, Bravo DM, Callaghan B. The gut as a sensory organ. *Nat Rev Gastroenterol Hepatol* 2013; **10**: 729-741 [PMID: 24061204 DOI: 10.1038/nrgastro.2013.180]

11 **Artis D**. Epithelial-cell recognition of commensal bacteria and maintenance of immune homeostasis in the gut. *Nat Rev Immunol* 2008; **8**: 411-420 [PMID: 18469830 DOI: 10.1038/nri2316]

12 **Macdonald TT**, Monteleone G. Immunity, inflammation, and allergy in the gut. *Science* 2005; **307**: 1920-1925 [PMID: 15790845 DOI: 10.1126/science.1106442]

13 **Liu H**, Tan B, Huang B, Li J, Wang J, Liao P, Guan G, Ji P, Yin Y. Involvement of calcium-sensing receptor activation in the alleviation of intestinal inflammation in a piglet model by dietary aromatic amino acid supplementation. *Br J Nutr* 2018; **120**: 1321-1331 [PMID: 30375295 DOI: 10.1017/S0007114518002891]

14 **Mine Y**, Zhang H. Calcium-sensing receptor (CaSR)-mediated anti-inflammatory effects of L-amino acids in intestinal epithelial cells. *J Agric Food Chem* 2015; **63**: 9987-9995 [PMID: 26551350 DOI: 10.1021/acs.jafc.5b03749]

15 **Nagarjun S**, Dhadde SB, Veerapur VP, Thippeswamy BS, Chandakavathe BN. Ameliorative effect of chromium-d-phenylalanine complex on indomethacin-induced inflammatory bowel disease in rats. *Biomed Pharmacother* 2017; **89**: 1061-1066 [PMID: 28292014 DOI: 10.1016/j.biopha.2017.02.042]

16 **Ravindran R**, Loebbermann J, Nakaya HI, Khan N, Ma H, Gama L, Machiah DK, Lawson B, Hakimpour P, Wang YC, Li S, Sharma P, Kaufman RJ, Martinez J, Pulendran B. The amino acid sensor GCN2 controls gut inflammation by inhibiting inflammasome activation. *Nature* 2016; **531**: 523-527 [PMID: 26982722 DOI: 10.1038/nature17186]

17 **Ren W**, Zou L, Li N, Wang Y, Liu G, Peng Y, Ding J, Cai L, Yin Y, Wu G. Dietary arginine supplementation enhances immune responses to inactivated Pasteurella multocida vaccination in mice. *Br J Nutr* 2013; **109**: 867-872 [PMID: 22809580 DOI: 10.1017/S0007114512002681]

18 **Revelo XS**, Winer S, Winer DA. Starving Intestinal Inflammation with the Amino Acid Sensor GCN2. *Cell Metab* 2016; **23**: 763-765 [PMID: 27166939 DOI: 10.1016/j.cmet.2016.04.020]

19 **Song Zh**, Tong G, Xiao K, Jiao le F, Ke Yl, Hu Ch. L-cysteine protects intestinal integrity, attenuates intestinal inflammation and oxidant stress, and modulates NF-κB and Nrf2 pathways in weaned piglets after LPS challenge. *Innate Immun* 2016; **22**: 152-161 [PMID: 26921254 DOI: 10.1177/1753425916632303]

20 **Jiao N**, Wu Z, Ji Y, Wang B, Dai Z, Wu G. L-Glutamate Enhances Barrier and Antioxidative Functions in Intestinal Porcine Epithelial Cells. *J Nutr* 2015; **145**: 2258-2264 [PMID: 26338884 DOI: 10.3945/jn.115.217661]

21 **Vargas Robles H**, Castro Ochoa KF, Nava P, Silva Olivares A, Shibayama M, Schnoor M. Analyzing Beneficial Effects of Nutritional Supplements on Intestinal Epithelial Barrier Functions During Experimental Colitis. *J Vis Exp* 2017; **119**: e55095 [PMID: 28117803 DOI: 10.3791/55095]

22 **Wils-Plotz EL**, Jenkins MC, Dilger RN. Modulation of the intestinal environment, innate immune response, and barrier function by dietary threonine and purified fiber during a coccidiosis challenge in broiler chicks. *Poult Sci* 2013; **92**: 735-745 [PMID: 23436524 DOI: 10.3382/ps.2012-02755]

23 **Wu G**. Amino acids: metabolism, functions, and nutrition. *Amino Acids* 2009; **37**: 1-17 [PMID: 19301095 DOI: 10.1007/s00726-009-0269-0]

24 **Yang Y**, Li W, Sun Y, Han F, Hu CA, Wu Z. Amino acid deprivation disrupts barrier function and induces protective autophagy in intestinal porcine epithelial cells. *Amino Acids* 2015; **47**: 2177-2184 [PMID: 25287255 DOI: 10.1007/s00726-014-1844-6]

25 **Luettig J**, Rosenthal R, Barmeyer C, Schulzke JD. Claudin-2 as a mediator of leaky gut barrier during intestinal inflammation. *Tissue Barriers* 2015; **3**: e977176 [PMID: 25838982 DOI: 10.4161/21688370.2014.977176]

26 **Wells JM**, Brummer RJ, Derrien M, MacDonald TT, Troost F, Cani PD, Theodorou V, Dekker J, Méheust A, de Vos WM, Mercenier A, Nauta A, Garcia-Rodenas CL. Homeostasis of the gut barrier and potential biomarkers. *Am J Physiol Gastrointest Liver Physiol* 2017; **312**: G171-G193 [PMID: 27908847 DOI: 10.1152/ajpgi.00048.2015]

27 **Furusawa Y**, Obata Y, Fukuda S, Endo TA, Nakato G, Takahashi D, Nakanishi Y, Uetake C, Kato K, Kato T, Takahashi M, Fukuda NN, Murakami S, Miyauchi E, Hino S, Atarashi K, Onawa S, Fujimura Y, Lockett T, Clarke JM, Topping DL, Tomita M, Hori S, Ohara O, Morita T, Koseki H, Kikuchi J, Honda K, Hase K, Ohno H. Commensal microbe-derived butyrate induces the differentiation of colonic regulatory T cells. *Nature* 2013; **504**: 446-450 [PMID: 24226770 DOI: 10.1038/nature12721]

28 **Natarajan N**, Pluznick JL. From microbe to man: the role of microbial short chain fatty acid metabolites in host cell biology. *Am J Physiol Cell Physiol* 2014; **307**: C979-C985 [PMID: 25273884 DOI: 10.1152/ajpcell.00228.2014]

29 **Tan J**, McKenzie C, Potamitis M, Thorburn AN, Mackay CR, Macia L. The role of short-chain fatty acids in health and disease. *Adv Immunol* 2014; **121**: 91-119 [PMID: 24388214 DOI: 10.1016/B978-0-12-800100-4.00003-9]

30 **Tana C**, Umesaki Y, Imaoka A, Handa T, Kanazawa M, Fukudo S. Altered profiles of intestinal microbiota and organic acids may be the origin of symptoms in irritable bowel syndrome. *Neurogastroenterol Motil* 2010; **22**: 512-519 [PMID: 19903265 DOI: 10.1111/j.1365-2982.2009.01427.x]

31 **Vinolo MA**, Rodrigues HG, Nachbar RT, Curi R. Regulation of inflammation by short chain fatty acids. *Nutrients* 2011; **3**: 858-876 [PMID: 22254083 DOI: 10.3390/nu3100858]

32 **Bellono NW**, Bayrer JR, Leitch DB, Castro J, Zhang C, O'Donnell TA, Brierley SM, Ingraham HA, Julius D. Enterochromaffin Cells Are Gut Chemosensors that Couple to Sensory Neural Pathways. *Cell* 2017; **170**: 185-198.e16 [PMID: 28648659 DOI: 10.1016/j.cell.2017.05.034]

33 **Ponnusamy K**, Choi JN, Kim J, Lee SY, Lee CH. Microbial community and metabolomic comparison of irritable bowel syndrome faeces. *J Med Microbiol* 2011; **60**: 817-827 [PMID: 21330412 DOI: 10.1099/jmm.0.028126-0]

34 **Shankar V**, Homer D, Rigsbee L, Khamis HJ, Michail S, Raymer M, Reo NV, Paliy O. The networks of

human gut microbe-metabolite associations are different between health and irritable bowel syndrome. *ISME J* 2015; **9**: 1899-1903 [PMID: 25635640 DOI: 10.1038/ismej.2014.258]
35 **Shankar V**, Reo NV, Paliy O. Simultaneous fecal microbial and metabolite profiling enables accurate classification of pediatric irritable bowel syndrome. *Microbiome* 2015; **3**: 73 [PMID: 26653757 DOI: 10.1186/s40168-015-0139-9]
36 **Mujagic Z**, Tigchelaar EF, Zhernakova A, Ludwig T, Ramiro-Garcia J, Baranska A, Swertz MA, Masclee AA, Wijmenga C, van Schooten FJ, Smolinska A, Jonkers DM. A novel biomarker panel for irritable bowel syndrome and the application in the general population. *Sci Rep* 2016; **6**: 26420 [PMID: 27263852 DOI: 10.1038/srep26420]
37 **Francis CY**, Morris J, Whorwell PJ. The irritable bowel severity scoring system: a simple method of monitoring irritable bowel syndrome and its progress. *Aliment Pharmacol Ther* 1997; **11**: 395-402 [PMID: 9146781 DOI: 10.1046/j.1365-2036.1997.142318000.x]
38 **Talley NJ**, Phillips SF, Melton J, Wiltgen C, Zinsmeister AR. A patient questionnaire to identify bowel disease. *Ann Intern Med* 1989; **111**: 671-674 [PMID: 2679285 DOI: 10.7326/0003-4819-111-8-671]
39 **Bjelland I**, Dahl AA, Haug TT, Neckelmann D. The validity of the Hospital Anxiety and Depression Scale. An updated literature review. *J Psychosom Res* 2002; **52**: 69-77 [PMID: 11832252 DOI: 10.1016/s0022-3999(01)00296-3]
40 **Zigmond AS**, Snaith RP. The hospital anxiety and depression scale. *Acta Psychiatr Scand* 1983; **67**: 361-370 [PMID: 6880820 DOI: 10.1111/j.1600-0447.1983.tb09716.x]
41 **Labus JS**, Bolus R, Chang L, Wiklund I, Naesdal J, Mayer EA, Naliboff BD. The Visceral Sensitivity Index: development and validation of a gastrointestinal symptom-specific anxiety scale. *Aliment Pharmacol Ther* 2004; **20**: 89-97 [PMID: 15225175 DOI: 10.1111/j.1365-2036.2004.02007.x]
42 **Saigo T**, Tayama J, Hamaguchi T, Nakaya N, Tomiie T, Bernick PJ, Kanazawa M, Labus JS, Naliboff BD, Shirabe S, Fukudo S. Gastrointestinal specific anxiety in irritable bowel syndrome: validation of the Japanese version of the visceral sensitivity index for university students. *Biopsychosoc Med* 2014; **8**: 10 [PMID: 24655428 DOI: 10.1186/1751-0759-8-10]
43 **Zhang Y**, Qin G, Liu DR, Wang Y, Yao SK. Increased expression of brain-derived neurotrophic factor is correlated with visceral hypersensitivity in patients with diarrhea-predominant irritable bowel syndrome. *World J Gastroenterol* 2019; **25**: 269-281 [PMID: 30670915 DOI: 10.3748/wjg.v25.i2.269]
44 **Bischoff SC**. 'Gut health': a new objective in medicine? *BMC Med* 2011; **9**: 24 [PMID: 21401922 DOI: 10.1186/1741-7015-9-24]
45 **He F**, Wu C, Li P, Li N, Zhang D, Zhu Q, Ren W, Peng Y. Functions and Signaling Pathways of Amino Acids in Intestinal Inflammation. *Biomed Res Int* 2018; **2018**: 1-13 [PMID: 29682569 DOI: 10.1155/2018/9171905]
46 **Zheng X**, Qiu Y, Zhong W, Baxter S, Su M, Li Q, Xie G, Ore BM, Qiao S, Spencer MD, Zeisel SH, Zhou Z, Zhao A, Jia W. A targeted metabolomic protocol for short-chain fatty acids and branched-chain amino acids. *Metabolomics* 2013; **9**: 818-827 [PMID: 23997757 DOI: 10.1007/s11306-013-0500-6]
47 **Fiori J**, Amadesi E, Fanelli F, Tropeano CV, Rugolo M, Gotti R. Cellular and mitochondrial determination of low molecular mass organic acids by LC-MS/MS. *J Pharm Biomed Anal* 2018; **150**: 33-38 [PMID: 29216582 DOI: 10.1016/j.jpba.2017.11.071]
48 **Boogers I**, Plugge W, Stokkermans YQ, Duchateau AL. Ultra-performance liquid chromatographic analysis of amino acids in protein hydrolysates using an automated pre-column derivatisation method. *J Chromatogr A* 2008; **1189**: 406-409 [PMID: 18070624 DOI: 10.1016/j.chroma.2007.11.052]
49 **Wei R**, Wang J, Jia E, Chen T, Ni Y, Jia W. GSimp: A Gibbs sampler based left-censored missing value imputation approach for metabolomics studies. *PLoS Comput Biol* 2018; **14**: e1005973 [PMID: 29385130 DOI: 10.1371/journal.pcbi.1005973]
50 **Demehri FR**, Barrett M, Ralls MW, Miyasaka EA, Feng Y, Teitelbaum DH. Intestinal epithelial cell apoptosis and loss of barrier function in the setting of altered microbiota with enteral nutrient deprivation. *Front Cell Infect Microbiol* 2013; **3**: 105 [PMID: 24392360 DOI: 10.3389/fcimb.2013.00105]
51 **Liu W**, Mi S, Ruan Z, Li J, Shu X, Yao K, Jiang M, Deng Z. Dietary Tryptophan Enhanced the Expression of Tight Junction Protein ZO-1 in Intestine. *J Food Sci* 2017; **82**: 562-567 [PMID: 28125771 DOI: 10.1111/1750-3841.13603]
52 **Wang H**, Ji Y, Wu G, Sun K, Sun Y, Li W, Wang B, He B, Zhang Q, Dai Z, Wu Z. l-Tryptophan Activates Mammalian Target of Rapamycin and Enhances Expression of Tight Junction Proteins in Intestinal Porcine Epithelial Cells. *J Nutr* 2015; **145**: 1156-1162 [PMID: 25878205 DOI: 10.3945/jn.114.209817]
53 **Tan B**, Huang B, Wang J, Guang GP, Yang CB, Yin YL. Aromatic amino acids alleviate intestinal inflammation in piglets through calcium-sensing receptor activation. J. *ournal of Animal Science* 2017; **95**: 201-202 [DOI: 10.2527/asasann.2017.408]
54 **Xin L**, Li N, Zhu W, Wu K, Zhang L, Zhai J, Wang Y, Zhu J, Wang X, Shi Y, Li N, Sha L, Wu Z, Zhang P, Wang X. An analysis of amino acid metabolic profile and its clinical significance in ulcerative colitis. *Zhonghua Neike Zazhi* 2015; **54**: 210-213 [PMID: 26269443 DOI: 10.3760/cma.j.issn.0578-1426.2015.03.010]
55 **De Palma G**, Lynch MD, Lu J, Dang VT, Deng Y, Jury J, Umeh G, Miranda PM, Pigrau Pastor M, Sidani S, Pinto-Sanchez MI, Philip V, McLean PG, Hagelsieb MG, Surette MG, Bergonzelli GE, Verdu EF, Britz-McKibbin P, Neufeld JD, Collins SM, Bercik P. Transplantation of fecal microbiota from patients with irritable bowel syndrome alters gut function and behavior in recipient mice. *Sci Transl Med* 2017; **9** [PMID: 28251905 DOI: 10.1126/scitranslmed.aaf6397]
56 **Bennet SM**, Ohman L, Simren M. Gut microbiota as potential orchestrators of irritable bowel syndrome. *Gut Liver* 2015; **9**: 318-331 [PMID: 25918261 DOI: 10.5009/gnl14344]
57 **Dupont HL**. Review article: evidence for the role of gut microbiota in irritable bowel syndrome and its potential influence on therapeutic targets. *Aliment Pharmacol Ther* 2014; **39**: 1033-1042 [PMID: 24665829 DOI: 10.1111/apt.12728]
58 **Harvie RM**, Chisholm AW, Bisanz JE, Burton JP, Herbison P, Schultz K, Schultz M. Long-term irritable bowel syndrome symptom control with reintroduction of selected FODMAPs. *World J Gastroenterol* 2017; **23**: 4632-4643 [PMID: 28740352 DOI: 10.3748/wjg.v23.i25.4632]
59 **Treem WR**, Ahsan N, Kastoff G, Hyams JS. Fecal short-chain fatty acids in patients with diarrhea-predominant irritable bowel syndrome: in vitro studies of carbohydrate fermentation. *J Pediatr Gastroenterol Nutr* 1996; **23**: 280-286 [PMID: 8890079 DOI: 10.1097/00005176-199610000-00013]
60 **Aerssens J**, Hillsley K, Peeters PJ, de Hoogt R, Stanisz A, Lin JH, Van den Wyngaert I, Göhlmann HW, Grundy D, Stead RH, Coulie B. Alterations in the brain-gut axis underlying visceral chemosensitivity in

Nippostrongylus brasiliensis-infected mice. *Gastroenterology* 2007; **132**: 1375-1387 [PMID: 17408648 DOI: 10.1053/j.gastro.2007.02.019]

61 **Bohórquez DV**, Shahid RA, Erdmann A, Kreger AM, Wang Y, Calakos N, Wang F, Liddle RA. Neuroepithelial circuit formed by innervation of sensory enteroendocrine cells. *J Clin Invest* 2015; **125**: 782-786 [PMID: 25555217 DOI: 10.1172/JCI78361]

62 **Mortensen PB**, Andersen JR, Arffmann S, Krag E. Short-chain fatty acids and the irritable bowel syndrome: the effect of wheat bran. *Scand J Gastroenterol* 1987; **22**: 185-192 [PMID: 3033815 DOI: 10.3109/00365528708991878]

63 **Xu D**, Wu X, Grabauskas G, Owyang C. Butyrate-induced colonic hypersensitivity is mediated by mitogen-activated protein kinase activation in rat dorsal root ganglia. *Gut* 2013; **62**: 1466-1474 [PMID: 22833396 DOI: 10.1136/gutjnl-2012-302260]

64 **Ford AC**, Moayyedi P. Meta-analysis: factors affecting placebo response rate in the irritable bowel syndrome. *Aliment Pharmacol Ther* 2010; **32**: 144-158 [PMID: 20412064 DOI: 10.1111/j.1365-2036.2010.04328.x]

65 **Chang L**, Di Lorenzo C, Farrugia G, Hamilton FA, Mawe GM, Pasricha PJ, Wiley JW. Functional Bowel Disorders: A Roadmap to Guide the Next Generation of Research. *Gastroenterology* 2018; **154**: 723-735 [PMID: 29288656 DOI: 10.1053/j.gastro.2017.12.010]

66 **De Filippis F**, Pellegrini N, Vannini L, Jeffery IB, La Storia A, Laghi L, Serrazanetti DI, Di Cagno R, Ferrocino I, Lazzi C, Turroni S, Cocolin L, Brigidi P, Neviani E, Gobbetti M, O'Toole PW, Ercolini D. High-level adherence to a Mediterranean diet beneficially impacts the gut microbiota and associated metabolome. *Gut* 2016; **65**: 1812-1821 [PMID: 26416813 DOI: 10.1136/gutjnl-2015-309957]

67 **De Giorgio R**, Volta U, Gibson PR. Sensitivity to wheat, gluten and FODMAPs in IBS: facts or fiction? *Gut* 2016; **65**: 169-178 [PMID: 26078292 DOI: 10.1136/gutjnl-2015-309757]

68 **Gibson PR**, Varney J, Malakar S, Muir JG. Food components and irritable bowel syndrome. *Gastroenterology* 2015; **148**: 1158-74.e4 [PMID: 25680668 DOI: 10.1053/j.gastro.2015.02.005]

69 **Staudacher HM**, Lomer MCE, Farquharson FM, Louis P, Fava F, Franciosi E, Scholz M, Tuohy KM, Lindsay JO, Irving PM, Whelan K. A Diet Low in FODMAPs Reduces Symptoms in Patients With Irritable Bowel Syndrome and A Probiotic Restores Bifidobacterium Species: A Randomized Controlled Trial. *Gastroenterology* 2017; **153**: 936-947 [PMID: 28625832 DOI: 10.1053/j.gastro.2017.06.010]

World Journal of Gastroenterology

Submit a Manuscript: https://www.f6publishing.com

World J Gastroenterol 2019 November 21; 25(43): 6430-6439

DOI: 10.3748/wjg.v25.i43.6430

ISSN 1007-9327 (print) ISSN 2219-2840 (online)

ORIGINAL ARTICLE

Retrospective Cohort Study

Segmental intrahepatic cholestasis as a technical complication of the transjugular intrahepatic porto-systemic shunt

Julian Nikolaus Bucher, Marcus Hollenbach, Steffen Strocka, Gereon Gaebelein, Michael Moche, Thorsten Kaiser, Michael Bartels, Albrecht Hoffmeister

ORCID number: Julian Nikolaus Bucher (0000-0002-8390-2143); Marcus Hollenbach (0000-0002-2654-3164); Steffen Strocka (0000-0003-2636-3072); Gereon Gaebelein (0000-0003-3286-1991); Michael Moche (0000-0001-7091-6821); Thorsten Kaiser (0000-0003-0523-3113); Michael Bartels (0000-0001-7395-1518); Albrecht Hoffmeister (0000-0002-9913-5313).

Author contributions: Bucher JN and Hoffmeister A designed research; Bucher JN, Strocka S, Gaebelein G, Moche M, Kaiser K, and Bartels M performed research; Strocka S and Moche M contributed analytic tools; Bucher JN and Hollenbach M analyzed data; Bucher JN, Hollenbach M and Hoffmeister A wrote the paper.

Institutional review board statement: The study was reviewed and approved for publication by our Institutional Reviewer.

Informed consent statement: Not applicable, weaver of informed consent due to retrospective study, Ethical Committee consented that no informed consent statement is necessary.

Conflict-of-interest statement: There is no conflict of interest associated with any of the senior author or other co-authors contributed their efforts in this manuscript. All the authors have no conflict of interest related to the manuscript.

Julian Nikolaus Bucher, Department of Surgery, Munich University Hospital at Großhadern, Bavaria, Munich 81377, Germany

Marcus Hollenbach, Medical Department II–Gastroenterology, Hepatology, Infectious Diseases, Pulmonology, University of Leipzig Medical Center, Saxony, Leipzig 04103, Germany

Steffen Strocka, Department of Diagnostic and Interventional Radiology, University of Leipzig Medical Center, Saxony, Leipzig 04103, Germany

Gereon Gaebelein, Department of General, Visceral, Vascular and Pediatric Surgery, University of Saarland, Saarland, Homburg 66421, Germany

Michael Moche, Department of Diagnostic and Interventional Radiology, Bavaria, Nuernberg 90411, Germany

Thorsten Kaiser, Institute of Laboratory Medicine, Clinical Chemistry and Molecular Diagnostics, University of Leipzig Medical Center, Saxony, Leipzig 04310, Germany

Michael Bartels, Department for General and Visceral Surgery, Helios Park-Klinikum Leipzig, Saxony, Leipzig 04289, Germany

Albrecht Hoffmeister, Medical Department II–Gastroenterology, Hepatology, Infectious Diseases, Pulmonology, University of Leipzig Medical Center, Leipzig 04103, Saxony, Germany

Corresponding author: Marcus Hollenbach, MD, Postdoc, Senior Researcher, Senior Scientist, Gastroenterologist, Medical Department II–Gastroenterology, Hepatology, Infectious Diseases, Pulmonology, University of Leipzig Medical Center, Liebigstraße 20, Leipzig 04103, Saxony, Germany. marcus.hollenbach@web.de
Telephone: +49-341-9712362
Fax: +49-341-9712209

Abstract

BACKGROUND

Segmental intrahepatic cholestasis caused by transjugular intrahepatic portosystemic shunt (TIPS) (SIC-T), is a rare complication of this technique and only referred by case reports. Thus, we conducted a systematic, retrospective analysis to provide evidence regarding prevalence and consequences of this TIPS-induced bile duct compression.

Data sharing statement: Technical appendix, statistical code, and dataset available from the corresponding author at marcus.hollenbach@web.de.

STROBE statement: The authors have read the STROBE Statement-checklist of items, and the manuscript was prepared and revised according to the STROBE Statement-checklist of items.

Manuscript source: Unsolicited manuscript

Received: July 31, 2019
Peer-review started: July 31, 2019
First decision: August 27, 2019
Revised: September 25, 2019
Accepted: November 7, 2019
Article in press: November 7, 2019
Published online: November 21, 2019

P-Reviewer: Gencdal G, Ruiz-Margáin A, Yang L
S-Editor: Wang J
L-Editor: A
E-Editor: Ma YJ

AIM
To assess prevalence and outcome of SIC-T in a large TIPS-cohort.

METHODS
In this retrospective cohort study, we screened the institutional databases for all consecutive patients that were treated by TIPS-placement or TIPS-revision between January 2005 and August 2013. We analyzed radiologic images for signs of biliary congestion. Cases that were indicative of SIC-T were reviewed by two independent radiologists and additional patient data was collected. Descriptive statistics of patient demographics, indications for TIPS and procedural details were registered. Logistic regression analysis was performed to identify predictors for the development of SIC-T.

RESULTS
We analyzed 135 cirrhotic patients who underwent TIPS (mean age 55 years, 79% male gender). Etiology of cirrhosis was alcohol in most cases and indications for TIPS were mainly refractory ascites and recurrent variceal bleeding. TIPS revision was necessary in 31 patients. We identified 4 cases (2.9%) of SIC-T in direct proximity of the TIPS-stent. Diagnosis was confirmed by CT-scan, MRI or endoscopic retrograde cholangio pancreaticography (ERCP). In two patients TIPS was implanted via the right and in one through the medial hepatic vein. One patient received TIPS-prolongation by multiple revisions. Most patients were asymptomatic but one cholangitic abscess necessitated a transhepatic drain. Logistic regression analysis identified TIPS-placement other than from medial hepatic vein to right portal vein as risk factor (OR 21.0) for SIC-T.

CONCLUSION
SIC-T ads to (mostly late) complications in the interventional treatment of cirrhotic portal hypertensions and can lead to cholangitic abscesses. Patients, particularly with multiple interventions, should be screened for SIC-T.

Key words: Transjugular intrahepatic portosystemic shunt; Cirrhosis; Ascites; Bleeding; Cholestasis; Biliary congestion

Core tip: Segmental intrahepatic cholestasis (SIC-T) is a rare and mostly late complication of transjugular intrahepatic portosystemic shunt (TIPS). Detection of SIC-T is performed by a combination of clinical, radiological and laboratory analyses. In the majority of patients, SIC-T requires no intervention but can lead to cholangitic abscesses. SIC-T contributes to late complications of TIPS-procedure. TIPS placement other than from the medial hepatic vein is an important risk factor for SIC-T development. Patients with atypical TIPS placements should be screened for SIC-T.

Citation: Bucher JN, Hollenbach M, Strocka S, Gaebelein G, Moche M, Kaiser T, Bartels M, Hoffmeister A. Segmental intrahepatic cholestasis as a technical complication of the transjugular intrahepatic porto-systemic shunt. *World J Gastroenterol* 2019; 25(43): 6430-6439
URL: https://www.wjgnet.com/1007-9327/full/v25/i43/6430.htm
DOI: https://dx.doi.org/10.3748/wjg.v25.i43.6430

INTRODUCTION

Portal hypertension is a consequence of chronic liver disease and the main cause of morbidity and mortality in patients with cirrhosis[1]. Although conservative therapy is an effective method to reduce portal hypertension[2], the implantation of a transjugular intrahepatic portosystemic shunt (TIPS) is the treatment of choice in refractory ascites (RA) and recurrent or refractory variceal bleeding (RVB)[3]. Moreover, recent data indicate that the use of a pre-emptive TIPS in variceal bleeding should be performed in all patients with end-stage liver disease[4,5].

Despite its convincing efficacy in reducing portal hypertension, a procedure related rate of major complications varies between less than 5%[6] and up to 10%[7]. Aside from life threatening acute complications that occur in less than 2%, post-interventional hepatic encephalopathy (up to 53.9%)[8] and shunt-dysfunction (15-43.9%)[9] are more frequent after TIPS. Rare chronic complications are isolated hyperbilirubinemia[10], stent migration[11], biliary fistula[12], migration[13] and liver infarction[14]. However, the use of covered and small diameter TIPS was associated with significantly less rates of complication but comparable efficacy and is now the standard of therapy[15-17].

Another rare complications of TIPS is a segmental intrahepatic cholestasis induced by TIPS-related compression of bile ducts (SIC-T)[18]. In order to identify prevalence and consequences of SIC-T in a large cohort, we evaluated all consecutive patients who underwent TIPS implantation or TIPS-revision at our institution since 2005. Moreover, we aimed to analyze risk factors for the development of SIC-T in regression analysis and described the management of SIC-T.

MATERIALS AND METHODS

Patient selection and procedure

The study protocol conforms to the ethical guidelines of the 1975 Declaration of Helsinki and was approved by the ethical review board of the Medical Faculty of the University of Leipzig (230/19-ek, June 16th 2019). In 2013 we reported a case of a segmental intrahepatic cholestasis caused by intrahepatic bile duct compression as a consequence of the TIPS-stent[18]. Thus, all patients with TIPS were identified by screening our institutional databases. Then, all consecutive patients who were treated by TIPS-placement or revision with prolongation of formerly placed TIPS stents between January 2005 and August 2013 were included to this study. We identified 135 Patients (107 males, 28 female) that met the selection criteria. Medical records were evaluated for patient demographics including age, gender as well as etiology of cirrhosis and indication for TIPS. All patients received TIPS-implantations as recommended by current guidelines[2] and Polytetrafluorethylene-(PTFE)-covered TIPS [VIATORR® TIPS-Stents (W.L. Gore, United States)] were used in all cases. Databases were also analyzed for the used techniques (puncture from the medial, right or left hepatic vein to the right or left portal vein). Here, the implantation of TIPS from the right hepatic vein to the right portal vein was considered as typical TIPS placement as described before. Also, the route from the medial hepatic vein to the right portal vein demonstrates an equivalent alternative[19-21]. Revisions and indication for revision of TIPS were assessed and follow-up time with patient's status at the end of follow-up was evaluated.

Imaging

All patients had at least one radiological imaging (ultrasound, contrast-enhanced CT or MRI) of the liver at our institution after TIPS-placement/-prolongation. The radiological imaging was reviewed by one radiologist who screened patients with TIPS for biliary congestion. Imaging, that showed signs of biliary congestion, was reviewed by a second radiologist and the diagnosis of SIC-T was either excluded or confirmed. For the patients with SIC-T we reviewed the medical history and the laboratory parameters that were indicative of biliary congestion in between the date of SIC-T diagnosis and the last imaging without signs of SIC-T. MRI was performed with 1.5 Tesla Siemens Symphony (Siemens Healthcare, Germany). For intravenous contrast, we used Gadoxetic acid (Bayer Healthcare Pharmaceuticals, Germany).

Statistical analysis

Statistical analysis was performed with SPSS 20 (IBM, Armonk, NY, United States). Data is presented with median as well as mean with lower and upper range or presented as "*n*" with a percentage (%) to each corresponding group. Logistic regression analysis was used to evaluate possible predictor for SIC-T. A P value ≤ 0.05 was considered statistically significant with except in regression analysis (P value less than 0.01 due to multiple testing). All statistical analyses were reviewed by an institutional biomedical statistician.

RESULTS

Patient cohort

Patients' characteristics are presented in Table 1. Patients underwent 121 primary TIPS-placements and 30 TIPS-revisions (22.2%), of which in two patients multiple

revisions per patient were performed (n = 4 and n = 2). Mean age was 54 years (19-84). The most frequent liver disease was alcoholic cirrhosis (84.3%) and the most frequent indications for TIPS-placement were RA (61.5%) and RVB (28.4%). In the majority of cases, the TIPS was placed from the medial hepatic vein to the right portal branch (79.3%). In 11.1% of the cases the TIPS was placed from the right hepatic vein to the right portal branch (together 90.4% typical TIPS placement) and in 2.2% an unconventional approach was performed for anatomical reasons. In 10 patients the anatomical route for TIPS-placement was not known because TIPS-placement was performed at another institution and follow-up was conducted by ultrasound. Indications for TIPS-revisions were hepatic encephalopathy because of high shunt-flow in 8 cases (26.7%) and RA because of low shunt flow or thrombosis in 8 and 14 cases (26.7% and 46.7% respectively). At the time of screening, the median retrospective follow-up after TIPS-placement per patient was 7 mo (mean/min/max = 19/0/148). Retrospective follow-up ended because of loss to clinical follow-up due to absence from our outpatient clinic or stop of retrospective follow up at the time of screening in 99 cases (73.3%), because of death with TIPS in 20 cases (14.8%) or because of consecutive liver transplantation in 17 cases (12.6%) (see Table 1). In 6 patients (4.4%) intrahepatic cholestasis was suspected in the initial screening because of tubular structures with fluid equivalent radiodensity converging in proximity to the TIPS stent. Two of these cases were identified as a hepatic vein obstruction by the reviewing radiologist while four cases of SIC-T (2.9%) were confirmed. Logistic regression analysis showed that TIPS-placement other than from the medial hepatic vein to the right portal branch was significantly associated with the occurrence of SIC-T (odds ratio 21.0, 95%CI: 0.7-5.4, P = 0.01). In contrast, age, male gender, RVB as TIPS indication or etiology of cirrhosis other than alcohol could not be identified as predictors for SIC-T (Tables 1-3). In addition, multivariate logistic regression failed to identify prediction parameters for SICT-T (data not shown).

Medical history, imaging and management of patients with SIC-T

Patient 1 is a 59 year-old male with an alcoholic Child B cirrhosis, who received a TIPS from the right hepatic vein to the right portal branch for RA and hepatorenal syndrome (HRS). Lab values were unremarkable. One month after the procedure the patient was free of ascites and the renal function had returned to the patient's baseline. No episode of hepatic encephalopathy occurred. A contrast enhanced abdominal CT scan for routine follow-up 6 years after TIPS-Placement incidentally showed the congestion of the intrahepatic bile ducts in segment VII. An MRI with liver specific, intravenous contrast and MRCP-sequence was performed to rule out hilar neoplasia and to clearly confirm the compression of the segmental bile duct by the TIPS-stent. It also showed a late contrast washout, that was highly suspicious for a hepatocellular carcinoma (HCC) in segment VIII unrelated to the biliopathy. Observational approach of the SIC-T was performed due to absence of cholangitis. The HCC was confirmed and treated by trans-arterial chemoembolisation and no episode of cholangitis or an attributable worsening of the cholestasis has occurred. After 2 years, a contrast enhanced CT-scan showed no signs of SIC-T. Unfortunately the patient developed bone metastases and had to be taken off the transplant waiting list.

Patient 2 is a 63 year old male with alcoholic Child B cirrhosis, who received a TIPS from the right hepatic vein to the right portal vein for RA. Lab values were inconspicuous. Reduction of ascites was sufficient and no episode of hepatic encephalopathy was registered. Although initial follow-up ultrasound was inconspicuous, a new, hypoechoic structure of 50 mm × 75 mm appeared 5 years after TIPS-placement in the right liver lobe. A contrast enhanced CT-scan revealed a tubular, cystic congestion of the intrahepatic bile ducts selectively in liver segment VII. The liver parenchyma in this segment was completely extinct by congested ducts. Tumorous compression was ruled out by MRI with MRCP-sequence and the SIC-T was confirmed (see Figure 1). The patient negotiated complaints, thus an observational approach was conducted. In last follow-up, the patient was in a stable condition.

Patient 3 is a 50 year-old female with alcoholic Child C cirrhosis who received a TIPS from the medial hepatic vein to the right portal vein branch for RA and HRS. Initial ascites reduction and improvement of renal function were satisfying and hepatic encephalopathy was absent. One month after TIPS-placement, she was re-admitted with a relapse of ascites and spontaneous bacterial peritonitis (SBP). Relapse of alcoholic abuse was reported. The hydropic decompensation was caused by a low shunt flow due to a protrusion of the covered part of the portal TIPS-end that was diagnosed by TIPS-angiography. Multiple TIPS-revisions and a stent-in-TIPS procedure were performed to elongate the stent into the extrahepatic portal vein. A significant reduction of ascites and a sustained clinical stability was achieved. Follow-

Table 1 Patient demographics and clinical data of retrospectively screened cohort

Characteristic	Value
Age[1]	55 (19, 54, 84)
Female	28 (20.7)
Male	107 (79.3)
Etiology of cirrhosis	
Alcoholic	114 (84.4)
NASH	7 (5.2)
BCS	4 (3.0)
Kryptogenic	3 (2.2)
HCV	2 (1.5)
PBC	1 (0.7)
Autoimmune	1 (0.7)
Hemochromatosis	1 (0.7)
HBV	1 (0.7)
Toxic	1 (0.7)
Indications for TIPS	
RA	83 (61.5)
RVB	38 (28.4)
HRS	10 (7.5)
BCS	3 (2.2)
Others	1 (0.7)
Technique	
MHV-RPV	107 (79.3)
RHV-RPV	15 (11.1)
LHV-LPV	2 (1.5)
MHV-LPV	1 (0.7)
Unknown	10 (7.4)
Time with TIPS[2]	7 (0, 19, 148)
Revision	
No revision	105 (77.8)
1 revision	28 (20.7)
More than 1 revision	2 (1.5)
Indications for revision	
Encephalopathy	8 (26.7)
Low shunt flow	8 (26.7)
Thrombosis	14 (46.7)
End of follow-up	
Loss to follow-up	99 (73.3)
Death with TIPS	20 (14.8)
Consecutive LTx	17 (12.6)

[1]At TIPS-placement in years; median; min; mean; max;
[2]At end of screening; in months; median; min; mean; max. NASH: Non alcoholic steatohepatitis; BCS: Budd Chiari Syndrome; HCV: Hepatitis C; PBC: Primary biliary cholangits; HBV: Hepatitis B; RA: Refractory ascites; HRS: Hepatorenal syndrome; MHV: Medial hepatic vein; RPV: Right portal branch; RHV: Right hepatic vein; RVB: Refractory variceal bleeding; LHV: Left hepatic vein; LPV: Left portal branch; LTx: Liver transplantation; TIPS: Transjugular intrahepatic portosystemic shunt.

up ultrasound and CT-scan revealed a biliary congestion of the intrahepatic bile ducts in segment V converging and ending in direct proximity of the TIPS stent. By reason of elevated cholestasis parameters (sudden hyperbilirubinemia from 98 to 493 μmol/L), an endoscopic retrograde cholangio pancreaticography (ERCP) was attempted but endoscopic access to the compressed bile duct could not be achieved. Decompression and biliary drainage through percutaneous transhepatic biliary drainage was not performed because of ascites. Thus, conservative therapy with antibiotic prophylaxis was initiated because the initial clinical deterioration of patient

Table 2 Characteristics of patients presenting with segmental intrahepatic cholestasis after intervention

Patient	Age[1]	Sex	Aetiology of cirrhosis	Indication for TIPS	TIPS-type	TIPS Localisation	Congested segments	SIC-T free intervall with TIPS[2]	Time from last imaging without SIC-T suspicion[2]	MELD before SIC-T diagnosis	MELD at SIC-T diagnosis	Relevant complications
1	51	M	Alcoholic	RA & HRS	PTFE-covered	RHV-RPV	VII	72	39	11	12	None
2	55	M	Alcoholic	RA	PTFE-covered	RHV-RPV	VII	83	26	19	16	None
3	49	F	alcoholic	RA & HRS	PTFE-covered	MHV-RPV	V	17	< 1	18	22	SBP
4	44	M	BCS	RA	PTFE-covered	Atypical	I	0,4	< 1	10	9	Hepatic abscess

[1]At TIPS-placement in years;
[2]In months. M: Male; F: Female; BCS: Budd Chiari Syndrome; RA: Therapy refractory ascites; HRS: Hepatorenal syndrome; PTFE: Polytetrafluorethylen; MHV: Medial hepatic vein; RHV : Right hepatic vein; RPV: Right portal branch; SIC-T: Segmental intrahepatic cholestasis caused by intrahepatic bile duct compression by the TIPS-stent; MELD: Model of endstage liverdisease; SBP: Spontaneous bacterial peritonitis; TIPS: Transjugular intrahepatic portosystemic shunt.

3 was rather attributable to the development of SBP and the relapsing alcohol abuse than to the SIC-T. The patient was discharged but unfortunately, the patient did not keep follow-up appointment due to continued alcohol abuse.

Patient 4 is a 44 year-old male with a Child B cirrhosis and Budd-Chiari syndrome. A first TIPS-attempt in another hospital for RA failed because of an atypical portal and hepatic venous anatomy. A single hepatic vein drained mainly the right liver lobe with multiple collaterals combined with an atypical portal-venous anatomy. A TIPS-placement was achieved through an atypical approach from the sole right hepatic vein into an atypically located portal branch. Ascites reduction was acceptable and the patient did not suffer from hepatic encephalopathy. Nevertheless, lab values showed increased inflammatory markers and a subtle but relevant peak in bilirubin (22.3 μmol/L), alkaline phosphatase (AP) and gamma-glutamyl transferase (gGT) (peak at 5.2 and 2.9 μkat/L). CT-scan indicated a segmental cholestasis and a cholangitic abscess in liver segment I that was treated with a percutaneous drain. Antibiotics were prescribed. An angiography of the drain showed a connection of the abscess with the segmental bile duct that appeared to be compressed by the TIPS-Stent (see Figure 2). A consecutively performed ERCP showed an abrupt ending of the segment I bile duct next to the TIPS-stent but internal stent-placement was not possible. Nevertheless, hilar neoplasia could be excluded. Lab values decreased at baseline levels after two weeks. Further follow-up was unremarkable.

Details of the patients with SIC-T can be found in Table 2. Additionally, all patients were instructed in detail about signs and symptoms of cholangitis and the necessity to urgently admit in our emergency room if these were present.

DISCUSSION

TIPS-placement is a well-established option to treat complications of portal hypertension secondary to cirrhosis[1]. Major complications related to the TIPS-procedure occur in 5 up to 10%[7] and minor complications in up to 53% of the cases. These can be stratified into acute complications through accidental damage of hepatic structures resulting in vascular occlusion, hemorrhage or bile-leak. Chronic complications result from the partial liver bypass or a progressive tissue proliferation that lead to stent occlusion[8,11,12]. In most cases chronic complications develop after an initial clinical improvement whereas acute challenges mostly present with immediate symptoms.

We described a segmental intrahepatic cholestasis as a new type of TIPS-related complication as case report before[18]. In our current study, we identified in our TIPS-cohort 4 cases of segmental intrahepatic cholestasis caused by the TIPS-stent (SIC-T), which can be assigned to the group of complications that result from damage of intrahepatic structures, yet in case of SIC-T without causing immediate symptoms in

Table 3 Univariate regression analysis for prediction of segmental intrahepatic cholestasis

Variable	OR	Univariate 95%CI	*P* value
Age	0.96	-0.1 - 0.1	0.40
Male gender	0.78	-2.6 - 2.1	0.83
Other than alcoholic cirrhosis	0.54	-2.9 - 1.7	0.60
RVB as TIPS indication	< 0.01	-5654.8 - 5620.0	0.99
TIPS placement other than MHV-RPV	21.0	0.7 - 5.4	0.01

RVB: Recurrent variceal bleeding; MHV: Medial hepatic vein; RPV: Right portal branch.

the majority of the patients. SIC-T can be defined as segmental cholestasis due to the mechanical obstruction of intrahepatic biliary branches by the stent graft after TIPS-procedure. This resulted in the significant congestion of the biliary system proximal to the obstructed intrahepatic bile duct in all identified cases.

In our retrospective analysis, SIC-T was detected with a relevant prevalence at our center (2.9%). Most cases could only be identified by a detailed review of the whole population that was treated with a TIPS or a TIPS-revision. Moreover, SIC-T was a late complication of TIPS (time from TIPS to SIC-T up to 83 mo). The reason for the delayed diagnosis could be explained on the one hand by the absence of distinct symptoms or conspicuous lab values in the majority of the cases (3 out of 4 cases; 75%) and on the other hand in the long period from TIPS-placement to development of SIC-T. Even in patients with regularly follow-up imaging, the interval from last inconspicuous imaging to diagnosis of SIC-T was up to 39 mo. However, one patient developed a cholangitic abscess immediate after onset of a symptomatic SIC-T and its severe clinical course. Remarkably, the TIPS-placement in this case was performed by an unconventional approach from one single hepatic vein to an atypically situated right portal branch because of anatomic variation. Consecutively, this results in a rather straight and central direction of the TIPS stent, which is suspected to have caused the interference with the segment I bile duct. In 3 out of 4 patients with SIC-T, TIPS-placement could not be performed out of the preferred medial hepatic vein. This finding was confirmed in the logistic regression analysis that identified TIPS-placement other than from medial hepatic vein as significant risk factor for SIC-T (OR 21.0). We are aware, that the preferred TIPS route in most centers is from the right hepatic vein to the right portal vein as described before[19,20] and is seen as the standard of procedure. Nevertheless, a TIPS placement from the medial hepatic vein to the right portal vein is an accepted alternative with equal results[21]. Moreover, our data also indicate that the MHV-RPV route might help to prevent the occurrence of SIC-T.

The pathophysiological etiology for the development of (late) SIC-T remains multifactorial and not elucidated yet. Three patients (1-3) had multiple unsuspicious imaging including contras-enhanced CT-scan between TIPS-placement and the detection of SIC-T. Thus, the biliopathy must have developed several months after TIPS-placement in the majority of the patients. Other factors that can lead to a segmental biliary congestion such as portal hypertensive biliopathy, cavernoma or tumor were ruled out by CT, MRI or ERCP. A combined interplay of a mechanical compression, ischemia through compression of the segmental artery or tissue encasement through a proliferative stimulus is assumable. Also, one could hypothesize that SIC-T will result from stent placement through the segmental bile duct. Before the use of covered stents, this would have resulted in a biliary fistula as previously described[12]. In this regard, again an atypical TIPS-placement is very likely to be associated with SIC-T. Moreover, other factors that could influence a TIPS-induced compression of the bile ducts or liver tissue, for instance the diameter of dilation or the length of the TIPS, but were not analyzed in our cohort. In addition, transient bacteremia during TIPS-implantation or pathologies of the bile duct system should also be considered to contribute to SIC-T.

However, our analysis showed some limitations. First this is a retrospective analysis and in the most patients with SIC-T no interventions was needed (but one cholangitic abscess). Moreover, statistical analysis was based on 4 cases with SIC-T that could have impacted the results as a consequence of a low patient number.

In conclusion, the unusual etiology of segmental intrahepatic cholestasis caused by intrahepatic bile duct compression due to TIPS-stent ads, with a remarkable prevalence of 2.9%, to the variety of TIPS-related complications. Furthermore, SIC-T could be relevant for the management of the affected patients and may lead to cholangitic abscesses. Therefore, we propose that TIPS-patients, in particular with TIPS-placement other than from the medial hepatic vein or multiple interventions,

Figure 1 Transversal T2w magnetic resonance imaging of the liver of patient 2 who presented with segmental intrahepatic cholestasis caused by intrahepatic bile duct compression after transjugular intrahepatic portosystemic shunt. The arrow indicates the intrahepatic portion of the stent. Note the tubular structure with fluid typical high T2w signal converging in direct proximity of the transjugular intrahepatic portosystemic shunt which represents the congested, intrahepatic bile ducts of liver segment VII. The segments' liver parenchyma is completely extinct by the dilated ducts. Other causes for bile duct obstruction were ruled out by T1w with liver specific contrast.

should be screened for SIC-T in their routine follow-ups.

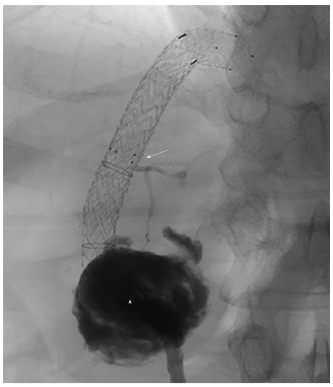

Figure 2 Angiography after contrast-injection through the interventional drain in patient 4. The abscess (triangle) is filled with contrast agent. The abscess is connected with the segmental bile duct (segment I) that is interrupted by the transjugular intrahepatic portosystemic shunt-stent as indicated by the arrowhead.

ARTICLE HIGHLIGHTS

Research background

Transjugular intrahepatic portosystemic shunt (TIPS) is an accepted and emerging intervention in ascites and variceal bleeding related to portal hypertension. Several complications have been described so far but a segmental intrahepatic cholestasis caused by TIPS (SIC-T) was only described as case report so far.

Research motivation

We aimed to perform a retrospective cohort analysis to obtain prevalence and consequences of SIC-T.

Research objectives

Our analysis aimed at prevalence, outcome and risk factors for development of SIC-T.

Research methods

This is a monocentric restrospective cohort analysis. All TIPS patients between January 2005 and August 2013 were screened for signs of biliary congestion. Cases that were conspicuous for SIC-T were reviewed by two independent radiologists. Patients data and procedural details were registered. Logistic regression analysis was performed to identify predictors for the development of SIC-T.

Research results

Out of 135 cirrhotic TIPS patients we identified 4 cases (2.9%) of SIC-T in direct proximity of the TIPS-stent. Main indications for TIPS were refractory ascites and variceal bleeding. Most patients were asymptomatic but one patient suffered from a cholangitic abscess. Logistic regression analysis identified TIPS-placement other than from medial hepatic vein to right portal vein as risk factor (OR 21.0) for SIC-T.

Research conclusions

SIC-T is a relatively rare and late complication of TIPS. Most patient do not require an intervention but severe infectious complications can occur. Patients with multiple interventions or atypical TIPS implantation should be screened for SIC-T.

Research perspectives

Future studies analyzing safety and complications of TIPS should include SIC-T as possible late complication of TIPS.

ACKNOWLEDGEMENTS

We acknowledge support from Universität Leipzig within the program of Open Access Publishing.

REFERENCES

1 **European Association for the Study of the Liver**. EASL clinical practice guidelines on the management of ascites, spontaneous bacterial peritonitis, and hepatorenal syndrome in cirrhosis. *J Hepatol* 2010; **53**: 397-417 [PMID: 20633946 DOI: 10.1016/j.jhep.2010.05.004]

2 **Boyer TD**, Haskal ZJ; American Association for the Study of Liver Diseases. The Role of Transjugular

Intrahepatic Portosystemic Shunt (TIPS) in the Management of Portal Hypertension: update 2009. *Hepatology* 2010; **51**: 306 [PMID: 19902484 DOI: 10.1002/hep.23383]

3 **Fagiuoli S**, Bruno R, Debernardi Venon W, Schepis F, Vizzutti F, Toniutto P, Senzolo M, Caraceni P, Salerno F, Angeli P, Cioni R, Vitale A, Grosso M, De Gasperi A, D'Amico G, Marzano A; AISF TIPS Special Conference. Consensus conference on TIPS management: Techniques, indications, contraindications. *Dig Liver Dis* 2017; **49**: 121-137 [PMID: 27884494 DOI: 10.1016/j.dld.2016.10.011]

4 **Hernández-Gea V**, Procopet Procopet B, Giráldez Á, Amitrano L, Villanueva C, Thabut D, Ibañez-Samaniego L, Silva-Junior G, Martinez J, Genescà J, Bureau C, Trebicka J, Llop E, Laleman W, Palazon JM, Castellote J, Rodrigues S, Gluud LL, Noronha Ferreira C, Barcelo R, Cañete N, Rodríguez M, Ferlitsch A, Mundi JL, Gronbaek H, Hernández-Guerra M, Sassatelli R, Dell'Era A, Senzolo M, Abraldes JG, Romero-Gómez M, Zipprich A, Casas M, Masnou H, Primignani M, Krag A, Nevens F, Calleja JL, Jansen C, Robic MA, Conejo I, Catalina MV, Albillos A, Rudler M, Alvarado E, Guardascione MA, Tantau M, Bosch J, Torres F, Garcia-Pagán JC;. International Variceal Bleeding Observational Study Group and Baveno Cooperation. Preemptive-TIPS Improves Outcome in High-Risk Variceal Bleeding: An Observational Study. *Hepatology* 2019; **69**: 282-293 [PMID: 30014519 DOI: 10.1002/hep.30182]

5 **García-Pagán JC**, Caca K, Bureau C, Laleman W, Appenrodt B, Luca A, Abraldes JG, Nevens F, Vinel JP, Mössner J, Bosch J; Early TIPS (Transjugular Intrahepatic Portosystemic Shunt) Cooperative Study Group. Early use of TIPS in patients with cirrhosis and variceal bleeding. *N Engl J Med* 2010; **362**: 2370-2379 [PMID: 20573925 DOI: 10.1056/NEJMoa0910102]

6 **Bettinger D**, Schultheiss M, Boettler T, Muljono M, Thimme R, Rössle M. Procedural and shunt-related complications and mortality of the transjugular intrahepatic portosystemic shunt (TIPSS). *Aliment Pharmacol Ther* 2016; **44**: 1051-1061 [PMID: 27670147 DOI: 10.1111/apt.13809]

7 **Rodrigues SG**, Sixt S, Abraldes JG, De Gottardi A, Klinger C, Bosch J, Baumgartner I, Berzigotti A. Systematic review with meta-analysis: portal vein recanalisation and transjugular intrahepatic portosystemic shunt for portal vein thrombosis. *Aliment Pharmacol Ther* 2019; **49**: 20-30 [PMID: 30450634 DOI: 10.1111/apt.15044]

8 **Dissegna D**, Sponza M, Falleti E, Fabris C, Vit A, Angeli P, Piano S, Cussigh A, Cmet S, Toniutto P. Morbidity and mortality after transjugular intrahepatic portosystemic shunt placement in patients with cirrhosis. *Eur J Gastroenterol Hepatol* 2019; **31**: 626-632 [PMID: 30550458 DOI: 10.1097/MEG.0000000000001342]

9 **Bureau C**, Garcia Pagan JC, Layrargues GP, Metivier S, Bellot P, Perreault P, Otal P, Abraldes JG, Peron JM, Rousseau H, Bosch J, Vinel JP. Patency of stents covered with polytetrafluoroethylene in patients treated by transjugular intrahepatic portosystemic shunts: long-term results of a randomized multicentre study. *Liver Int* 2007; **27**: 742-747 [PMID: 17617116 DOI: 10.1111/j.1478-3231.2007.01522.x]

10 **Rouillard SS**, Bass NM, Roberts JP, Doherty CA, Gee L, Bacchetti P, Somberg KA. Severe hyperbilirubinemia after creation of transjugular intrahepatic portosystemic shunts: natural history and predictors of outcome. *Ann Intern Med* 1998; **128**: 374-377 [PMID: 9490598 DOI: 10.7326/0003-4819-128-5-199803010-00006]

11 **Silva RF**, Arroyo PC, Duca WJ, Silva AA, Reis LF, Cabral CM, Sgnolf A, Domingues RB, Barao GT, Coelho DJ, Deberaldini M, Felício HC, Silva RC. Complications following transjugular intrahepatic portosystemic shunt: a retrospective analysis. *Transplant Proc* 2004; **36**: 926-928 [PMID: 15194319 DOI: 10.1016/j.transproceed.2004.03.117]

12 **Freedman AM**, Sanyal AJ, Tisnado J, Cole PE, Shiffman ML, Luketic VA, Purdum PP, Darcy MD, Posner MP. Complications of transjugular intrahepatic portosystemic shunt: a comprehensive review. *Radiographics* 1993; **13**: 1185-1210 [PMID: 8290720 DOI: 10.1148/radiographics.13.6.8290720]

13 **Paterno F**, Khan A, Cavaness K, Asolati M, Campsen J, McKenna GJ, Onaca N, Ruiz R, Trotter J, Klintmalm GB. Malpositioned transjugular intrahepatic portosystemic shunt in the common hepatic duct leading to biliary obstruction and liver transplantation. *Liver Transpl* 2011; **17**: 344-346 [PMID: 21384518 DOI: 10.1002/lt.22255]

14 **Mayan H**, Kantor R, Rimon U, Golubev N, Heyman Z, Goshen E, Shalmon B, Weiss P. Fatal liver infarction after transjugular intrahepatic portosystemic shunt procedure. *Liver* 2001; **21**: 361-364 [PMID: 11589774 DOI: 10.1034/j.1600-0676.2001.210510.x]

15 **Sauerbruch T**, Mengel M, Dollinger M, Zipprich A, Rössle M, Panther E, Wiest R, Caca K, Hoffmeister A, Lutz H, Schoo R, Lorenzen H, Trebicka J, Appenrodt B, Schepke M, Fimmers R; German Study Group for Prophylaxis of Variceal Rebleeding. Prevention of Rebleeding From Esophageal Varices in Patients With Cirrhosis Receiving Small-Diameter Stents Versus Hemodynamically Controlled Medical Therapy. *Gastroenterology* 2015; **149**: 660-8.e1 [PMID: 25989386 DOI: 10.1053/j.gastro.2015.05.011]

16 **Schepis F**, Vizzutti F, Garcia-Tsao G, Marzocchi G, Rega L, De Maria N, Di Maira T, Gitto S, Caporali C, Colopi S, De Santis M, Arena U, Rampoldi A, Airoldi A, Cannavale A, Fanelli F, Mosconi C, Renzulli M, Agazzi R, Nani R, Quaretti P, Fiorina I, Moramarco L, Miraglia R, Luca A, Bruno R, Fagiuoli S, Golfieri R, Torricelli P, Di Benedetto F, Belli LS, Banchelli F, Laffi G, Marra F, Villa E. Under-dilated TIPS Associate With Efficacy and Reduced Encephalopathy in a Prospective, Non-randomized Study of Patients With Cirrhosis. *Clin Gastroenterol Hepatol* 2018; **16**: 1153-1162.e7 [PMID: 29378312 DOI: 10.1016/j.cgh.2018.01.029]

17 **Li YH**, Xu ZY, Wu HM, Yang LH, Xu Y, Wu XN, Wan YM. Long-term shunt patency and overall survival of transjugular intrahepatic portosystemic shunt placement using covered stents with bare stents versus covered stents alone. *Clin Radiol* 2018; **73**: 580-587 [PMID: 29475551 DOI: 10.1016/j.crad.2018.01.014]

18 **Karlas T**, Hoffmeister A, Fuchs J, Tröltzsch M, Keim V. Bile duct obstruction after transjugular intrahepatic portosystemic shunt implantation. *Endoscopy* 2013; **45** Suppl 2 UCTN: E47-E48 [PMID: 23526512 DOI: 10.1055/s-0032-1325898]

19 **Rössle M**, Haag K, Ochs A, Sellinger M, Nöldge G, Perarnau JM, Berger E, Blum U, Gabelmann A, Hauenstein K. The transjugular intrahepatic portosystemic stent-shunt procedure for variceal bleeding. *N Engl J Med* 1994; **330**: 165-171 [PMID: 8264738 DOI: 10.1056/NEJM199401203300303]

20 **Rössle M**, Ochs A, Gülberg V, Siegerstetter V, Holl J, Deibert P, Olschewski M, Reiser M, Gerbes AL. A comparison of paracentesis and transjugular intrahepatic portosystemic shunting in patients with ascites. *N Engl J Med* 2000; **342**: 1701-1707 [PMID: 10841872 DOI: 10.1056/NEJM200006083422303]

21 **Rössle M**. TIPS: 25 years later. *J Hepatol* 2013; **59**: 1081-1093 [PMID: 23811307 DOI: 10.1016/j.jhep.2013.06.014]

World Journal of Gastroenterology

Submit a Manuscript: https://www.f6publishing.com

World J Gastroenterol 2019 November 21; 25(43): 6440-6450

DOI: 10.3748/wjg.v25.i43.6440

ISSN 1007-9327 (print) ISSN 2219-2840 (online)

ORIGINAL ARTICLE

Retrospective Study

Serum amyloid A levels in patients with liver diseases

Zi-Ying Yuan, Xing-Xin Zhang, Yu-Jing Wu, Zhi-Ping Zeng, Wei-Min She, Shi-Yao Chen, Yuan-Qing Zhang, Jin-Sheng Guo

ORCID number: Zi-Ying Yuan (0000 0001 5899 8705); Xing-Xin Zhang (0000-0003-3327-7316); Yu-Jing Wu (0000-0001-6339-4631); Zhi-Ping Zeng (0000-0001-5713-2221); Wei-Min She (0000-0002-8583-0358); Shi-Yao Chen (0000-0002-0873-9198); Yuan-Qing Zhang (0000-0002-6815-2147); Jin-Sheng Guo (0000-0002-9980-8725).

Author contributions: Guo JS designed the research; Yuan ZY and Zhang XX performed the research; Wu YJ, Zeng ZP, She WM, and Zhang YQ contributed to data collection; Yuan ZY, Zhang XX and Chen SY analyzed the data; Yuan ZY and Guo JS wrote the paper.

Supported by the National Natural Science Foundation of China, No. 91129705, No. 81070340, and No. 30570825; and Science and Technology Commission of Shanghai Municipality, Shanghai Pujiang Talent Program, No. 09PJ1402600.

Institutional review board statement: This research was approved by Ethics Committee of Zhongshan Hospital Affiliated to Fudan University.

Informed consent statement: Informed consent was obtained from all subjects.

Conflict-of-interest statement: All authors declare that they have no conflicts of interest to disclose.

Data sharing statement: Data are available from the corresponding author at guo.jinsheng@zs-hospital.sh.cn.

Zi-Ying Yuan, Xing-Xin Zhang, Yu-Jing Wu, Zhi-Ping Zeng, Wei-Min She, Shi-Yao Chen, Jin-Sheng Guo, Department of Gastroenterology and Hepatology, Zhongshan Hospital, Fudan University, Shanghai 200032, China

Zi-Ying Yuan, Xing-Xin Zhang, Yu-Jing Wu, Zhi-Ping Zeng, Wei-Min She, Shi-Yao Chen, Jin-Sheng Guo, Shanghai Institute of Liver Diseases, Shanghai 200032, China

Zi-Ying Yuan, Department of Gastroenterology, Peking University Third Hospital, Beijing 100191, China

Yuan-Qing Zhang, The First Affiliated Hospital, Yunnan Institute of Digestive Disease, Kunming Medical University, Kunming 650000, Yunnan Province, China

Corresponding author: Jin-Sheng Guo, MD, PhD, Chief Physician of Medicine, Department of Gastroenterology and Hepatology, Zhongshan Hospital, Fudan University, Shanghai Institute of Liver Diseases, 180 Fenglin Road, Shanghai 200032, China.
guo.jinsheng@zs-hospital.sh.cn
Telephone: +86-21-64041990-2424
Fax: +86-21-64038472

Abstract

BACKGROUND

Serum amyloid A (SAA) is an acute phase protein mainly synthesized by the liver. SAA induces inflammatory phenotype and promotes cell proliferation in activated hepatic stellate cells, the major scar forming cells in the liver. However, few studies have reported on the serum levels of SAA in human liver disease and its clinical significance in various liver diseases.

AIM

To investigate the serum levels of SAA in patients with different liver diseases and analyze the factors associated with the alteration of SAA levels in chronic hepatitis B (CHB) patients.

METHODS

Two hundred and seventy-eight patients with different liver diseases and 117 healthy controls were included in this study. The patients included 205 with CHB, 22 with active autoimmune liver disease (AILD), 21 with nonalcoholic steatohepatitis (NASH), 14 with drug-induced liver injury (DILI), and 16 with pyogenic liver abscess. Serum levels of SAA and other clinical parameters were collected for the analysis of the factors associated with SAA level. Mann-Whitney *U* test was used to compare the serum SAA levels of patients with various liver diseases with those of healthy controls. Bonferroni test was applied for post hoc

Manuscript source: Unsolicited manuscript

Received: June 24, 2019
Peer-review started: June 26, 2019
First decision: August 28, 2019
Revised: September 23, 2019
Accepted: November 7, 2019
Article in press: November 7, 2019
Published online: November 21, 2019

P-Reviewer: Ciccone MM, Gencdal G
S-Editor: Gong ZM
L-Editor: Wang TQ
E-Editor: Ma YJ

comparisons to control the probability of type 1 error (alpha = 0.05/6 = 0.008). For statistical tests of other variables, $P < 0.05$ was considered statistically significant. Statistically significant factors determined by single factor analysis were further analyzed by binary multivariate logistic regression analysis.

RESULTS

All patients with active liver diseases had higher serum SAA levels than healthy controls and the inactive CHB patients, with the highest SAA level found in patients with pyogenic liver abscess (398.4 ± 246.8 mg/L). Patients with active AILD (19.73 ± 24.81 mg/L) or DILI (8.036 ± 5.685 mg/L) showed higher SAA levels than those with active CHB (6.621 ± 6.776 mg/L) and NASH (6.624 ± 4.891 mg/L). Single ($P < 0.001$) and multivariate logistic regression analyses ($P = 0.039$) for the CHB patients suggested that patients with active CHB were associated with an SAA serum level higher than 6.4 mg/L. Serum levels of SAA and CRP (C-reactive protein) were positively correlated in patients with CHB ($P < 0.001$), pyogenic liver abscess ($P = 0.045$), and active AILD ($P = 0.02$). Serum levels of SAA (0.80-871.0 mg/L) had a broader fluctuation range than CRP (0.30-271.3 mg/L).

CONCLUSION

Serum level of SAA is a sensitive biomarker for inflammatory activity of pyogenic liver abscess. It may also be a weak marker reflecting milder inflammatory status in the liver of patients with CHB and other active liver diseases.

Key words: Serum amyloid A; Liver diseases; Pyogenic liver abscess; Chronic hepatitis B; Inflammation

Core tip: Serum amyloid A (SAA) is an acute phase protein known to have diagnostic and prognostic value in many diseases. However, the SAA level and its clinical significance in various liver diseases have not been reported. Our study found that serum level of SAA is a sensitive biomarker for inflammatory activity of pyogenic liver abscess, and to a less extent, to reflect mild inflammatory status in autoimmune liver diseases, drug-induced liver injury, chronic active hepatitis B, and nonalcoholic steatohepatitis. Serum level of SAA can be confounded by various inflammatory diseases, thus it is not a specific indicator for certain diseases.

Citation: Yuan ZY, Zhang XX, Wu YJ, Zeng ZP, She WM, Chen SY, Zhang YQ, Guo JS. Serum amyloid A levels in patients with liver diseases. *World J Gastroenterol* 2019; 25(43): 6440-6450
URL: https://www.wjgnet.com/1007-9327/full/v25/i43/6440.htm
DOI: https://dx.doi.org/10.3748/wjg.v25.i43.6440

INTRODUCTION

Serum amyloid A (SAA) is an acute phase protein mainly synthesized by the liver[1]. SAA1 and SAA2 are the major isoforms of acute phase SAA (A-SAA) in humans, which act on various receptors and signal pathways that participate in the pathological process of various diseases, with inflammatory, immune regulatory, and anti-microbial effects[1]. The increase of SAA level is not only a consequence of inflammation or tissue injury stimulated by inflammatory cytokines and mediators[2-4], but also acts as a promoting factor by itself to intensify disease processes. SAA was found to activate formyl peptide receptor 2 (FPR2)[5] and Toll like receptors (TLRs)[6,7] to exert chemotactic effects, and also to promote the synthesis and secretion of other inflammatory factors[1]. The serum level of SAA fluctuates with the severity of inflammation in many diseases such as amyloidosis[8], chronic obstructive pulmonary disease[9,10], rheumatoid arthritis[3,11], atherosclerosis[12], inflammatory bowel disease[13], and certain neoplastic diseases[14,15], in which SAA has important diagnostic and prognostic value. Up-regulation of local SAA1 and SAA2 expression in injured tissues

and cells stimulated by inflammatory mediators was detected in chronic lung diseases, accompanied by accumulation of macrophages[9,10].

Long-term inflammatory stimulation occurs in the liver as a consequence of a variety of disease etiologies including chronic hepatitis B (CHB), and this can lead to the formation of diffuse liver fibrosis *via* the activation of hepatic stellate cells (HSCs). Activated HSCs are the major scar forming cells in the inflamed liver, and they express a number of fibrogenic signaling pathways which, if unchecked, may further lead to liver cirrhosis and decompensated cirrhosis with fatal complications. The activation of HSCs is therefore a central event of liver fibrogenesis and a driver of cirrhosis. Apart from the important fibrogenic activity of HSCs, they have emerged as key effectors of the liver's inflammatory response by regulating leukocyte trafficking and Kupffer cell recruitment and activation *via* secretion of cytokines and chemokines. It has been demonstrated that SAA may effectively activate c-Jun N-terminal kinase (JNK), Erk, Akt, IκB kinase, and NF-κB in primary human and rat HSCs. These provide mechanisms by which SAA promotes HSC proliferation and stimulates the production of inflammatory factors such as MCP-1, RANTES, and MMP9. The transcription of SAA mRNA has been shown to be significantly elevated in mouse models of liver fibrosis induced by carbon tetrachloride injection and bile duct ligation[16]. However, few studies have reported on the levels of SAA in human liver disease and the clinical significance of SAA in various liver diseases. In this study, serum levels of SAA in patients with common liver diseases were examined. The factors associated with the alteration of SAA levels in chronic liver diseases were analyzed.

MATERIALS AND METHODS

Study population

This research was approved by the ethics committee of Zhongshan Hospital Affiliated to Fudan University. The study protocol conformed to the provisions of the Declaration of Helsinki. Informed consent was obtained from all subjects. A total of 278 patients with different liver diseases and 117 healthy controls from Zhongshan Hospital Affiliated to Fudan University were enrolled in this study. The patients include 205 with chronic hepatitis B (146 with inactive hepatitis and 59 with active hepatitis), 22 with active autoimmune liver disease (AILD; 13 with primary biliary cholangitis, 6 with autoimmune hepatitis, and 3 with overlap syndromes), 21 with nonalcoholic steatohepatitis (NASH), 14 with drug-induced liver injury (DILI), and 16 with pyogenic liver abscess. The flow chart of the study is shown in Figure 1.

The diagnosis of liver diseases and their active status were referred to most recent AASLD guidelines (https://www.aasld.org/publications/practice-guidelines). The diagnostic criteria for active hepatitis B included: (1) HBsAg present for no less than 6 months; (2) Serum HBV DNA > 20000 IU/mL in HBeAg-positive CHB and > 2000 IU/mL in HBeAg-negative CHB; and (3) Intermittently or persistently elevated ALT and/or AST levels, or liver biopsy results showing chronic hepatitis with moderate or severe necroinflammation. The diagnostic criteria for inactive hepatitis B were: (1) HBsAg present for no less than 6 months; (2) Serum HBV DNA < 2000 IU/mL; (3) Persistently normal ALT and/or AST levels; and (4) Liver biopsy or noninvasive test results showing absence of significant necroinflammation. Individuals in the healthy control group were people who came to the hospital for medical examination with negative findings.

The exclusion criteria were: (1) Patients with chronic liver disease caused by viruses other than HBV and other liver diseases such as genetic liver diseases (*e.g.*, hepatolenticular degeneration and hereditary hyperbilirubinemia) and parasitic liver diseases; (2) Patients who have received immunomodulatory therapy in the past three months; (3) Patients with advanced malignant tumors except liver cancer; and (4) Patients with two or more comorbidities that may affect the serum level of SAA, including systematic inflammation, diabetes, infectious ascites, *etc*.

Data collection

Peripheral blood tests and other related examinations were provided by the Laboratory Department of Zhongshan Hospital. Serum SAA level was detected by the scattering turbidimetry method (OQMP11 Germany/Siemens). The human serum samples were stored at 4 °C and tested within 24 hours after collection. The upper normal limits of SAA and CRP in the clinical laboratory of Zhongshan Hospital were 6.4 mg/L and 3 mg/L, respectively. Other clinical parameters including liver function test and serum CRP level were collected for the analysis of the factors associated with SAA levels.

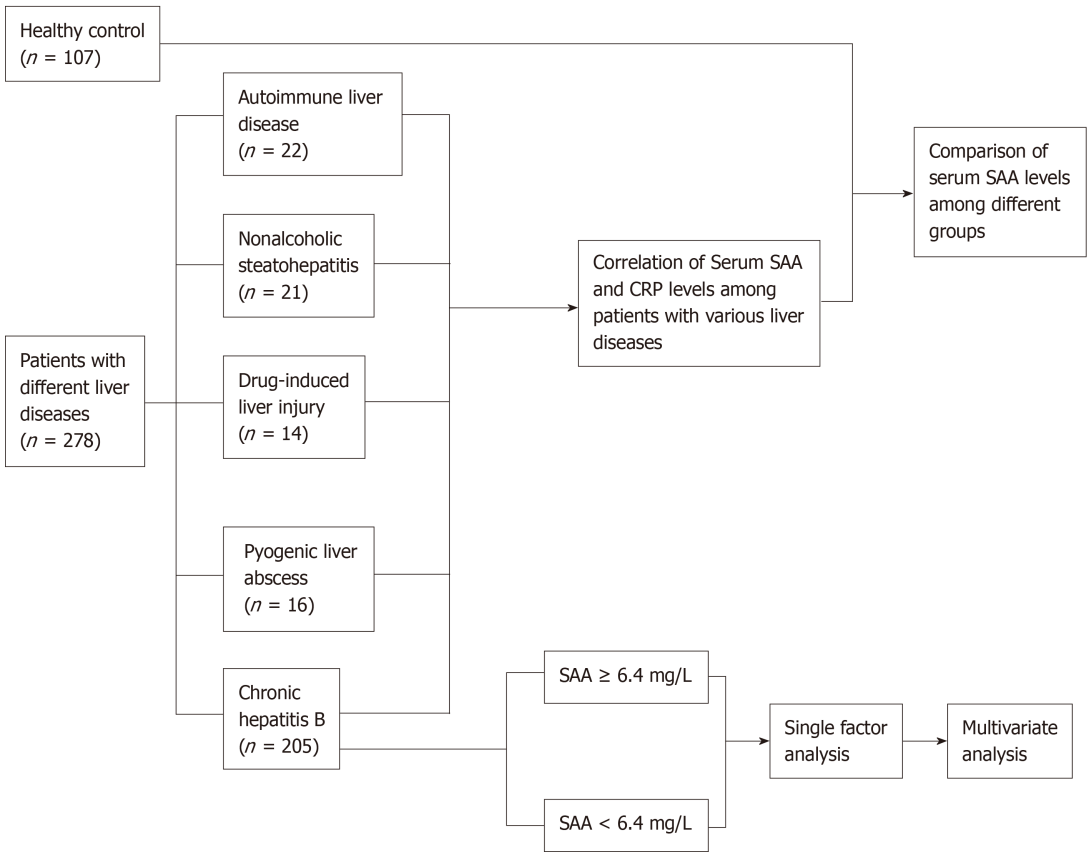

Figure 1 Flow chart of the study. SAA: Serum amyloid A; CRP: C-reactive protein.

Statistical analysis

Statistical analyses were performed using SPSS22.0 software. Continuous normal distribution data were analyzed by the *t*-test to determine the difference between two groups. Continuous non-normal distribution data were analyzed by the Mann-Whitney *U*-test, or the data were grouped based on the normal reference value and compared by the chi-square test. Enumeration data were analyzed by the chi-square test. The Spearman's rank correlation test was used to determine the correlation between two groups of consecutive non-normal distribution data. Statistically significant factors determined by single factor analysis were further analyzed by binary multivariate logistic regression analysis. The Mann-Whitney *U* test was used to compare the serum levels of SAA between various liver disease groups and the healthy control group. Bonferroni method was applied for post hoc comparisons to control the probability of type 1 error (alpha = 0.05/6 = 0.008). For statistical tests of other variables, $P < 0.05$ was considered statistically significant.

RESULTS

Analysis of serum levels of SAA in different groups of subjects

Serum SAA levels in patients with various liver diseases and healthy controls are shown in Table 1. All patients except those with inactive CHB had higher serum SAA levels than healthy controls. Specifically, patients with pyogenic liver abscess had the highest SAA level (mean value: 398.4 ± 246.8 mg/L; median value: 413.5 mg/L). Serum SAA levels in patients with AILD, DILI, and pyogenic liver abscess were higher than those in patients with active CHB. No difference in SAA levels was found between patients with NASH and active CHB. No difference between the healthy control and the inactive CHB patient groups was found by univariate and covariance (ANCOVA) analyses after adjusting baseline data of gender, age, and CRP level (data not shown).

Differences in serum levels of SAA and their association factors in patients with CHB

Two hundred and five patients with CHB (59 active hepatitis and 146 inactive

Table 1 Serum levels of serum amyloid A in different groups of subjects

Subjects (*n*)	mean ± SD, (mg/L)	Median (minimum-maximum), (mg/L)	Z[1] (compared with healthy controls/active CHB)	*P*[1] (compared with healthy controls/ active CHB)
Healthy controls (117)	2.902 ± 1.801	2.250 (0.797-9.040)	-	-
Inactive CHB (146)	2.936 ± 3.092	2.350 (0.800-29.90)	-1.129/-7.281	0.259/< 0.001
Active CHB (59)	6.621 ± 6.776	4.000 (1.700-39.90)	-5.980	< 0.001
NASH (21)	6.624 ± 4.891	5.500 (2.800-23.00)	-4.867	< 0.001
Drug-induced liver injury (14)	8.036 ± 5.685	6.800 (3.400-26.20)	-4.992	< 0.001
Autoimmune liver disease (22)	19.73 ± 24.81	13.70 (3.300-108.0)	-6.870	< 0.001
Pyogenic liver abscess (16)	398.4 ± 246.8	413.5 (62.20-871.0)	-6.474	< 0.001

[1]Mann-Whitney *U* test was used to compare the serum amyloid A levels between various liver disease groups and the healthy control group, and Bonferroni test was applied for post hoc comparisons to control the probability of type 1 error (alpha = 0.05/6 = 0.008). CHB: Chronic hepatitis B; NASH: Nonalcoholic steatohepatitis.

hepatitis) were divided into SAA ≥ 6.4 mg/L and SAA < 6.4 mg/L groups. Single factor analysis showed that patients with active CHB (χ^2 = 16.78, P < 0.001, OR = 5.881), ALP ≥ 135 U/L (χ^2 = 4.592, P = 0.032, OR = 4.093), and CRP ≥ 3 mg/L (χ^2 = 17.01, P < 0.001, OR = 6.993) were associated with SAA levels higher than 6.4 mg/L (Table 2). Other liver function parameters, hepatitis B virus markers, and blood routine test results were not statistically different between the SAA ≥ 6.4 mg/L group and SAA < 6.4 mg/L group.

Active CHB (P = 0.039, OR = 6.222) was the independent factor associated with SAA serum levels higher than 6.4 mg/L by binary multivariate logistic regression analysis (Table 3).

The disease history of the CHB patients ranged from 1 year to 40 years. No significant difference was found in serum SAA levels between cirrhotic and non-cirrhotic patients (P = 0.537), or between patients with or without receiving oral antiviral drugs (P = 0.634). Eighteen of the 59 active hepatitis patients and 82 of the 146 inactive hepatitis patients were receiving antiviral therapy. The types and proportions of antiviral drugs used by the patients were enticavir (ETV) monotherapy (58%), adefovir (ADV) monotherapy (12%), ETV and ADV combination therapy (2%), lamivudine monotherapy (6%), lamivudine and ADV combination therapy (5%), telbivudine (12%), telbivudine and ADV combination therapy (2%), and TDF monotherapy (3%). Among patients who were receiving antiviral therapy, patients with inactive hepatitis (n = 82) had significantly lower blood SAA levels than those with active hepatitis (n = 18) (Z value = -4.077, P = 0.000) (Table 4).

Correlation between serum levels of SAA and CRP in patients with CHB, autoimmune liver disease, and pyogenic liver abscess

Spearman's rank correlation test revealed that serum levels of SAA and CRP were positively correlated in patients with CHB (r = 0.620, P < 0.001), AILD (r = 0.504, P = 0.020), and pyogenic liver abscess (r = 0.508, P = 0.045). Serum levels of SAA (0.80-871.0 mg/L) displayed a broader fluctuation range than CRP (0.30-271.3 mg/L) (Table 5). We found no significant correlation between CRP and SAA levels in patients with DILI.

DISCUSSION

SAA and liver diseases

In this study, the serum levels of SAA in patients with different liver diseases were investigated and the association factors were analyzed. Patients with pyogenic liver abscess, active AILD, DILI, NASH, and active CHB were found to have higher serum SAA levels than patients with inactive CHB and healthy controls. The results extend the diagnostic and prognostic value of SAA as a sensitive inflammatory marker in liver diseases, especially liver abscess.

Patients with pyogenic liver abscess had the highest blood levels of SAA, which can be hundred times higher than those of inactive CHB and healthy controls. This may be due to a systemic release of inflammatory factors in the context of bacterial infection, which in turn may stimulate the production of SAA, forming a positive

Table 2 Single factor analysis of serum levels of serum amyloid A in patients with chronic hepatitis B

Factor	SAA < 6.4 mg/L	SAA ≥ 6.4 mg/L	χ^2/t value[1]	*P*[1] value	OR (95%CI)
	Positive cases/total cases (%)	Positive cases/total cases (%)			
Female	39/182 (21.4%)	6/23 (26.1%)	0.259	0.611	1.294 (0.478-3.503)
Age (yr)	47.87 ± 13.17	49.26 ± 14.476	-0.471	0.638	-
ALT ≥ 40 U/L	53/178 (29.8%)	7/22 (31.8%)	0.039	0.844	1.101 (0.424-2.854)
AST ≥ 35 U/L	68/178 (38.2%)	7/22 (31.8%)	0.340	0.560	0.755 (0.293-1.946)
γ-GT ≥ 45 U/L	60/178 (33.7%)	9/22 (40.9%)	0.449	0.503	1.362 (0.551-3.365)
ALP ≥ 135 U/L	12/179 (6.70%)	5/22 (22.7%)	4.592	***0.032***	4.093 (1.288-13.011)
Elevated ALP or γ-GT level	63/178 (35.4%)	10/22 (45.5%)	0.855	0.355	1.521 (0.622-3.718)
AFP ≥ 20 ng/mL	16/173 (9.2%)	3/22 (13.6%)	0.074	0.786	1.549 (0.413-5.810)
A/G ≤ 1.2	32/177 (18.1%)	7/22 (31.8%)	1.553	0.213	2.115 (0.797-5.608)
Active CHB	44/182 (24.2%)	15/23 (65.2%)	16.78	< 0.001	5.881 (2.337-14.797)
Child-Pugh grade B or C	19/182 (10.4%)	6/23 (26.1%)	3.322	0.068	1.212 (0.946-1.552)
Complicated by UGIB	5/152 (3.29%)	1/20 (5.00%)	0.000	1.000	1.547 (0.172-13.959)
Complicated by HE	4/152 (2.63%)	1/20 (5.00%)	0.000	1.000	1.947 (0.207-18.343)
Complicated by ascites	19/152 (12.5%)	6/20 (30.0%)	3.062	0.080	3.000 (1.029-8.749)
Complicated by UGIB or HE or ascites	23/152 (15.1%)	6/20 (30.0%)	1.828	0.176	2.404 (0.838-6.898)
Complicated by HCC	28/182 (15.4%)	3/23 (13.0%)	0.000	1.000	0.825 (0.230-2.963)
CRP ≥ 3 mg/L	5/35 (14.3%)	7/7 (100%)	17.01	< 0.001	6.993 (3.106-15.873)
HBsAg	160/168 (95.2%)	20/22 (90.9%)	0.121	0.728	0.500 (0.099-2.521)
HBV DNA ≥ 2000 IU/mL	43/177 (24.3%)	4/21 (19.0%)	0.285	0.593	0.733 (0.234-2.297)
Received antiviral therapy	87/162 (53.7%)	13/22 (59.1%)	0.227	0.634	1.245 (0.504-3.076)

[1]Continuous normal distribution data were analyzed by the *t*-test to determine the difference between two groups. Enumeration data were analyzed by the chi-square test to analyze the difference between groups. ALT: Alanine transaminase; AST: Aspartate transaminase; γ-GT: γ-glutamyltransferase; ALP: Alkaline phosphatase; AFP: Alpha-fetoprotein; A/G: Albumin/globulin ratio; HCC: Hepatocellular carcinoma; CRP: C-reactive protein; UGIB: Upper gastrointestinal bleeding; HE: Hepatic encephalopathy; SAA: Serum amyloid A; CHB: Chronic hepatitis B.

feedback loop to amplify inflammation.

The performance of SAA in reflecting liver inflammation and fibrogenesis was also tested in non-abscess liver diseases with milder inflammatory status such as CHB. By single factor analysis of 205 patients with CHB, it was observed that serum SAA levels were significantly higher in patients with active CHB than in those with inactive CHB. Patients with active CHB have intermittently or persistently elevated ALT and/or AST levels, which are markers reflecting hepatocyte and biliary destruction. Elevated serum levels of ALP and/or γ-GT usually indicate impaired biliary drainage. Studies have shown that ALP has a higher specificity than γ-GT in the diagnosis of cholestasis[17]. In the present study, the elevation of ALP level, rather than γ-GT, was associated with higher SAA levels by single factor analysis. The association between SAA and cholestasis and the underlying mechanisms warrant further investigation.

Serum SAA level has been found to be an indicator of disease activity in autoimmune diseases such as rheumatoid arthritis[18]. SAA participates in the disease's progression by promoting formation of synovial pannus and inducing local synthesis of cytokines and chemokines[11]. In this study, serum levels of SAA in patients with autoimmune liver disease were also remarkably increased, indicating that SAA may also exert pro-inflammatory properties and be involved in the pathological process of autoimmune responses in the liver.

It can also be concluded that SAA lacks specificity in the judgment of disease activity. The analysis of serum SAA level can be complicated by other local or systemic inflammatory diseases such as pyogenic liver abscess and inflammatory bowel disease. It is therefore necessary to consider the patient's disease status systemically when using SAA as a parameter of the disease activity of aforementioned liver diseases.

SAA and CRP

Similar to SAA, CRP is also an acute phase protein produced by the liver, with a half-life of 46.4 ± 21.7 h compared with 34.9 ± 28.7 h for SAA[19]. IL-1, IL-6, and TNF-α

Table 3 Multivariate analysis of serum levels of serum amyloid A in patients with chronic hepatitis B

Factor	Regression coefficient	*P* value	OR	95%CI
Active CHB	1.828	0.039	6.222	1.095-35.36

CHB: Chronic hepatitis B.

stimulate the production of SAA as well as CRP in the liver[20]. CRP is not sensitive in the detection of liver injury and dysfunction in clinical practice. Comparative studies have demonstrated that SAA has a higher sensitivity and specificity, as well as a broader range of serum level than CRP in viral inflammation[21], infection after kidney transplantation[22], acute appendicitis, and inflammatory bowel disease[23]. The present study demonstrated that serum levels of SAA were positively correlated with CRP levels in patients with CHB, AILD, and pyogenic liver abscess. SAA has a broader range of serum levels than CRP in liver diseases and thus is a more sensitive and better indicator to capture mild inflammation[21].

There may be functional similarity and difference between CRP and SAA in liver diseases. Many studies have reported the pro-inflammatory effects of CRP[24,25]. Intraperitoneal injection of CRP in rats resulted in a significant increase in superoxide anion, NF-κB activity, and the release of biomarkers of inflammation from macrophages[26]. *In vitro*, the expression of intercellular cell adhesion molecule-1 (ICAM-1) remarkably increased in human umbilical vein endothelial cells and human coronary artery endothelial cells stimulated by CRP. CRP also promotes MCP-1 production. Similarly, SAA promotes the synthesis of inflammatory factors, and strengthens the inflammatory response as aforementioned, but with an additional property to stimulate HSC activities during liver injury and hepatitis. SAA may be a potential fibrogenic factor that dynamically changes with liver fibrogenesis.

SAA and active CHB

By single and multivariate logistic regression analyses, it was revealed that active CHB was the independent factor associated with SAA serum levels higher than 6.4 mg/L among CHB patients. Oral antiviral drug treatment itself was not associated with significant changes of SAA level. Among patients who were receiving antiviral drugs, those with inactive hepatitis had lower blood SAA levels than patients with active hepatitis, albeit their mean level of SAA (6.289 ± 6.042 mg/L) was under the upper normal limit. This may reflect a confounded status of insufficient or ineffective antiviral therapy in these active CHB patients, and is in line with the result that patients with active CHB had higher levels of SAA than those with inactive CHB. Piotti *et al*[27] showed immunopositivity for SAA protein in the liver biopsy specimens of hepatitis C and B patients with active chronic hepatitis and early fibrosis. The functional impact of SAA in the progression of chronic hepatitis B and various other liver diseases warrants further studies.

Single factor analysis in this study showed that SAA level ≥ 6.4 mg/L was not associated with albumin/globulin ratio, globulin level, aspartate aminotransferase-to-platelet ration index score, Child-Pugh score/grade, or major complications of cirrhosis such as upper gastrointestinal bleeding, hepatic encephalopathy, or ascites in CHB patients. These results are in line with the inflammatory property of SAA, and thus the increase coordinates with active hepatitis, rather than cirrhosis.

Although there was no statistical difference of SAA levels in patients with ascites alone compared with patients without ascites by continuous calibration chi-square test (P = 0.080), the OR value of SAA levels above 6.4 mg/L in patients with ascites alone was found to be 3.000 (95%CI: 1.029-8.749; Table 2). This may be due to the slight inflammatory state in patients with ascites, or the small sample size. Follow-up studies may expand the research by enrolling patients with spontaneous bacterial peritonitis.

The positive rates and quantitative values of HBV markers were not associated with SAA levels. There was also no difference of SAA levels in patients with or without receiving antiviral therapy. HBV markers are important in reflecting viral infection status and viral replication activity, whereas the carrying and amplification of HBV alone may not induce immune response that causes liver injury and inflammation.

Summary

Serum level of SAA is a sensitive biomarker for the inflammatory activity of pyogenic liver abscess, and to a lesser extent can reflect the mild inflammatory status of AILD,

Table 4 Comparison of serum amyloid A levels between active and inactive chronic hepatitis B patients with oral antiviral therapy

Status of patients with antiviral therapy	*n*	mean ± SD of SAA (mg/L)	Average rank of SAA	*Z*[1] value	*P*[1] value
Active CHB	18	6.289 ± 6.042	74.92	-4.077	0.000
Inactive CHB	82	3.379 ± 4.726	44.46		

[1]The Mann-Whitney *U* test was used to compare the serum amyloid A levels between various liver disease groups. SAA: Serum amyloid A; CHB: Chronic hepatitis B.

DILI, CHB, and NASH. SAA lacks specificity in the judgment of inflammatory diseases. It is therefore necessary to comprehensively consider the patient's systemic status before making judgment.

Table 5 Correlation of serum amyloid A and C-reactive protein levels among patients with various liver diseases

Disease	SAA (mg/L)		CRP (mg/L)		[1]Spearman's rank correlation coefficient	*P* value
	mean ± SD	Median (minimum-maximum)	mean ± SD	Median (minimum-maximum)		
CHB	3.984 ± 4.743	3.250 (0.80-39.90)	4.398 ± 6.522	1.500 (0.30-25.40)	0.620	< 0.001
Autoimmune liver disease	19.73 ± 24.81	13.70 (3.30-108.0)	9.633 ± 5.977	9.100 (1.20-19.60)	0.504	0.020
Pyogenic liver abscess	398.4 ± 246.8	413.5 (62.20-871.0)	138.8 ± 57.46	141.1 (22.90-271.3)	0.508	0.045
Drug-induced liver injury	8.036 ± 1.519	6.800 (3.40-26.20)	6.490 ± 2.616	2.850 (0.30-25.30)	0.219	0.544

[1]The Spearman's rank correlation test was used to determine correlation between groups. SAA: Serum amyloid A; CRP: C-reactive protein.

ARTICLE HIGHLIGHTS

Research background

Serum amyloid A (SAA) is an acute phase protein mainly synthesized by the liver, which participates in the pathological process of a varieties of inflammatory diseases. Immune and inflammatory responses participate in chronic liver injuries and fibrogenesis of various liver diseases including chronic hepatitis B (CHB) *via* activating hepatic stellate cells (HSCs), the key fibrogenic cells in the liver. It has been demonstrated that SAA induces inflammatory phenotype and promotes cell proliferation in activated HSCs. However, few studies have been reported on the serum levels of SAA in human liver diseases. It is of interest to investigate the diagnostic value and clinical significance of serum SAA level in patients with inflammatory liver diseases.

Research motivation

Few studies have been reported on the serum level of SAA and its clinical significance in human liver diseases. Yet many studies have demonstrated that the increase of serum SAA level is not only a consequence of inflammation or tissue injury, but also a promoting factor by itself to intensify the disease process. It has been reported that the transcription of SAA in the liver was significantly elevated in mouse models of liver fibrogenesis. SAA induces inflammatory phenotype and promotes cell proliferation in activated HSCs. The present study aimed at investigating the clinical significance of serum SAA levels in various liver diseases. The results will help to delineate whether SAA level may serve as an indicator of liver inflammation and fibrogenesis, and the potential impact of SAA on the diseases' progression. The upstream regulation of SAA expression in various liver diseases will also be of great interest.

Research objectives

The main objective of this study was to investigate the serum levels of SAA in patients with various liver diseases, especially chronic hepatitis B, and analyze the factors associated with the alteration of SAA levels.

Research methods

Two hundred and seventy-eight patients with different liver diseases and 117 healthy controls were enrolled in this study. The patients included 205 with chronic hepatitis B (CHB), 22 with active autoimmune liver disease (AILD), 21 with nonalcoholic steatohepatitis (NASH), 14 with drug-induced liver injury (DILI), and 16 with pyogenic liver abscess. The Mann-Whitney *U* test was used to compare the serum SAA levels of patients with various liver diseases and those of healthy controls. Bonferroni test was applied for post hoc comparisons to control the probability of type 1 error. Serum levels of SAA and other clinical parameters were collected for the analysis of the factors associated with SAA levels. The 205 patients with CHB (59 active hepatitis and 146 inactive hepatitis) were divided into SAA ≥ 6.4 mg/L and SAA < 6.4 mg/L groups. The *t*-test or Chi-square test was used to perform single factor analysis of serum levels of SAA in patients with CHB. Then multivariate analysis was used to determine the independent risk factors for high serum levels of SAA in patients with CHB. Finally, the Spearman's rank correlation test was used to determine correlation of SAA levels and CRP among patients with different liver diseases.

Research results

All patients except those with inactive CHB had higher serum SAA levels than healthy controls. Specifically, patients with pyogenic liver abscess had the highest SAA level (mean value: 398.4 ± 246.8 mg/L; median value: 413.5 mg/L). The serum SAA levels in patients with AILD, DILI, and pyogenic liver abscess were higher than those in patients with active CHB. Active CHB (χ^2 = 16.78, P < 0.001, OR = 5.881), ALP ≥ 135 U/L (χ^2 = 4.592, P = 0.032, OR = 4.093), and CRP ≥ 3 mg/L (χ^2 = 17.01, P < 0.001, OR = 6.993) were associated with SAA levels higher than 6.4 mg/L. Active CHB (P = 0.039, OR = 6.222) was the independent factor associated with SAA serum

levels higher than 6.4 mg/L by binary multivariate logistic regression analysis. Serum levels of SAA and CRP were positively correlated in patients with CHB (r = 0.620, P < 0.001), AILD (r = 0.504, P = 0.020), and pyogenic liver abscess (r = 0.508, P = 0.045). Serum levels of SAA (0.80-871.0 mg/L) displayed a broader fluctuation range than CRP (0.30-271.3 mg/L).

Research conclusions

It was found in the present study that serum level of SAA is a sensitive biomarker for the inflammatory activity of pyogenic liver abscess, and to a lesser extent can reflect the mild inflammatory status of AILD, DILI, CHB, and NASH. SAA lacks specificity in the judgment of inflammatory diseases. It is therefore necessary to comprehensively consider the patient's systemic status before making judgment.

Research perspectives

Previous studies and our data have showed that SAA participates in inflammatory response in human liver diseases. It may own an additional property to stimulate HSC activities during chronic liver injury and hepatitis. We speculate that SAA may be a potential fibrogenic factor that dynamically changes during liver fibrogenesis. The value of SAA detection in monitoring the prognosis of liver abscess and other liver diseases, the potential impact and underlying mechanisms of SAA on liver diseases' progression, the upstream regulation of SAA expression in various liver diseases, and whether SAA may become a treatment target for inflammatory liver diseases warrant further investigation.

ACKNOWLEDGEMENTS

The authors thank Professor Derek A. Mann of Newcastle University, England for language modification of this manuscript.

REFERENCES

1 **Sun L**, Ye RD. Serum amyloid A1: Structure, function and gene polymorphism. *Gene* 2016; **583**: 48-57 [PMID: 26945629 DOI: 10.1016/j.gene.2016.02.044]
2 **Meek RL**, Urieli-Shoval S, Benditt EP. Expression of apolipoprotein serum amyloid A mRNA in human atherosclerotic lesions and cultured vascular cells: implications for serum amyloid A function. *Proc Natl Acad Sci USA* 1994; **91**: 3186-3190 [PMID: 8159722 DOI: 10.1073/pnas.91.8.3186]
3 **O'Hara R**, Murphy EP, Whitehead AS, FitzGerald O, Bresnihan B. Local expression of the serum amyloid A and formyl peptide receptor-like 1 genes in synovial tissue is associated with matrix metalloproteinase production in patients with inflammatory arthritis. *Arthritis Rheum* 2004; **50**: 1788-1799 [PMID: 15188355 DOI: 10.1002/art.20301]
4 **Sung HJ**, Ahn JM, Yoon YH, Rhim TY, Park CS, Park JY, Lee SY, Kim JW, Cho JY. Identification and validation of SAA as a potential lung cancer biomarker and its involvement in metastatic pathogenesis of lung cancer. *J Proteome Res* 2011; **10**: 1383-1395 [PMID: 21141971 DOI: 10.1021/pr101154j]
5 **Gouwy M**, De Buck M, Pörtner N, Opdenakker G, Proost P, Struyf S, Van Damme J. Serum amyloid A chemoattracts immature dendritic cells and indirectly provokes monocyte chemotaxis by induction of cooperating CC and CXC chemokines. *Eur J Immunol* 2015; **45**: 101-112 [PMID: 25345597 DOI: 10.1002/eji.201444818]
6 **Guo J**, Friedman SL. Toll-like receptor 4 signaling in liver injury and hepatic fibrogenesis. *Fibrogenesis Tissue Repair* 2010; **3**: 21 [PMID: 20964825 DOI: 10.1186/1755-1536-3-21]
7 **Sandri S**, Rodriguez D, Gomes E, Monteiro HP, Russo M, Campa A. Is serum amyloid A an endogenous TLR4 agonist? *J Leukoc Biol* 2008; **83**: 1174-1180 [PMID: 18252871 DOI: 10.1189/jlb.0407203]
8 **Westermark GT**, Fändrich M, Westermark P. AA amyloidosis: pathogenesis and targeted therapy. *Annu Rev Pathol* 2015; **10**: 321-344 [PMID: 25387054 DOI: 10.1146/annurev-pathol-020712-163913]
9 **Anthony D**, Seow HJ, Uddin M, Thompson M, Dousha L, Vlahos R, Irving LB, Levy BD, Anderson GP, Bozinovski S. Serum amyloid A promotes lung neutrophilia by increasing IL-17A levels in the mucosa and γδ T cells. *Am J Respir Crit Care Med* 2013; **188**: 179-186 [PMID: 23627303 DOI: 10.1164/rccm.201211-2139OC]
10 **Bozinovski S**, Hutchinson A, Thompson M, Macgregor L, Black J, Giannakis E, Karlsson AS, Silvestrini R, Smallwood D, Vlahos R, Irving LB, Anderson GP. Serum amyloid a is a biomarker of acute exacerbations of chronic obstructive pulmonary disease. *Am J Respir Crit Care Med* 2008; **177**: 269-278 [PMID: 18006888 DOI: 10.1164/rccm.200705-678OC]
11 **Connolly M**, Marrelli A, Blades M, McCormick J, Maderna P, Godson C, Mullan R, FitzGerald O, Bresnihan B, Pitzalis C, Veale DJ, Fearon U. Acute serum amyloid A induces migration, angiogenesis, and inflammation in synovial cells in vitro and in a human rheumatoid arthritis/SCID mouse chimera model. *J Immunol* 2010; **184**: 6427-6437 [PMID: 20435930 DOI: 10.4049/jimmunol.0902941]
12 **Fyfe AI**, Rothenberg LS, DeBeer FC, Cantor RM, Rotter JI, Lusis AJ. Association between serum amyloid A proteins and coronary artery disease: evidence from two distinct arteriosclerotic processes. *Circulation* 1997; **96**: 2914-2919 [PMID: 9386157 DOI: 10.1161/01.CIR.96.9.2914]
13 **Niederau C**, Backmerhoff F, Schumacher B, Niederau C. Inflammatory mediators and acute phase proteins in patients with Crohn's disease and ulcerative colitis. *Hepatogastroenterology* 1997; **44**: 90-107 [PMID: 9058126]
14 **Biran H**, Friedman N, Neumann L, Pras M, Shainkin-Kestenbaum R. Serum amyloid A (SAA) variations in patients with cancer: correlation with disease activity, stage, primary site, and prognosis. *J Clin Pathol* 1986; **39**: 794-797 [PMID: 3734116 DOI: 10.1136/jcp.39.7.794]
15 **Lee JW**, Stone ML, Porrett PM, Thomas SK, Komar CA, Li JH, Delman D, Graham K, Gladney WL, Hua X, Black TA, Chien AL, Majmundar KS, Thompson JC, Yee SS, O'Hara MH, Aggarwal C, Xin D, Shaked A, Gao M, Liu D, Borad MJ, Ramanathan RK, Carpenter EL, Ji A, de Beer MC, de Beer FC, Webb NR,

Beatty GL. Hepatocytes direct the formation of a pro-metastatic niche in the liver. *Nature* 2019; **567**: 249-252 [PMID: 30842658 DOI: 10.1038/s41586-019-1004-y]

16 **Siegmund SV**, Schlosser M, Schildberg FA, Seki E, De Minicis S, Uchinami H, Kuntzen C, Knolle PA, Strassburg CP, Schwabe RF. Serum Amyloid A Induces Inflammation, Proliferation and Cell Death in Activated Hepatic Stellate Cells. *PLoS One* 2016; **11**: e0150893 [PMID: 26937641 DOI: 10.1371/journal.pone.0150893]

17 **European Association for the Study of the Liver**. EASL Clinical Practice Guidelines: management of cholestatic liver diseases. *J Hepatol* 2009; **51**: 237-267 [PMID: 19501929 DOI: 10.1016/j.jhep.2009.04.009]

18 **Shen C**, Sun XG, Liu N, Mu Y, Hong CC, Wei W, Zheng F. Increased serum amyloid A and its association with autoantibodies, acute phase reactants and disease activity in patients with rheumatoid arthritis. *Mol Med Rep* 2015; **11**: 1528-1534 [PMID: 25352049 DOI: 10.3892/mmr.2014.2804]

19 **Takata S**, Wada H, Tamura M, Koide T, Higaki M, Mikura SI, Yasutake T, Hirao S, Nakamura M, Honda K, Nagatomo T, Tanaka Y, Sohara E, Watanabe M, Yokoyama T, Saraya T, Kurai D, Ishii H, Goto H. Kinetics of c-reactive protein (CRP) and serum amyloid A protein (SAA) in patients with community-acquired pneumonia (CAP), as presented with biologic half-life times. *Biomarkers* 2011; **16**: 530-535 [PMID: 21854219 DOI: 10.3109/1354750X.2011.607189]

20 **Yeh ET**. CRP as a mediator of disease. *Circulation* 2004; **109**: II11-II14 [PMID: 15173057 DOI: 10.1161/01.CIR.0000129507.12719.80]

21 **Wu TL I**, Chen Tsai, Chang PY, Tsao KC, Sun CF, Wu LL, Wu JT. Establishment of an in-house ELISA and the reference range for serum amyloid A (SAA): complementarity between SAA and C-reactive protein as markers of inflammation. *Clin Chim Acta* 2007; **376**: 72-76 [PMID: 16916504 DOI: 10.1016/j.cca.2006.07.012]

22 **Yamada T**. Serum amyloid A (SAA): a concise review of biology, assay methods and clinical usefulness. *Clin Chem Lab Med* 1999; **37**: 381-388 [PMID: 10369107 DOI: 10.1515/CCLM.1999.063]

23 **Yarur AJ**, Quintero MA, Jain A, Czul F, Barkin JS, Abreu MT. Serum Amyloid A as a Surrogate Marker for Mucosal and Histologic Inflammation in Patients with Crohn's Disease. *Inflamm Bowel Dis* 2017; **23**: 158-164 [PMID: 27930409 DOI: 10.1097/MIB.0000000000000991]

24 **Wu Y**, Potempa LA, El Kebir D, Filep JG. C-reactive protein and inflammation: conformational changes affect function. *Biol Chem* 2015; **396**: 1181-1197 [PMID: 26040008 DOI: 10.1515/hsz-2015-0149]

25 **Kushner I**, Agrawal A. CRP can play both pro-inflammatory and anti-inflammatory roles. *Mol Immunol* 2007; **44**: 670-671 [PMID: 16540170 DOI: 10.1016/j.molimm.2006.02.001]

26 **Jialal I**, Devaraj S, Smith G, Lam KS, Kumaresan PR. A novel peptide inhibitor attenuates C-reactive protein's pro-inflammatory effects in-vivo. *Int J Cardiol* 2013; **168**: 3909-3912 [PMID: 23871616 DOI: 10.1016/j.ijcard.2013.06.047]

27 **Piotti KC**, Yantiss RK, Chen Z, Jessurun J. Serum amyloid A immunohistochemical staining patterns in hepatitis. *Histopathology* 2016; **69**: 937-942 [PMID: 27302660 DOI: 10.1111/his.13016]

World Journal of Gastroenterology

Submit a Manuscript: https://www.f6publishing.com

World J Gastroenterol 2019 November 21; 25(43): 6451-6464

DOI: 10.3748/wjg.v25.i43.6451

ISSN 1007-9327 (print) ISSN 2219-2840 (online)

ORIGINAL ARTICLE

Retrospective Study

Application of preoperative artificial neural network based on blood biomarkers and clinicopathological parameters for predicting long-term survival of patients with gastric cancer

Si-Jin Que, Qi-Yue Chen, Qing-Zhong, Zhi-Yu Liu, Jia-Bin Wang, Jian-Xian Lin, Jun Lu, Long-Long Cao, Mi Lin, Ru-Hong Tu, Ze-Ning Huang, Ju-Li Lin, Hua-Long Zheng, Ping Li, Chao-Hui Zheng, Chang-Ming Huang, Jian-Wei Xie

ORCID number: Si-Jin Que (0000-0002-4156-0659); Qi-Yue Chen (0000-0001-6391-4043); Qing Zhong (0000-0002-8214-9129); Zhi-Yu Liu (0000-0002-2207-2932); Jia-Bin Wang (0000-0002-2023-0183); Jian-Xian Lin (0000-0002-5006-4454); Jun Lu (0000-0002-8459-4867); Long-Long Cao (0000-0003-3144-3050); Mi Lin (0000-0001-7299-6159); Ru-Hong Tu (0000-0002-7491-3879); Ze-Ning Huang (0000-0001-7284-3689); Juli Lin (0000-0002-6518-9372); Hua-Long Zheng (0000-0002-2749-0113); Ping Li (0000-0002-9418-9339); Chao-Hui Zheng (0000-0003-0157-5167); Chang-Ming Huang (0000-0002-0019-885X); Jian-Wei Xie (0000-0001-9000-5638).

Author contributions: Que SJ and Chen QY contributed equally to this work. Huang CM, Zheng CH, Chen QY, and Que SJ designed the research; Que SJ, Chen QY, Zhong Q, Liu ZY, Xie JW, Wang JB, Lin JX, Lu J, Cao LL, Lin M, Tu RH, Huang ZN, Lin JL, Zheng HL, Li P, Zheng CH, and Huang CM performed the research; Que SJ, Chen QY, Zhong Q, and Liu ZY contributed new reagents or analytic tools; Que SJ, Chen QY, Zhong Q, Liu ZY, Huang ZN, Lin JL, Zheng HL, Zheng CH, and Huang CM, Li P analyzed the data; Que SJ, Chen QY, Zhong Q, Liu ZY, Huang CM, and Li P wrote the paper.

Supported by the Scientific and Technological Innovation Joint

Si-Jin Que, Qi-Yue Chen, Qing-Zhong, Zhi-Yu Liu, Jia-Bin Wang, Jian-Xian Lin, Jun Lu, Long-Long Cao, Mi Lin, Ru-Hong Tu, Ze-Ning Huang, Ju-Li Lin, Hua-Long Zheng, Ping Li, Chao-Hui Zheng, Chang-Ming Huang, Jian-Wei Xie, Department of Gastric Surgery and Department of General Surgery, Fujian Medical University Union Hospital, Fuzhou 350001, Fujian Province, China

Si-Jin Que, Qi-Yue Chen, Qing-Zhong, Zhi-Yu Liu, Jia-Bin Wang, Jian-Xian Lin, Jun Lu, Long-Long Cao, Mi Lin, Ru-Hong Tu, Ze-Ning Huang, Ju-Li Lin, Hua-Long Zheng, Ping Li, Chao-Hui Zheng, Chang-Ming Huang, Jian-Wei Xie, Key Laboratory of Ministry of Education of Gastrointestinal Cancer, Fujian Medical University, Fuzhou 350108, Fujian Province, China

Si-Jin Que, Qi-Yue Chen, Qing-Zhong, Zhi-Yu Liu, Jia-Bin Wang, Jian-Xian Lin, Jun Lu, Long-Long Cao, Mi Lin, Ru-Hong Tu, Ze-Ning Huang, Ju-Li Lin, Hua-Long Zheng, Ping Li, Chao-Hui Zheng, Chang-Ming Huang, Jian-Wei Xie, Fujian Key Laboratory of Tumor Microbiology, Fujian Medical University, Fuzhou 350108, Fujian Province, China

Corresponding author: Jian-Wei Xie, MD, PhD, Doctor, Professor, Department of Gastric Surgery, Fujian Medical University Union Hospital, No. 29, Xinquan Road, Fuzhou 350001, Fujian Province, China. xjwhw2019@163.com
Telephone: +86-591-83363366
Fax: +86-591-83363366

Abstract

BACKGROUND

Because of the powerful abilities of self-learning and handling complex biological information, artificial neural network (ANN) models have been widely applied to disease diagnosis, imaging analysis, and prognosis prediction. However, there has been no trained preoperative ANN (preope-ANN) model to preoperatively predict the prognosis of patients with gastric cancer (GC).

AIM

To establish a neural network model that can predict long-term survival of GC patients before surgery to evaluate the tumor condition before the operation.

METHODS

The clinicopathological data of 1608 GC patients treated from January 2011 to

Capital Projects of Fujian Province, No. 2016Y9031; the Construction Project of Fujian Province Minimally Invasive Medical Center, No. [2017]171; the General Project of Miaopu Scientific Research Fund of Fujian Medical University, No. 2015MP021; the Youth Project of Fujian Provincial Health and Family Planning Commission, No. 2016-1-41; the Fujian Province Medical Innovation Project, Chinese Physicians Association Young Physician Respiratory Research Fund, No. 2015-CXB-16; and the Fujian Science and Technology Innovation Joint Fund Project, No. 2017Y9004.

Institutional review board statement: This retrospective study was approved by the Ethics Committee of Fujian Medical University Union Hospital.

Informed consent statement: The patients were not required to give informed consent to the study because the analysis used anonymous clinical data that were obtained after each patient agreed to treatment by written consent.

Conflict-of-interest statement: All authors declare that they have no conflicts of interest.

Data sharing statement: No additional data are available.

Manuscript source: Unsolicited manuscript

Received: August 19, 2019
Peer-review started: August 19, 2019
First decision: September 10, 2019
Revised: September 17, 2019
Accepted: October 17, 2019
Article in press: October 17, 2019
Published online: November 21, 2019

P-Reviewer: Lazăr DC, de Melo FF, Nagem RG
S-Editor: Tang JZ

April 2015 at the Department of Gastric Surgery, Fujian Medical University Union Hospital were analyzed retrospectively. The patients were randomly divided into a training set (70%) for establishing a preope-ANN model and a testing set (30%). The prognostic evaluation ability of the preope-ANN model was compared with that of the American Joint Commission on Cancer (8th edition) clinical TNM (cTNM) and pathological TNM (pTNM) staging through the receiver operating characteristic curve, Akaike information criterion index, Harrell's C index, and likelihood ratio chi-square.

RESULTS

We used the variables that were statistically significant factors for the 3-year overall survival as input-layer variables to develop a preope-ANN in the training set. The survival curves within each score of the preope-ANN had good discrimination ($P < 0.05$). Comparing the preope-ANN model, cTNM, and pTNM in both the training and testing sets, the preope-ANN model was superior to cTNM in predictive discrimination (C index), predictive homogeneity (likelihood ratio chi-square), and prediction accuracy (area under the curve). The prediction efficiency of the preope-ANN model is similar to that of pTNM.

CONCLUSION

The preope-ANN model can accurately predict the long-term survival of GC patients, and its predictive efficiency is not inferior to that of pTNM stage.

Key words: Gastric cancer; Artificial neural network model; Prognostic model; Preoperative; Blood biomarkers; Long-term survival

Core tip: We established an artificial neural network model before surgery that can predict the long-term survival of patients with gastric cancer, and its predictive efficiency is not inferior to that of pathological TNM stage.

Citation: Que SJ, Chen QY, Qing-Zhong, Liu ZY, Wang JB, Lin JX, Lu J, Cao LL, Lin M, Tu RH, Huang ZN, Lin JL, Zheng HL, Li P, Zheng CH, Huang CM, Xie JW. Application of preoperative artificial neural network based on blood biomarkers and clinicopathological parameters for predicting long-term survival of patients with gastric cancer. *World J Gastroenterol* 2019; 25(43): 6451-6464
URL: https://www.wjgnet.com/1007-9327/full/v25/i43/6451.htm
DOI: https://dx.doi.org/10.3748/wjg.v25.i43.6451

INTRODUCTION

Gastric cancer (GC) is one of the five most common malignant tumors in the world, and it is the third leading cause of death in cancer patients[1]. Despite the progress in the diagnosis and treatment of GC, the prognosis of GC patients is still very poor, especially the long-term survival of advanced GC patients, for which the 5-year survival rate is only 10%[2]. Most scholars have focused on how to accurately distinguish the stages of GC in patients. The improved postoperative American Joint Commission on Cancer (AJCC) TNM staging system based on pathological examination is currently the most important and recognized prognostic staging system for GC[3-5]. However, this scoring system needs to be performed based on the pathological analysis of tumor specimens and examination of lymph nodes after surgery, which cannot provide a reference for preoperative treatment and consultation. Recently, the treatment for GC has gradually changed from simple surgical treatment to comprehensive treatment with the core being surgical treatment. Accurate preoperative tumor assessment providing a reasonable individualized treatment for GC patients is the key to improving the prognosis of patients with GC. However, the single traditional index, namely, the clinical TNM (cTNM) staging system based on the imaging examination, does not show the ideal accuracy of preoperative tumor assessment. Therefore, it has been a challenge in clinical work to explore the markers and methods for preoperative accurate tumor assessment.

L-Editor: Wang TQ
E-Editor: Ma YJ

In recent years, increasingly more scholars have believed that the inflammation indexes are relevant to the survival of cancer patients[6,7]. Some scholars have reported that inflammatory cells may promote tumor growth and progression of the disease, rather than produce an effective host antitumor response. Consequently, the inflammatory biomarkers in peripheral blood are potential predictors of cancer prognosis[8-11]. It has been reported that several indexes from peripheral blood, such as the neutrophil-lymphocyte ratio (NLR), platelet-lymphocyte ratio (PLR), and albumin-globulin ratio (AGR), have a powerful impact on the prognosis of GC[8,11-14]. The prognostic nutrition index (PNI) based on lymphocyte and albumin levels is a feasible parameter to reflect the immune and nutritional status of patients with a malignant tumor and is regarded as a good index to evaluate the prognosis of patients with GC[3,15]. Although the previously established inflammatory models could predict the prognosis of patients with GC, their accuracy was still not satisfactory. Furthermore, many pathophysiological processes of malignant tumors are nonlinear processes, which cannot be well reflected through traditional linear analysis methods. Many studies have shown that artificial neural networks (ANNs) can deal with the nonlinear statistical relationship better than the traditional analysis methods, including studies on the prognosis of various cancers[16-18]. It has been reported that ANNs had a more accurate prognostic ability than TNM staging in patients with breast and rectal cancers[19]. However, there is no study on the relationship between a preoperative ANN (preope-ANN) and the prognosis in GC patients. Therefore, this study combined the preoperative blood biomarkers and preoperative tumor data to establish an ANN model in order to build a reliable preoperative prediction system that can achieve the same effect of postoperative TNM staging. The aim of this study was to evaluate the prognosis of patients with GC and to provide a reasonable individualized treatment plan for patients.

MATERIALS AND METHODS

Patients

The clinicopathological data of 1860 GC patients treated at the Department of Gastric Surgery, Fujian Medical University Union Hospital from January 2011 to April 2015 were analyzed retrospectively. The inclusion criteria were that all patients were diagnosed with GC and accepted radical surgery at our center. The exclusion criteria were as follows: (1) The general clinical data were incomplete, including age, sex, body mass index (BMI), American society of anesthesiologists (ASA) score, carcinoembryonic antigen (CEA), carbohydrate antigen 19-9 (CA199), alpha fetoprotein (AFP), NLR, PLR, AGR, PNI, preoperative complications, tumor size, primary site, clinical T stage (cT), and clinical N stage (cN); (2) The follow-up data were missing; and (3) Patients receiving neoadjuvant chemotherapy. A total of 1608 patients were included (Supplementary Figure 1). The study was approved by the Ethics Committee of Fujian Medical University Union Hospital.

Data

All patients underwent routine preoperative examinations, including upper gastrointestinal endoscopy and upper gastrointestinal angiography, to assess tumor location. Preoperative clinical staging was assessed using chest radiography, total abdominal computed tomography (CT), abdominal ultrasound, and, if necessary, PET-CT, and bone scans. The 8th edition of the AJCC tumor staging system was used for cTNM and pathological TNM (pTNM) staging (Supplementary Figure 1). The overall survival (OS) time was the time from the operation to the last follow-up time or death.

All patients were randomly divided into a training set (n = 1104, 70%) and a testing set (n = 504, 30%), and the testing set was separated for evaluation of the final model. The training data were used five times for cross-validation to optimize the neural network. Finally, the separated data of the testing set were used to evaluate the model.

Blood sample analysis

Routine blood biochemistry and tumor markers were assessed within 1 wk before the operation. Using X-tile software, the optimal critical values of the NLR for OS were 1.91 and 3.87 (P < 0.05). According to optimal critical values, the patients were divided into three groups as follows: Low NLR group (NLR ≤ 1.91, n = 632), middle NLR group (1.91 < NLR ≤ 3.87, n = 753), and high NLR group (NLR > 3.87, n = 223). Similarly, the patients were divided into a low PLR group (PLR ≤ 89.5, n = 258), middle PLR group (89.5 < PLR ≤ 162.3, n = 777), and high PLR group (PLR > 162.3, n =

573). According to the AGR, the patients were divided into a low AGR group (AGR ≤ 6.59, n = 474), middle AGR group (6.59 < AGR ≤ 7.81, n = 612), and high AGR group (AGR > 7.81, n = 522). Furthermore, according to the PNI, the patients were divided into a low PNI group (PNI ≤ 371.01, n = 495), middle PNI group (371.0 < PNI ≤ 430.0, n = 771), and high PNI group (PNI > 430.0, n = 342).

Preope-ANN model

First, logistic univariate analysis was used to analyze 1104 cases in the training set to screen the variables that affected the 3-year survival and to determine these variable items as the input nodes of the ANN.

We used the multilayer perceptron to develop the preope-ANN (Figure 1). The input layer of the preope-ANN model consisted of the screened general clinicopathological data and preoperative blood biomarkers using logistic analysis and the 3-year survival condition. The ANN intelligently analyzed the 3-year survival of the patients according to the input data and generated the outcome compared with the real value. The output layer consisted of two values: (1) The patient's 3-year survival (death or survival); and (2) The continuous variables from 0 to 1, which represent the predictive probability of the outcome of the patient's 3-year survival. The network architecture of the preope-ANN model was composed of seven hidden layers, and the input layer was composed of 16 nodes (including 14 general clinical data and blood biomarkers and two survival conditions related to the 3-year OS). The hidden layer was activated by the hyperbolic tangent function, and the output layer was composed of two nodes activated by the softmax function, including the survival condition and survival probability. According to the survival probability predicted by the preope-ANN model, the patients were divided into seven subgroups: The survival probability was 0%-30% for group A, 30%-50% for group B, 50%-65% for group C, 65%-80% for group D, 80%-90% for group E, 90%-97% for group F, and 97%-100% for group G.

Statistical analysis

All data were analyzed using SPSS 20.0 (SPSS Inc. Chicago, IL, United States) and R software (version 3.5.4). The classified variables were tested using the χ^2 test or Fisher's exact test. The X-tile software was used to determine the best cut-off point of the counting data. Mann-Whitney U test was used to test the receiver operating characteristic (ROC) curve and the area under the curve (AUC), and the Z test was used to compare the AUCs (MedCal software). We used Harrell's C index to measure the discriminatory ability of the different models[4,20]. The likelihood ratio chi-square was calculated by Cox regression to measure homogeneity; a higher score means better homogeneity[21]. The Akaike information criterion (AIC) within the Cox regression model was used to compare performances between two prognostic models; smaller AIC values represent better optimistic prognostic stratification[22]. We calculated the relative likelihood of two models using the following formula: Exp {[AIC (model A) - AIC (model B)]/2}. The relative likelihood represents the probability that model A minimizes information as effectively as model B and could thus be interpreted as a P value for the comparison of both AIC values[23]. P < 0.05 was considered statistically significant.

RESULTS

General information

Table 1 shows the clinical data of 1608 patients with GC. Among them, 1104 cases were in the training set, and 504 cases were in the testing set. The average age of all patients diagnosed was 60.72 years (range, 12-101 years), and the male to female ratio was 2.84:1. The proportion of patients diagnosed with stages I, II, III, and IVA disease in the cTNM system was 11.6%, 38.2%, 45.6%, and 4.6%, respectively. The proportion of patients diagnosed with stage I, II, and III disease in the pTNM system was 22.6%, 24.9%, and 52.5%, respectively.

Univariate logistic analysis of the survival of patients in the training set

In the training set, the univariate logistics regression analysis (Table 2) showed that age, sex, BMI, CEA, CA199, AFP, NLR, PLR, AGR, PNI, ASA score, tumor location, tumor size, cT stage, and cN stage were significant factors for the 3-year OS of the patients (P < 0.05 for all).

Performance evaluation of the preope-ANN model

The accuracy, sensitivity, and specificity of the preope-ANN model in the training set were 77.3%, 88.5%, and 50.1%, respectively. For the preope-ANN model in the testing

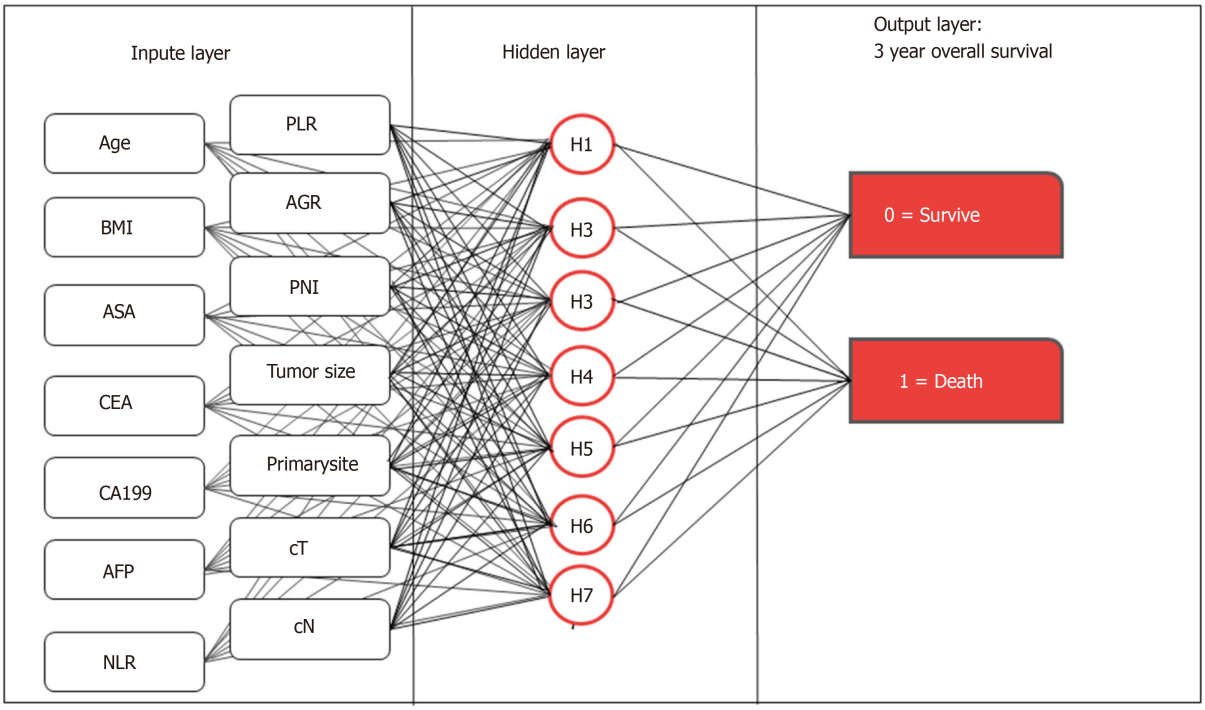

Figure 1 Structure diagram of the preoperative artificial neural network model. Age, sex, body mass index, American society of anesthesiologists score, tumor location, tumor size, prognostic nutrition index, albumin-globulin ratio, neutrophil-lymphocyte ratio, platelet-lymphocyte ratio, clinical T stage, clinical N stage, carcinoembryonic antigen, carbohydrate antigen 19-9, and alpha fetoprotein are the input variables. All weighted values passed to the hidden layer node are summed on the hidden layer node and passed to the output node through the sigmoid function. All weighted values entering the output node are summed again and passed through the sigmoid function. For each patient, the probability of output is 0-1.0. In the training of the artificial neural network, the output values are compared with the real results of each patient. The weight is adjusted so that the next time the patient appears on the network, the network output is closer to the real result. NLR: Neutrophil-lymphocyte ratio; PLR: Platelet-lymphocyte ratio; AGR: Albumin-globulin ratio; PNI: Prognostic nutrition index; BMI: Body mass index; ASA: American society of anesthesiologists score; cT: Clinical T stage; cN: Clinical N stage; CEA: Carcinoembryonic antigen; CA199: Carbohydrate antigen 19-9; AFP: Alpha fetoprotein.

set, the accuracy was 75.2%, the sensitivity was 86.5%, and the specificity was 43.8% (Figure 2).

Subgroups of the preope-ANN model for Kaplan-Meier survival analysis

In Figure 3, the prediction results of the preope-ANN model were divided into seven subgroups. The Kaplan-Meier survival curve showed that the survival curve of each subgroup within the preope-ANN model had good discrimination in both the training and testing sets ($P < 0.05$). For cTNM staging, the survival curve in the training set showed (Figure 4) that the substages of the TNM system were well differentiated ($P < 0.05$). However, the survival curve of the testing set showed that the curve of stage III was close to that of stage IVA ($P = 0.335$). Figure 5 shows the survival analysis of the pTNM staging. In the training set, the survival curve discrimination between stages IA and IB was poor ($P = 0.240$), and there was no significant difference between stages IIA and IIB and stages IIB and IIIA ($P < 0.05$). In the testing set, there was no significant difference in survival curves between stages IA and IB, IIA and IIB, and IIIA and IIIB ($P > 0.05$).

Accuracy of each model

Figure 6 shows the ROC curves of the preope-ANN model, cTNM stage, and pTNM stage in both the training set and the testing set. In the training set, the AUC values of the preope-ANN model, cTNM stage, and pTNM stage were 0.820 (0.800-0.838), 0.740 (0.718-0.762), and 0.803 (0.782-0.822), respectively. The predictive performance of the preope-ANN was better than that of the cTNM stage ($P < 0.05$) and was similar to that of the pTNM stage ($P = 0.130$). In the testing set, the AUC values of the preope-ANN model, cTNM stage, and pTNM stage were 0.790 (0.752- 0.825), 0.687 (0.644-0.727), and 0.786 (0.748-0.821), respectively. Comparison of the AUC showed that the prediction performance of the preope-ANN was better than that of the cTNM stage ($P < 0.05$), and was similar to that of the pTNM ($P = 0.858$).

Comparison of the three models

As shown in Table 3, for Harrell's C index, the preope-ANN model was superior to

Table 1 General clinicopathological data, *n* (%)

Variable	All patients (*n* = 1608)	Training set (*n* = 1104)	Testing set (*n* = 504)
Age (yr)			
< 57	593 (36.9)	413 (37.4)	180 (35.7)
57-74	838 (52.1)	565 (51.2)	273 (54.2)
> 74	177 (11.0)	126 (11.4)	51 (10.1)
Sex			
Female	412 (25.6)	299 (27.1)	113 (22.4)
Male	1196 (74.4)	805 (72.9)	391 (77.6)
BMI			
< 18.5	156 (9.7)	98 (8.9)	58 (11.5)
18.5-23.5	960 (59.7)	670 (60.7)	290 (57.5)
> 23.5	492 (30.6)	336 (30.4)	156 (31.0)
CEA			
< 2.8	932 (58.0)	626 (56.7)	306 (60.7)
2.8-4.8	328 (20.4)	226 (20.5)	102 (20.2)
> 4.8	348 (21.6)	252 (22.8)	96 (19.0)
CA199			
< 15.0	1043 (64.9)	696 (63.0)	347 (68.8)
15.0-39.2	348 (21.6)	255 (23.1)	93 (18.5)
> 39.2	217 (13.5)	153 (13.9)	64 (12.7)
AFP			
< 2	496 (30.8)	344 (31.2)	152 (30.2)
2-5.29	916 (57.0)	631 (57.2)	285 (56.5)
> 5.3	196 (12.2)	129 (11.7)	67 (13.3)
NLR			
< 1.91	632 (39.3)	422 (38.2)	210 (41.7)
1.91-3.87	753 (46.8)	525 (47.6)	228 (45.2)
> 3.87	223 (13.9)	157 (14.2)	66 (13.1)
PLR			
< 89.5	258 (16.0)	177 (16.0)	81 (16.1)
89.5-162.3	777 (48.3)	540 (48.9)	237 (47.0)
>162.3	573 (35.6)	387 (35.1)	186 (36.9)
AGR			
< 6.59	474 (29.5)	332 (30.1)	142 (28.2)
6.59-7.81	612 (38.1)	426 (38.6)	186 (36.9)
> 7.81	522 (32.5)	346 (31.3)	176 (34.9)
PNI			
< 371	495 (30.8)	347 (31.4)	148 (29.4)
371-430	771 (47.9)	531 (48.1)	240 (47.6)
> 430	342 (21.3)	226 (20.5)	116 (23.0)
ASA			
I	983 (61.1)	677 (61.3)	306 (60.7)
II	561 (34.9)	379 (34.3)	182 (36.1)
III-IV	64 (4.0)	48 (4.3)	16 (3.2)
Comorbidity			
No	1133 (70.5)	779 (70.6)	354 (70.2)
Yes	475 (29.5)	325 (29.4)	150 (29.8)
Primary site			
Lower	671 (41.7)	476 (43.1)	195 (38.7)
Middle	350 (21.8)	231 (20.9)	119 (23.6)
Upper	401 (24.9)	257 (23.3)	144 (28.6)
Overlapping	186 (11.6)	140 (12.7)	46 (9.1)
Tumor size (mm)			

< 30	578 (35.9)	404 (36.6)	174 (34.5)
30-60	711 (44.2)	477 (43.2)	234 (46.4)
> 60	319 (19.8)	223 (20.2)	96 (19.0)
cT			
T1	167 (10.4)	108 (9.8)	59 (11.7)
T2	185 (11.5)	135 (12.2)	50 (9.9)
T3	429 (26.7)	292 (26.4)	137 (27.2)
T4	827 (51.4)	569 (51.5)	258 (51.2)
cN			
N0	662 (41.2)	457 (41.4)	205 (40.7)
N1	376 (23.4)	257 (23.3)	119 (23.6)
N2	362 (22.5)	245 (22.2)	117 (23.2)
N3	208 (12.9)	145 (13.1)	63 (12.5)
Follow-up duration (mo)	48 (3-91)	48 (3-91)	50 (3-89)

BMI: Body mass index; CEA: Carcinoembryonic antigen; CA199: Carbohydrate antigen 19-9; AFP: Alpha fetoprotein; NLR: Neutrophil-lymphocyte ratio; PLR: Platelet-lymphocyte ratio; AGR: Albumin-globulin ratio; PNI: Prognostic nutrition index; ASA: American society of anesthesiologists; cT: Clinical T stage; cN: Clinical N stage.

the cTNM staging model and had the same performance as the pTNM staging model in both the training and testing sets. (In the training set: Preope-ANN *vs* cTNM = 0.773 *vs* 0.663, respectively, $P < 0.001$; preope-ANN *vs* pTNM = 0.773 *vs* 0.757, respectively, $P = 0.120$; in the testing set: Preope-ANN *vs* cTNM = 0.752 *vs* 0.652, respectively, $P < 0.001$; preope-ANN *vs* pTNM =0.752 *vs* 0.740, respectively, $P = 0.539$). The AIC analysis showed that the preope-ANN model of the training set had a better fitting degree than both the cTNM staging and pTNM staging (preope-ANN *vs* cTNM = 4977.83 *vs* 5176.70, respectively, relative likelihood < 0.001; preope-ANN *vs* pTNM = 4977.83 *vs* 4999.80, respectively, relative likelihood < 0.001). The fitting degree of the preope-ANN model in the testing set was better than that of the cTNM staging (preope-ANN *vs* cTNM = 1952.94 *vs* 2020.37, respectively, relative likelihood < 0.001), and the fitting degree of the preope-ANN model was not inferior to that of the pTNM staging (preope-ANN 1952.94 *vs* pTNM 1951.84, respectively, relative likelihood = 1.733). Therefore, the performance of the preope-ANN was better than that of the cTNM staging and was similar to that of the pTNM staging.

DISCUSSION

Presently, GC remains a common malignant tumor worldwide and the third leading cancer cause of death. As is known, it is very important to develop a GC prognostic model in order to provide valuable prognosis information for the patients and help clinicians formulate reasonable treatment regimens for the patients[19]. The TNM staging system proposed by the AJCC is the most important prognostic evaluation system for GC, and it has served as the main instruction for clinicians to choose the treatment plan. However, pTNM staging needs both grouping information and prognostic information from the postoperative histopathology results of the tumor specimen, which prevents the approach from guiding the preoperative treatment decision[24]. The exact pretreatment clinical stage is essential to customize the treatment strategy for each patient. Park *et al*[25] suggested that the clinical staging based on endoscopy and the CT scan has predictive value, where cTNM staging can be used to guide the treatment of GC patients; however, its accuracy depends on the imaging experience of the physician. Some scholars found that this method had limitations in evaluating the cT stage of large tumors, while the accuracy of cN was only 20%; and over 80% of pN0 patients are overestimated[26,27]. Thus, there is an urgent need for a more accurate preoperative prognostic model to guide the choice of treatment options.

In recent years, increasingly more studies have shown that blood inflammatory markers are associated with a poor prognosis in cancer patients[28]. The NLR, PLR, and PNI in cancer patients have been proven to be prognostic markers for various malignant tumors[29-32]. In our study, logistic analysis confirmed that the preoperative NLR, PLR, PNI, and AGR were significant prognostic factors for the 3-year survival, which is consistent with previous studies. However, because of the nonlinearity of biological information in the human body, the traditional model inevitably has had

Table 2 Univariate logistics regression analysis of risk factors for the 3-year survival

Variable	Training set			
	OR	95CI		*P* value
Age (yr)				
< 57	REF			
57-74	0.38	0.25	0.58	< 0.001
> 74	0.63	0.42	0.93	0.020
Sex				
Male	REF			
Female	0.96	0.72	1.29	0.782
BMI				
< 18.5	REF			
18.5-23.5	3.04	1.90	4.85	< 0.001
> 23.5	1.28 357	0.95	1.73	0.111
CEA				
< 2.8	REF			
2.8-4.8	0.33	0.24	0.45	< 0.001
> 4.8	0.46	0.31	0.67	< 0.001
CA199				
< 15.0	REF			
15.0-39.2	0.20	0.14	0.29	< 0.001
> 39.2	0.33	0.22	0.50	< 0.001
AFP				
< 2	REF			< 0.001
2-5.29	0.78	0.51	1.18	0.240
> 5.3	0.50	0.33	0.74	0.001
NLR				
< 1.91	REF			
1.91-3.87	0.32	0.22	0.48	< 0.001
> 3.87	0.48	0.33	0.69	< 0.001
PLR				
< 89.5	REF			
89.5-162.3	0.26	0.16	0.42	< 0.001
> 162.3	0.59	0.45	0.78	< 0.001
AGR				
< 6.59	REF			
6.59-7.81	2.11	1.50	2.98	< 0.001
> 7.81	1.58	1.13	2.20	0.007
PNI				
< 371	REF			
371-430	3.98	2.62	6.06	< 0.001
> 430	1.94	1.29	2.92	0.002
ASA				
I	REF			
II	0.44	0.24	0.79	0.006
III-IV	0.53	0.29	0.97	0.041
Comorbidity				
No	REF			
Yes	0.99	0.74	1.31	0.933
Primary site				
Lower	REF			
Middle	0.30	0.20	0.45	< 0.001
Upper	0.54	0.35	0.83	0.001
Overlapping lesion of the stomach	0.47	0.31	0.73	< 0.001

Tumor size (mm)				
< 30	REF			
30-60	0.08	0.06	0.13	< 0.001
> 60	0.43	0.31	0.60	< 0.001
cT				
T1	REF			
T2	0.05	0.02	0.13	< 0.001
T3	0.18	0.11	0.32	< 0.001
T4	0.24	0.17	0.34	< 0.001
cN				
N0	REF			
N1	0.18	0.12	0.27	< 0.001
N2	0.28	0.18	0.43	< 0.001
N3	0.67	0.44	1.007	0.054

BMI: Body mass index; CEA: Carcinoembryonic antigen; CA199: Carbohydrate antigen 19-9; AFP: Alpha fetoprotein; NLR: Neutrophil-lymphocyte ratio; PLR: Platelet-lymphocyte ratio; AGR: Albumin-globulin ratio; PNI: Prognostic nutrition index; ASA: American society of anesthesiologists; cT: Clinical T stage; cN: Clinical N stage; OR: Odds ratio; CI: Confidence interval.

some limitations when the traditional linear analysis method was used to construct the prognostic model in previous studies. At the same time, the growth of a tumor is a process of interaction between the human body and the tumor, which depends on the nutritional status of the body, the immune system, and the tumor malignancy; thus, the application of a single index for forecasting may lack accuracy[18]. Consequently, we need a new statistical model that can synthesize the biological indicators and better address the nonlinear relationship among the indicators.

The ANN is a new computational model developed by simulating the function of human brain; this method can establish a nonlinear statistical model to evaluate complex biological systems and address the relationship between complex biological indicators more flexibly[33]. In recent years, ANNs have been successfully applied to the field for the identification of lesions in pathological specimens, automatic detection of breast X-ray injury, and disease diagnosis and treatment[33,34].

We synthesized preoperative blood biomarkers (the inflammatory indicators and PNI) and preoperative clinical data to establish the preope-ANN, which are easily available compared with the need for postoperative pathological results. At the same time, we used the ANN to reduce the error of human interference, ensuring the objectivity and accuracy of the results. The verification results showed that the accuracy of the preope-ANN model in predicting the 3-year survival rate was 91.7%. In addition, the comparison of Harrell's C index and AIC analysis showed that the accuracy and the fitting degree of the preope-ANN model were better than those of cTNM staging, and the preope-ANN model could achieve the same prediction effect as pTNM staging. The TNM staging system divides the patients into different risk groups, and our preope-ANN model can provide an even more detailed prediction for each patient, which is better than grouping the predictions. The preope-ANN model can be used to predict the long-term survival of patients before surgery and to choose a reasonable individualized treatment according to the prognosis. We can obtain the possible poor prognosis information of those patients with a low score before surgery and improve the prognosis by adopting neoadjuvant radiotherapy and chemotherapy.

This study still has some limitations. First, some patients had a follow-up period less than 5 years, and we only conducted the study for the 3-year survival outcome, not for the longer-term survival outcome. Second, this was a retrospective study, and some potential biases were still unavoidable. Moreover, this study included all postoperative patients, and the results are not suitable for the evaluation of the prognosis of patients with unresectable advanced GC. Nevertheless, this study first confirmed that the preope-ANN is a novel and convenient prognostic model through the use of a large sample data size, which can effectively predict the prognosis of GC patients. In the clinic, the preope-ANN model can be considered as part of preoperative risk stratification to guide the individualized treatment of patients with GC. The next challenge is to establish a web version of the preope-ANN model that can be dynamically adjusted for the input of different sample data; with this approach, the model accuracy would be closer to the real value and more flexibly applied to the evaluation of clinical patients.

Table 3 Comparison of the area under the curve values and Harrell's C index between the pathological TNM stage, clinical TNM stage, and preoperative artificial neural network

	Training set			Testing set			Bio-ANN	Cli-ANN
	Preope-ANN	cTNM	pTNM	Preope-ANN	cTNM	pTNM		
Harrell's C index	0.773 (0.753-0.795)	0.663 (0.640-0.687)	0.757 (0.735-0.779)	0.752 (0.719-0.785)	0.652 (0.615-0.688)	0.740 (0.707-0.775)	0.722 (0.698-0.746)	0.760 (0.738-0.782)
P value		< 0.001	0.120		< 0.001	0.539	[a]*P* < 0.001; [b]*P* = 0.000; [c]*P* = 0.018	[d]*P* < 0.001 [e]*P* < 0.000; [f]*P* = 0.827
AIC	4977.83	5176.70	4999.80	1952.94	2020.37	1951.84	5115.9	5011.9
Relative likelihood		< 0.001	< 0.001		<0.001	1.733	[a]*P* < 0.001; [b]*P* > 1 [c]*P* < 0.001	[d]*P* = 0.001 E > 1 [f]*P* = 0.06

[a]*P*, Bio-artificial neural network (ANN) *vs* preoperative ANN (preope-ANN);
[b]*P*, Bio-ANN *vs* clinical TNM (cTNM);
[c]*P*, Bio-ANN *vs* pathological TNM (pTNM).
[d]*P*, cli-ANN *vs* preope-ANN;
[e]*P*, cli-ANN *vs* cTNM;
[f]*P*, cli-ANN *vs* pTNM. pTNM: Pathological TNM; cTNM: Clinical TNM; preope-ANN: Preoperative artificial neural network; AIC: Akaike information criterion.

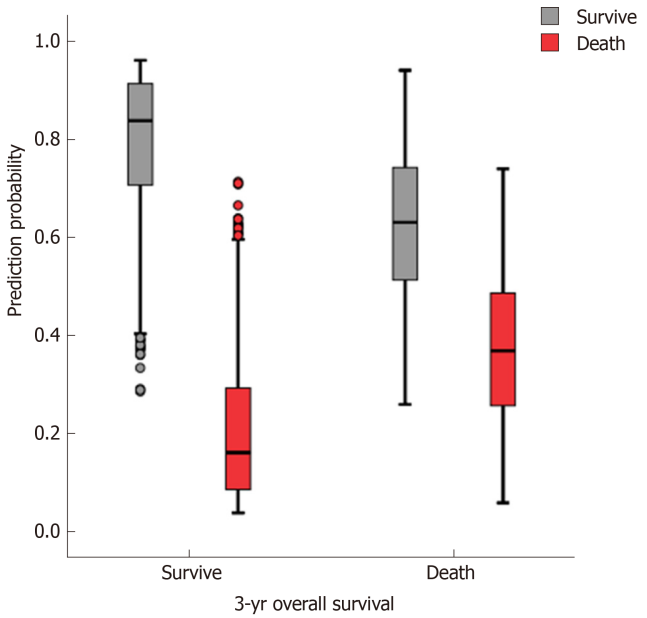

Figure 2 Prediction of the 3-year survival of patients using the preoperative artificial neural network. In the training set, the predictive accuracy rate was 77.3%. The sensitivity and specificity of the centralized training model were 88.5% and 50.1%, respectively. The accuracy of the testing set model for survival prediction was 75.2%. The sensitivity and specificity of the test set model were 86.5% and 43.1%, respectively.

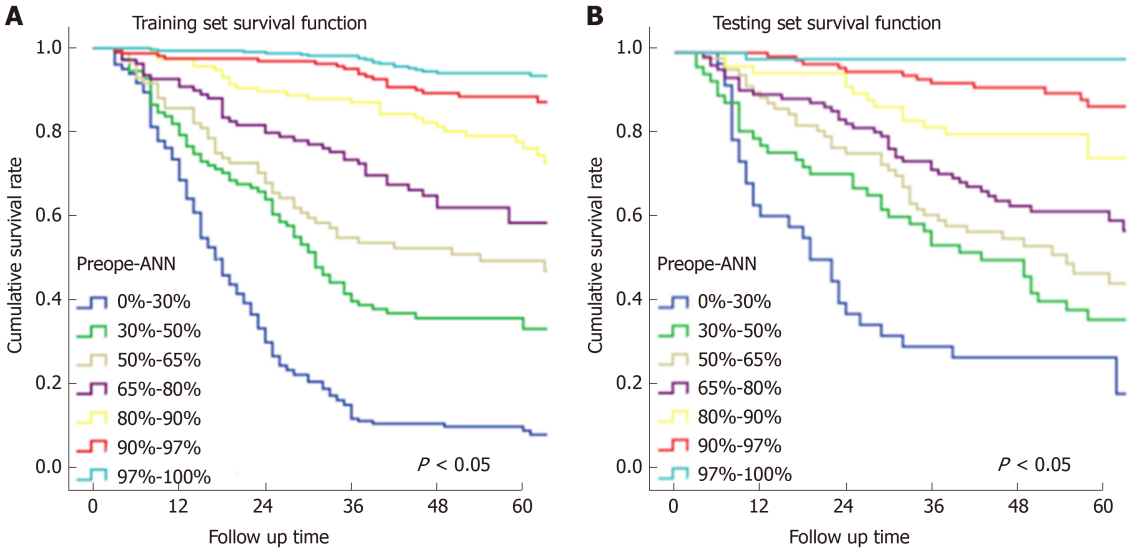

Figure 3 Subgroup survival curves of the preoperative artificial neural network. A: The survival curve of each subgroup of the preoperative artificial neural network model showed good discrimination in the training and testing sets ($P < 0.05$). B: The survival analysis of the training set showed that the substages of the TNM system were well differentiated ($P < 0.05$). Preope-ANN: Preoperative artificial neural network.

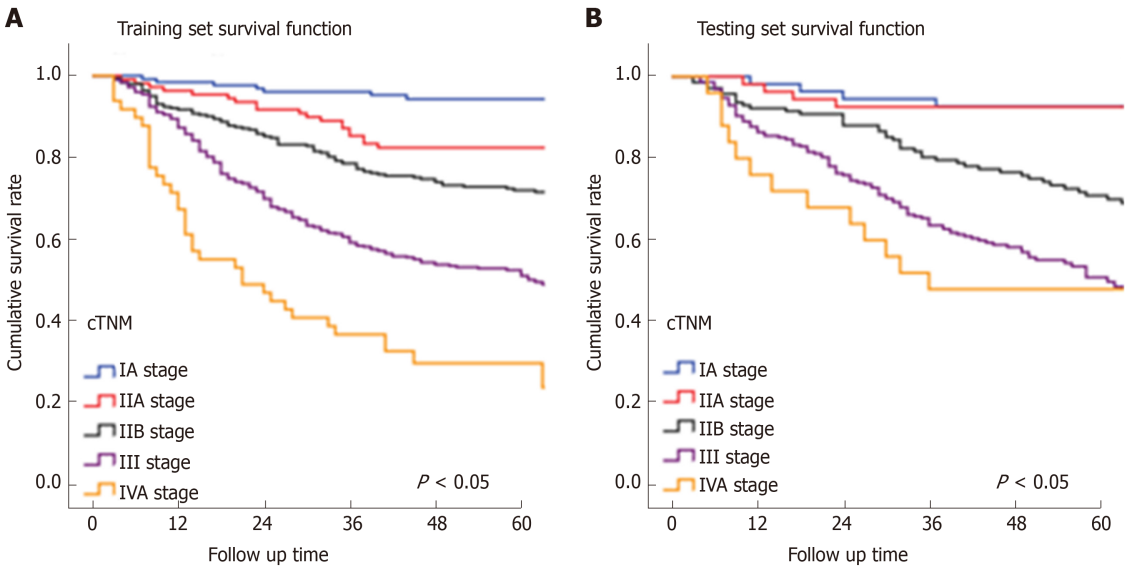

Figure 4 Survival curves of the clinical TNM staging. A: The discrimination between the survival curves of each stage of the clinical TNM (cTNM) system in the training set was good ($P < 0.05$). B: There was no significant difference in the survival curves between the cTNM stages I and II A ($P = 0.935$), and between stages III and IVA ($P = 0.355$). cTNM: Clinical TNM.

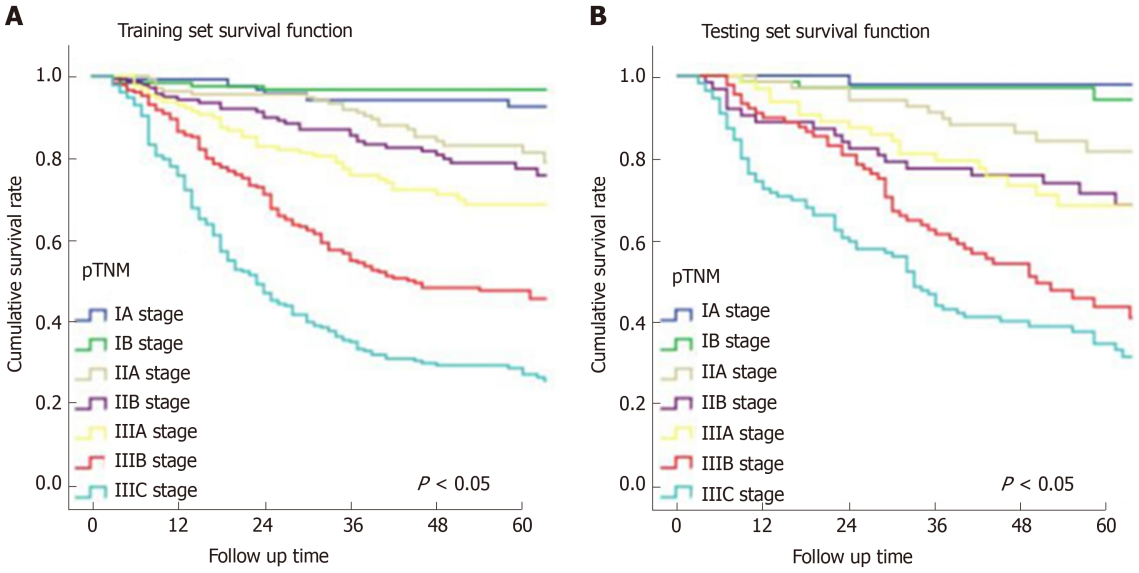

Figure 5 Survival curves of the pathological TNM staging. A: In the training set, the survival curve discrimination between stages IA and IB was poor ($P = 0.240$), and there was no significant difference in the survival curves between stages IIA and IIB and IIB and IIIA ($P < 0.05$). B: In the testing set, there was no significant difference in survival curves between stages IA and IB, IIA and IIB, and IIIA and IIIB of the pathological TNM staging ($P > 0.05$). pTNM: Pathological TNM.

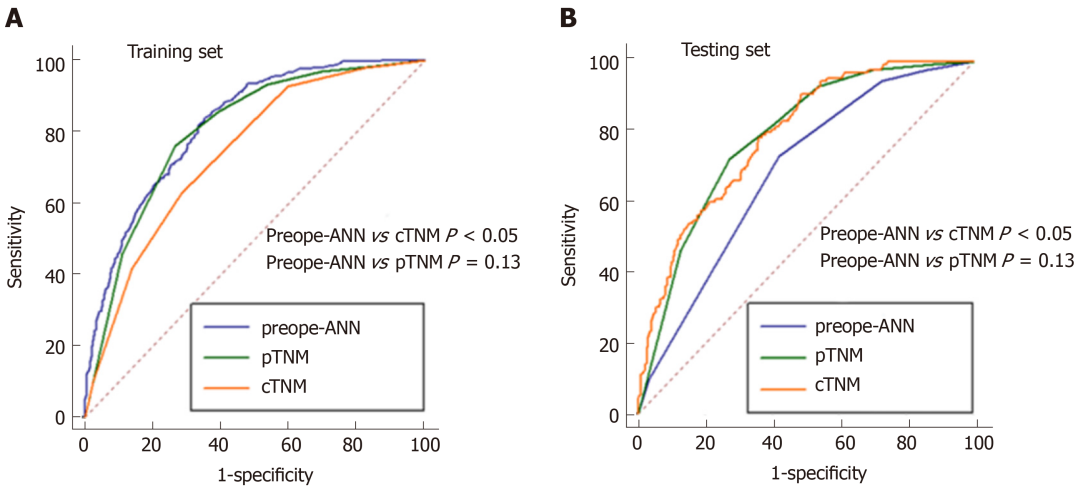

Figure 6 Comparison of the receiver operating characteristic curves among the preope-ANN model, clinical TNM stage, and pathological TNM stage. A: In the training set, the area under the curve (AUC) values of the preoperative artificial neural network (preope-ANN) model, clinical TNM (cTNM) staging, and pathological TNM (pTNM) staging were 0.820 (0.800-0.838), 0.740 (0.718-0.762), and 0.803 (0.782-0.822), respectively. The comparison of the AUC values in the training set showed that the predictive performance of the preope-ANN was better than that of the cTNM stage ($P < 0.05$), and similar to that of pTNM stage ($P = 0.130$). B: In the testing set, the AUC values of the preope-ANN model, cTNM staging, and pTNM staging were 0.790 (0.752-0.825), 0.687 (0.644-0.727), and 0.786 (0.748-0.821), respectively. The comparison of the AUC values in the testing set showed that the prediction performance of the preope-ANN and the pTNM stage was better than that of the cTNM stage ($P < 0.05$), and the prediction performance of the preope-ANN was similar to that of the pTNM stage ($P = 0.858$). pTNM: Pathological TNM; cTNM: Clinical TNM; preope-ANN: Preoperative artificial neural network.

ARTICLE HIGHLIGHTS

Research background

Because of the powerful abilities of self-learning and handling complex biological information, artificial neural network (ANN) models have been widely applied to disease diagnosis, imaging analysis, and prognosis prediction. However, there has been no trained preoperative ANN (preope-ANN) model to preoperatively predict the prognosis of patients with gastric cancer (GC).

Research motivation

This study combined the preoperative blood biomarkers and preoperative tumor data to establish an ANN model in order to build a reliable preoperative prediction system that can achieve the same effect as postoperative TNM staging. The aim of this study was to evaluate the

prognosis of patients with GC and to provide a reasonable individualized treatment plan for patients.

Research objectives
We aimed to establish a neural network model that can predict long-term survival of GC patients before surgery to evaluate the tumor condition before the operation.

Research methods
The clinicopathological data of 1608 GC patients treated from January 2011 to April 2015 at the Department of Gastric Surgery, Fujian Medical University Union Hospital were analyzed retrospectively. Patients were randomly divided into a training set (70%) for establishing a preope-ANN model and a testing set (30%). The prognostic evaluation ability of the preope-ANN model was compared with that of the American Joint Commission on Cancer (8th edition) clinical TNM stage (cTNM) and pathological TNM stage (pTNM) through the receiver operating characteristic curve, Akaike information criterion index, Harrell's C index, and likelihood ratio chi-square.

Research results
We used the variables that were statistically significant factors for the 3-year overall survival as input-layer variables to develop a preope-ANN in the training set. The survival curves within each score of the preope-ANN had good discrimination ($P < 0.05$). Comparing the preope-ANN model, cTNM, and pTNM in both the training and testing sets, the preope-ANN model was superior to cTNM in predictive discrimination (C index), predictive homogeneity (likelihood ratio chi-square), and prediction accuracy (area under the curve). The prediction efficiency of the preope-ANN model was similar to that of pTNM.

Research conclusions
The preope-ANN model can accurately predict the long-term survival of GC patients, and its predictive efficiency is not inferior to pTNM staging.

Research perspectives
This study for the first time confirmed that the preope-ANN is a novel and convenient prognostic model through the use of a large sample data size, which can effectively predict the prognosis of GC patients. In the clinic, preope-ANN can be considered as part of preoperative risk stratification to guide the individualized treatment of patients with GC. The next challenge is to establish a web version of the preope-ANN model that can be dynamically adjusted for the input of different sample data; with this approach, the model accuracy would be closer to the real value and more flexibly applied to the evaluation of clinical patients.

REFERENCES

1 **Bray F**, Ferlay J, Soerjomataram I, Siegel RL, Torre LA, Jemal A. Global cancer statistics 2018: GLOBOCAN estimates of incidence and mortality worldwide for 36 cancers in 185 countries. *CA Cancer J Clin* 2018; **68**: 394-424 [PMID: 30207593 DOI: 10.3322/caac.21492]

2 **Dassen AE**, Dikken JL, van de Velde CJ, Wouters MW, Bosscha K, Lemmens VE. Changes in treatment patterns and their influence on long-term survival in patients with stages I-III gastric cancer in The Netherlands. *Int J Cancer* 2013; **133**: 1859-1866 [PMID: 23564267 DOI: 10.1002/ijc.28192]

3 **Hanahan D**, Weinberg RA. Hallmarks of cancer: the next generation. *Cell* 2011; **144**: 646-674 [PMID: 21376230 DOI: 10.1016/j.cell.2011.02.013]

4 **Harrell FE**, Califf RM, Pryor DB, Lee KL, Rosati RA. Evaluating the yield of medical tests. *JAMA* 1982; **247**: 2543-2546 [PMID: 7069920 DOI: 10.1001/jama.1982.03320430047030]

5 **Hirahara N**, Tajima Y, Fujii Y, Yamamoto T, Hyakudomi R, Taniura T, Kaji S, Kawabata Y. Preoperative Prognostic Nutritional Index Predicts Long-term Outcome in Gastric Cancer: A Propensity Score-matched Analysis. *Anticancer Res* 2018; **38**: 4735-4746 [PMID: 30061243 DOI: 10.21873/anticanres.12781]

6 **Balkwill F**, Mantovani A. Inflammation and cancer: back to Virchow? *Lancet* 2001; **357**: 539-545 [PMID: 11229684 DOI: 10.1016/S0140-6736(00)04046-0]

7 **Coussens LM**, Werb Z. Inflammation and cancer. *Nature* 2002; **420**: 860-867 [PMID: 12490959 DOI: 10.1038/nature01322]

8 **Roxburgh CS**, McMillan DC. Role of systemic inflammatory response in predicting survival in patients with primary operable cancer. *Future Oncol* 2010; **6**: 149-163 [PMID: 20021215 DOI: 10.2217/fon.09.136]

9 **Deng Q**, He B, Liu X, Yue J, Ying H, Pan Y, Sun H, Chen J, Wang F, Gao T, Zhang L, Wang S. Prognostic value of pre-operative inflammatory response biomarkers in gastric cancer patients and the construction of a predictive model. *J Transl Med* 2015; **13**: 66 [PMID: 25885254 DOI: 10.1186/s12967-015-0409-0]

10 **Pan QX**, Su ZJ, Zhang JH, Wang CR, Ke SY. A comparison of the prognostic value of preoperative inflammation-based scores and TNM stage in patients with gastric cancer. *Onco Targets Ther* 2015; **8**: 1375-1385 [PMID: 26124667 DOI: 10.2147/OTT.S82437]

11 **Liu X**, Wu Z, Lin E, Li W, Chen Y, Sun X, Zhou Z. Systemic prognostic score and nomogram based on inflammatory, nutritional and tumor markers predict cancer-specific survival in stage II-III gastric cancer patients with adjuvant chemotherapy. *Clin Nutr* 2019; **38**: 1853-1860 [PMID: 30075998 DOI: 10.1016/j.clnu.2018.07.015]

12 **Cucchetti A**, Piscaglia F, Grigioni AD, Ravaioli M, Cescon M, Zanello M, Grazi GL, Golfieri R, Grigioni WF, Pinna AD. Preoperative prediction of hepatocellular carcinoma tumour grade and micro-vascular invasion by means of artificial neural network: a pilot study. *J Hepatol* 2010; **52**: 880-888 [PMID:

20409605 DOI: 10.1016/j.jhep.2009.12.037]
13 **McQuade JL**, Daniel CR, Hess KR, Mak C, Wang DY, Rai RR, Park JJ, Haydu LE, Spencer C, Wongchenko M, Lane S, Lee DY, Kaper M, McKean M, Beckermann KE, Rubinstein SM, Rooney I, Musib L, Budha N, Hsu J, Nowicki TS, Avila A, Haas T, Puligandla M, Lee S, Fang S, Wargo JA, Gershenwald JE, Lee JE, Hwu P, Chapman PB, Sosman JA, Schadendorf D, Grob JJ, Flaherty KT, Walker D, Yan Y, McKenna E, Legos JJ, Carlino MS, Ribas A, Kirkwood JM, Long GV, Johnson DB, Menzies AM, Davies MA. Association of body-mass index and outcomes in patients with metastatic melanoma treated with targeted therapy, immunotherapy, or chemotherapy: a retrospective, multicohort analysis. *Lancet Oncol* 2018; **19**: 310-322 [PMID: 29449192 DOI: 10.1016/S1470-2045(18)30078-0]
14 **Liu X**, Sun X, Liu J, Kong P, Chen S, Zhan Y, Xu D. Preoperative C-Reactive Protein/Albumin Ratio Predicts Prognosis of Patients after Curative Resection for Gastric Cancer. *Transl Oncol* 2015; **8**: 339-345 [PMID: 26310380 DOI: 10.1016/j.tranon.2015.06.006]
15 **Ma M**, Wang J, Hu Y, Weng M, Liu X, Wang Y. Prognostic Value of Inflammatory Biomarkers in Gastric Cancer Patients and the Construction of a Predictive Model. *Dig Surg* 2019; **36**: 433-442 [PMID: 30300879 DOI: 10.1159/000493432]
16 **Burke HB**, Goodman PH, Rosen DB, Henson DE, Weinstein JN, Harrell FE, Marks JR, Winchester DP, Bostwick DG. Artificial neural networks improve the accuracy of cancer survival prediction. *Cancer* 1997; **79**: 857-862 [PMID: 9024725 DOI: 10.1002/(sici)1097-0142(19970215)79:4<857::aid-cncr24>3.0.co;2-y]
17 **Lancashire LJ**, Lemetre C, Ball GR. An introduction to artificial neural networks in bioinformatics--application to complex microarray and mass spectrometry datasets in cancer studies. *Brief Bioinform* 2009; **10**: 315-329 [PMID: 19307287 DOI: 10.1093/bib/bbp012]
18 **Davies AR**, Gossage JA, Zylstra J, Mattsson F, Lagergren J, Maisey N, Smyth EC, Cunningham D, Allum WH, Mason RC. Tumor stage after neoadjuvant chemotherapy determines survival after surgery for adenocarcinoma of the esophagus and esophagogastric junction. *J Clin Oncol* 2014; **32**: 2983-2990 [PMID: 25071104 DOI: 10.1200/JCO.2014.55.9070]
19 **Marrelli D**, Morgagni P, de Manzoni G, Coniglio A, Marchet A, Saragoni L, Tiberio G, Roviello F; Italian Research Group for Gastric Cancer (IRGGC). Prognostic value of the 7th AJCC/UICC TNM classification of noncardia gastric cancer: analysis of a large series from specialized Western centers. *Ann Surg* 2012; **255**: 486-491 [PMID: 22167003 DOI: 10.1097/SLA.0b013e3182389b1a]
20 **Harrell FE**, Lee KL, Mark DB. Multivariable prognostic models: issues in developing models, evaluating assumptions and adequacy, and measuring and reducing errors. *Stat Med* 1996; **15**: 361-387 [PMID: 8668867 DOI: 10.1002/(SICI)1097-0258(19960229)15:4<361::AID-SIM168>3.0.CO;2-4]
21 **Yoon HM**, Ryu KW, Nam BH, Cho SJ, Park SR, Lee JY, Lee JH, Kook MC, Choi IJ, Kim YW. Is the new seventh AJCC/UICC staging system appropriate for patients with gastric cancer? *J Am Coll Surg* 2012; **214**: 88-96 [PMID: 22036661 DOI: 10.1016/j.jamcollsurg.2011.09.018]
22 **Vrieze SI**. Model selection and psychological theory: a discussion of the differences between the Akaike information criterion (AIC) and the Bayesian information criterion (BIC). *Psychol Methods* 2012; **17**: 228-243 [PMID: 22309957 DOI: 10.1037/a0027127]
23 **Edeline J**, Blanc JF, Johnson P, Campillo-Gimenez B, Ross P, Ma YT, King J, Hubner RA, Sumpter K, Darby S, Evans J, Iwuji C, Swinson D, Collins P, Patel K, Muazzam I, Palmer DH, Meyer T. A multicentre comparison between Child Pugh and Albumin-Bilirubin scores in patients treated with sorafenib for Hepatocellular Carcinoma. *Liver Int* 2016; **36**: 1821-1828 [PMID: 27214151 DOI: 10.1111/liv.13170]
24 **Krittanawong C**, Johnson KW, Rosenson RS, Wang Z, Aydar M, Baber U, Min JK, Tang WHW, Halperin JL, Narayan SM. Deep learning for cardiovascular medicine: a practical primer. *Eur Heart J* 2019; **40**: 2058-2073 [PMID: 30815669 DOI: 10.1093/eurheartj/ehz056]
25 **Park SR**, Kim MJ, Ryu KW, Lee JH, Lee JS, Nam BH, Choi IJ, Kim YW. Prognostic value of preoperative clinical staging assessed by computed tomography in resectable gastric cancer patients: a viewpoint in the era of preoperative treatment. *Ann Surg* 2010; **251**: 428-435 [PMID: 20179530 DOI: 10.1097/SLA.0b013e3181ca69a7]
26 **Shimizu K**, Ito K, Matsunaga N, Shimizu A, Kawakami Y. Diagnosis of gastric cancer with MDCT using the water-filling method and multiplanar reconstruction: CT-histologic correlation. *AJR Am J Roentgenol* 2005; **185**: 1152-1158 [PMID: 16247125 DOI: 10.2214/AJR.04.0651]
27 **Blank S**, Bläker H, Schaible A, Lordick F, Grenacher L, Buechler M, Ott K. Impact of pretherapeutic routine clinical staging for the individualization of treatment in gastric cancer patients. *Langenbecks Arch Surg* 2012; **397**: 45-55 [PMID: 21598045 DOI: 10.1007/s00423-011-0805-8]
28 **Zheng L**, Zou K, Yang C, Chen F, Guo T, Xiong B. Inflammation-based indexes and clinicopathologic features are strong predictive values of preoperative circulating tumor cell detection in gastric cancer patients. *Clin Transl Oncol* 2017; **19**: 1125-1132 [PMID: 28315180 DOI: 10.1007/s12094-017-1649-7]
29 **Shimada H**, Takiguchi N, Kainuma O, Soda H, Ikeda A, Cho A, Miyazaki A, Gunji H, Yamamoto H, Nagata M. High preoperative neutrophil-lymphocyte ratio predicts poor survival in patients with gastric cancer. *Gastric Cancer* 2010; **13**: 170-176 [PMID: 20820986 DOI: 10.1007/s10120-010-0554-3]
30 **Wang Z**, Wang Y, Zhang X, Zhang T. Pretreatment prognostic nutritional index as a prognostic factor in lung cancer: Review and meta-analysis. *Clin Chim Acta* 2018; **486**: 303-310 [PMID: 30138620 DOI: 10.1016/j.cca.2018.08.030]
31 **Mohri Y**, Inoue Y, Tanaka K, Hiro J, Uchida K, Kusunoki M. Prognostic nutritional index predicts postoperative outcome in colorectal cancer. *World J Surg* 2013; **37**: 2688-2692 [PMID: 23884382 DOI: 10.1007/s00268-013-2156-9]
32 **Eo WK**, Chang HJ, Suh J, Ahn J, Shin J, Hur JY, Kim GY, Lee S, Park S, Lee S. The Prognostic Nutritional Index Predicts Survival and Identifies Aggressiveness of Gastric Cancer. *Nutr Cancer* 2015; **67**: 1260-1267 [PMID: 26583916 DOI: 10.1080/01635581.2015.1082112]
33 **Kim JH**, Kim HS, Seo WY, Nam CM, Kim KY, Jeung HC, Lai JF, Chung HC, Noh SH, Rha SY. External validation of nomogram for the prediction of recurrence after curative resection in early gastric cancer. *Ann Oncol* 2012; **23**: 361-367 [PMID: 21566150 DOI: 10.1093/annonc/mdr118]
34 **Yoshida H**, Shimazu T, Kiyuna T, Marugame A, Yamashita Y, Cosatto E, Taniguchi H, Sekine S, Ochiai A. Automated histological classification of whole-slide images of gastric biopsy specimens. *Gastric Cancer* 2018; **21**: 249-257 [PMID: 28577229 DOI: 10.1007/s10120-017-0731-8]

World Journal of Gastroenterology

Submit a Manuscript: https://www.f6publishing.com

World J Gastroenterol 2019 November 21; 25(43): 6465-6482

DOI: 10.3748/wjg.v25.i43.6465

ISSN 1007-9327 (print) ISSN 2219-2840 (online)

ORIGINAL ARTICLE

Observational Study

Metabolic syndrome attenuates ulcerative colitis: Correlation with interleukin-10 and galectin-3 expression

Marina Jovanovic, Bojana Simovic Markovic, Nevena Gajovic, Milena Jurisevic, Aleksandar Djukic, Ivan Jovanovic, Nebojsa Arsenijevic, Aleksandra Lukic, Natasa Zdravkovic

ORCID number: Marina Jovanovic (0000-0002-7691-6133); Bojana Simovic Markovic (0000-0001-8408-4624); Nevena Gajovic (0000-0003-0535-2964); Milena Jurisevic (0000-0002-0553-1156); Aleksandar Djukic (0000-0003-4123-2177); Ivan Jovanovic (0000-0002-1169-2378); Nebojsa Arsenijevic (0000-0002-2107-3490); Aleksandra Lukic (0000-0001-6744-2856); Natasa Zdravkovic (0000-0001-9843-8550).

Author contributions: Jovanovic M, Jovanovic I, Djukic A and Zdravkovic N designed the study; Jovanovic M, Simovic Markovic B and Gajovic N performed the study; Jovanovic M, Simovic Markovic B and Gajovic N collected data; and Jovanovic I, Gajovic N and Jovanovic M analyzed data; Jovanovic M, Lukic A, Arsenijevic N and Jovanovic I wrote the paper; All authors discussed the results and implications and commented on the manuscript at all stages.

Institutional review board statement: The study was reviewed and approved by the Clinical Center of Kragujevac and Faculty of Medical Sciences, University of Kragujevac, Serbia Institutional Review Board.

Informed consent statement: All study participants, or their legal guardian, provided informed written consent prior to study enrollment.

Conflict-of-interest statement: There is no conflict of interest to be

Marina Jovanovic, Natasa Zdravkovic, Department of Internal Medicine, Faculty of Medical Sciences, University of Kragujevac, Kragujevac 34000, Serbia

Bojana Simovic Markovic, Nevena Gajovic, Ivan Jovanovic, Nebojsa Arsenijevic, Center for Molecular Medicine and Stem Cell Research, Faculty of Medical Sciences, University of Kragujevac, Kragujevac 34000, Serbia

Milena Jurisevic, Department of Pharmacy, Faculty of Medical Sciences, University of Kragujevac, Kragujevac 34000, Serbia

Aleksandar Djukic, Department of Pathophysiology, Faculty of Medical Sciences, University of Kragujevac, Kragujevac 34000, Serbia

Aleksandra Lukic, Department of Dentistry, Faculty of Medical Sciences, University of Kragujevac, Kragujevac 34000, Serbia

Corresponding author: Bojana Simovic Markovic, MD, PhD, Research Assistant Professor, Center for Molecular Medicine and Stem Cell Research, Faculty of Medical Sciences, University of Kragujevac, Svetozara Markovica 69, Kragujevac 34000, Serbia.
bojana.simovicmarkovic@medf.kg.ac.rs
Telephone: +381-34-306800
Fax: +381-34-306800

Abstract

BACKGROUND

Ulcerative colitis (UC) is a chronic disease characterized by inflammation of intestinal epithelium, primarily of the colon. An increasing prevalence of metabolic syndrome (MetS) in patients with UC has been documented recently. Still, there is no evidence that MetS alters the course of the UC.

AIM

To test the influence of the MetS on the severity of UC and the local and systemic immune status.

METHODS

Eighty nine patients with *de novo* histologically confirmed UC were divided in two groups, according to ATP III criteria: Group without MetS (no MetS) and group with MetS.

RESULTS

reported.

Data sharing statement: All data used to support the findings of this study are included within the article. Technical appendix, statistical code, and dataset available from the corresponding author at bojana.simovicmarkovic@medf.kg.ac.rs.

STROBE statement: The authors have read the STROBE Statement-checklist of items, and the manuscript was prepared and revised according to the STROBE Statement-checklist of items.

Manuscript source: Unsolicited manuscript

Received: July 25, 2019
Peer-review started: July 25, 2019
First decision: August 27, 2019
Revised: October 24, 2019
Accepted: November 7, 2019
Article in press: November 7, 2019
Published online: November 21, 2019

P-Reviewer: Chiba T, Blanco JR
S-Editor: Tang JZ
L-Editor: A
E-Editor: Ma YJ

Clinically and histologically milder disease with higher serum level of immunosuppressive cytokine interleukin-10 (IL-10) and fecal content of Galectin-3 (Gal-3) was observed in subjects with UC and MetS, compared to subjects suffering from UC only. This was accompanied with predomination of IL-10 over pro-inflammatory cytokines tumor necrosis factor α (TNF-α), interleukin-6 (IL-6), and interleukin-17 (IL-17) in the sera as well as Gal-3 over TNF-α and IL-17 in feces of UC patients with MetS. Further, the patients with both conditions (UC and MetS) had higher percentage of IL-10 producing and Gal-3 expressing innate and acquired immune cells in lamina propria.

CONCLUSION
Local dominance of Gal-3 and IL-10 over pro-inflammatory mediators in patients with MetS may present a mechanism for limiting the inflammatory process and subsequent tissue damage in UC.

Key words: Ulcerative colitis; Metabolic syndrome; Galectin-3; Inflammation; Interleukin-10; Systemic immune response

Core tip: Metabolic syndrome (MetS) is among most common ulcerative colitis (UC) comorbidity. Still, there is no data considering whether the comorbidity of UC and MetS affects the pathology of UC. The aim of this study was to investigate the effects of MetS on severity and immunopathology of UC. Our results revealed that patients with MetS have milder form of UC accompanied with higher level of Galectin-3 and interleukin-10 and altered functional phenotype and intracellular content of lymphocytes infiltrating affected tissue.

Citation: Jovanovic M, Simovic Markovic B, Gajovic N, Jurisevic M, Djukic A, Jovanovic I, Arsenijevic N, Lukic A, Zdravkovic N. Metabolic syndrome attenuates ulcerative colitis: Correlation with interleukin-10 and galectin-3 expression. *World J Gastroenterol* 2019; 25(43): 6465-6482
URL: https://www.wjgnet.com/1007-9327/full/v25/i43/6465.htm
DOI: https://dx.doi.org/10.3748/wjg.v25.i43.6465

INTRODUCTION

Ulcerative colitis (UC) is an inflammatory bowel disease (IBD), characterized by inflammation of the intestinal lamina propria, starting from the rectum and potentially involving the whole colonic mucosa. The course of UC is unpredictable, characterized by spontaneous remission and relapses[1,2]. There is evidence suggesting that the disease occurs in genetically susceptible subjects, triggered by environmental factors, which lead to an exaggerated and uncontrolled immune response to the intestinal flora[1].

It is established that many other diseases are associated with UC such as rheumatoid arthritis, multiple sclerosis, lupus, psoriasis, hypothyroidism, and metabolic syndrome (MetS)[3-6]. Among these diseases, the MetS is the most common comorbidity with pathogenic, clinical and therapeutic implications[3]. MetS represents significant public health concern for its high global prevalence and association with an increased risk for developing chronic diseases[7]. In addition, MetS has been found to have suppressive effect on the immune response, which is confirmed by the higher incidence of unsuccessful vaccinations and complications in infections registered in patients with MetS[8,9].

There is no data considering whether the comorbidity of UC and MetS affects the pathology of UC[3]. Although specific studies dealing with the very mechanism of this aspect have not yet been implemented, this phenomenon deserves attention.

Despite the sustained interest of the researchers in Galectin-3 (Gal-3) and the pronounced and constitutive expression of this molecule in the epithelium of the digestive tract of mice and humans, only a few studies have addressed the possible role of this member of β-galactoside binding proteins in IBDs[10,11]. Gal-3 is produced mainly by monocytes/macrophages and in UC is expressed on $CD68^+$ colon-

infiltrating macrophages[12,13].

The aim of our study was to investigate the effects of MetS on severity and immunopathology of UC.

Herewith, we provide the evidence that patients with MetS have milder form of UC accompanied with higher fecal and serum level of Gal-3 and altered functional phenotype and intracellular content of lymphocytes infiltrating affected tissue.

MATERIALS AND METHODS

Study population

Eighty nine patients (52 male and 37 female), between 21 and 80 years of age, with *de novo* histologically confirmed UC, were included in observational cross-sectional study. Recruited UC patients were divided in two groups, using ATP III criteria for the diagnosis of MetS: Group without MetS (no MetS) and group with MetS[25]. According to these criteria, for the diagnosis of the MetS, it is necessary that patients have at least 3 of 5 disorders: Disglycemia (fasting plasma glucose higher than 5.5 mmol/L and/or 2 h-post load plasma glucose higher than 7.8 mmol/L or active treatment of disglycemia), arterial hypertension (arterial tension higher than 130/85 mmHg or active treatment), central type of obesity, and high-density lipoprotein cholesterol below and triglycerides higher than reference values. All patients within UC + MetS group fulfill all of these criteria.

In each individual case, the diagnosis and assessment of the severity of UC was determined by histological and clinical scores[14-18]. All endoscopies were performed by the same experienced endoscopist (NZ) thus ensuring uniformity in mucosal assessment. The severity of endoscopic lesions was defined using the Mayo endoscopic sub-score that includes erosions/ulcerations, mucosal erythema, visibility of vascular pattern and bleeding provoked/spontaneous, with scores ranging from 0 to 3[17,18]. The clinical score was determined using the *Truelove* and *Witts* clinical activity index and the Mayo clinical index[15,19,20]. Histological score was determined based on Geboes grading[16] and histological sections were examined in a blinded manner by two pathologists, independently. Sections were analyzed for architectural changes, crypt destruction, erosion of the mucous membranes, eosinophilic infiltration, neutrophilic infiltration and chronic inflammatory infiltration. Patients with UC were classified according to Montreal classification of the localization of the UC lesions, as E1 (proctitis), E2 (left-sided colitis), or E3 (pancolitis)[21]. Thirty-four patients had detectable extraintestinal manifestations (fatty liver metamorphosis, primary sclerosing cholangitis, cholelithiasis, bone-joint changes, hematopoietic changes, changes in the reproductive system, eye changes, and dermatologic manifestations- pyoderma gangrenosum or erythema nodosum).

For all study participants, demographic and clinical data were entered in SPSS database. Patients with previously diagnosed colorectal cancer, as well as patients with Crohn's disease or UC who were previously treated with antibiotics, aminosalicylates, corticosteroids, immunosuppressive agents, statins, and biological therapy were not included in the study. All patients had complete medical history, including physical examination, routine laboratory tests and diagnostic imaging (chest X-ray, abdominal ultrasound, abdominal computed tomography scan, and endoscopy). The study was conducted at Center for Gastroenterology, Clinical Center of Kragujevac and Center for Molecular Medicine and Stem Cell Research, Faculty of Medical Sciences, University of Kragujevac, Serbia and was approved by Ethics Committees of these institutions. Additionally, adherence was made to the Principle of Good Clinical Practice and the Declaration of Helsinki at all times. All patients gave their informed consent for blood and tissue analysis. Patients were under continuous medical supervision at the Clinical Center Kragujevac.

Measurements of fecal and serum cytokines levels

Fecal samples were prepared as previously described[22]. Briefly, 1g of fecal samples was diluted, mixed, and homogenized in 5mL of protease inhibitor cocktail (Sigma Aldrich, St. Louis, MO, United States; P83401)[22]. Blood was obtained from patients and healthy control subjects at 8 am and serums were separated, collected and stored at 80 °C before use. Concentrations of tumor necrosis factor α (TNF-α), interleukin-6 (IL-6), interleukin-10 (IL-10), interleukin-17 (IL-17), and Gal-3 were measured in serum and fecal supernatants of UC patients by using commercially available ELISA tests, according to the manufacturer's instructions.

Flow cytometry analysis of colon infiltrating cells in patients with UC

Immune cells were isolated from colons of patients with UC, as previously

described[23,24]. Briefly, after biopsy, tissue samples were washed and incubate in medium with 1 mmol/L EDTA for 10 min at 37 °C with gentle shaking to remove intestinal epithelial cells. Further, specimens were incubated for 20-30 min in 2 mL Dulbecco's Modified Eagle Medium (Lonza, Basel, Swiss) with 1 mg/mL collagenase type I, 0.1 mg/mL DNase and 1 mg/mL hyaluronidase (Sigma-Aldrich, St-Louis, MO, United States, respectively) without fetal bovine serum at 37 °C. Cells were washed and finally submitted to Ficoll density gradient centrifugation for 20 min at 690 *g*. The interphase was carefully removed. Single-cell suspensions were obtained and the cells were washed twice with FACS medium.

For flow cytometry, 1 × 10^6 cells per sample were incubated with anti-human CD4, CD8, CD56, and Gal-3 antibodies conjugated with fluorescein isothiocyanate (FITC; BD Biosciences, Franklin Lakes, NJ, United States), phycoerythrin (PE; BD Biosciences), Peridinin Chlorophyll A Protein (PerCP; BD Biosciences), or allophycocyanin (APC; BD Biosciences). For the intracellular staining, cells were stimulated with phorbol myristate acetate and ionomycin for 4 h at 37 °C with the addition of 1 μg/mL Golgi plug. Intracellular staining for IL-10 and Foxp3 was performed using the BD Bioscience fixation/ permeabilization buffer kit. Flow cytometry was conducted on a BD Biosciences FACSCalibur and the data were analyzed using FlowJo (Tree Star).

Statistical analysis

Data were analyzed using commercially available software (SPSS version 22). Results were analyzed using Student's *t* test, Mann-Whitney *U* test, Chi-squared test or Kruskal-Wallis test where appropriate. Data are presented as mean ± standard error of the mean and the difference was considered significant when $P < 0.05$.

RESULTS

Clinical feature and MetS in patients with UC

Laboratory findings and clinical features of all patients are presented in Table 1. We have compared laboratory findings. Significantly lower white blood cells count (WBC) and increased blood cholesterol, triglycerides, low-density lipoprotein, aspartateaminotransferase, alanine aminotransferase, as well as urea and creatinine were detected in UC patients with MetS, compared to UC patients without MetS (Table 1). There was no significant difference in platelet count and in the concentration of hemoglobin, albumin and globulin between patients with MetS and without MetS (Table 1).

Patients with MetS have milder form of UC

Despite the fact that cholesterol, triglycerides and liver enzymes were higher in MetS, the local findings of UC were milder in MetS + UC patients. Patients with UC and MetS had significantly lower Mayo endoscopic subscore ($P = 0.038$; Figure 1A) and Mayo clinical score ($P = 0.005$; Figure 1B). Within these group of patients (UC + MetS), Mayo ES 1 was recorded in 56.95% patients, while Mayo CS 1 was recorded in 59.72% patients. Therefore, the Mayo ESs and CSs classified the majority of the patients with MetS as having mild UC. We have also registered lower Truelove and Witts clinical score of disease in patients with MetS, but the difference did not reach statistical significance (Figure 1C). Endoscopic data are illustrated in Figure 1D. Endoscopic findings in patients with UC + Mets revealed normal mucosa or slight mucosal erythema, decreased vascular pattern, mild friability, comparing to frank friability, marked erythema, absent vascular pattern and erosions that are characteristic for UC patients without MetS (Figure 1D). Clinical and endoscopic data are supported by pathohistological findings (Figure 2): Chronic inflammatory infiltration ($P = 0.044$; Figure 2A) and eosinophilic infiltration ($P = 0.031$; Figure 2B) in affected tissue of UC patients with MetS were milder than in UC patients without MetS. Neutrophil infiltration, crypt destruction, erosion of the mucous membranes, architectural changes were also milder in UC patients with MetS, but these differences did not reach statistical significance (Figure 2C-F). Representative pathohistological characteristics are shown in Figure 2G.

MetS affects inflammatory and regulatory cytokines in sera and feces of patients with UC

We have assessed concentration of pro and anti-inflammatory cytokines in sera and fecal liquid fraction of all UC patients (Figure 3). Patients with MetS had significantly lower serum level of pro-inflammatory cytokine IL-17 ($P = 0.045$; Figure 3A), while immunosuppressive IL-10 was significantly higher ($P = 0.045$; Figure 3B). There was

Table 1 Clinical and laboratory findings in ulcerative colitis patients

Characteristics	All (*n* = 89)	Without MetS (*n* = 17)	With MetS (*n* = 72)	*P* value
Age (yr)				
Median (range)	50 (21-80)	34 (23-54)	53 (21-80)	0.001
Gender, *n* (%)				
Male	52 (58.43)	11 (64.71)	41 (56.95)	> 0.05
Female	37 (41.57)	6 (35.29)	31 (43.05)	
Smoking status, *n* (%)				
Yes	42 (47.19)	7 (41.18)	35 (48.61)	> 0.05
No	47 (52.81)	10 (58.82)	37 (51.39)	
Localization (PT/LC/PC)	13/51/25	3/7/7	10/44/18	> 0.05
Extraintestinal manifestations (+/-)	34/55	7/10	27/45	> 0.05
WBC (10^9/L)	8.18 ± 0.48	10.27 ± 1.04	7.69 ± 0.49	0.025
Platelet (10^9/L)	377.2 ± 11.4	400.80 ± 28.10	371.60 ± 11.60	> 0.05
Hb (g/L)	125.7 ± 1.97	120.90 ± 4.10	126.80 ± 2.10	> 0.05
Cholesterol (mmol/L)	4.91 ± 0.18	3.71 ± 0.21	5.19 ± 0.19	0.001
Triglycerides (mmol/L)	1.63 ± 0.11	0.89 ± 0.07	1.81 ± 0.11	0.001
HDL (mmol/L)	1.54 ± 0.07	1.73 ± 0.14	1.50 ± 0.07	> 0.05
LDL (mmol/L)	2.62 ± 0.18	1.49 ± 0.28	2.89 ± 0.19	0.001
AST (U/L)	30.08 ± 1.87	20.65 ± 2.27	32.31 ± 2.07	0.002
ALT (U/L)	33.19 ± 4.50	23.29 ± 2.24	35.53 ± 5.28	0.039
GGT (U/L)	36.00 ± 6.70	20.94 ± 2.51	39.56 ± 7.88	> 0.05
Urea (mmol/L)	5.13 ± 0.30	3.69 ± 0.43	5.47 ± 0.33	0.014
Creatinine (μmol/L)	81.89 ± 2.79	68.71 ± 3.31	85.00 ± 3.09	0.014
Albumin (g/L)	41.33 ± 0.88	41.88 ± 0.88	41.19 ± 0.40	> 0.05
Globulin (g/L)	27.44 ± 0.37	27.82 ± 0.59	27.35 ± 0.42	> 0.05

Values are expressed as mean ± standard error of the mean. PT: Proctitis; LC: Left-sided colitis; PC: Pancolitis; MetS: Metabolic syndrome; WBC: White blood cells count; Hb: Hemoglobin; HDL: High-density lipoprotein; LDL: Low-density lipoprotein; AST: Aspartateaminotransferase; ALT: Alanine aminotransferase; GGT: Gamma-glutamyl transpeptidase.

no significant difference in systemic concentration of proinflammatory TNF-α between patients with and without MetS (P = 0.542; Figure 3C).

It is considered that the ratio of counter-regulatory cytokines can be relevant indicator of disease activity[22]. Ratios of TNF-α/IL-10, IL-6/IL-10, and IL-17/IL-10 were significantly lower in the group of patients with MetS (P = 0.014; P = 0.018; P = 0.017; respectively; Figure 3D).

In feces samples, there was no significant difference in the concentration of any tested cytokine. However, there was strikingly higher level of Gal-3 in UC + MetS patients, compared to UC patients (Figure 3E). Accordingly, ratios of Gal-3 and the two inflammatory cytokines (TNF-α and IL-17, were significantly higher in UC + MetS patients in comparison to UC patients (P = 0.039; P = 0.029; respectively; Figure 3F).

MetS alters inflammatory and regulatory cytokines in sera and feces in all endoscopic, clinical and histopathological stages of UC

We further analyzed serum level of cytokines of interest and fecal level of Gal-3 in groups with and without MetS in especially same clinical, endoscopic and histopathological stage of UC, respectively. We detected significantly lower serum level of IL-17 in MetS patients with Mayo endoscopic subscore 1 (P = 0.049) and 3 (P = 0.017), Mayo clinical score 2 (P = 0.031) and 3 (P = 0.032), Truelove and Witts clinical score 2 (P = 0.027) and 3 (P = 0.024) as well as chronic inflammatory infiltration score 3 (P = 0.030), in comparison to UC patients without MetS but in exactly the same scores (Figure 4A). There was no significant difference in systemic concentration of TNF-α between patients with and without MetS in same endoscopic, clinical and histopathological scores (data not shown). Higher serum level of IL-10 was detected in MetS patients with Mayo endoscopic subscore 2 (P = 0.028) and 3 (P = 0.029), Mayo clinical score 1 (P = 0.031), all 3 Truelove and Witts clinical scores (P = 0.035; P = 0.048; P = 0.031, respectively) and chronic inflammatory infiltration score 1 (P = 0.042) (Figure 4B). Higher level of Gal-3 in feces was observed in MetS patients with all

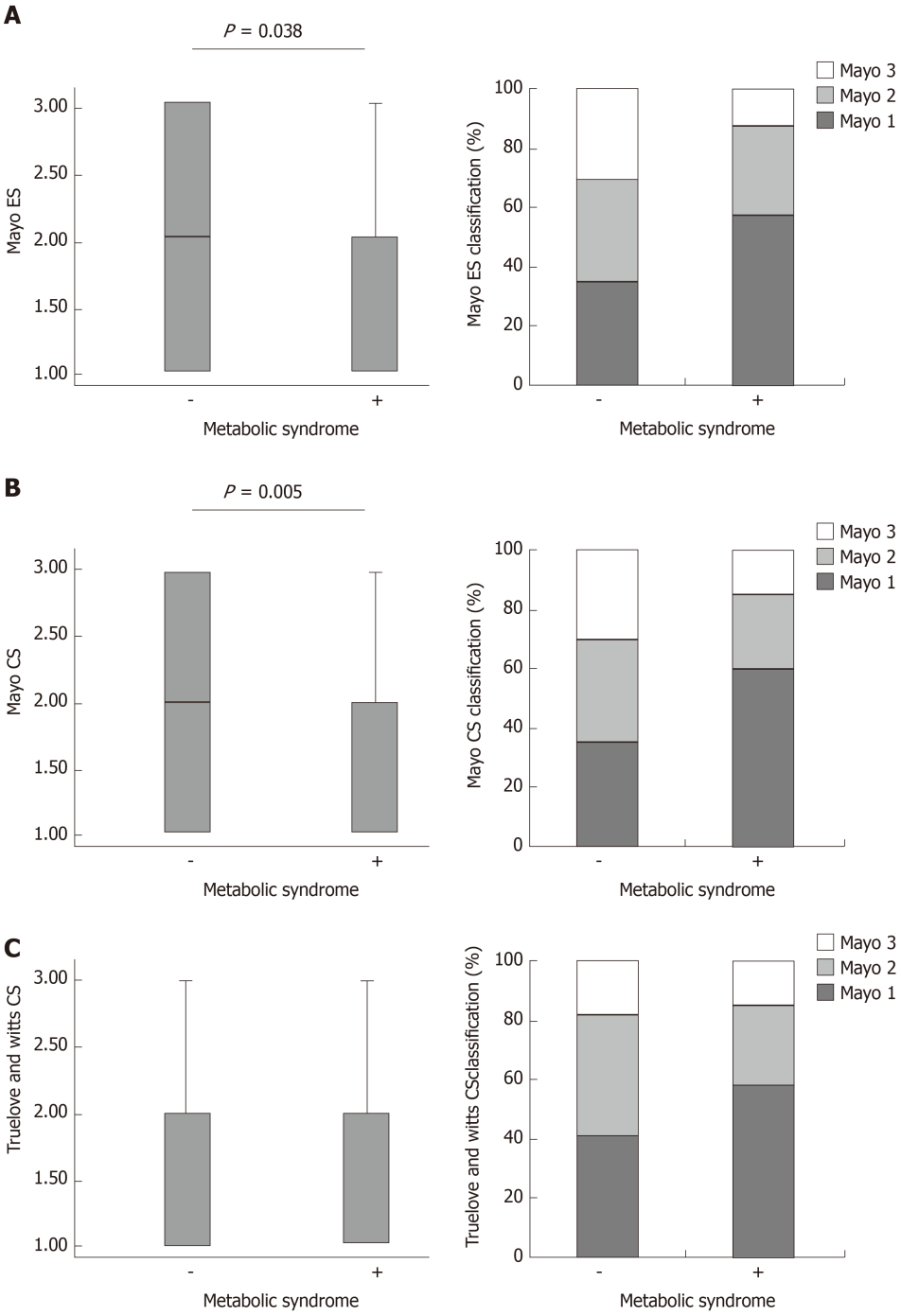
A
P = 0.038
Mayo ES
3.00
2.50
2.00
1.50
1.00
-
+
Metabolic syndrome
Mayo ES classification (%)
100
80
60
40
20
0
Mayo 3
Mayo 2
Mayo 1
B
P = 0.005
Mayo CS
Mayo CS classification (%)
C
Truelove and witts CS
Truelove and witts CSclassification (%)

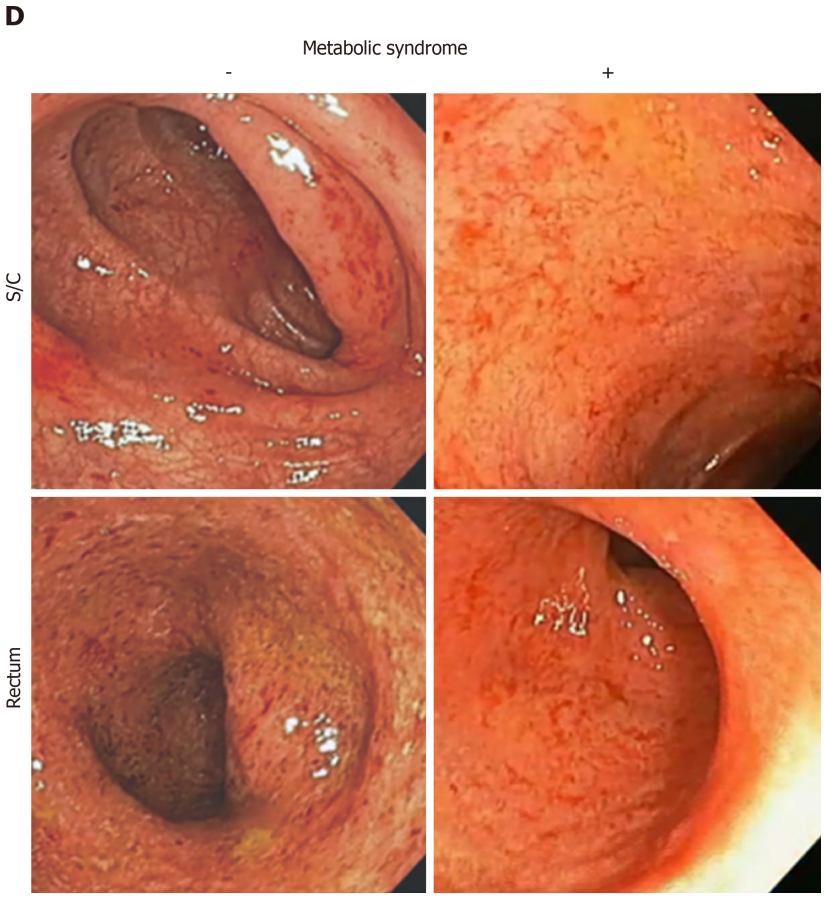

Figure 1 Clinical feature of ulcerative colitis in patients with metabolic syndrome. A: Comparison of Mayo endoscopic subscore between ulcerative colitis (UC) patients without and with metabolic syndrome (MetS) was performed by the Chi-squared test or Kruskal-Wallis test and *P* values are presented above the box plots. B: Mayo clinical scores (CS) between UC patients without and with MetS was performed by the Chi-squared test or Kruskal-Wallis test and *P* values are presented above the box plots. C: Truelove and Witts CS between UC patients without and with MetS was performed by the Chi-squared test or Kruskal-Wallis test and *P* values are presented above the box plots. D: Representative images was presented. ES: Sndoscopic subscore; CS: Clinical scores.

Mayo endoscopic subscores (P = 0.038; P = 0.028; P = 0.038, respectively), Mayo clinical scores (P = 0.017; P = 0.035; P = 0.019, respectively) Truelove and Witts clinical scores (P = 0.038; P = 0.008; P = 0.017, respectively) and chronic inflammatory infiltration scores (P = 0.013; P =0.048; P = 0.020, respectively) (Figure 4C). The same trend was observed for cytokines of interest in all other histopathological scores (eosinophilic infiltration, neutrophil infiltration, crypt destruction, erosion of the mucous membranes, architectural changes), but the difference did not reached statistical significance (data not shown).

Predominance of regulatory cells in colon of patients with UC and MetS

Flow cytometric analysis of colon infiltrating lymphocytes showed no significant differences in the percentage of $CD56^+$ NK cells, $CD3^+CD56^+$ NKT cells, $CD4^+$Th cells and $CD19^+$ B cells (data not shown). Significantly lower percentage of $CD8^+$ T cells (P = 0.035) and higher percentage of $CD4^+Foxp3^+$ regulatory T cells (P = 0.025) were detected in UC patients with MetS (Figure 5A and B). Interestingly, percentage of both, $CD3^+CD56^+$ NKT cells and $CD8^+Foxp3^+$ regulatory T cells expressing Gal-3 was significantly higher in UC + MetS patients (P = 0.029; P = 0.034; respectively; Figure 5C and D). Finally, we analyzed cytokine content in infiltrating immune cells. We have not found the difference in the percentage of infiltrating Th cells, $CD8^+$ T cells and NK cells producing pro-inflammatory cytokines IFN-γ and IL-17 (data not shown). There was higher percentage of regulatory innate $CD56^+$ NK cells and $CD4^+$Th cells producing IL-10 in lamina propria of patients with UC + MetS *vs* UC only (P = 0.034; P = 0.012; respectively; Figure 5E and F).

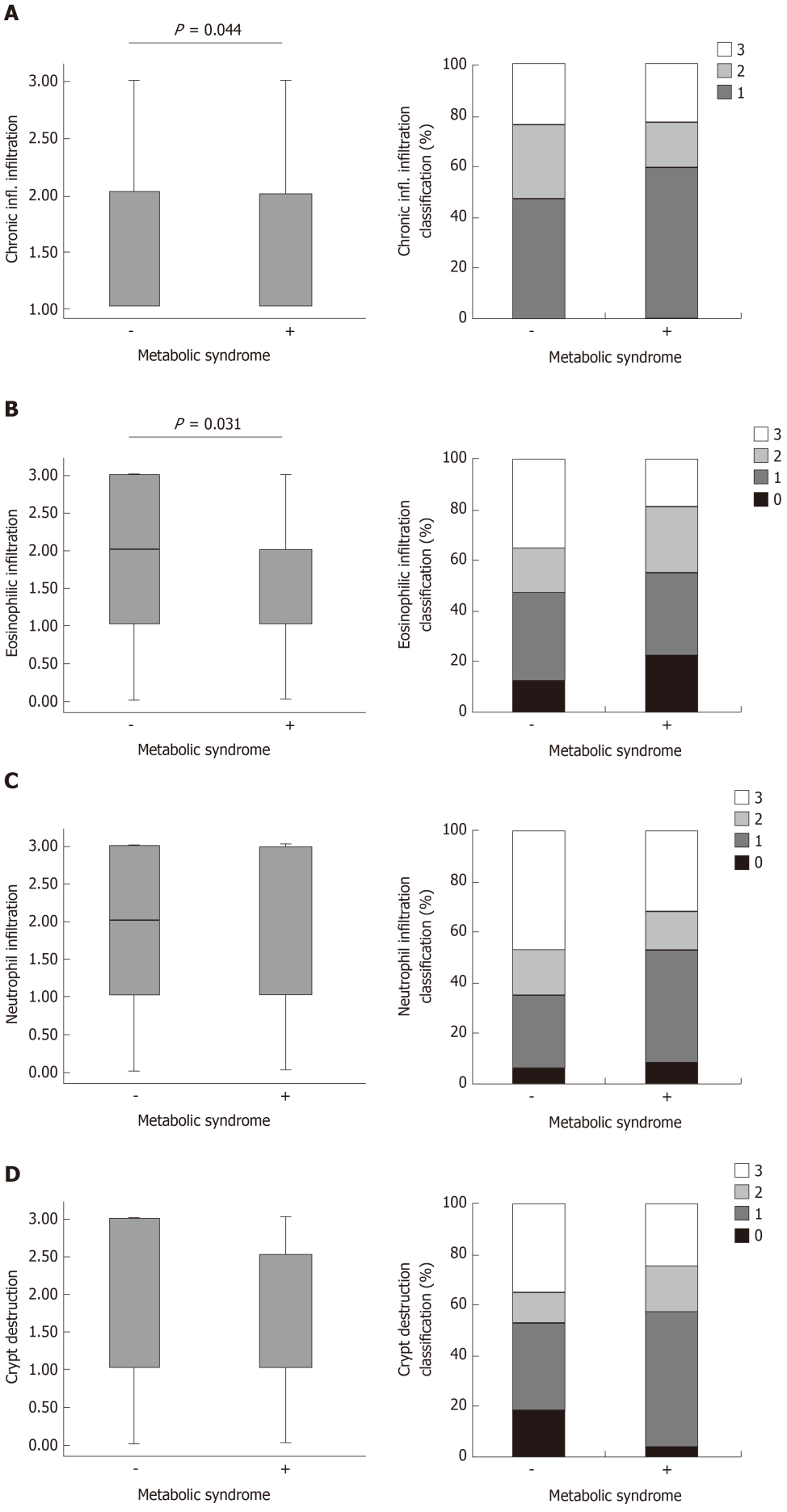
A
P = 0.044
Chronic infl. infiltration
3.00
2.50
2.00
1.50
1.00
-
+
Metabolic syndrome
Chronic infl. infiltration classification (%)
100
80
60
40
20
0
3
2
1
B
P = 0.031
Eosinophilic infiltration
0.50
0.00
Eosinophilic infiltration classification (%)
0
C
Neutrophil infiltration
Neutrophil infiltration classification (%)
D
Crypt destruction
Crypt destruction classification (%)

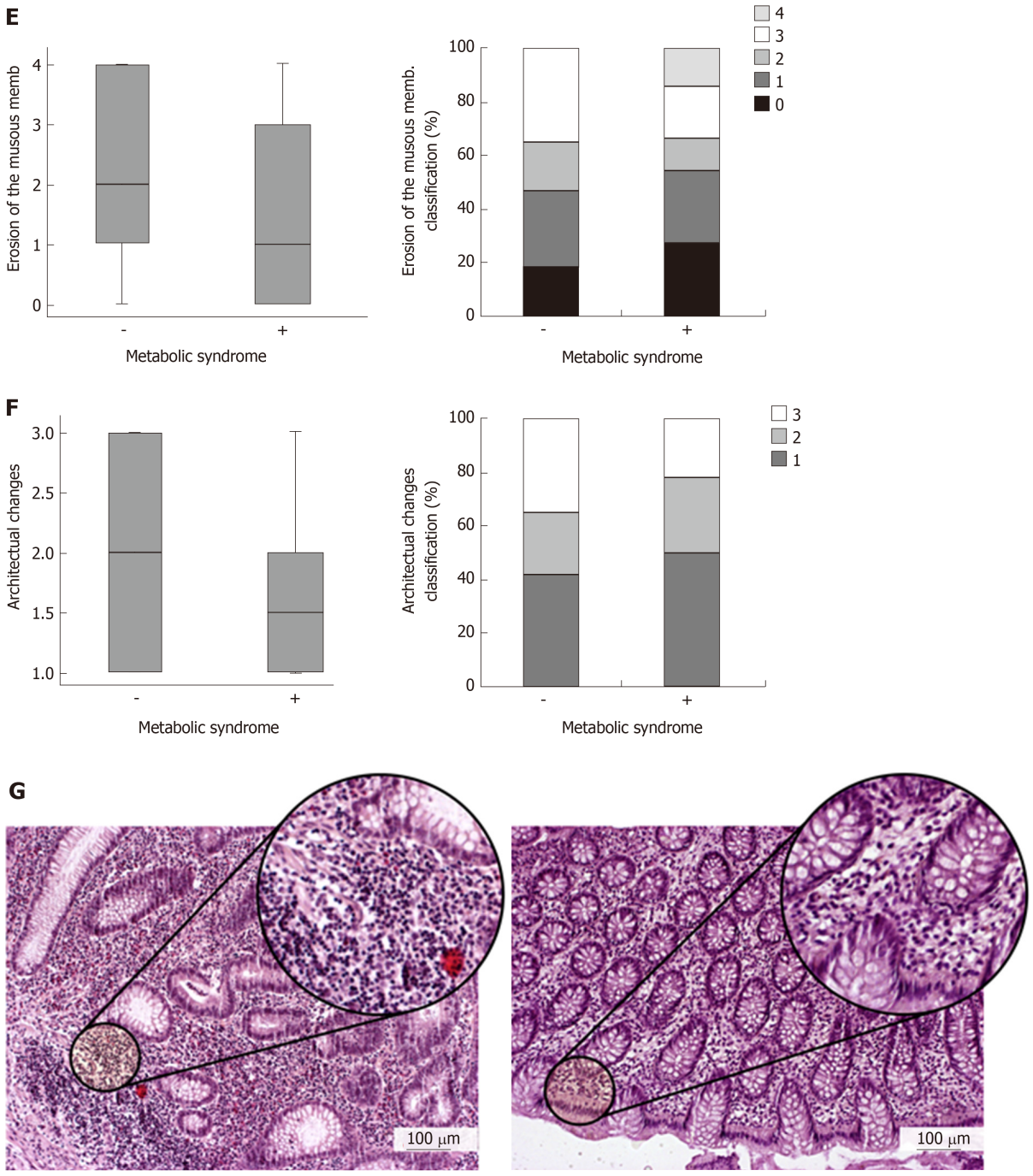

Figure 2 Pathohistological parameters of ulcerative colitis in patients with metabolic syndrome. A-G: Histological score was analyzed for chronic inflammatory infiltration, eosinophilic infiltration, neutrophilic infiltration, crypt destruction, erosion of the mucous membranes and architectural changes. Ulcerative colitis patients without metabolic syndrome (MetS) confirmed the presence of chronic inflammatory infiltration and eosinophilic infiltration in the injured colons (down left panel, 200 x). On the contrary, damage of colon tissue in patients with MetS was manifested by resolution of inflammation, less chronic inflammatory infiltration and eosinophilic infiltration in the colon (down right panel, 200 x).

DISCUSSION

We analyzed the effect of MetS as comorbidity in patients with UC. In this study we included *de novo* histologically confirmed UC patients without previous treatment with antibiotics, aminosalicylates for at least two mo, without corticosteroids, statins, immunosuppressive agents as well as any kind of biological therapy previously. The limitation of our work is that this was cross-sectional study with only one time point evaluation. Patients with MetS are significantly older than patients without MetS (Table 1). As all patients were *de novo* diagnosed with UC and MetS, we could not elucidate the influence of MetS durability on UC severity. Our findings suggest that in general MetS attenuates inflammatory and immunopathogenic correlates of UC. Protective effect of MetS is reflected by clinical and endoscopic score (Figure 1) as well

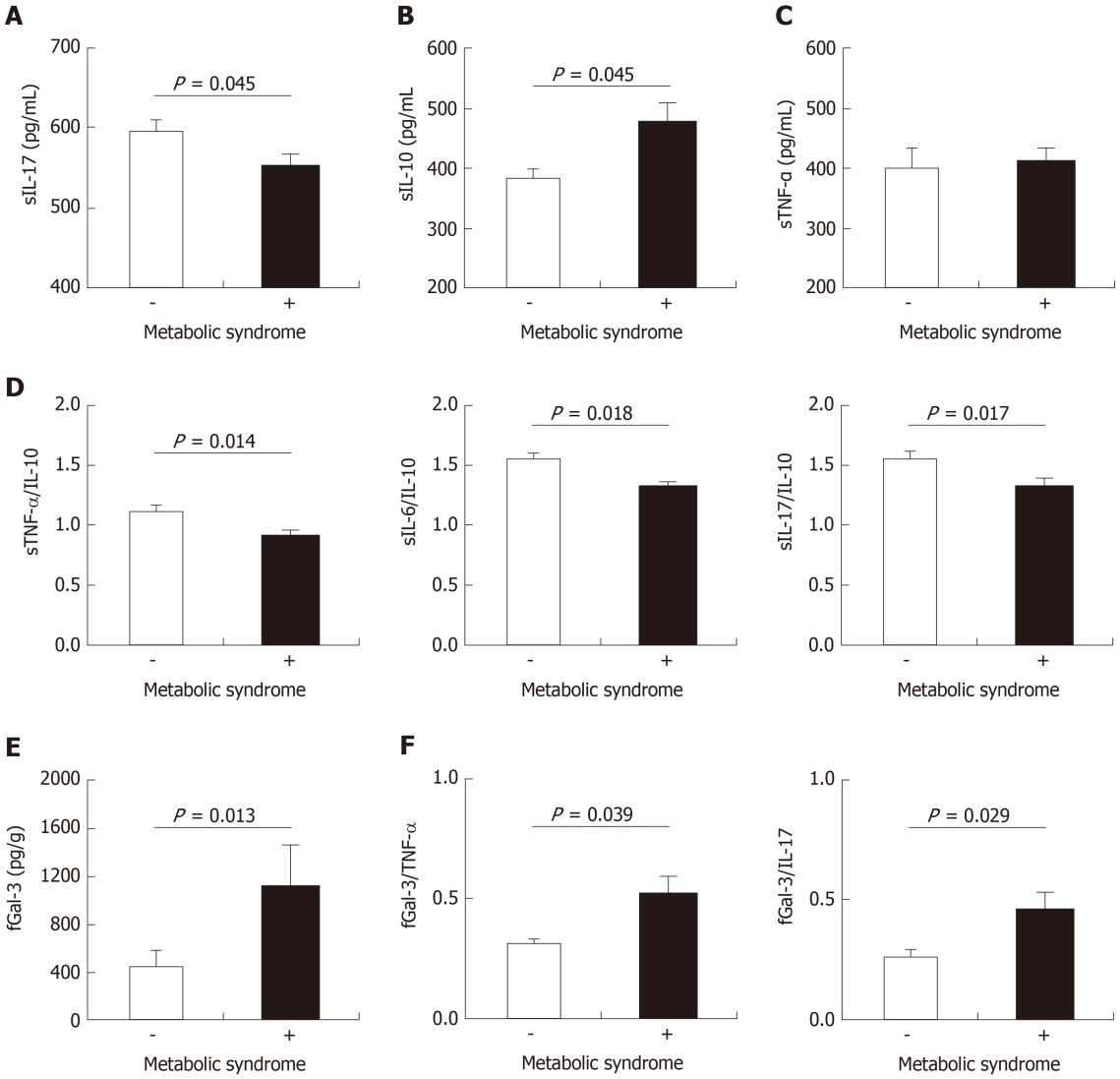

Figure 3 Systemic and local cytokine profile of ulcerative colitis patients according to metabolic syndrome. A: Interleukin-17 (IL-17) were measured by ELISA in the sera of ulcerative colitis (UC) patients without and with metabolic syndrome (MetS). B: Interleukin-10 (IL-10) were measured by ELISA in the sera of UC patients without and with MetS. C: Tumor necrosis factor α (TNF-α) were measured by ELISA in the sera of UC patients without and with MetS. D: sTNF-α/IL-10, sIL-6/IL-10 and sIL-17/IL-10 ratios were evaluated for each patient, separately. E: Concentration of fecal Galectin-3 (Gal-3) was determined in UC patients without and with MetS. F: Ratio of fGal-3/TNF-α and fGal-3/IL-17 in UC patients according to MetS was evaluated for each patient, separately. Patients with UC were divided into two groups: without and with metabolic syndrome (negative "-" or positive "+"). The Student's *t* or Mann-Whitney *U* test was applied as appropriate to evaluate statistical significant differences. TNF-α: Tumor necrosis factor α; IL-17: Interleukin-17; IL-10: Interleukin-10; Gal-3: Galectin-3.

as on histopathology (Figure 2), phenotype of inflammatory cells (Figure 4) and cytokine levels in liquid fraction of feces (Figure 3).

It is believed that immunopathology is the main mechanism in the genesis and progression of UC[1]. The destruction of the intestinal epithelium, which is directly related to the severity of the disease, is due to an intense immune response[26]. There are ample evidences that both, cells of innate and acquired immunity participate in immunopathogenesis of UC[1,2]. This is clearly showed in human[11-13] and experimental studies in animal models by us[10] and others[27-29]. It appears that MetS favors immunosuppressive environment in diseased colon, as evidenced by increased percentage of Foxp3$^+$ regulatory T cells (Figure 5) and IL-10 production (Figures 3 and 5). The lower systemic values of pro-inflammatory IL-17, with higher IL-10 values, and lower ratios of TNF-α/IL-10, IL-6/IL-10, and IL-17/IL-10 (Figure 3A-C) support the prevalence of immunosuppressive over pro-inflammatory mediators in the serum of subjects with MetS. In order to clarify the correlation between UC and cytokine levels in patients with or without MetS, we analyzed serum cytokines and fecal Gal-3 in the same endoscopic, clinical or histopathological score. Significantly lower serum level of IL-17 with higher IL-10 values in sera and Gal-3 values in feces in MetS patients with almost all Mayo endoscopic subscores, Mayo clinical scores, Truelove and Witts clinical scores and chronic inflammatory infiltration scores (Figure 4)

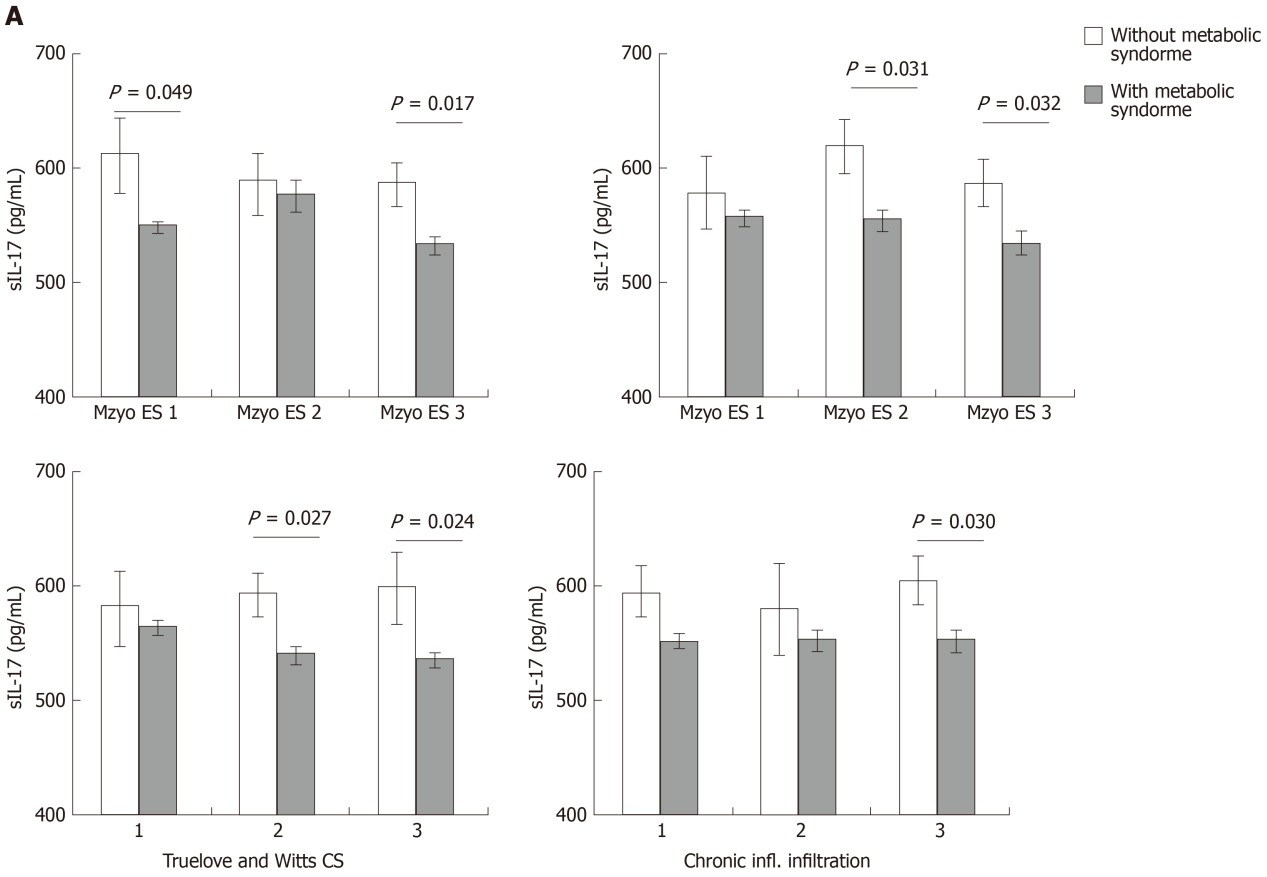
A
Without metabolic syndorme
With metabolic syndorme
sIL-17 (pg/mL)
700
600
500
400
P = 0.049
P = 0.017
Mzyo ES 1
Mzyo ES 2
Mzyo ES 3
P = 0.031
P = 0.032
P = 0.027
P = 0.024
1
2
3
Truelove and Witts CS
P = 0.030
Chronic infl. infiltration

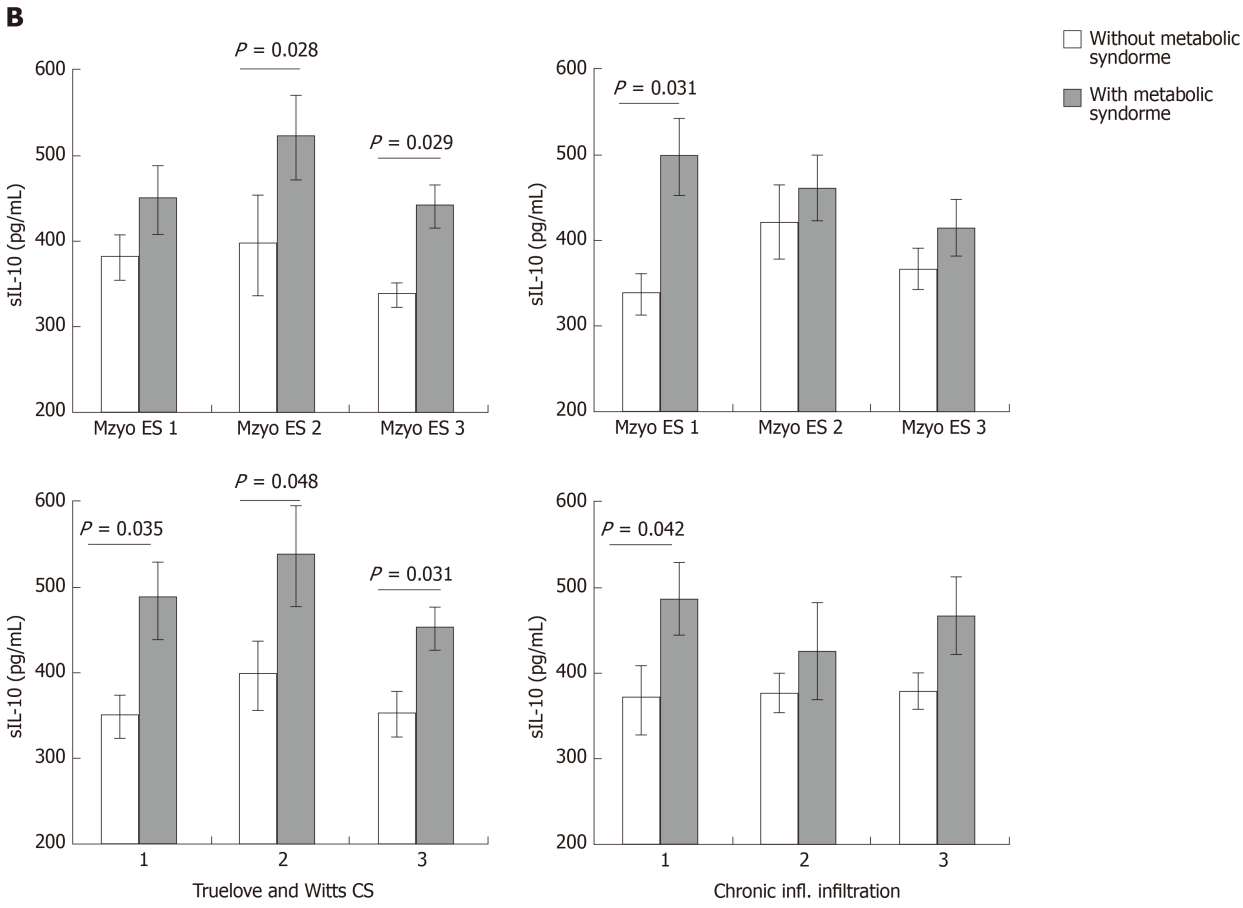
B
Without metabolic syndorme
With metabolic syndorme
sIL-10 (pg/mL)
600
500
400
300
200
P = 0.028
P = 0.029
Mzyo ES 1
Mzyo ES 2
Mzyo ES 3
P = 0.031
P = 0.035
P = 0.048
P = 0.031
1
2
3
Truelove and Witts CS
P = 0.042
Chronic infl. infiltration

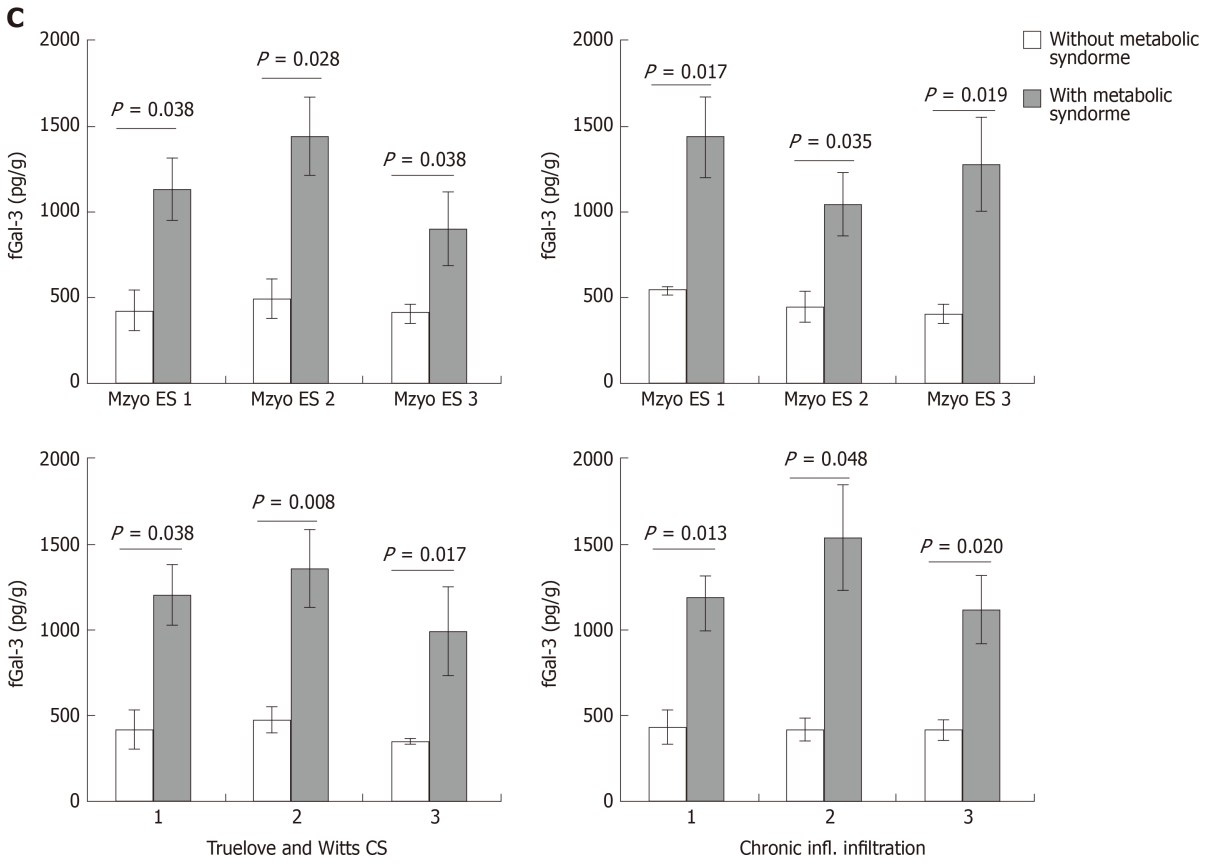

Figure 4 Systemic and local cytokine profile of patients with especially same clinical, endoscopic and histopathological stage of ulcerative colitis, according to metabolic syndrome. Patients with ulcerative colitis (UC) were divided into groups according to clinical, endoscopic and histopathological stage of UC, respectively. A: Interleukin-17 were measured by ELISA in the sera of UC patients without and with metabolic syndrome (MetS). B: Interleukin-10 were measured by ELISA in the sera of UC patients without and with MetS. C: Galectin-3 were measured by ELISA in the sera of UC patients without and with MetS. The Student's *t* or Mann-Whitney U test was applied as appropriate to evaluate statistical significant differences. IL-17: Interleukin-17; IL-10: Interleukin-10; Gal-3: Galectin-3.

implicate that disease severity does not affect difference in the concentration of systemic and fecal proinflammatory and immunosuppressive cytokines between UC patients with and without MetS.

Analysis of functional phenotype of lymphoid cells revealed increased accumulation of IL-10 producing NK cells and Th lymphocytes (Figures 3B, 5E and F), in agreement with higher IL-10 level in the serum of the patients with MetS. In line with our finding, study on UC patients, by Acovic *et al*[24], revealed that mucosal healing was accompanied by decreased serum and fecal levels of pro-inflammatory cytokines and elevation of anti-inflammatory IL-10 as well as significantly higher percentage of immunosuppressive regulatory T cells- Tregs, IL-10- producing Th lymphocytes and NK cells, indicating that the milder form of UC in subjects with MetS is most likely due to altered local immune response. Other study[30] showed two fold increase of the number of peripheral Th lymphocytes in patients with MetS, compared to healthy controls, with the prevalence of Th2 cells. Increased percentage of Th lymphocytes and reduced percentage of $CD8^+$ T lymphocytes in peripheral blood of patients with MetS which is in line with our results was also recorded[31].

Recent studies have suggested the association of MetSs with immune system dysfunction[32,33]. MetS induces the activation of the immune system in some tissues, which is often manifested by slightly elevated markers of chronic inflammation[32,33], but also negatively affects the immune response, which is confirmed by the higher incidence of unsuccessful vaccinations and complications in infections[8,9].

Gal-3 concentration is significantly increased in feces of UC + MetS patients, as well as Gal-3/TNF-α and Gal-3/IL-17 ratios (Figure 3E and F). Recently, Li *et al*[34] have shown that Gal-3 causes cellular and systemic insulin resistance. It is also interesting that Gal-3 appears to be involved in protective role of MetS in UC (Figures 3-5). Despite that Gal-3 has been found to promote inflammation in some experimental models[11,35], there is also evidence that it may attenuate pathologic condition in the others[36,37]. Our recent research has shown higher systemic concentration of Gal-3 in end stage renal disease patients infected with hepatitis C virus, suggesting on hepatoprotective role of Gal-3 from virus destruction[38]. Our other study revealed

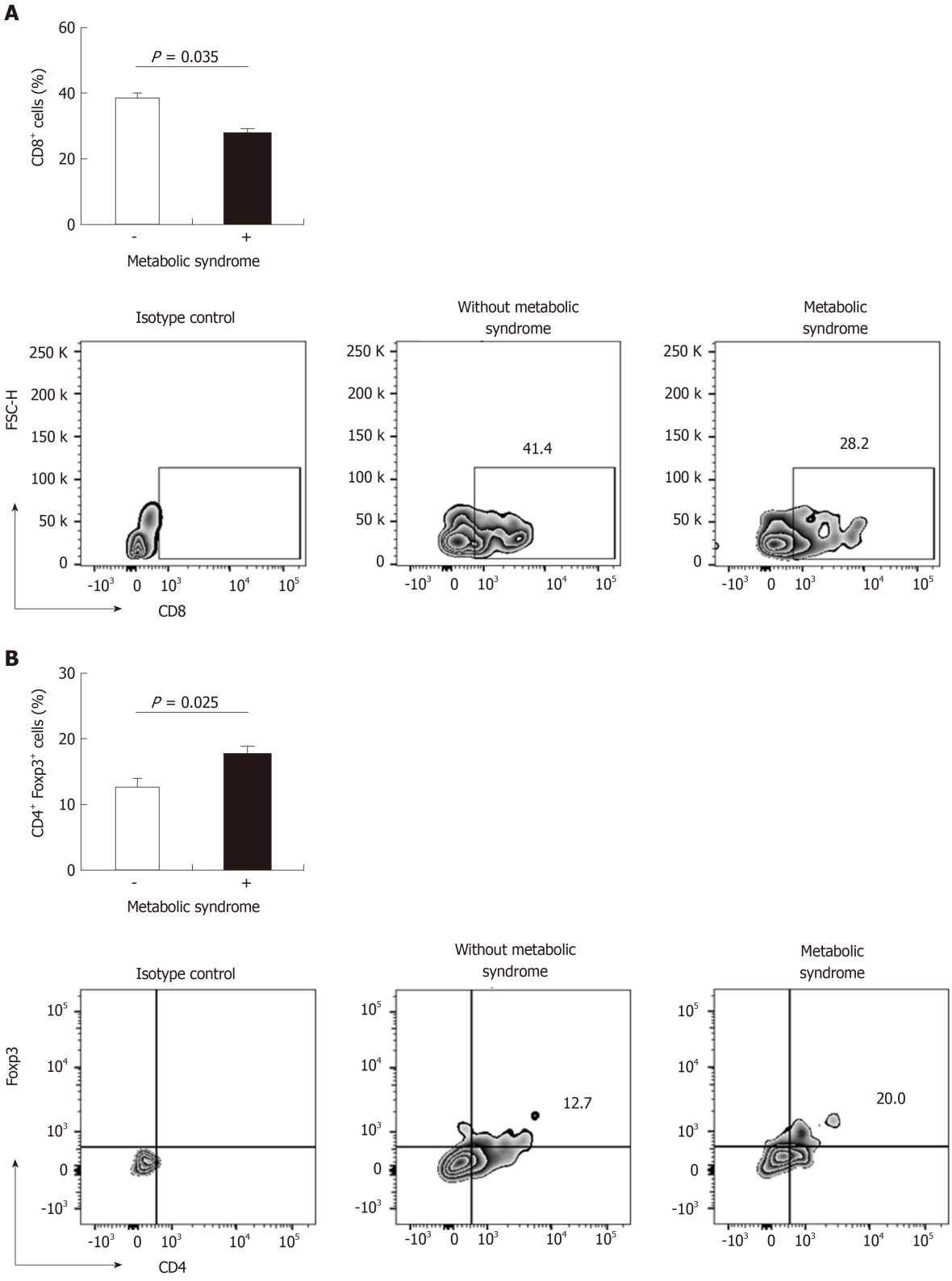
A
P = 0.035
CD8+ cells (%)
Metabolic syndrome
Isotype control
Without metabolic syndrome
Metabolic syndrome
FSC-H
CD8
41.4
28.2
B
P = 0.025
CD4+ Foxp3+ cells (%)
Metabolic syndrome
Isotype control
Without metabolic syndrome
Metabolic syndrome
Foxp3
CD4
12.7
20.0

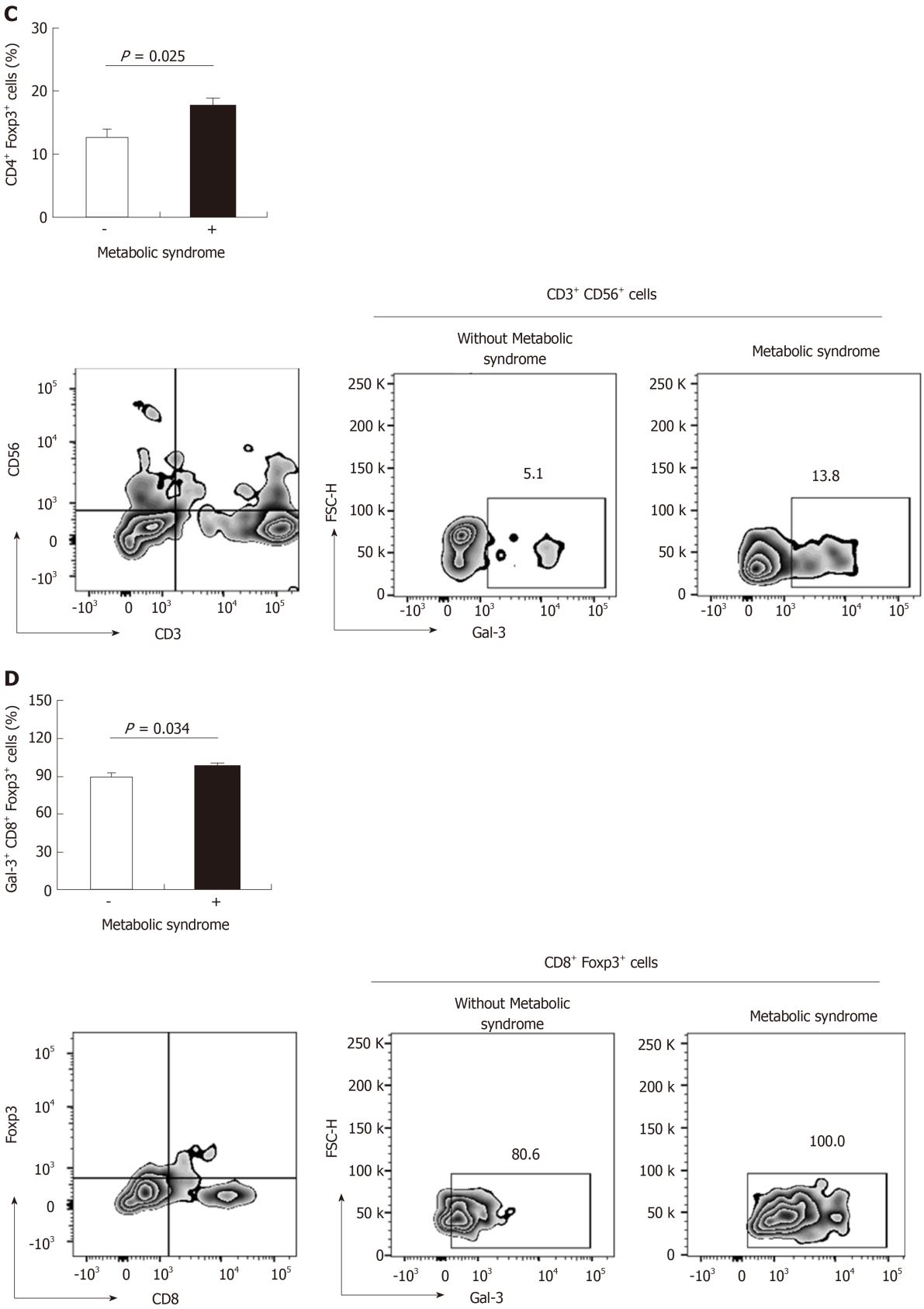
C
CD4+ Foxp3+ cells (%)
P = 0.025
Metabolic syndrome
CD3+ CD56+ cells
Without Metabolic syndrome
Metabolic syndrome
CD56
CD3
FSC-H
Gal-3
5.1
13.8
D
Gal-3+ CD8+ Foxp3+ cells (%)
P = 0.034
Metabolic syndrome
CD8+ Foxp3+ cells
Without Metabolic syndrome
Metabolic syndrome
Foxp3
CD8
FSC-H
Gal-3
80.6
100.0

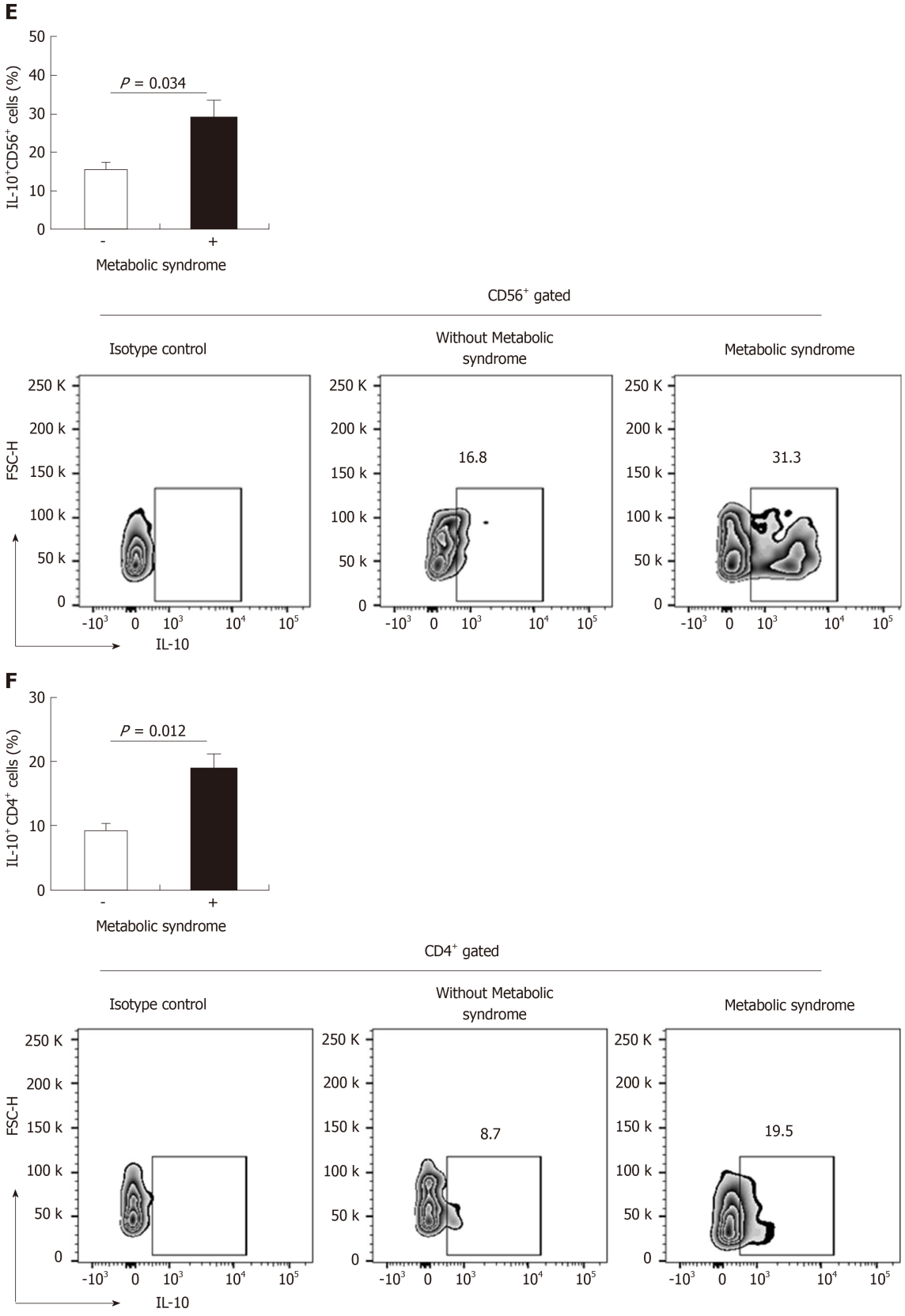

Figure 5 Functional phenotype of immune cells in colonic mucosa. A: The graph and representative FACS plots displaying the percentage of $CD8^+$ T cells derived from colonic mucosa of ulcerative colitis (UC) patients without and with metabolic syndrome (MetS). B: The graph and representative FACS plots displaying the percentage of T regulatory cells ($CD4^+Fox3^+$) derived from colonic mucosa of UC patients without and with MetS. C: The graph and representative FACS plots displaying the percentage of Galectin-3^+ (Gal-3^+) NKT ($CD3^+CD56^+$) cells derived from colonic mucosa of UC patients without and with MetS. D: The graph and representative FACS plots displaying the percentage of $CD8^+Foxp3^+$ cells derived from colonic mucosa of UC patients without and with MetS. E and F: The graph and representative FACS plots displaying the percentage of Interleukin-10 producing $CD56^+$ and $CD4^+$ cells derived from colonic mucosa of UC patients without and with MetS. Cellular make up of colon-infiltrating immune cells were examined by flow cytometry. The Student's *t* or Mann-Whitney U test was applied to evaluate statistical significant differences among the two groups. IL-10: Interleukin-10; Gal-3: Galectin-3.

higher fecal concentration of Gal-3 and higher Gal-3/TNF-α ratio in patients with more severe form of colorectal cancer, thus suggesting immunosuppressive effect of Gal-3 on antitumor immune response[39]. Moreover, Tsai *et al*[40] showed that Gal-3 favors accumulation of regulatory T cells in the colon mucosa which suppresses inflammation and decreases the severity of dextran sulfate sodium-induced colitis. In line with these studies are our results showing significantly higher number of NKT cells and $CD8^+$ regulatory T cells expressing Gal-3 in affected lamina propria derived from UC + MetS patients (Figure 5). Moreover, significantly higher fecal values of Gal-3 and Gal-3/TNF -α and Gal-3/IL-17 ratios (Figure 3D) indicate pronounced local Gal-3 predominance over pro-inflammatory mediators in patients with MetS.

In summary, our data shows for the first time clinically and endoscopically milder disease in UC patients with MetS. The presence of MetS may attenuate colon inflammation, possibly by deviating local inflammatory response toward enhanced participation of immunosuppressive cells and molecules. The increase in systemic IL-10 and local Gal-3 production as well as expression on Tregs and immunocompetent cells accumulating in affected colon tissue implicate on IL-10 and Gal-3 dependent immunomodulation. The precise mechanism of Gal-3 effect in MetS and UC comorbidity is still to be clarified.

ARTICLE HIGHLIGHTS

Research background

Ulcerative colitis (UC) is a chronic disease associated with many other diseases such as rheumatoid arthritis, multiple sclerosis, lupus, psoriasis, hypothyroidism, and metabolic syndrome (MetS). Among these diseases, the MetS is the most common comorbidity. There is no evidence considering whether the comorbidity with MetS alters the course of the UC.

Research motivation

We hope to offer reliable evidence that MetS affects the outcome of the UC, given the increasingly common comorbidity.

Research objectives

Test the impact of the MetS on the severity of UC and the local and systemic immune response.

Research methods

A total of 89 patients with *de novo* confirmed UC were enrolled in this cross-sectional study, and they were further divided in two groups, according to ATP III criteria: group without MetS (no MetS) and group with MetS. Severity of UC was determined by histological and clinical scores, fecal and serum cytokines levels were determined using an enzyme-linked immunosorbent assay, while cellular makeup of colon infiltrations was determined by flow cytometry.

Research resultsWhen compared to UC patients without MetS, clinically and histologically milder disease with higher serum level of immunosuppressive cytokine interleukin- 10 (IL-10) and fecal content of Galectin-3 (Gal-3) was observed in subjects with UC and MetS. This was accompanied with predomination of IL-10 over pro-inflammatory cytokines tumor necrosis factor α (TNF-α), interleukin-6, and interleukin-17 (IL-17) in the sera as well as Gal-3 over TNF-α and IL-17 in feces of UC patients with MetS. Significantly lower systemic values of IL-17, higher values of IL-10 and Gal-3 values in feces were determined in MetS patients in especially same clinical, endoscopic and histopathological stage of UC as patients without MetS. In addition, UC + MetS patients had higher percentage of IL-10 producing and Gal-3 expressing innate and acquired immune cells in lamina propria of affected colon tissue.

Research conclusions

UC patients with MetS have clinically and histologically milder disease. Predominance of Gal-3 and IL-10 over pro-inflammatory mediators in patients with MetS may present a mechanism for limiting the inflammatory process and subsequent tissue damage in UC.

Research perspectives

Future studies are needed to investigate the exact mechanism underlying the protective effect of MetS in biology of UC. And it is necessary to determinate the influence of developmental stages of MetS on the severity of UC. Large sample size studies are also required to confirm the current findings.

ACKNOWLEDGEMENTS

We particularly want to thank Milomir Simovic MD, PhD from United States. Army Institute of Surgical Research, Department of Pathology for verifying the language of the manuscript. Also the authors would like to thank Aleksandar Ilic and Milan Milojevic for excellent technical assistance.

REFERENCES

1 **Bouma G**, Strober W. The immunological and genetic basis of inflammatory bowel disease. *Nat Rev Immunol* 2003; **3**: 521-533 [PMID: 12876555 DOI: 10.1038/nri1132]
2 **Xavier RJ**, Podolsky DK. Unravelling the pathogenesis of inflammatory bowel disease. *Nature* 2007; **448**: 427-434 [PMID: 17653185 DOI: 10.1038/nature06005]
3 **Maconi G**, Furfaro F, Sciurti R, Bezzio C, Ardizzone S, de Franchis R. Glucose intolerance and diabetes mellitus in ulcerative colitis: pathogenetic and therapeutic implications. *World J Gastroenterol* 2014; **20**: 3507-3515 [PMID: 24707133 DOI: 10.3748/wjg.v20.i13.3507]
4 **Bernstein CN**, Wajda A, Blanchard JF. The clustering of other chronic inflammatory diseases in inflammatory bowel disease: a population-based study. *Gastroenterology* 2005; **129**: 827-836 [PMID: 16143122 DOI: 10.1053/j.gastro.2005.06.021]
5 **Cohen R**, Robinson D, Paramore C, Fraeman K, Renahan K, Bala M. Autoimmune disease concomitance among inflammatory bowel disease patients in the United States, 2001-2002. *Inflamm Bowel Dis* 2008; **14**: 738-743 [PMID: 18300281 DOI: 10.1002/ibd.20406]
6 **Bardella MT**, Elli L, De Matteis S, Floriani I, Torri V, Piodi L. Autoimmune disorders in patients affected by celiac sprue and inflammatory bowel disease. *Ann Med* 2009; **41**: 139-143 [PMID: 18777226 DOI: 10.1080/07853890802378817]
7 **Ford ES**. Risks for all-cause mortality, cardiovascular disease, and diabetes associated with the metabolic syndrome: a summary of the evidence. *Diabetes Care* 2005; **28**: 1769-1778 [PMID: 15983333 DOI: 10.2337/diacare.28.7.1769]
8 **Bandaru P**, Rajkumar H, Nappanveettil G. The impact of obesity on immune response to infection and vaccine: an insight into plausible mechanisms. *Endocrinol Metab Syndr* 2013; **2**: 113 [DOI: 10.4172/2161-1017.1000113]
9 **Sheridan PA**, Paich HA, Handy J, Karlsson EA, Hudgens MG, Sammon AB, Holland LA, Weir S, Noah TL, Beck MA. Obesity is associated with impaired immune response to influenza vaccination in humans. *Int J Obes* (*. Lond)* 2012; **36**: 1072-1077 [PMID: 22024641 DOI: 10.1038/ijo.2011.208]
10 **Simovic Markovic B**, Nikolic A, Gazdic M, Bojic S, Vucicevic L, Kosic M, Mitrovic S, Milosavljevic M, Besra G, Trajkovic V, Arsenijevic N, Lukic ML, Volarevic V. Galectin-3 Plays an Important Pro-inflammatory Role in the Induction Phase of Acute Colitis by Promoting Activation of NLRP3 Inflammasome and Production of IL-1β in Macrophages. *J Crohns Colitis* 2016; **10**: 593-606 [PMID: 26786981 DOI: 10.1093/ecco-jcc/jjw013]
11 **Frol'ová L**, Smetana K, Borovská D, Kitanovicová A, Klimesová K, Janatková I, Malícková K, Lukás M, Drastich P, Benes Z, Tucková L, Manning JC, André S, Gabius HJ, Tlaskalová-Hogenová H. Detection of galectin-3 in patients with inflammatory bowel diseases: new serum marker of active forms of IBD? *Inflamm Res* 2009; **58**: 503-512 [PMID: 19271150 DOI: 10.1007/s00011-009-0016-8]
12 **Müller S**, Schaffer T, Flogerzi B, Fleetwood A, Weimann R, Schoepfer AM, Seibold F. Galectin-3 modulates T cell activity and is reduced in the inflamed intestinal epithelium in IBD. *Inflamm Bowel Dis* 2006; **12**: 588-597 [PMID: 16804396 DOI: 10.1097/01.MIB.0000225341.37226.7c]
13 **Brazowski E**, Dotan I, Tulchinsky H, Filip I, Eisenthal A. Galectin-3 expression in pouchitis in patients with ulcerative colitis who underwent ileal pouch-anal anastomosis (IPAA). *Pathol Res Pract* 2009; **205**: 551-558 [PMID: 19278794 DOI: 10.1016/j.prp.2009.02.001]
14 **Pineton de Chambrun G**, Peyrin-Biroulet L, Lémann M, Colombel JF. Clinical implications of mucosal healing for the management of IBD. *Nat Rev Gastroenterol Hepatol* 2010; **7**: 15-29 [PMID: 19949430 DOI: 10.1038/nrgastro.2009.203]
15 **TRUELOVE SC**, WITTS LJ. Cortisone in ulcerative colitis; final report on a therapeutic trial. *Br Med J* 1955; **2**: 1041-1048 [PMID: 13260656 DOI: 10.1136/bmj.2.4947.1041]
16 **Geboes K**, Riddell R, Ost A, Jensfelt B, Persson T, Löfberg R. A reproducible grading scale for histological assessment of inflammation in ulcerative colitis. *Gut* 2000; **47**: 404-409 [PMID: 10940279 DOI: 10.1136/gut.47.3.404]
17 **Magro F**, Gionchetti P, Eliakim R, Ardizzone S, Armuzzi A, Barreiro-de Acosta M, Burisch J, Gecse KB, Hart AL, Hindryckx P, Langner C, Limdi JK, Pellino G, Zagórowicz E, Raine T, Harbord M, Rieder F. European Crohn´s and Colitis Organisation [ECCO]. Third European Evidence-based Consensus on Diagnosis and Management of Ulcerative Colitis. Part 1: Definitions, Diagnosis, Extra-intestinal Manifestations, Pregnancy, Cancer Surveillance, Surgery, and Ileo-anal Pouch Disorders. *J Crohns Colitis* 2017; **11**: 649-670 [PMID: 28158501 DOI: 10.1093/ecco-jcc/jjx008]
18 **Rutgeerts P**, Sandborn WJ, Feagan BG, Reinisch W, Olson A, Johanns J, Travers S, Rachmilewitz D, Hanauer SB, Lichtenstein GR, de Villiers WJ, Present D, Sands BE, Colombel JF. Infliximab for induction and maintenance therapy for ulcerative colitis. *N Engl J Med* 2005; **353**: 2462-2476 [PMID: 16339095 DOI: 10.1056/NEJMoa050516]
19 **Gomollón F**, García-López S, Sicilia B, Gisbert JP, Hinojosa J; Grupo Espa˜nol de Trabajo en Enfermedad de Crohn y Colitis Ulcerosa. Therapeutic guidelines on ulcerative colitis: a GRADE methodology based effort of GETECCU. *Gastroenterol Hepatol* 2013; **36**: 104-114 [PMID: 23332546 DOI: 10.1016/j.gastrohep.2012.09.006]
20 **Walsh AJ**, Ghosh A, Brain AO, Buchel O, Burger D, Thomas S, White L, Collins GS, Keshav S, Travis SP. Comparing disease activity indices in ulcerative colitis. *J Crohns Colitis* 2014; **8**: 318-325 [PMID: 24120021 DOI: 10.1016/j.crohns.2013.09.010]
21 **Satsangi J**, Silverberg MS, Vermeire S, Colombel JF. The Montreal classification of inflammatory bowel disease: controversies, consensus, and implications. *Gut* 2006; **55**: 749-753 [PMID: 16698746 DOI: 10.1136/gut.2005.082909]
22 **Jovanovic M**, Gajovic N, Jurisevic M, Simovic-Markovic B, Maric V, Jovanovic M, Arsenijevic N, Zdravkovic N. Fecal sST2 correlates with disease severity of ulcerative colitis. *Vojnosanit pregl* 2018; In press [DOI: 10.2298/VSP171225026J]
23 **Rogler G**, Hausmann M, Vogl D, Aschenbrenner E, Andus T, Falk W, Andreesen R, Schölmerich J, Gross V. Isolation and phenotypic characterization of colonic macrophages. *Clin Exp Immunol* 1998; **112**: 205-215 [PMID: 9649182 DOI: 10.1046/j.1365-2249.1998.00557.x]
24 **Acovic A**, Simovic Markovic B, Gazdic M, Arsenijevic A, Jovicic N, Gajovic N, Jovanovic M, Zdravkovic N, Kanjevac T, Harrell CR, Fellabaum C, Dolicanin Z, Djonov V, Arsenijevic N, Lukic ML, Volarevic V. Indoleamine 2,3-dioxygenase-dependent expansion of T-regulatory cells maintains mucosal healing in ulcerative colitis. *Therap Adv Gastroenterol* 2018; **11**: 1756284818793558 [PMID: 30159037 DOI: 10.1177/1756284818793558]

25 **Huang PL**. A comprehensive definition for metabolic syndrome. *Dis Model Mech* 2009; **2**: 231-237 [PMID: 19407331 DOI: 10.1242/dmm.001180]

26 **Krausgruber T**, Schiering C, Adelmann K, Harrison OJ, Chomka A, Pearson C, Ahern PP, Shale M, Oukka M, Powrie F. T-bet is a key modulator of IL-23-driven pathogenic CD4(+) T cell responses in the intestine. *Nat Commun* 2016; **7**: 11627 [PMID: 27193261 DOI: 10.1038/ncomms11627]

27 **Knosp CA**, Schiering C, Spence S, Carroll HP, Nel HJ, Osbourn M, Jackson R, Lyubomska O, Malissen B, Ingram R, Fitzgerald DC, Powrie F, Fallon PG, Johnston JA, Kissenpfennig A. Regulation of Foxp3+ inducible regulatory T cell stability by SOCS2. *J Immunol* 2013; **190**: 3235-3245 [PMID: 23455506 DOI: 10.4049/jimmunol.1201396]

28 **Laffont S**, Siddiqui KR, Powrie F. Intestinal inflammation abrogates the tolerogenic properties of MLN CD103+ dendritic cells. *Eur J Immunol* 2010; **40**: 1877-1883 [PMID: 20432234 DOI: 10.1002/eji.200939957]

29 **Hall LJ**, Murphy CT, Quinlan A, Hurley G, Shanahan F, Nally K, Melgar S. Natural killer cells protect mice from DSS-induced colitis by regulating neutrophil function via the NKG2A receptor. *Mucosal Immunol* 2013; **6**: 1016-1026 [PMID: 23340823 DOI: 10.1038/mi.2012.140]

30 **van der Weerd K**, Dik WA, Schrijver B, Schweitzer DH, Langerak AW, Drexhage HA, Kiewiet RM, van Aken MO, van Huisstede A, van Dongen JJ, van der Lelij AJ, Staal FJ, van Hagen PM. Morbidly obese human subjects have increased peripheral blood CD4+ T cells with skewing toward a Treg- and Th2-dominated phenotype. *Diabetes* 2012; **61**: 401-408 [PMID: 22228716 DOI: 10.2337/db11-1065]

31 **O'Rourke RW**, Kay T, Scholz MH, Diggs B, Jobe BA, Lewinsohn DM, Bakke AC. Alterations in T-cell subset frequency in peripheral blood in obesity. *Obes Surg* 2005; **15**: 1463-1468 [PMID: 16354528 DOI: 10.1381/096089205774859308]

32 **Kanneganti TD**, Dixit VD. Immunological complications of obesity. *Nat Immunol* 2012; **13**: 707-712 [PMID: 22814340 DOI: 10.1038/ni.2343]

33 **Guilherme A**, Virbasius JV, Puri V, Czech MP. Adipocyte dysfunctions linking obesity to insulin resistance and type 2 diabetes. *Nat Rev Mol Cell Biol* 2008; **9**: 367-377 [PMID: 18401346 DOI: 10.1038/nrm2391]

34 **Li P**, Liu S, Lu M, Bandyopadhyay G, Oh D, Imamura T, Johnson AMF, Sears D, Shen Z, Cui B, Kong L, Hou S, Liang X, Iovino S, Watkins SM, Ying W, Osborn O, Wollam J, Brenner M, Olefsky JM. Hematopoietic-Derived Galectin-3 Causes Cellular and Systemic Insulin Resistance. *Cell* 2016; **167**: 973-984.e12 [PMID: 27814523 DOI: 10.1016/j.cell.2016.10.025]

35 **Volarevic V**, Milovanovic M, Ljujic B, Pejnovic N, Arsenijevic N, Nilsson U, Leffler H, Lukic ML. Galectin-3 deficiency prevents concanavalin A-induced hepatitis in mice. *Hepatology* 2012; **55**: 1954-1964 [PMID: 22213244 DOI: 10.1002/hep.25542]

36 **Arsenijevic A**, Milovanovic M, Milovanovic J, Stojanovic B, Zdravkovic N, Leung PS, Liu FT, Gershwin ME, Lukic ML. Deletion of Galectin-3 Enhances Xenobiotic Induced Murine Primary Biliary Cholangitis by Facilitating Apoptosis of BECs and Release of Autoantigens. *Sci Rep* 2016; **6**: 23348 [PMID: 26996208 DOI: 10.1038/srep23348]

37 **Pejnovic NN**, Pantic JM, Jovanovic IP, Radosavljevic GD, Milovanovic MZ, Nikolic IG, Zdravkovic NS, Djukic AL, Arsenijevic NN, Lukic ML. Galectin-3 deficiency accelerates high-fat diet-induced obesity and amplifies inflammation in adipose tissue and pancreatic islets. *Diabetes* 2013; **62**: 1932-1944 [PMID: 23349493 DOI: 10.2337/db12-0222]

38 **Lukic R**, Gajovic N, Jovanovic I, Jurisevic M, Mijailovic Z, Maric V, Popovska Jovicic B, Arsenijevic N. Potential Hepatoprotective Role of Galectin-3 during HCV Infection in End-Stage Renal Disease Patients. *Dis Markers* 2017; **2017**: 6275987 [PMID: 28487598 DOI: 10.1155/2017/6275987]

39 **Jovanovic M**, Gajovic N, Zdravkovic N, Jovanovic M, Jurisevic M, Vojvodic D, Maric V, Arsenijevic A, Jovanovic I. Fecal Galectin-3: A New Promising Biomarker for Severity and Progression of Colorectal Carcinoma. *Mediators Inflamm* 2018; **2018**: 8031328 [PMID: 29849497 DOI: 10.1155/2018/8031328]

40 **Tsai HF**, Wu CS, Chen YL, Liao HJ, Chyuan IT, Hsu PN. Galectin-3 suppresses mucosal inflammation and reduces disease severity in experimental colitis. *J Mol Med* (Berl). 2016; **94**: 545-556 [PMID: 26631140 DOI: 10.1007/s00109-015-1368-x]

Published By Baishideng Publishing Group Inc
7041 Koll Center Parkway, Suite 160, Pleasanton, CA 94566, USA
Telephone: +1-925-2238242
E-mail: bpgoffice@wjgnet.com
Help Desk:http://www.f6publishing.com/helpdesk
http://www.wjgnet.com